Comments on

ENVIRONMENTAL PROTECTION AGENCY
40 CFR Part 50
[EPA–HQ–OAR–2007–1145; FRL–9441–2]
RIN 2060–AO72
Secondary National Ambient Air Quality Standards for Oxides of Nitrogen and Sulfur

Federal Register / Vol. 76, No. 147 / Monday, August 1, 2011 / 46084-46147

Submitted by the Electric Power Research Institute (EPRI)

Eladio M. Knipping, Ph.D.
Senior Technical Manager, Environment
Electric Power Research Institute (EPRI)
2000 L Street NW Suite 805, Washington, DC 20036 USA
Phone: 202.293.6343 • **Mobile:** 650.799.7088 • **Fax:** 202.293.2697
Email: eknippin@epri.com

Acknowledgements: Steven A. Gherini[1], Robert A. Goldstein[2], David F. Grigal[3], Bonyoung Koo[4], Ralph E. Morris[4], Ronald K. Munson[5], Piti Piyachaturawat[4], John Rath[1], Karen Summers[1], Joy L. Valentini[1]

[1] Tetra Tech, Inc.
[2] Electric Power Research Institute (EPRI)
[3] University of Minnesota (retired)
[4] ENVIRON International Corporation
[5] Leonardo Technologies, Inc.

Monday, October 10, 2011

Comments on

ENVIRONMENTAL PROTECTION AGENCY
40 CFR Part 50
[EPA–HQ–OAR–2007–1145; FRL–9441–2]
RIN 2060–AO72
Secondary National Ambient Air Quality Standards for Oxides of Nitrogen and Sulfur

Federal Register / Vol. 76, No. 147 / Monday, August 1, 2011 / 46084-46147

Submitted by the Electric Power Research Institute
Monday, October 10, 2011

Principal Comments

On August 1, 2011, the United States Environmental Protection Agency (EPA) published in the Federal Register [76 FR 147] a proposed rule revising the Secondary National Ambient Air Quality Standards (NAAQS) for oxides of nitrogen (NOx) and oxides of sulfur (SOx) (EPA, 2011). A final rulemaking is scheduled for spring 2012. As summarized in the proposed rulemaking:

> *Based on its review, EPA proposes to retain the current nitrogen dioxide (NO_2) and sulfur dioxide (SO_2) secondary standards to provide requisite protection for the direct effects on vegetation resulting from exposure to gaseous oxides of nitrogen and sulfur in the ambient air. Additionally, with regard to protection from the deposition of oxides of nitrogen and sulfur to sensitive aquatic and terrestrial ecosystems, including acidification and nutrient enrichment effects, EPA is proposing to add secondary standards identical to the NO_2 and SO_2 primary 1- hour standards and not set a new multipollutant secondary standard in this review. The proposed 1-hour secondary NO_2 standard would be set at a level of 100 ppb and the proposed 1-hour secondary SO_2 standard would be set at 75 ppb. In addition, EPA has decided to undertake a field pilot program to gather and analyze additional relevant data so as to enhance the Agency's understanding of the degree of protectiveness that a new multipollutant approach, defined in terms of an aquatic acidification index (AAI), would afford and to support development of an appropriate monitoring network for such a standard.*

The existing secondary standards for NOx and SOx are

- NO_2 at 0.053 ppm (parts per million) averaged over a year; and
- SO_2 at 0.5 ppm averaged over three hours, not to be exceeded more than once per year

During its review of the secondary NAAQS for NOx and SOx, EPA for the first time considered a multipollutant and multimedia approach in its assessment of the National Ambient Air Quality Standards (NAAQS). This approach, expressed in terms of an aquatic acidification index (AAI), would be multimedia since it would provide a standard that would address concentrations of NOx and SOx concurrently. The approach would be a multimedia approach not only because it would consider the effects of

atmospheric deposition of NOx and SOx on aquatic acidification, but also because the "level" of the standard would be based on the water quality variable of Acid Neutralizing Capacity (ANC).

As noted in EPA's proposed rulemaking, EPA is planning to develop a five-year pilot field program in several acid-sensitive ecoregions. The goal of this pilot program is to inform a future decision on secondary standards for NOx and SOx. There is currently very little detail given about this pilot program, but it focuses on developing new Federal Reference Method (FRM) monitors that measure the atmospheric concentrations of oxides of sulfur (SOx)[1] and total oxides of nitrogen (NOy)[2].

In addition to the FRM development, the program will also estimate dry deposition fluxes and measure wet deposition fluxes of NOy, SOx and reduced nitrogen compounds (NHx)[3]. These fluxes, along with the concurrent concentration measurements, can be used to test the performance of atmospheric models and evaluate the concept of "transference ratios" (e.g., test the ability of models to reproduce measured values, and their spatial and temporal variability) introduced as part of the Aquatic Acidification Index. In order to estimate dry deposition fluxes, the program proposes to use atmospheric concentrations and prescribed deposition velocities. This combination of measurements and model-derived deposition velocities is the approach employed by EPA's Clean Air Status and Trends Network (CASTNet) to assess dry deposition fluxes of particulate sulfate (SO_4^{2-}), nitric acid (HNO_3) and particulate nitrate (NO_3^-). To assess wet deposition fluxes of NOy, SOx, and NHx , the EPA currently uses, and proposes to continue to rely on, measurements collected by the National Atmospheric Deposition Program (NADP). The NADP consists of over 100 sites where weekly precipitation samples are collected and analyzed for pH and key *inorganic* ions (such as SO_4^{2-}; NO_3^-;NH_4^+; chloride, Cl^-; calcium, Ca^{2+}; magnesium, Mg^{2+}; and sodium, Na^+). In addition to these wet deposition flux measurements, a new program named AMoN has been initiated under the auspices of NADP and will be used by the pilot program. For AMoN, two-week composite atmospheric NH_3 samples are taken and analyzed. By combining this ambient measurement with model deposition velocities, ammonia (NH_3) fluxes will be evaluated as the other dry deposition assessments mentioned earlier.

Although the stated objectives of the pilot program is to "*enhance the Agency's understanding of the degree of protectiveness that a new multipollutant approach, defined in terms of an aquatic acidification index (AAI), would afford and to support development of an appropriate monitoring network for such a standard*," the program described fails to address key scientific concerns with the new approach and is limited to measuring ambient concentrations with very coarse technologies. In order to meet its stated objectives, the pilot program must address a number of scientific concerns with respect to the proposed methodology based on the Aquatic Acidification Index.

---

[1] SOx[1] = sulfur dioxide, SO_2, + particulate sulfate, SO_4^{2-}, and organic forms of oxides of sulfur in gases and particles

[2] NOy = nitric oxide, NO, + nitrogen dioxide, NO_2, + nitric acid, HNO_3, + particulate nitrate, NO_3^- + other forms of oxides of nitrogen, inorganic and organic, in gases and particles

[3] NHx = ammonia, NH_3, particulate ammonium, NH_4^+, and organic forms of reduced organic nitrogen in gases and particles

The Electric Power Research Institute (EPRI) submitted comments to EPA on the Second Draft Policy Assessment Document (PAD) on the review of the Secondary NAAQS for NOx and SOx underscoring key concerns with the proposed methodology based on the Aquatic Acidification Index. EPRI later provided additional comments to the Clean Air Scientific Advisory Committee (CASAC) Review Panel that emphasized additional scientific concerns with the proposed methodology as presented in the Final Policy Assessment Document—the same methodology described in the proposed rulemaking—which emphasized that current databases needed to support a national standard based on this methodology are inadequate[4]. A compendium of detailed EPRI comments and observations is provided as an Appendix A to this document.[5] These comments, summarized below, should inform the development of a broader research program, beyond the scope of the current pilot program, and additional studies in order to address key knowledge and data gaps necessary to properly evaluate the adequacy of the proposed EPA methodology. The proposed rulemaking makes the presumption that a methodology based on the Aquatic Acidification Index can be proposed at a future date. We recommend that EPA use the development of a research program to test the AAI methodology and explore other alternatives to better understand and address ecosystem impacts attributed to atmospheric deposition.

1. The Adequacy of ANC as a Universal Indicator of Ecosystem Sustainability Requires Evaluation; Other Alternative Indicators Need to Be Explored

As described in detail in the Appendix A, EPA proposes to use the water chemistry parameter of Acid Neutralizing Capacity, ANC, as the "ecological indicator" on which the "level" of the standard is based. However, EPA has not explored the adequacy of this parameter in terms of its appropriateness as a universal indicator of the viability of waterbodies (e.g., lakes and streams) to support aquatic biota.

EPA has established the use of ANC based on data collected in the Adirondacks (and to some extent data from the Shenandoah region). However, the use of ANC alone is insufficient. As recognized by EPA in its Final PAD, the toxicity of lakes has a causal relationship to pH levels and concentrations of inorganic monomeric aluminum, [Al_{im}]; ANC per se does not cause adverse impacts to aquatic habitats.

EPA's research program should explore the relationships—in watersheds across the nation and within regions believed to be sensitive, moderately sensitive and insensitive to acidification due to atmospheric deposition—between ANC, pH and [Al_{im}] before the influence of SOx, NOy and

[4] EPRI comments also underscored even in areas where waterbodies have been studied extensively, such as Adirondacks lakes and Shenandoah streams, the waterbodies selected for study are not representative of the overall population distribution of waterbodies or the distribution of other parameters such as lake area or stream length.

[5] The comments and presentations provided to the EPA CASAC Review Panel on the Final Policy Assessment Document are also attached for completeness.

total reduced nitrogen (NHx) can be determined. Of critical importance, it is essential to collect detailed water chemistry data—including, in particular, levels of dissolved organic carbon (DOC), inorganic monomeric aluminum (Al_{im}) and total aluminum (AL_T)—in different waterbodies across the nation within regions of different sensitivity to acidification from deposition in order to understand their influence on pH levels and the concentrations of Al_{im}.

After determining the influence of different limnological factors on water chemistry (also discussed in a subsequent comment on water chemistry modeling), it is important to relate chemical parameters to biological parameters. EPA's research program should explore the relationship of fish population and fish species diversity (two key ecosystem services identified as affected by acidification) to different water chemistry variables.

At this moment, EPA is depending on data collected primarily from Adirondack lakes and, in part, Shenandoah streams. EPA should collect fish population and species data in waterbodies located in other regions of the country in order to understand the applicability of their proposed methodology for a national ambient air quality standard. It also important to focus on areas considered sensitive, moderately sensitive, and non- sensitive to acidification due to atmospheric deposition since the standard would address the requisite level of protections across all regions in the United States.

2. The Research Program Should Evaluate the Adequacy of the Omernik Ecoregion Approach as a Method of Waterbody Aggregation for Critical Load Calculations; It Should Determine the Representativeness of Data Used for Critical Load Calculations in Any Regionalization Scheme

As described in detail in the Appendix A, EPA's regionalization methodology, based on Omernik ecoregions, emphasizes vegetation differences, not key water-quality or limnological variables. EPA should evaluate the adequacy of different geospatial classification methods—such as ecological regionalization schemes or hydrological unit classification (HUC) levels—for use in aggregating populations of waterbodies that would employ a similar set of parameters in critical load calculations. One important methodology to explore is the application of multivariate methods that would emphasize variables that determine the sensitivity of the waterbodies to acidification. Several of these variables are discussed in the subsequent section on critical load modeling.

Regardless of the regionalization scheme used for aggregation of waterbodies, EPA should conduct an analysis of available water quality data to evaluate the representativeness of waterbodies for which critical loads can be calculated in any region. Such an analysis would ensure that the population of streams and lakes in the region—and corresponding stream length and lake area—are representative of the distribution of geology, limnology, biota, and sensitivity to acidification in the region.

3. The Research Program Should Explore Different Methods for Calculating Critical Loads, Collect Essential Data and Employ Mechanistic Water Chemistry Models

It is important to note that a research program should be able to recognize that not all acidic waterbodies have reached those conditions due to anthropogenic influences. In other words, it is important to understand which waterbodies have been "acidified" and to understand the extent to which atmospheric deposition of NOx and SOx have contributed to acidification. It is also important to establish the extent to which acidification influences the ecosystem services of concern, i.e. fish population and fish species diversity. It is important to understand that there are several processes that influence these services and that different populations and habitats respond differently to atmospheric deposition.

The proposed future approach for a secondary national ambient air quality standard uses a simple steady-state water chemistry model to develop critical loads for different regions of the country. However, as discussed in Appendix A, these simple parameterizations and models fail to represent key processes, conditions and watershed characteristics that determine the chemical composition of waterbodies.

EPA should improve the modeling of key watershed characteristics—such as weathering rates, ion uptake, ion exchange, soil composition, soil depth, and flow paths—that affect water chemistry. This effort would require the evaluation of different modeling approaches, but more importantly would also necessitate a broad data collection effort, as described at the conclusion of these comments.

A data collection effort should also evaluate the impact of organic acids on water chemistry across different regions of the country. Both weak and strong organic acids should be measured in order to understand the amount of expected recovery. The age of soils and the presence of carbonate rocks and other sedimentary materials should also be evaluated. It is also important to characterize the cation exchange capacity of different soils, understand how it varies with soil depth and evaluate the base cation saturation of different soil layers. As noted earlier, any data collection campaign should focus on areas considered acid-sensitive, moderately acid-sensitive and non-acid-sensitive since the standard must address the requisite level of protection across all regions in the United States.

It is evident from our analysis that the Henriksen f-factor approach for calculating preindustrial (or preacidification) base cation concentrations is insufficient, not only because it relies on data based from Norwegian studies but also because it fails to reproduce the temporal variability exhibited in natural systems. In fact, as shown in Appendix A, it even fails to reproduce the range of observed values in the two most-highly studied areas of the U.S.

A research effort to advance the development of mechanistic models that include key physical and chemical processes is necessary. These models should be tested across a wide variety of regions (sensitive, moderately sensitive and non-sensitive) and should be able to differentiate between ion uptake (including sulfate adsorption, nitrogen uptake, and base cation uptake), ion exchange and weathering rates, properly simulating each process. Models such as the Integrated Lake-Watershed Acidification Study (ILWAS) model, the Regional Integrated Lake-Watershed Acidification Study (RILWAS) model and the Watershed Risk Management Framework (WARMF) model should also be evaluated.

4. The Research Program Should Include Testing of Dry Deposition Measurement Methods and Evaluate the Ability of Atmospheric Models to Simulate Accurate Concentrations and Fluxes of SOx, NOy and NHx

As noted earlier, there is currently very little detail on EPA's proposed program, but it appears to focus on developing new Federal Reference Method (FRM) monitors that measure the atmospheric concentrations of SOx and NOy. In addition to the FRM portion of the program, dry deposition fluxes would be estimated by relying on modeled deposition velocities and wet deposition fluxes would be obtained from CASTNET-type methods and NADP measurements. The AMoN network would be used to collect two-week composite atmospheric NH_3 and estimate dry NH_3 fluxes. These fluxes, along with the concurrent concentration measurements, can be used to test the performance of atmospheric models and evaluate the concept of "transference ratios" (e.g., test the ability of models to reproduce values, and their spatial and temporal variability) introduced as part of the Aquatic Acidification Index.

EPA should expand this program in several ways. First, it should explore several alternate methods to measure concentrations of SOx, NOy and NHx in the atmosphere, including methods with high-time resolution and methods that target specific components of these three families of chemical compounds; moreover, EPA should target methods that can differentiate between organic and inorganic constituents of gases and particles.

Perhaps most importantly given the objectives of the program, EPA should promote the development of instruments to measure actual dry deposition fluxes of these species instead of relying on a combination of ambient concentrations and modeled deposition velocities. An emphasis should be given to methods that would be amenable to operation in routine networks; these methods should be robust, relatively low-cost, and provide continuous data on the flux of SOx, NOy and NHx. Consideration should be given to the use of Leaf Areas Indices (LAI) in combination with flux measurements to better develop algorithms for estimating dry deposition fluxes that accurately represent the role of the forest canopy.

EPA should also promote the continued development of atmospheric models such that they include missing emissions sources (such as emissions or organic reduced-nitrogen gases) and the accurate temporal and spatial distribution of emissions. In addition, atmospheric models should simulate the bi-directional flux of NOy and NHx species. This will also require better land-use and characterization data for use within the modeling systems.

Atmospheric models should also accurately represent the gas-particle partitioning of chemical compounds, in particular the formation of ammonium nitrate under different meteorological and air quality conditions.

Improved atmospheric models will also require better methods for estimating precipitation and the formation of convective clouds within three-dimensional models. Adjusting atmospheric modeling results *a-posteriori* with methods such as the Parametric Regression on Independent Slopes Models (PRISM) to wet-deposition only introduces mass-balance concerns and questions the adequacy of the overall modeling system.

Improvements to atmospheric models can only be gauged by comparison to ambient measurement of concentrations and deposition fluxes. Given the proposed use of the models, it is imperative to collect actual deposition data in addition to concentrations in order to test the suitability of the transference ratio concept. In doing so, data must be collected at different locations of any regionalization schemes being considered (as expressed in earlier comments) in order to evaluate the spatial variability of these ratios across the different spatial geospatial classification methods. These data should then be compared to model simulations as part of a rigorous model evaluation study, as illustrated in the Appendix A to these comments. Any model evaluation study should also incorporate more than one atmospheric model (and test various model configurations) in order to test the robustness of results provided from an individual atmospheric simulation versus an ensemble of simulations to ensure that comparisons and evaluation to ambient data are not based on the results of a single simulation. It is important to note once again that such an effort should focus on both areas considered acid-sensitive and non-acid-sensitive since the standard must address the requisite level of protections across all regions in the United States.

5. A Rigorous Uncertainty and Variability Analysis of the Aquatic Acidification Index Needs to be Conducted as Part of the Research Program

Consideration of uncertainty is an essential part of any scientific analysis. As it relates to the SOx and NOx Secondary NAAQS, an uncertainty analysis can be used to determine the potential for any proposed standards to be effective in protecting ecosystems. Given the large uncertainty in many parameters of the AAI, it is imperative that a full uncertainty analysis of the overall

standard be conducted as part of the pilot program. EPA is proposing to use average values of parameters used as part of critical load calculations and other factors (such as transference ratios and runoff rates) that form part of the Aquatic Acidification Index. However, the variability of these parameters in any a regionalization scheme can have a large impact on the range of uncertainty of the standard.

Uncertainty and variability are indeed two different concepts. However, the variability in the parameters must be included in an uncertainty analysis due to the design of the AAI equation. For example, if a region with 10 monitors were to add 2 new monitors, the location of existing monitors and the choice of location of the two new monitors could have a significant impact on the new average value of any given parameter due to the extent of the variability in the ecoregion, particularly if data representativeness in the waterbody distribution is not adequately tested (as noted in an earlier comment).

The extent by which the new "mean" values, as well as the representative critical load, could change must be assessed when there is high variability in the data and a lack of clearly defined representativeness in the waterbody population. The distribution of the actual individual parameters, such as TSOx and TNOy, in a region needs to be considered in a combined uncertainty and variability analysis.

With an increasing level of homogeneity in a region, the impact of variability diminishes. It is at this moment that the "certainty" of the standard is influenced by the uncertainty in the measurements or estimations of the AAI parameters. EPA should perform uncertainty analyses that consider the impact of variability to estimate the uncertainty in the standard. An example of such an analysis is given in Appendix A.

Overarching Comments and Concluding Remarks

An overarching point from these comments is that in order to conduct a nationwide assessment of any proposed methodology for a future Secondary NAAQS for NOx and SOx based on ecological impacts such as acidification, EPA needs to ensure the existence of a nationwide database of water chemistry that includes representative data for every region[6] of the country, including regions that are believed to be sensitive, moderately sensitive and non-sensitive to acidification from atmospheric deposition. These data sets would include, but not be limited to:

- Key water quality variables related to acidification: ANC; DOC; pH; the concentration of total aluminum [AL_T]; the total concentration of other key inorganic bases such as calcium [Ca_T], magnesium [Mg_T], sodium [Na_T], and potassium [K_T]; the partial pressure of CO_2 (pCO_2) or the

[6] For every region as defined by a proposed regionalization scheme.

concentration of total inorganic carbon[7]; the concentrations of key acid anions, such as sulfate [SO_4^{2-}], nitrate [NO_3^-] and chloride [Cl^-]; and the concentration of aqueous silica [SiO_2].

- Key aquatic biota variables, such as fish data (e.g., population, species diversity,) and other key biological, physical and chemical variables that influence or indicate the trophic state and health of aquatic communities: phytoplankton counts, zooplankton counts, temperature, dissolved oxygen, chlorophyll-a, total phosphorus, total nitrogen and sediment data.
- Key soil chemistry variables: cation exchange capacity, base saturation ratio, sulfate adsorption, nitrogen uptake, base cation uptake and base cation weathering.
- Landscape features: soil depth, slope, vegetative cover, bedrock type, elevation, and watershed area.

EPA should first assess the spatial and temporal (vintage) representativeness of existing data bases, including consideration of potential spatial aggregation schemes, and then plan a sampling program to fill in important data gaps. One possibility would be to coordinate efforts with the EPA National Aquatic Resource Surveys[8], run by EPA's Office of Water, which has taken over the monitoring of the nation's water resources from the Environmental Monitoring & Assessment Program (EMAP)[9] that operated from 1990-2006.

In locations that have been affected by atmospheric deposition, it is important to understand to what extent the distribution of lakes and streams—and the distribution of lake area and stream length—have been affected in a particular region. Additional areas of research include understanding the potential for additional acidification under current emissions and future emissions trends. In addition, one must also evaluate the potential for recovery in these systems and corresponding response times so that we can properly adjust our expectations of recovery.

Attachments (in PDF Format)

- Main Comments (this file)
- Appendix Part 1–Appendix A: Review of Alternate Approach for Secondary NAAQS for NOx and SOx
- Appendix Part 2–Appendices B-D1: Supporting Information to Appendix A
- Appendix Part 3–Appendices D2-E: Supporting Information to Appendix A
- Text of comments presented to CASAC Review Panel on Final Policy Assessment Document
- Short presentation presented in conjunction with comments presented to CASAC Review Panel on Final Policy Assessment Document
- Long presentation with additional information, comments and analysis presented to CASAC Review Panel on Final Policy Assessment Document

---

[7] The concentration of total inorganic carbon (TIC)—also referred to as total carbonate, TC or [C_T], or dissolved inorganic carbon (DIC)—is equal to the sum of the concentrations of dissolved CO_2 ($CO_2 \cdot H_2O$), bicarbonate [HCO_3^-] and carbonate [CO_3^{2-}].

[8] http://water.epa.gov/type/watersheds/monitoring/aquaticsurvey_index.cfm

[9] http://www.epa.gov/emap2/

Appendix A – Review of Alternate Approach for Secondary NAAQS for NOx and SOx

Introduction

Under the notice of proposed rulemaking for the Secondary National Ambient Air Quality Standards (NAAQS) for Oxides of Nitrogen (NOx) and Oxides of Sulfur (SOx), EPA includes a discussion of an alternate secondary NAAQS for NOx and SOx which would have addressed these pollutants jointly. This alternate approach for a joint secondary NAAQS was first introduced by EPA during the Policy Assessment phase of the Secondary NAAQS Review Process. EPA is postponing their introduction of this joint approach until additional data are collected as part of pilot program as described in the proposed rulemaking. The Electric Power Research Institute (EPRI) has provided comments, observations and recommendations on the pilot program in its "Main Comments" section. This appendix supports those comments and provides additional details on several aspects of the proposed future methodology that need to be explored.

In past evaluations of the secondary standards of SOx and NOx, EPA considered the potential for adverse impacts from the presence of these pollutants—taken individually—in ambient air on vegetation. As part of this Secondary NAAQS process, EPA considered the potential adverse effects of these pollutants—taken jointly—on ecosystems by means of their deposition on soils and waters. As part of the review process, EPA prepared two documents. The purpose of the first document, the Integrated Science Assessment (EPA, 2008), was to summarize the science of NOx and SOx in the atmosphere and how these pollutants may adversely affect public welfare through a wide-range of environment effects. The purpose of the second document, the Risk and Exposure Assessment (EPA, 2009), was to evaluate and quantify the extent that adverse impacts are occurring in the environment throughout the United States. EPA identified four new ecological impacts of concern in these documents, although they limited their analyses to a handful of "case study" regions. The four ecological endpoints were:

- Aquatic Acidification
- Terrestrial Acidification
- Aquatic Nutrient Enrichment
- Terrestrial Nutrient Enrichment

EPA concluded that current state of the science would support a new approach to address the first of these ecological endpoints, aquatic acidification. In doing so, EPA developed a new approach for a secondary standard that was unprecedented in several ways.

1. The approach would result in an effective multimedia NAAQS as it would address the control of air emissions to address a concern in a separate environmental medium (surface waters such as lakes and streams), i.e., aquatic acidification attributed to atmospheric deposition.

2. The approach would rely heavily on aquatic and atmospheric models to develop a new parameter, the aquatic acidification index (AAI), which would define the "form" of the standard. In essence though, this parameter would define the levels of NOx and SOx needed to satisfy the standard.
3. The approach would result in a non-uniform atmospheric level of concentrations required to satisfy the NAAQS. The approach would use a water quality variable, the acid neutralizing capacity (ANC), to define the regulatory "level" of the standard. Actual ambient concentrations needed to satisfy the standard (for a given level of ANC) would vary across the country.

In this Appendix, we briefly summarize the alternate methodology that EPA proposed in the Final Policy Assessment Document and may propose in a future rulemaking and then discuss the key issues of concern that require further research and should be addressed before reaching a determination as to the adequacy of the approach.

Elements of the Standard

A National Ambient Air Quality Standard (NAAQS), whether primary or secondary, is defined by four "elements." The elements of the standard are the indicator, level, averaging time and form. In the case of this joint approach the elements can be summarized as follows (EPA, 2011):

- **Indicators:**

  SOx: sum of SO_2 and SO_4^{2-}

  NOy: sum of NO + NO_2 + HNO_3 + NO_3^- + all other forms of oxidized nitrogen (inorganic and organic) in gas and particles. In atmospheric science, the term NOx signifies the sum of two oxides of nitrogen (NO and NO_2); the scientific term NOy is used to represent all oxides of nitrogen in the atmosphere. This term will be used henceforth to avoid confusion between the established scientific terms.

  The indicators are ambient concentrations measured in order to determine compliance with the standard.

- **Level:**

  Although the indicators as stated above are ambient concentrations of substances in air, the level of the new approach is based on the "ecological indicator" of Acid Neutralizing Capacity (ANC); EPA staff suggests values in the range of 20-75 μeq L^{-1}. A more complete discussion of ANC is discussed in subsequent sections.

- **Averaging Time:** 3-5 years

  This averaging time applies only to the indicators of SOx and NOy measured in ambient air. As indicated in the following discussion, the form of the standard uses several parameters and model results. Our comments will show that the averaging time for these parameters and model

results has not been evaluated completely. In fact, the vintage (date or dates of measurement or modeling) are a key concern in the overall process.

- **Form:** Aquatic Acidification Index

  The form of standard is discussed in detailed in the following section.

The Aquatic Acidification Index

The aquatic acidification index is described by the following equation (EPA, 2011)

$$\mathbf{AAI = F1 - F2 - F3[NOy] - F4[SOx]} \qquad \text{Equation 1}$$

These four factors (F1, F2, F3, and F4) would be provided by EPA for 84 ecoregions in the United States. EPA has chosen a specific ecoregion approach to define different areas of the country for which these factors would be calculated. Although these four factors would be constant within any specific ecoregion, these factors vary across ecoregions. (The ecoregion approach used by EPA is discussed in subsequent sections.)

If the AAI for a particular ecoregion of the country is LESS than the statutory level of standard based on a "target" ANC, then that region is found to be in non-attainment. From inspection, a high level of AAI can only be achieved by lowering concentrations of NOy and SOx. The relative magnitude of F3 and F4 determine the extent by which NOy or SOx controls may influence the AAI. (In a special case discussed later, the F2 and F3 factors may be simplified to zero, leaving only two terms to the AAI equation).

Since these factors vary across ecoregions, the stringency of the standard with respect to ambient levels of NOy and SOx varies across the country. The individual variables that make up these factors are

- $F1 = ANC_{lim} + CL_r/Q_r$
- $F2 = NHx/Q_r$
- $F3 = TNOy/Q_r$
- $F4 = TSOx/Q_r$

… where …

- ANC_{lim} is the limiting ("target") ANC
- CL_r is the representative critical load, assuming a steady-state water chemistry (SSWC) model, calculated as the value to protect a certain percentile of waterbodies in an ecoregion with sufficient data for critical load calculations. (Comments on the concept and modeling of critical loads are included in subsequent sections.)
- Q_r is the representative hydrologic run-off rate, calculated as the median of all waterbodies with data in an ecoregion.
- NHx is the wet and dry deposition of reduced nitrogen, taken as sum of NH_3 and NH_4^+ deposition loads from EPA's Community Multiscale Air Quality (CMAQ) model spatially averaged over an ecoregion.

- TSOx and TNOy are the transference ratios that convert annual ambient air concentrations of SOx and NOy to annual deposition loads of SOx and NOy, respectively, also derived from the CMAQ model spatially averaged over an ecoregion. These ratios are discussed in more detail in the following sections.

The AAI is applied by taking the following steps:

1. Divide the country into different regions
   - EPA staff has selected Omernik Level III ecoregions
2. Classify ecoregions as acid-sensitive and non-acid sensitive based on EPA staff criteria:
   - Sensitive ecoregions are those with **1%** of waterbodies with measurements of **ANC < 100 µeq L^{-1}** and **5%** of waterbodies with measurements of **ANC < 200 µeq L^{-1}**
   - **The sensitivity of this screening process has not been explored in any documents by EPA.**
   - Set a limiting ("target") ANC (ANC_{lim}): **ANC_{lim} is a decision of the Administrator**
3. Calculate critical loads for each waterbody having sufficient data using **steady state** assumptions
   - Use the critical load at a certain percentile of the distribution in AAI equation: CL_r
   - Percentiles from 70th to 90th suggested by EPA staff for acid sensitive regions
   - Median (50th percentile) suggested by EPA staff for non-acid-sensitive regions
   - **These percentiles of protection are also a decision of the Administrator**
   - Calculate F1 for each ecoregion using the regional median runoff rate: Qr
   - Note that population of waterbodies that are used to determine sensitivity are likely different than those used to calculate CL_r and Q_r.
4. Calculate F2, a value for annual reduced nitrogen (ammonia and ammonium) total (wet and dry) deposition load from CMAQ air quality model, spatially averaged across the ecoregions: (NHx)
   - EPA is considering alternative estimation methods for the NHx deposition load
5. Calculate F3 and F4, transference ratios (effective deposition velocities): annual aggregate, wet + dry, deposition load of all species of SOx or NOy ÷ annual aggregate concentrations of all species of SOx or NOy, respectively; data obtained from the CMAQ air quality model, spatially averaged across the ecoregions (TSOx and TNOy)
6. Calculate AAI by using these values and measured annual atmospheric concentrations of SOx and NOy averaged over 3-5 years
   - **The details of spatial and temporal averaging for CL_r, Q_r, NHx, TSOx and TNOy are unclear**
7. **Ecoregions where AAI < ANC_{lim} are designated as non-attainment**

As this appendix will elucidate, the elements of the approach described by EPA are (1) unconstrained due to a lack of data availability, (2) introduce concepts that have not been thoroughly tested by the scientific community, (3) exhibit an overreliance on aquatic and atmospheric models that have not been evaluated with a rigor commensurate with the significance of their anticipated use within a nationwide standard, and (4) fail to objectively recognize key fundamentals in the science of aquatic acidification.

We address several overarching issues regarding concerns over the use of ANC as an universal indicator of ecosystem health; concerns over the regionalization scheme adopted by EPA, spatial aggregation, representativeness of available data; the use of the steady state approach for critical load calculations; the application of aquatic and atmospheric models without rigorous testing and evaluation with ambient data; and a deficient methodology for evaluating the overall uncertainty of the AAI approach.

Acid Neutralizing Capacity is Not an Adequate Universal Indicator of Ecosystem Sustainability

Acid Neutralizing Capacity

Acid neutralizing capacity (ANC) is a measure of the net strong base in solution, or strong acid if the ANC value is negative. ANC is usually determined by titration with a strong acid or strong base. It can also be determined by calculation (See Sidebar 1 for pertinent derivations). In distilled water the value of ANC is zero; in seawater the ANC is about 2200 µeq L^{-1}. Most natural waters have values between about 100 and 5,000 µeq L^{-1} (Stumm and Morgan, 1981). Natural waters acquire their ANC predominantly from the weathering of minerals and ion exchange. Waters thought to be susceptible to acid deposition may have ANC values of 20-50 µeq L^{-1} or less.

ANC can be calculated in two ways that have been shown to be mathematically equivalent (Gherini, et al., 1985, and Munson and Gherini, 1991a). See Sidebar 1 “Derivation of ANC” for ANC derivation and other background information on ANC.

Sidebar 1: Derivation of ANC

Throughout EPA's PAD report, the term 'ANC' is used repeatedly. However, an accurate definition is never provided, and some of the uses for ANC in the report are appropriate while others are not.

Acid neutralizing capacity, or ANC, is a measurable parameter that indicates the net strong base in solution, or net strong acid if its value is negative. It is routinely measured by titration with strong acid or base to an equivalence point. At the equivalence point, the strong base in solution matches the strong acid and ANC is zero. The Gran (1952) procedure is the most commonly-used of several analytical procedures that have been developed to identify the equivalence point.

ANC is defined as the concentration of hydrogen-ion acceptors in solution minus the concentration of hydrogen-ion donors. For most fresh waters, bicarbonate ion is quantitatively the most important hydrogen-ion acceptor. For low ANC waters, other hydrogen-ion acceptors can become more important. Using the definition of ANC and the requirement of electroneutrality, a mathematically equivalent representation of ANC can be derived (See Derivation below) yielding:

$$\mathrm{ANC} = \sum \mathrm{C_B} - \sum \mathrm{C_A}$$

where,

$$\sum \mathrm{C_B} = 2[\mathrm{Ca_T}] + 2[\mathrm{Mg_T}] + [\mathrm{Na_T}] + [\mathrm{K_T}] + [\mathrm{NH_{4_T}}] + 2[\mathrm{Al_T}] + 2[\mathrm{Mn_T}] + 2[\mathrm{Fe_T}]$$

and

$$\sum \mathrm{C_A} = 2[\mathrm{SO_{4_T}}] + [\mathrm{NO_{3_T}}] + [\mathrm{Cl_T}] + [\mathrm{F_T}]$$

where

$[\ _T]$ = the total concentration of a species in µmoles L^{-1}

Note that this definition of ANC is different than that included in the PAD report. The primary difference is in the treatment of aluminum. The form presented above is more consistent with the definition of ANC and with what is measured in the Gran procedure (Gran, 1952). The form in the PAD report removes Al_T from $\sum \mathrm{C_B}$, presumably due to the negative impact of aluminum on biota.

This, however, represents a fundamental misuse of the ANC concept. ANC is concerned with acid-base chemistry of waters. It is not a measure of the suitability of waters for biota. Biota do not respond directly to changes in ANC. As discussed in more detail earlier in this review, biota respond to elevated aluminum concentrations and, at times, to elevated hydrogen-ion concentrations, but not to ANC. Florida lakes with low DOC provide an example of this phenomenon. Lake Barco and Lake Five-O were evaluated as part of the Hydrology and Acidity of Seepage Lakes study. Both have low ANC and low pH (elevated hydrogen-ion concentration); it is also important to note that the low ANC and low pH of these systems is not a result of high DOC levels, but rather a characteristic due to the nature of the soils in the region. However, because neither lake receives significant inputs from terrestrial sources, both have low aluminum concentrations and thus thriving fisheries (Pollman et al, 1991).

The normal conceptualization of ANC (e.g., Stumm and Morgan 1981) is the concentration of all hydrogen ion acceptors minus hydrogen ion donors:

$$\mathrm{ANC} = [\mathrm{HCO_3^-}] + 2[\mathrm{CO_3^{2-}}] + [\mathrm{OH^-}] + [\text{other } \mathrm{H^+}\text{-ion acceptors}] - [\mathrm{H^+}\text{-ion donors}]$$

An alternative representation of solution-phase ANC that is mathematically equivalent to the above equation is derived as follows (Gherini et al. 1985; Munson and Gherini, 1991a). The derivation is based upon the ANC definition and the solution electro-neutrality condition. The derivation is for a metal that hydrolyzes, $\mathrm{M(OH)}^{n^-}{}_{(z+n)}$, and a strong acid, HA. This approach can be readily extended to yield the general form for the ANC equation commonly used today. The solution charge balance gives

$$[\mathrm{H}^+] + z\left[\mathrm{M}^{z^+}\right] + (z-1)\left[\mathrm{M(OH)}^{(z-1)}\right] + \cdots + \left[\mathrm{M(OH)}^+{}_{(z-1)}\right] = [\mathrm{OH}^-] + n\left[\mathrm{M(OH)}^{n^-}{}_{(z+n)}\right] + \cdots + [\mathrm{A}^-] \tag{a}$$

where:

z	=	valence state of the metal M
n	=	species charge

From the ANC definition (ANC = concentration of the hydrogen ion acceptors minus the concentration of hydrogen ion donors; proton reference level = H_2O and M^{z^+}), we have

$$\mathrm{ANC} = [\mathrm{OH}^-] + \left[\mathrm{M(OH)}^{(z-1)^+}\right] + \cdots + (z-1)\left[\mathrm{M(OH)}^+{}_{(z-1)}\right] + z[\mathrm{M(OH)}_z] + \cdots + (z+n)\left[\mathrm{M(OH)}^{n^-}{}_{(z+n)}\right] + \cdots - [\mathrm{HA}] - [\mathrm{H}^+] \tag{b}$$

Solving the charge balance (Equation a) for $[OH^-]$-$[H^+]$ and substituting into the ANC definition (Equation b) yields

$$\mathrm{ANC} = -[\mathrm{HA}] - [\mathrm{A}^-] + z\left[\mathrm{M}^{z^+}\right] + (z-1)\left[\mathrm{M(OH)}^{(z-1)^+}\right] + \left[\mathrm{M(OH)}^{(z-1)^+}\right] + \cdots + \left[\mathrm{M(OH)}^+{}_{(z-1)}\right] + (z-1)\left[\mathrm{M(OH)}^+{}_{(z-1)}\right] + z[\mathrm{M(OH)}_z] + \cdots + (z+n)\left[\mathrm{M(OH)}^{n^-}{}_{(z+n)}\right] - n\left[\mathrm{M(OH)}^{n^-}{}_{(z+n)}\right] \tag{c}$$

Letting

$$\mathrm{M}_T = \left[\mathrm{M}^{z^+}\right] + \left[\mathrm{M(OH)}^{(z-1)^+}\right] + \cdots + \left[\mathrm{M(OH)}^+{}_{(n-1)}\right] + [\mathrm{M(OH)}_z] + \cdots + \left[\mathrm{M(OH)}^{n^-}{}_{(z+n)}\right] \tag{d}$$

and

$$\mathrm{A}_T = [\mathrm{HA}] + [\mathrm{A}^-] \tag{e}$$

Yields

$$\mathrm{ANC} = z \cdot \mathrm{M}_T - \mathrm{A}_T \tag{f}$$

Expansion to multiple acid and base systems yields

$$\mathrm{ANC} = \sum_{i=1}^{n} |z_i| \mathrm{M}_{T_i} - \sum_{j=1}^{\mathrm{m}} |z_j| \mathrm{A}_{T_j} = \sum C_B - \sum C_A \tag{g}$$

Differentially, $\Delta\mathrm{ANC} = \Delta \sum \mathrm{C_B} - \Delta \sum \mathrm{C_A}$

The ANC equation relates ANC to the difference between the sum of the base cation concentrations times their predominant charge at the equivalence point minus the sum of the strong acid anion concentrations times their predominant charge at the equivalence point. In most natural waters, these sums can be represented as

$$\sum_{i=1}^{n} |z_i|\, \mathrm{M}_{T_i} = \sum C_B = 2[\mathrm{Ca}_T] + 2[\mathrm{Mg}_T] + [\mathrm{Na}_T] + [\mathrm{K}_T] + [\mathrm{NH}_{4_T}] + 2[\mathrm{Al}_T] + 2[\mathrm{Mn}_T] + 2[\mathrm{Fe}_T] \tag{h}$$

and

$$\sum_{j=1}^{m} |z_j|\, \mathrm{A}_{T_j} = \sum C_A = 2[\mathrm{SO}_{4_T}] + [\mathrm{NO}_{3_T}] + [\mathrm{Cl}_T] + [\mathrm{F}_T] \tag{i}$$

Dissolved organic carbon (DOC) contains about 15 µeq of charge sites per mg DOC. About 4.5 to 5 µeq per mg L^{-1} DOC are strong sites (pK_a <v3). This 4.5 to 5 µeq per mg DOC should be added to $\sum C_A$ to accommodate waters with dissolved organic carbon (Munson and Gherini, 1993).

The classical means of representing ANC is as the sum of the hydrogen acceptors minus the hydrogen ion donors. ANC historically was called alkalinity and focused on the aqueous CO_2 system (Stumm and Morgan, 1981):

$$\mathrm{ANC} = [HCO_3^-] + 2[CO_3^{2-}] + [OH^-] + [\text{other hydrogen ion acceptors}] - [H^+],$$

where

ANC = strong acid neutralizing capacity, if positive, or strong base neutralizing capacity, if negative, in µeq L^{-1} and all species concentrations expressed in µeq L^{-1}

The mathematically equivalent method can be expressed as follows (See Sidebar 1):

$$\mathrm{ANC} = \Sigma C_B - \Sigma C_A$$

where

$\sum C_B$ = the sum of the base cation concentrations in µeq L^{-1}

$\sum C_A$ = the sum of the strong acid anion concentrations in µeq L^{-1}.

In long form,

$$\mathrm{ANC} = 2[Ca_T] + 2[Mg_T] + [K_T] + [Na_T] + [NH_{4T}] + 2[Al_T] + 2[Mn_T] + 2[Fe_T] - 2\,[SO_{4T}] - [NO_{3T}] - [Cl_T] - [F_T]$$

where

ANC = acid neutralizing capacity, µeq L^{-1}

[ ] = concentrations in µmoles L^{-1}, and

$_T$ = signifies analytical totals

The actual concentrations used are the analytical measurement results. For example, $[Ca_T]$ is the laboratory concentration for total calcium. This makes usage of this method relatively easy. In most cases, some minor term concentrations (e.g., $[Mn_T]$ or $[Fe_T]$), are very low, and are omitted.

The following alternative statement of ANC is commonly used, particularly in modeling, and in differential analyses:

In the differential mode the expression for ANC simply becomes:

$$\Delta ANC = \Delta\Sigma C_B - \Delta\Sigma C_A$$

where

ΔANC = change in ANC, μeq L^{-1}

$\Delta\Sigma C_B$ = change in the sum of the base cations, μeq L^{-1}

$\Delta\Sigma C_A$ = change in the sum of the strong acid anions, μeq L^{-1}

This is a convenient form. The effects of changes in ion concentrations on ANC can be readily determined. For example, adding one μeq of calcium ion to a liter solution will simply increase ANC by one μeq L^{-1}; adding one μeq of nitrate to a liter solution will decrease the ANC by one μeq L^{-1}.

Consideration of ANC as the "Ecological Indicator"

EPA's consideration of the use of ANC as the "ecological indicator" within the approach suggested for a future joint secondary NAAQS for NOx and SOx is based primarily on data collected from a select number of lakes in the Adirondacks shown in Figure 1. However, as recognized by EPA in its review documents (as illustrated in Figure 2), the toxicity of lakes has a causal relationship to pH and inorganic monomeric aluminum (Al_{im}) concentrations and that ANC per se does not cause adverse impacts to aquatic habitats.

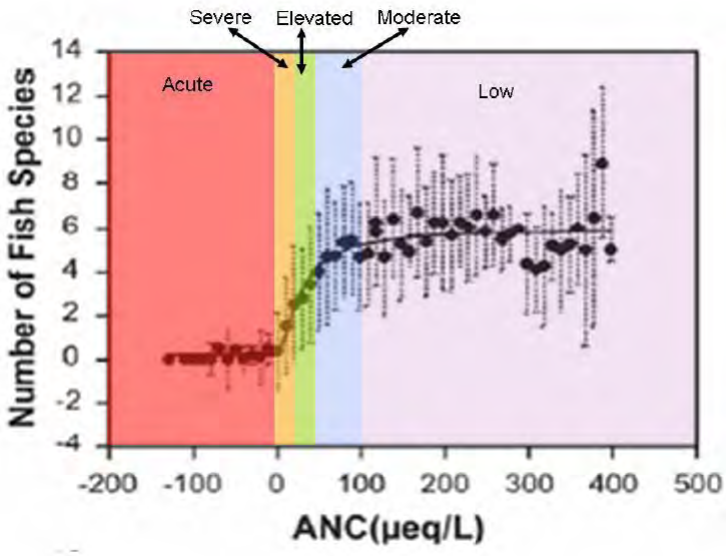

Figure 1: Relationship between ANC and number of fish species in the Adirondacks
Source: EPA PA (EPA, 2011 and references therein

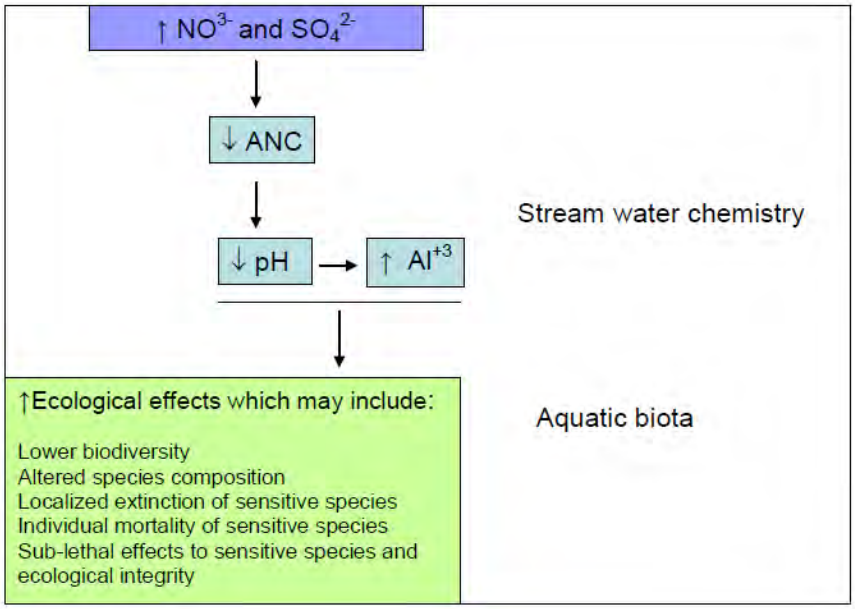

Figure 2: Relationship between ecological effects on aquatic biota and stream water chemistry
Source: EPA PA (EPA, 2011 and references therein

The bioavailability of aluminum is determined by the pH of the water. If (1) the relationship between ANC and pH were universal **AND** (2) aluminum in all waterbodies existed in equal concentrations, then ANC alone would be an appropriate indicator of aquatic acidification effects. However, neither of these

two conditions is true. In Figure 3, we show that the **relationship between ANC and pH is not universal**; whereas the figure from the EPA Policy Assessment on the left shows theoretical and measured curves of pH vs ANC for a solution of Gibbsite in equilibrium with ambient CO_2, the figure on the right shows data obtained from over 1400 waterbodies illustrating the deviation from this curve. This spread in the data reflects the broad distributions of dissolved organic carbon (DOC), dissolved CO_2 and dissolved aluminum in real waters.

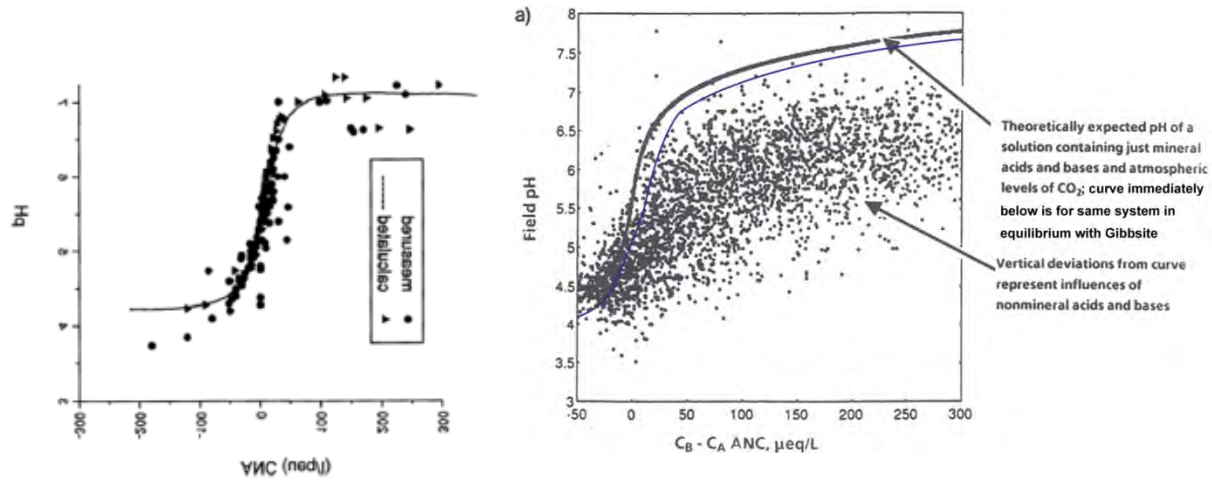

Figure 3: Relationship of ANC with pH; figure on left is flipped and rotated to match figure on right. Left Figure Source: EPA PA (EPA, 2011); Right Figure Source: Baker and Gherini, 1990

It is also important to note that the amount of aluminum in solution is paramount. In Figure 4, the relationship of fish species to pH is less sensitive in Florida than elsewhere (including the Adirondacks) as these waters are low in aluminum; although these waters are characterized by low ANC and low pH (and have low, not high, DOC), the scarcity of aluminum results in thriving fish habitats. Limiting the use of comparisons of number of species to a limited number of regions is problematic. As seen in Figure 4, the correlation of number of species is not universal even to pH, a more causal indicator of ecosystem viability. Due to the variability in the relationship between ANC and pH, relationship of ecosystem viability based on ANC would be more disparate. It is also important to note that other factors—such as temperature (particularly for shallow freezing lakes), precipitation, diet, and spawning habitat—can all impact the population and diversity of fish species in a waterbody.

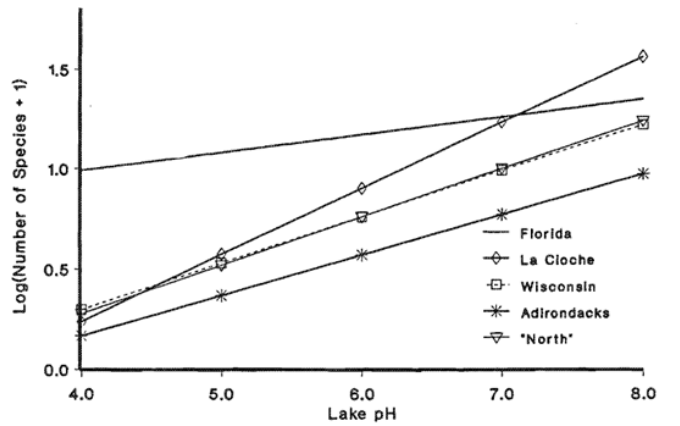

FIG. 1. Regression lines for number of fish species vs. pH for Florida, Wisconsin (Rahel 1982), La Cloche (Harvey 1975), Adirondack Mountain (Adirondack Lake Survey Corp. 1989) lakes, and the merged north-temperate data "North." All are significant ($P \leq 0.05$). F: $Y = 0.09$ (pH) + 0.63; $R^2 = 0.33$. C: $Y = 0.33$ (pH) − 1.08; $R^2 = 0.35$. W: $Y = 0.23$ (pH) − 0.62; $R^2 = 0.50$. NY: $Y = 0.20$ (pH) − 0.63; $R^2 = 0.43$. N: $Y = 0.24$ (pH) − 0.68; $R^2 = 0.38$.

Figure 4: Relationship between number of fish species and lake pH in different regions (Source: Keller and Crisman, 1990)

The relationship between ANC and pH and the levels of aluminum is also depicted in Figure 5, which reveals that in the Shenandoah National Park, aquatic habitats for *brook trout* are considered non-acidic starting at ANC values of 50 µeq L^{-1}. Similarly, Figure 6 shows that for populations of *blacknose dace*, the "Shenandoah National Park: Fish in Sensitive Habitats (FISH)" study found the highest fish density in streamwaters with ANC near 20 µeq L^{-1}.

Table 1. Brook trout stream categories, ANC classes, and ANC thresholds for brook trout responses to acidification in forested headwater catchments in western Virginia (Bulger et al. 1999).

Brook trout stream category	ANC class	ANC range (µequiv.·L^{-1})	Brook trout response
Suitable	Not acidic	>50	Reproducing brook trout populations expected where habitat suitable
Indeterminate	Indeterminate	20–50	Extremely sensitive to acidification; brook trout response variable
Marginal	Episodically acidic	0–20	Sublethal and (or) lethal effects on brook trout possible
Unsuitable	Chronically acidic	<0	Lethal effects on brook trout probable

Figure 5: Reproduction of Table 1 from Bulger et al., 2000 reflecting brook trout sensitivity to ANC in western Virginia

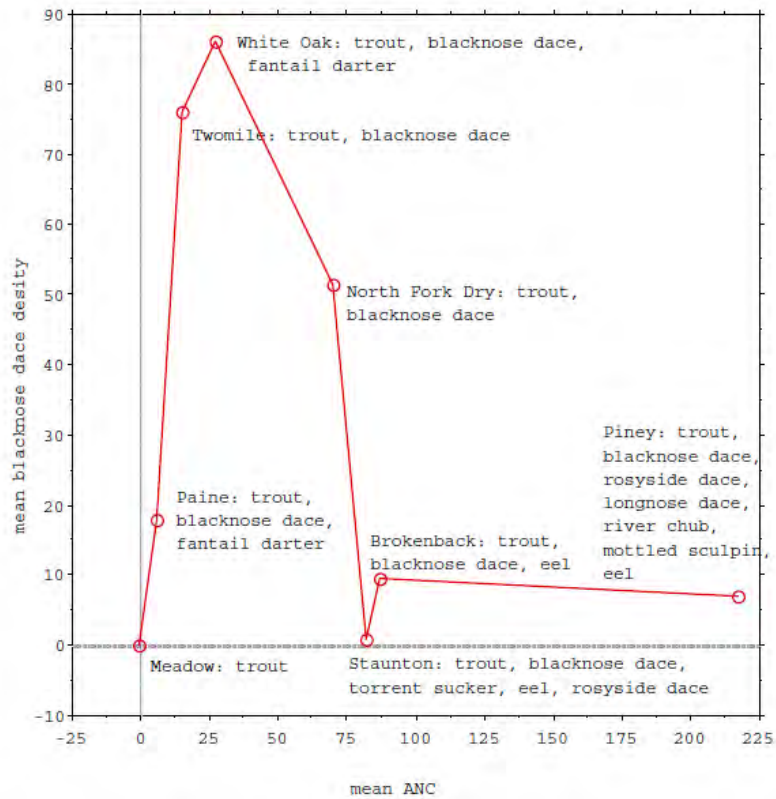

Figure E-4. Blacknose dace density (number of individuals per 100 m^2 of habitat) in the FISH project's three intensive and five extensive streams, versus mean ANC. Other fish species present in each stream are shown after the stream name on the graph.

Figure 6: Reproduction of Figure E-4 from Bulger et al., 1996 reflecting blacknose dace density observed in the FISH project

In summary, EPA suggests the use an ecological indicator, ANC, on the basis that ANC is more amenable to implementing within a standard—due to the mass conservative aspects of the variable—and not on its adequacy as a universal indicator of aquatic ecosystem viability and health. Simply stated, ANC alone is inappropriate. With appropriate information, the relationships between ANC, pH and [Ali_m] can be calculated for waterbodies and the influence of SOx, NOy and NHx deposition on these variables can be determined.

The argument that mass conservation is critical to a standard is not scientific and conflicts with the nature of existing standards. The fact that ANC maintains mass balance is a property of the parameter, not a scientific requirement for an indicator. For example, ozone (O3) is formed through highly non-linear reactions of ambient VOC and NOx, as well as O_2 and H_2O as reactants, and does not have a mass-balance relationship with the emissions of its controlled precursors (VOC and NOx). Further examples of non-mass-conservative standards are temperature-based discharge standards to protect aquatic habitats. Ultimately, one should target the indicator(s) most closely related to the causative agent(s).

The Regionalization Scheme Proposed by EPA Has Not Been Thoroughly Evaluated and Data Representativeness Has Not Been Explored

EPA's Final Policy Assessment (PA) document (EPA, 2011) recognizes that while air quality standards are national in scope, the effects of SOx and NOy deposition are not the same in different areas of the country. The EPA also acknowledged that there may be lands used for commercial agriculture and forestry that are likely to be impacted adversely by the current atmospheric deposition levels. The proposed approach for a future standard is intended to account for different sensitivity to acid deposition by protecting sensitive areas, expected to be "relatively pristine and wild and generally in rural areas, and the services provided by such sensitive ecosystems, without requiring more protection than is needed elsewhere" (EPA, 2011). The approach of EPA is to protect sensitive populations of water bodies, rather than individual water bodies.

In the PA document, EPA considered using one region for the entire continental US or multiple ecoregions based on three different classification systems: (1) the Omernik ecoregion classification system (Omernik, 1987), (2) the National Ecological Observatory Network (NEON) domain system (Hargrove and Hoffman, 1999, 2004, 2009; Schimel et al., 2009), and (3) the Bailey ecoregion classification system developed for the US Forest Service (USFS) (Bailey et al, 1994; Bailey, 1995, 1998, 2004). Use of one ecoregion was dropped because it would not consider the variability in atmospheric and ecological factors that are important to development of the aquatic acidification index (AAI). The EPA selected Omernik's Level III ecoregion map for use in developing the proposed secondary standard for SOx and NOy.

The EPA's stated reasons for using the Level III map were that it is widely used, well-documented, and that the basis for the map is understood. The EPA did not consider whether there were any advantages in using the two alternative systems considered, Bailey's system for the USFS or NEON. EPA's other reasons for deciding not to use Bailey's USFS system or NEON were that neither of these systems had undergone a comparable peer review to that of Omernik's system and that the NEON system is still under development. However, EPA failed to evaluate whether the Omernik classification system *per se* was inherently appropriate for the stated purpose of supporting an acidification-based national standard. The following section describes the Omernik ecoregion classification system and tests its adequacy as a proper method for defining different regions as part of potential future multimedia-based NAAQS.

Omernik Ecoregion Classification System

There are four levels of detail for the ecoregion maps that are derived from Omernik's original ecoregions map from 1987 (Omernik, 1987); maps at all levels are available from a US EPA Website (*http://www.epa.gov/wed/pages/ecoregions.htm*). The Level I, II, and III maps have been completed (EPA, 2010). The Level IV map is currently being developed by the National Interagency Technical Team (NITT), which is comprised of 8 representatives of federal agencies including the National Health and Environmental Effects Laboratory of US EPA, Natural Resources Conservation Service, Forest Service, Agricultural Research Service, Bureau of Land Management, National Park Service, US Fish and Wildlife Service, and the US Geological Survey. The Level I map has 15 regions in the US, but encompasses all of

North America. The names and defined areas of the regions indicate that climate and vegetation were the primary factors, and explain why nearly the entire eastern half of the US was assigned to one region. The Level II map has 52 ecoregions in the continental US. The most recent version of the Level III map has 85 ecoregions in the continental US (Figure 7). A larger version of the Level III map with labels for each ecoregion is included in Appendix B. The Level IV map uses the Level III ecoregions, and then subdivides them into smaller divisions. The Level IV map is complete, except for California and Arizona, where initial divisions have been made, but they have not been approved.

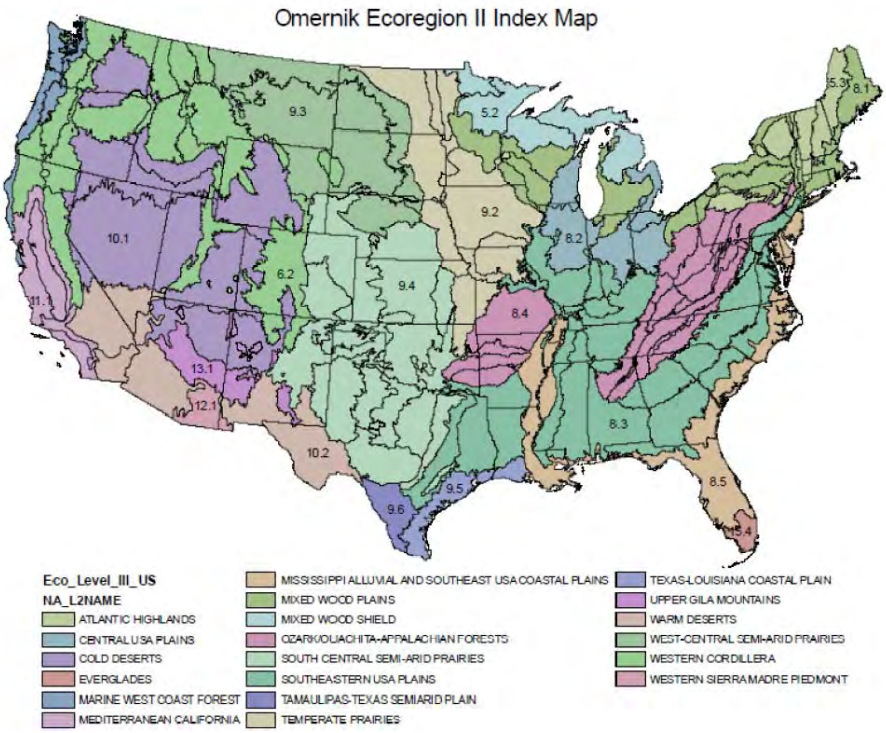

Figure 7: Ecoregion Map showing Level II Index Map with Level III Subdivisions (EPA, 2007)

The basis for Omernik's first effort at defining ecoregions was based on alkalinity, "driving" factors considered to influence alkalinity (geology, soils, land surface form, and climate), and "integrating" factors thought to reflect combinations of driving factors (land use and potential natural vegetation (Omernik and Powers, 1983). The resulting map is presented in Omernik (1987a) and described further in Omernik (1987b). Omernik and Griffith (1986) also developed a map using alkalinity for the upper Midwest to classify sensitivity to acidic inputs. For the upper Midwest map, comparisons were made between alkalinity of surface waters and other characteristics including land use, geology, and physiography. The conclusions from this effort were that alkalinity is influenced by a "complex set of factors" and that the relative influence of a given factor varied from one place to another. Part of the original reason for moving away from classification based on hydrologic units or watershed boundaries was that in the dry western states and glaciated areas of the upper Midwest, defining watersheds based on topographic boundaries was difficult and in some areas did not represent the contributing zones of groundwater recharge to a surface waterbody (Omernik and Bailey, 1997).

The later refinements of Omernik's 1987 ecoregion map considered geology, physiology, vegetation, climate, soils, land use, wildlife, and hydrology and were intended to integrate the various factors, rather than being based primarily on maps of single factors. The developers recognized that the relative importance of a given factor would vary from one ecoregion to another. The intent of the ecoregion concept is to improve ecosystem management across agencies that emphasize different resources (Bryce et al, 1999). However, other key factors such as soil depth were not used, which in an important influence on hydrologic flowpaths in drainage basins and consequent water chemistry as discussed subsequently.

Examples of Ecoregions and Comparison to Underlying Factors

One feature of using the Level III map is that some ecoregions are comprised of non-contiguous areas. Examples are the Adirondacks, which is combined with the inland part of New England and the Catskills, as shown in Figure 8 for the Northeastern Highlands (Ecoregion 5.3.1). Because of the much greater number of waterbodies with data for the Adirondacks than the other areas, the critical load selected at a given percentile for this ecoregion is dominated by the Adirondacks data set. In fact, 65 percent of the lakes with sufficient data to estimate critical loads for this ecoregion were from the Adirondacks, a known acid-sensitive area. Another example of combining areas with different characteristics is the Southeastern Plains (Ecoregion 8.3.5), where one ecoregion extends from South Carolina north through the southern half of New Jersey. This Level III ecoregion is part of the Level II Ecoregion 8.3, which is identified in Figure 3-1 of this section.

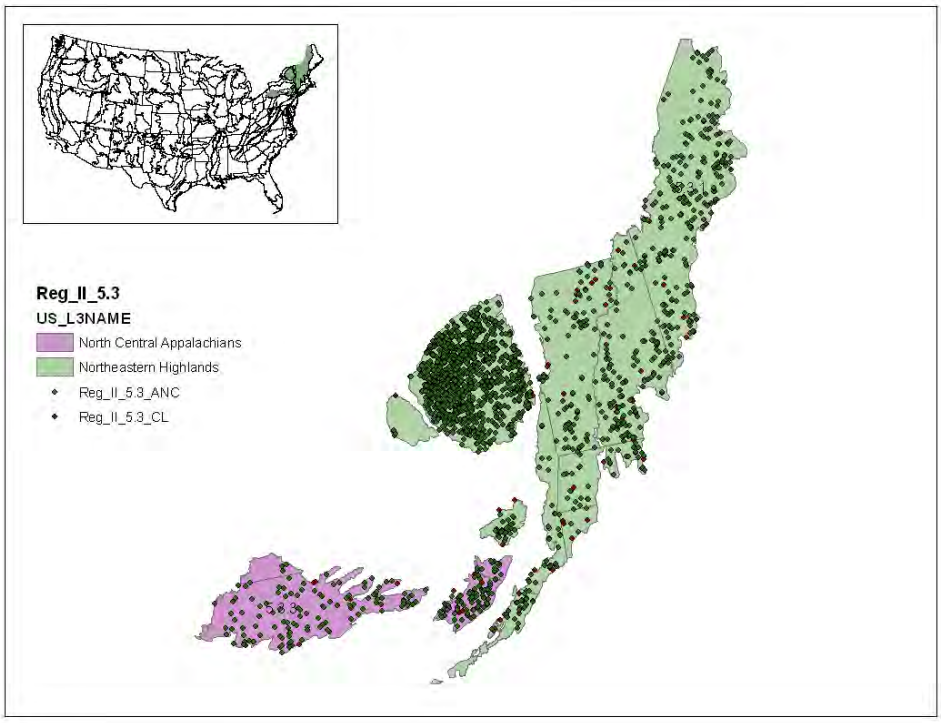

Figure 8: Map showing Level III Ecoregion 5.3.1 Northeastern Highlands, Consisting of the Adirondacks, the Higher Elevation Catskills, and Part of New England and Ecoregion 5.3.3 North Central Appalachians, consisting of the lower elevation Catskills and nearby

In some cases, the ecoregions are small and appear to be defined primarily by vegetation as it changes with elevation, particularly in the southern Appalachian area, which has been divided into a series of small ecoregions (Figure 9). Differences in data availability are also apparent in this area. The Shenandoah National Park area has been widely studied, while the western parts of the individual ecoregions have much less data.

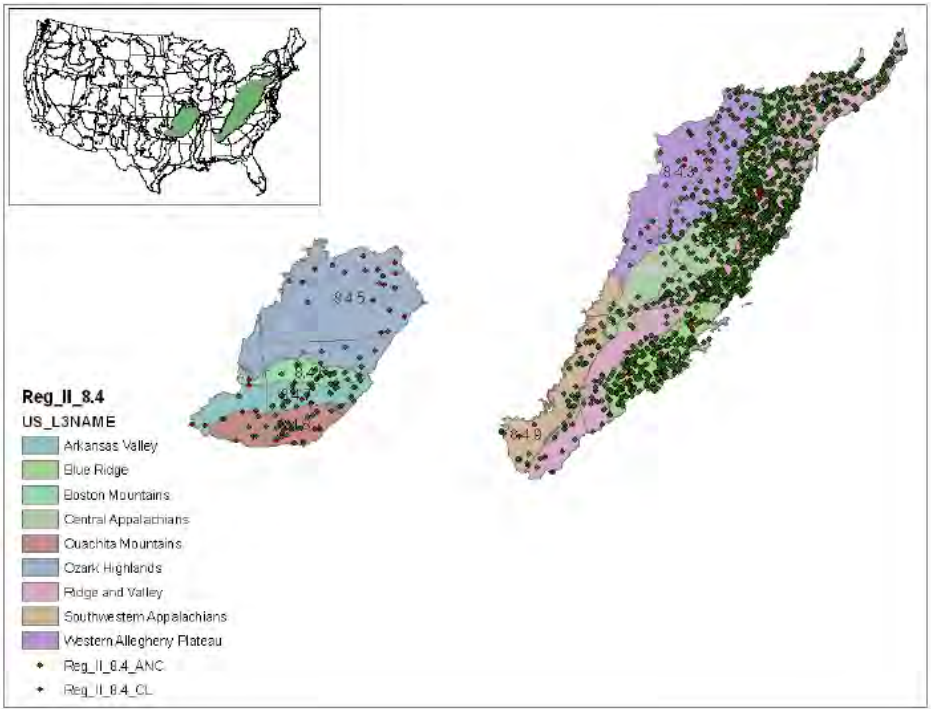

Figure 9: Map of Ecoregions in Level II Region 8.4, Ozark/Ouachita-Appalachian Forests, which Includes the Well-studied Level III Ecoregions of the Blue Ridge (8.4.4) and the Ridge and Valley (8.4.1)

Two examples of comparing ecoregions and the primary factors used to define them were reviewed. One example is for New England and eastern Canada (Dupont et al, 2005) and the other is for the southern Appalachian Mountains (Sullivan et al, 2007a). The study in New England used the SSWC model to compute critical loads of sulfate and nitrate deposition in surface waters (Figure 10, top). This was one of the models used by EPA for development of the proposed approach for a future secondary standard. The bedrock map included in the Dupont study used four bedrock categories (Figure 10, bottom), as listed below and assigned sensitivity to acid precipitation to each category:

1. Limestone – very low
2. Sedimentary rocks - low
3. Volcanic and old meta-sedimentary rocks - medium
4. Plutonic and igneous rocks – high.

Most of New England was classified as having sedimentary rocks, and hence was considered to have low sensitivity to acid precipitation. *The map (Figure 10, bottom) showed that nearly all of the areas assigned to the category "low sensitivity to acid precipitation" based on bedrock type had waterbodies rated as "very low sensitivity" based on critical load, defined as greater than 100 meq m^{-2} y^{-1}*. In contrast,

the EPA identified the entire region of New England as sensitive based on both ANC and critical loads, discussed later in this section.

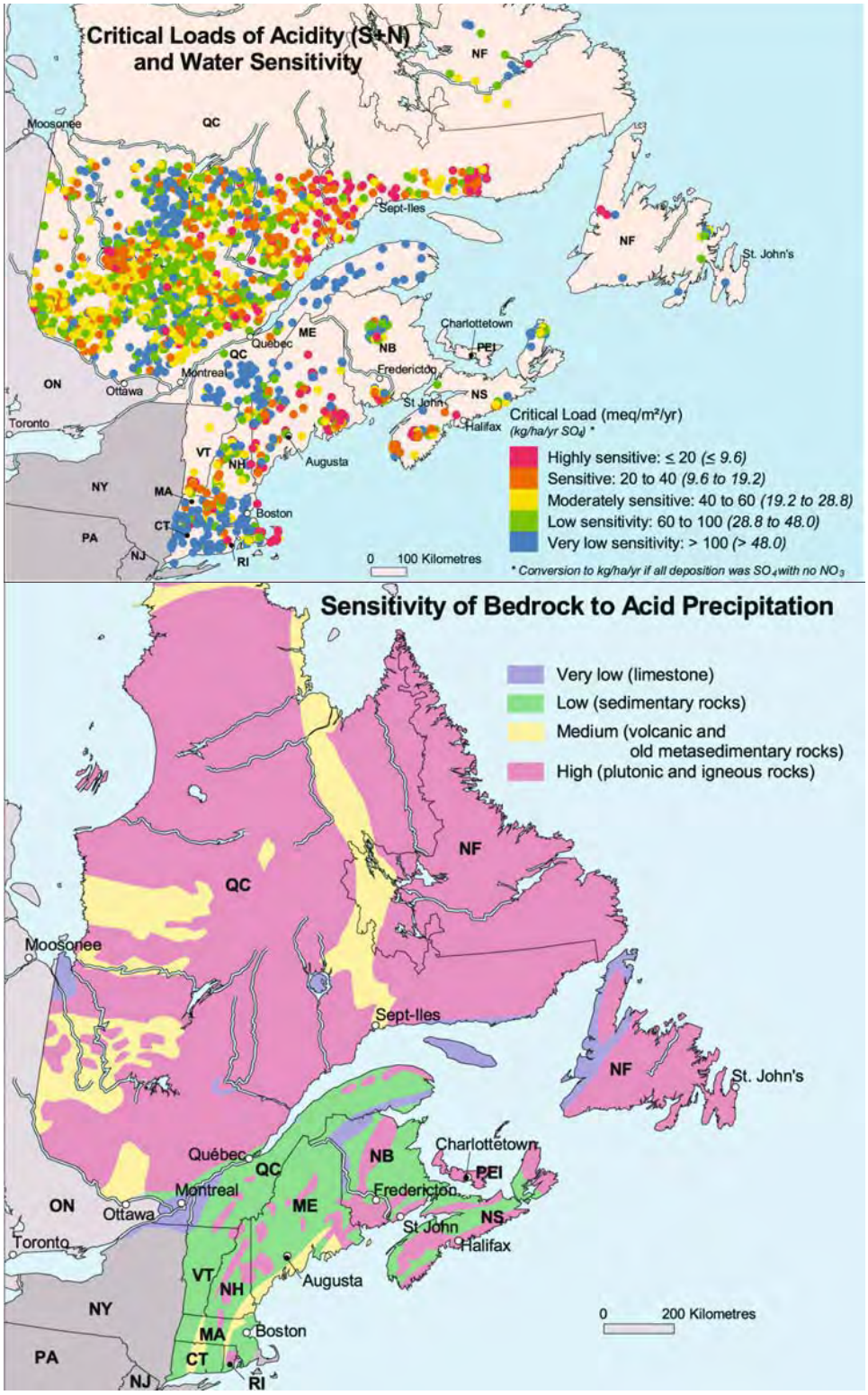

Figure 10: Comparison of (top) Critical Load Estimates and (bottom) Bedrock Types in New England and Eastern Canada (Dupont et al, 2005)

In the Southern Appalachian Mountains, a comparison was made between ANC in streams and other factors, which included bedrock lithology, elevation, watershed area, watershed relief, forest vegetation type, soil type, and ecoregion. Bedrock was divided into five types as follows:

1. Siliceous – sandstone, quartzite
2. Argillaceous – shale, siltstone
3. Felsic – granite, gneiss
4. Mafic – basalt, anorthosite
5. Carbonate – limestone, dolomite.

While the general propensity to weather follows this order, from least likely to weather at the top (siliceous) to most likely to weather near the bottom (mafic and carbonate), a classification solely based on lithology does not consider other factors that influence weathering such as grain size, degree of fracturing, or hydrologic flow paths. The evaluation system based on lithology and landscape could distinguish between ANC greater than or equal to 50 µeq L^{-1}, but was not a good predictor of stream ANC (Sullivan et al, 2007). A further factor, elevation, was then used to improve the acid sensitivity classification system based on ANC < 0 µeq L^{-1} or ANC between 0-20 µeq L^{-1}. Using elevation can be a proxy for quantity of precipitation. The classification system showed a scattering of low ANC streams. The evaluation by Sullivan indicated that the addition of vegetation-related factors were not necessary to achieve an initial acid sensitivity classification system. This finding is in contrast to the Level III ecoregion system used by EPA, which is based primarily on climate and vegetation related factors and does not include specific water quality parameters.

EPA's Classification of Ecoregions by Acid Sensitivity

The EPA classified the Level III ecoregions into those considered acid-sensitive and non-acid-sensitive. The acid-sensitive ecoregions were identified as ecoregions that have greater than 5 percent of waterbodies with ANC less than 200 µeq L^{-1} and greater than 1 percent of waterbodies with ANC values less than 100 µeq L^{-1}. This step resulted in 29 ecoregions being selected as acid-sensitive. Ecoregions that met the above two criteria, but had less than 20 waterbodies with ANC data were classified as "likely sensitive", as shown in the top map of Figure 11. The areas classified as acid-sensitive based on the above definition are overly broad and expand the extent of acid-sensitive regions partly by linking areas with ANC less than 100 µeq L^{-1}. The increased size of the acid-sensitive ecoregions can be seen by comparing the lower map on Figure 11 to Figure 12, which shows ANC in waterbodies and labels those with ANC greater than 100 µeq L^{-1} as "Low Acidification".

Another finding from reviewing these maps is that in much of the country there are minimal to no ANC data, and that previous investigations have targeted known acid-sensitive areas. Twelve non-acid-sensitive ecoregions had data for less than ten water bodies in the ecoregion. As seen in Figure 11, non-acid-sensitive regions cover large parts of the Midwest and West. Several ecoregions had even fewer waterbodies with sufficient data to estimate critical loads.

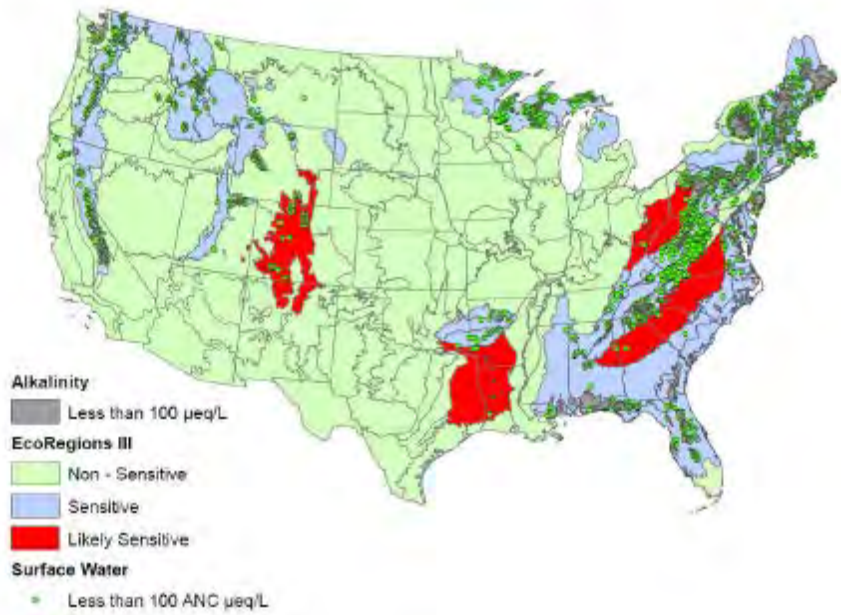

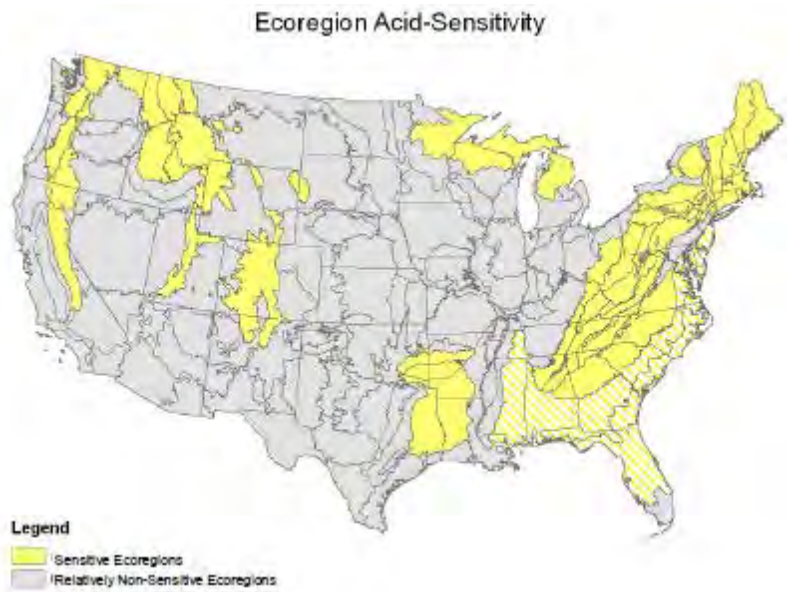

Figure 11: EPA's Classification of Acid-sensitivity using ANC Data (EPA, 2011). Note: In the top figure, the "green" areas are waterbodies with ANC <100 ueq L^{-1}, while the larger "blue" areas are the ecoregions considered sensitive by EPA. The "red" areas are ecoregions with less than 20 waterbodies with ANC data. In the bottom figure, the cross-hatched ecoregions are low elevation coastal plains with (in some locations) DOC levels above 5 mg L^{-1} and low base cation supply, where low ANC was not considered to be due to acid deposition, and thus these ecoregions were classified by EPA as non-acid-sensitive.

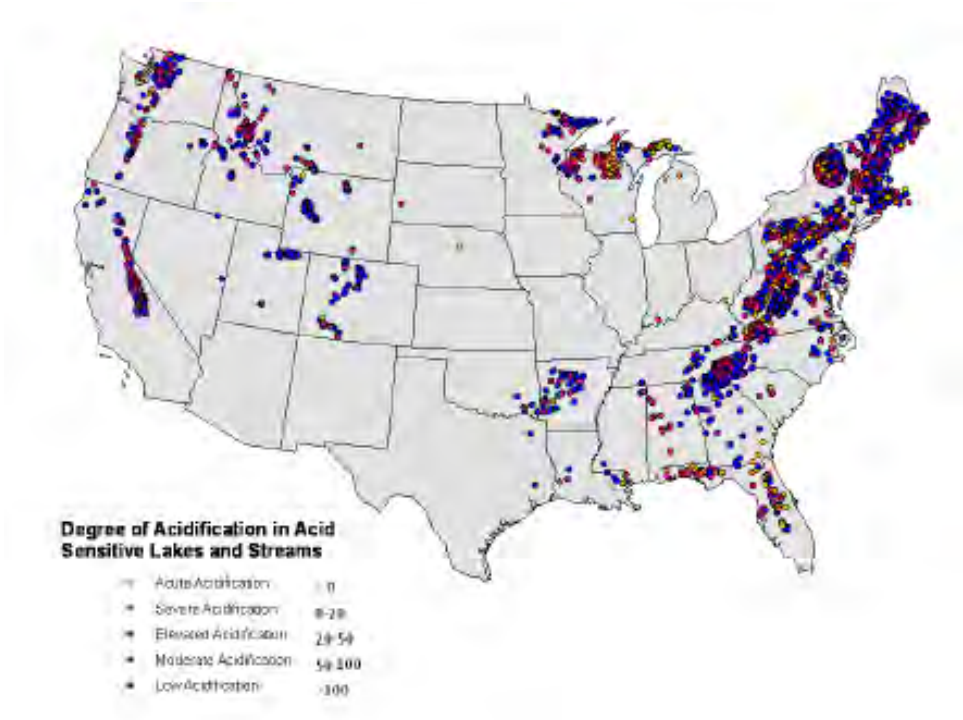

Figure 12: Map Showing ANC Data (EPA, 2011).

Table 1 summarizes the number of waterbodies in each EPA-designated acid-sensitive ecoregion and the range of ANC, pH, SO_4 and DOC for each ecoregion. The number of waterbodies per acid-sensitive ecoregion with ANC data ranged from a minimum of 24 in Ecoregion 8.4.6 (Boston Mountains in part of Arkansas and eastern Oklahoma) to a maximum of 2,414 in 5.3.1 (Northern Appalachians and Atlantic Maritime Highlands, which includes the Adirondacks and the non-coastal regions of New England). Seven ecoregions had a total of 50 or less waterbodies with ANC data. While these ecoregions were classified as acid-sensitive, partly because larger areas have been combined into one ecoregion, not all the waterbodies in a given ecoregion are actually acid-sensitive. For example, there were five acid-sensitive ecoregions where the minimum measured pH was greater than 6. Eleven of the ecoregions did not have minimum pH values less than 5.45. The minimum ANC in these ecoregions ranged from 6.0 to 44.4 µeq L^{-1} and three of these five ecoregions had minimum ANC values greater than 20 µeq L^{-1}. In some cases, the lowest ANC values represented older data from 1985–1987, and in some ecoregions there was only one ANC less than 0 from the older data. The data used for a given ecoregion often spanned multiple years with no screen for "older" data. The maximum ANC values in all ecoregions ranged from 802.6 to 9,273.8 µeq L^{-1} and the maximum pH values ranged from 7.2 to 9.8; such values are clearly not indicative of acid-sensitive waterbodies.

In addition to inclusion of non-acidic waterbodies, there are other concerns with the data used in the EPA analyses, particularly for DOC and SO_4. The maximum DOC concentration is above 10 mg L^{-1} for 20 of the 29 ecoregions, and six ecoregions had maximum DOC concentrations above 30 mg L^{-1}. High DOC occurs in the coastal plain regions (e.g., 171 mg L^{-1} in ecoregion 8.5.3 Southern Coastal Plain), as might be expected due to swamps and wetlands, but inland areas also have elevated DOC maximum

concentrations such as in the North Appalachians & Atlantic Maritime Highlands and Middle Rockies. The plan in the Second PA Document was to exclude waterbodies with DOC above 10 mg L^{-1}, since elevated DOC can mitigate aluminum toxicity by forming Al-organic complexes. The form of concern to fish is inorganic monomeric aluminum. However, this method was not used in the analyses for the Final PA Document.

The plan in the Second PA Document was also to exclude waterbodies with SO_4 above 400 mg L^{-1}. As with DOC, this method was not used in the analyses for the Final PA Document. Maximum sulfate concentrations were quite high in many of the ecoregions. The maximum SO_4 concentrations ranged from 165.9 to 44,590 µeq L^{-1}; eight ecoregions had maximum values over 10,000 µeq L^{-1}. Waterbodies with high SO_4 concentrations, particularly in the Appalachians and Midwest could be influenced by other factors such as acid-mine drainage or other anthropogenic discharges. In addition, there are additional sources of geologic sulfate in soils such as the by-products of pyrite oxidation, natural gypsum sources, and evaporite deposits (Mayer et al, 2009). The EPA considered that all sulfate was derived from atmospheric deposition, but this is not always the case. SO_4 concentrations are used in the critical load calculations. The critical load values are then used in the calculation of AAI. The next step would be to select a given percentile of the AAI distribution from 70 to 90 percent for acid-sensitive ecoregions. Thus, atypical values that influence the AAI could affect the selected value from the distribution. Another concern with sulfate is that the method for estimating BC_0 does not consider sulfate adsorption by old, highly weathered soils, except for the streams in the Shenandoah area where the MAGIC model was used. Such soils are present in part of the nearby ecoregions of the southern Appalachian Mountains. The sulfate adsorption process was acknowledged by EPA for the regions south of the glaciated areas based on work by Rochelle and Church, 1987 and Rochelle et al, 1987. However, the EPA stated that the process is potentially reversible, and hence could contribute to acidification if the sulfate was released in the soil solution. The time required for this to occur in the soils in the southeast was not addressed.

Table 1: Key Water Chemistry Parameters in EPA-designated Acid-sensitive Ecoregions

Ecoregion	Name	Count	ANC, $\mu eq\ L^{-1}$		pH		SO_4, $\mu eq\ L^{-1}$		DOC, $mg\ L^{-1}$	
			Min	Max	Min	Max	Min	Max	Min	Max
5.2.1	N Lakes & Forests	740	-51	5287	4.4	8.7	2	2039	0	29
5.3.1	N Appalachians & Atlantic Maritime Highlands	2414	-134	1544	3.8	9.4	2	473	0	35
5.3.3	N Central Appalachians	234	-1162	2079	3.6	8.2	30	5845	0	16
6.2.3	Columbia Mts/N Rockies	78	23	3788	6.2	8.8	1	488	0	10
6.2.4	Canadian Rockies	29	21	3932	6.6	8.6	6	187	0	4
6.2.5	N Cascades	145	15	5845	5.8	9.6	1	362	0	10
6.2.7	Cascades	111	3	803	6.0	8.0	0	222	0	7
6.2.10	Middle Rockies	249	-24	9274	4.8	9.5	5	34089	0	74
6.2.12	Sierra Nevada	156	13	2095	5.8	8.9	0	166	0	11
6.2.13	Wasatch & Uinta Mountains	27	44	1206	6.6	9.6	9	2360	0	15
6.2.14	S Rockies	238	6	9199	6.0	9.8	3	14120	0	19
6.2.15	Idaho Batholith	115	19	2504	6.3	8.7	3	361	0	10
8.1.3	N Appalachians Plateau & Uplands	131	-104	2736	4.0	9.1	72	2088	1	20
8.1.7	NE Coastal Zone	204	-61	2113	4.2	9.1	41	880	1	22
8.1.8	Maine/New Brunswick Plains & Hills	250	-63	2000	4.3	9.3	11	544	0	20
8.3.4	Piedmont	260	47	2132	5.5	8.6	8	1475	0	10
8.3.5*	SE Plains	182	-46	3831	4.5	7.9	1	5234	0	33
8.3.7	S Central Plains	59	29	6443	5.4	8.0	3	728	0	28
8.5.1*	Middle Atlantic Coastal Plain	50	-63	1754	4.6	7.9	15	1810	1	31
8.5.3*	Southern Coastal Plain	201	-645	3702	3.4	9.0	1	44591	0	171
8.5.4*	Atlantic Coastal Pine Barrens	86	-442	1779	3.5	8.3	48	30238	0	32
8.4.1	Ridge and Valley	738	-352	6432	4.4	8.9	14	11578	0	8
8.4.2	Central Appalachians	300	-2120	3970	2.9	8.6	65	33786	0	9
8.4.3	Western Allegheny Plateau	112	-213	4575	4.0	8.9	144	28569	1	8
8.4.4	Blue Ridge	517	-15	1882	5.9	8.9	6	829	0	15
8.4.6	Boston Mountains	24	54	1356	5.8	7.2	39	224	0	5
8.4.7	Arkansas Valley	41	65	5588	5.5	7.6	46	802	0	12
8.4.8	Ouachita Mountains	44	-156	1675	3.9	8.2	32	382	0	5
8.4.9	SW Appalachians	49	-319	4982	3.7	8.0	40	26302	0	12
Data obtained from US EPA supplied file name: ANC.csv.										
* These four ecoregions have low ANC waterbodies, but EPA considered that this was not due to acid deposition.										

Representativeness

Lakes in Ecoregion 5.3.1

Using the National Hydrologic GIS Database, the numbers of lakes, reservoirs, and marshes with surface areas greater than one acre (1 acre = 0.004 km^2 = 0.4 ha) were quantified for Ecoregion 5.3.1. The intent is to compare the number of waterbodies sampled and used by EPA to the total number present in the ecoregion. The total number of waterbodies in Ecoregion 5.3.1 is 9,938, of which most were lakes. The breakdown by waterbody type by numbers of waterbodies and total surface area is shown below in Table 2:

Table 2: Distribution of Waterbody Types in Ecoregion 5.3.1 (Northeastern Highlands)

Ecoregion 5.3.1 Northeastern Highlands		
Waterbody Type	**Count**	**Total Area, km^2**
Lake	8447	4341.7
Reservoir	15	0.6
Marsh	1476	1178.5
Total	9938	5520.8

A more detailed breakdown by lake area is shown in Table 3.

Table 3: Number of Lakes in Ecoregion 5.3.1 and Sampled Data Sets

Area Category km^2	**All Lakes in Ecoregion**		**ADR Data Sets***				**All TIME Lakes**	
			LTM Lakes		**TIME Lakes**			
≥ 100	5	0.1%	0	0%	0	0%	0	0%
[50, 100)	5	0.1%	0	0%	0	0%	0	0%
[10, 50)	53	0.6%	0	0%	5	4.4%	14	4.6%
[5, 10)	66	0.8%	1	2%	5	4.4%	19	6.3%
[1, 5)	379	4.5%	3	6%	19	16.7%	48	15.8%
[0.1, 1)	2,305	27.3%	26	52%	51	44.7%	149	49.0%
[0.01, 0.1)	5,369	63.6%	20	40%	34	29.8%	73	24.0%
[0.004, 0.01)	265	3.1%	0	0%	0	0%	1	0.3%
Total Number of Lakes	8,447	100%	50	100%	114	100%	304	100%
Total Area, km^2	4,342		20.2		0.70		542.30	

*ADR is Adirondacks area. (1 acre = 0.004 km2 = 0.4 ha; 1 km^2 = 100 ha = 247.1 acre)

Most of the lakes sampled were between 0.01 km^2 (0.1 ha, 2.47 acre) and 1 km^2 (100 ha, 247 acre) for all three data sets. A comparison of average ANC in lakes based on number and lake area is shown in Table 4 for the LTM and TIME lakes in the Adirondacks and all TIME lakes in the ecoregion.

Table 4: Comparison of ANC in Lakes in Ecoregion 5.3.1 by Number of Lakes and Lake Area

	LTM-ADR Lakes				TIME Lakes			
ANC Range ($\mu eq\ L^{-1}$)	**Number**		**Area (km^2)**		**Number**		**Area (km^2)**	
≥ 50	13	26%	3.6	17.8%	239	79%	508	93.8%
[20, 50)	10	20%	3.9	19.3%	34	11%	23	4.2%
[0, 20)	16	32%	11.6	57.4%	19	6%	9	1.7%
< 0	11	22%	1.1	5.5%	12	4%	2	0.3%
Total	50	100%	20.2	100.0%	304	100%	542	100.0%

In both data sets, the lakes with depleted ANC (<0 $\mu eq\ L^{-1}$) were a smaller percent of the total based on lake size (total surface area) than based on number. The difference between using number or size was greater for the lakes outside the Adirondacks, because the proportion of large, less sensitive lakes sampled was larger. For the Adirondacks, lakes with ANC <0 $\mu eq\ L^{-1}$ represented about 20% of the lakes based on number, but about 5% based on total lake area. In the other parts of Ecoregion 5.3.1, lakes with ANC <0 $\mu eq\ L^{-1}$ represented about 4% of the lakes based on number, but about 0.3% based on total lake area.

Another way to review the data sets used by EPA was to determine how many lakes had ANC data and how many had sufficient data to estimate critical loads. In Ecoregion 5.3.1, there were

- 8447 total lakes greater than one acre in area,
- 2414 lakes with ANC data, but only
- 448 lakes had enough information to estimate critical loads.

The number of lakes with enough data to calculate critical loads, shown in Figure 13, represents roughly 5% (448/8447) of the total lakes in the ecoregion. In addition, of the lakes with enough data to calculate critical loads, over one third (158 of 448 lakes, or 35%) were in the Adirondacks. This is of particular concern given recent results evaluating the extent to which well-studied lakes in the Adirondacks are representative of the Adirondacks region, let alone Ecoregion 5.3.1 as a whole. As stated by Sullivan et al., 2007b:

> *Based on modeling results reported here for the lakes that were studied, ALTM [Adirondacks Long-Term Monitoring] and AEAP [Adirondack Effects Assessment Program] modeling results appear to be well-distributed across a gradient of highly acid-sensitive conditions.* ***They are not, however, representative of the overall population of Adirondack lakes, or even the subset of Adirondack lakes that includes those having ANC ≤ 200 $\mu eq\ L^{-1}$ [emphasis added].*** *In particular, the ALTM and AEAP monitoring lakes having the longest records of monitoring data represent a group of lakes that largely receive high S deposition and exhibit a high degree of sensitivity to chemical change in response to acidic deposition.*

The representativeness of waterbodies used to calculate critical loads is important because, under EPA's proposed future approach for the Secondary NAAQS for NOx and SOx, the EPA Administrator will select a given percentile from the critical load distribution (ranging from the 70th to 90th percentile) as one of the key inputs to compute the AAI for the entire ecoregion. (See AAI equation and CL equation shown in the Introduction to this Appendix.) For the designated non-sensitive ecoregions, EPA proposes to select the 50th percentile of the critical load distribution to compute the AAI value. The distribution of the estimated critical loads in Ecoregion 5.3.1 is shown in Table 5.

Table 5: Distribution of Critical Loads in Ecoregion 5.3.1

Critical Load Category meq km^2 y^{-1}	**Number**	**Percent**
≤ 0	12	3%
(0, 20]	27	6%
(20, 50]	75	17%
(50, 75]	56	13%
(75, 100]	55	12%
> 100	223	50%
Total	448	100%

The above distribution shows that low critical loads (CL ≤ 50 meq m^{-2} y^{-1}) were estimated for about 25% of the lakes, and about 3% of the lakes had essentially no allowable load, which would imply that those lakes cannot be brought to the target ANC based on limiting atmospheric deposition alone. On the upper end, the critical loads were high (>100 meq m^{-2} y^{-1}) for about 50 percent of the lakes, even in this EPA designated acid-sensitive region which is highly influenced by a large number of non-representative data from the Adirondacks.

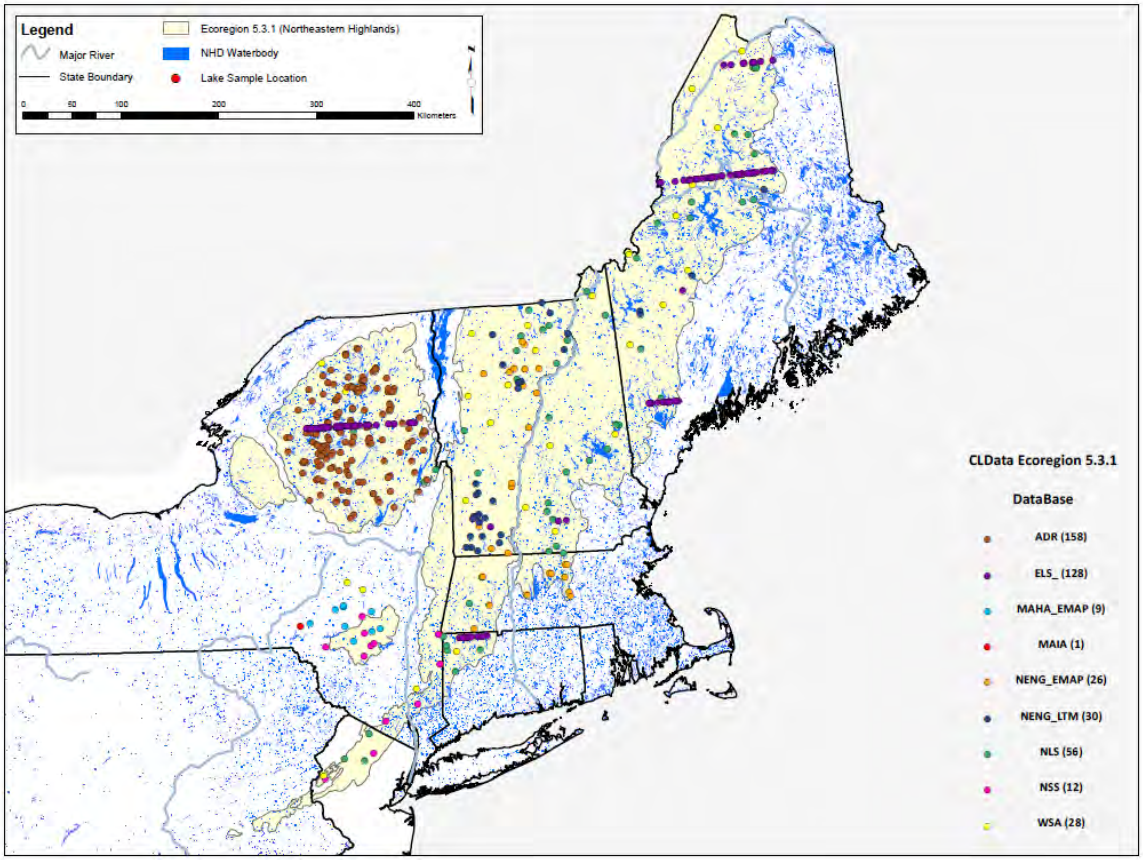

Figure 13: Lakes with Critical Load Values in Ecoregion 5.3.1. Note: Blue areas are individual lakes or streams from the National Hydrologic Database (NHD). The colored dots are the sampled waterbodies with sufficient data to estimate critical loads.

Streams in Southern Appalachian Mountains

The Southern Appalachian Mountains Investigation area (SAMI) is not placed in one ecoregion, rather it is divided into three regions, which also extend further south and sometimes north of the areas in Virginia considered to be acid-sensitive. The three ecoregions are Ecoregion 8.4.1 Ridge and Valley, and Ecoregion 8.4.2 Central Appalachians, and 8.4.4 Blue Ridge. Figure 14 shows the location of the three regions in this area. Maps for each of the four ecoregions showing the specific data sets used by EPA are included in Appendix B.

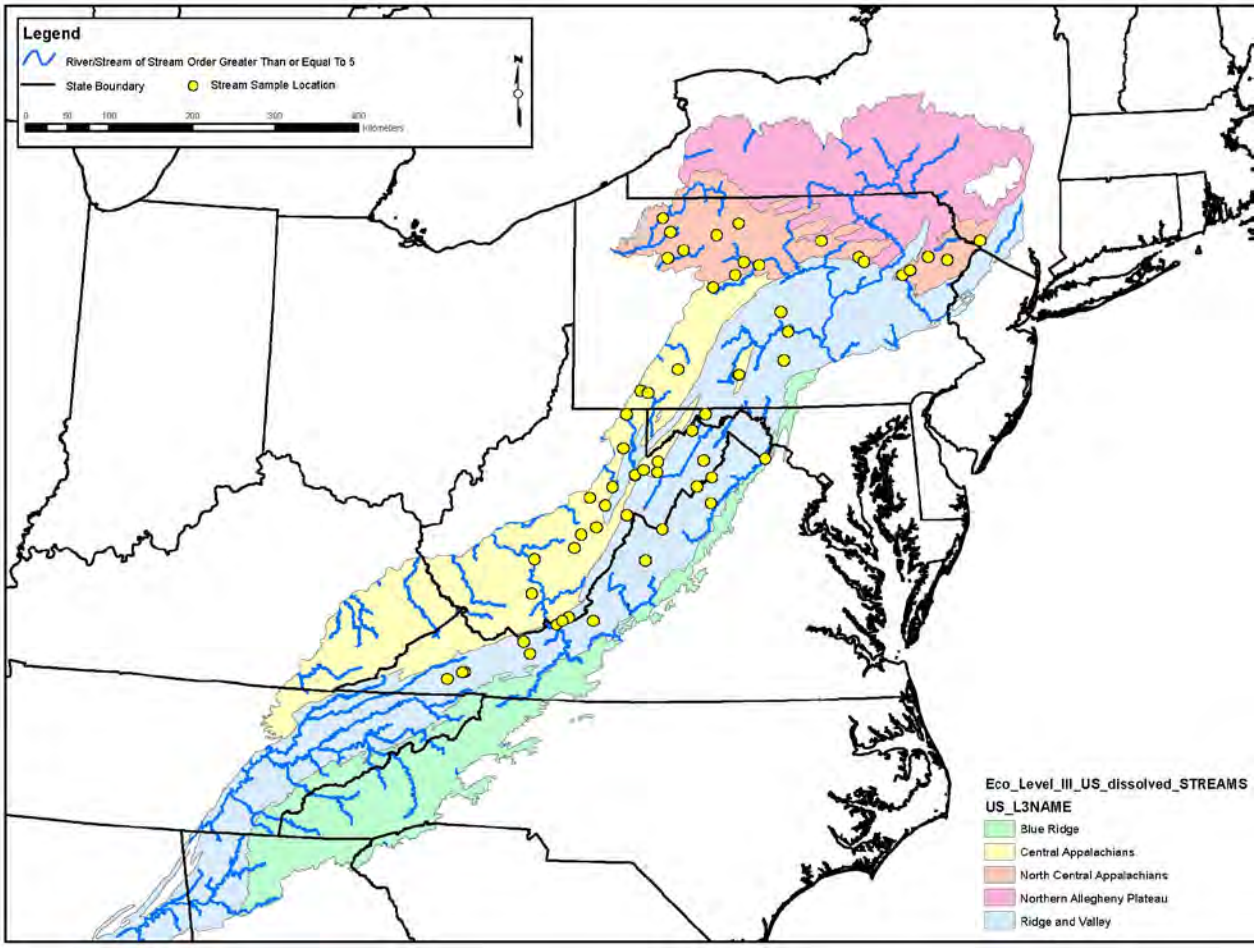

Figure 14: Map Showing Locations of the Ecoregions in the SAMI area (Note: not all data are shown on this map. Detailed maps for each ecoregion are included in Appendix B)

In Virginia, most of the research has been conducted on streams in the western part of the state, which are parts of Ecoregion 8.4.1 Ridge and Valley and 8.4.4 Blue Ridge. An initial estimate was made that 440 streams supported naturally reproducing populations of native brook trout (Bulger et al, 2000). The Virginia Trout Stream Survey (VTSS) program conducted an initial survey in 1987 of 344 streams. A subset of 60 streams was then selected for quarterly sampling. VTSS data were used by EPA in the Policy Assessment document.

The total stream length estimated to be suitable as potential trout streams in the Southern Appalachian Mountains was 53,000 km based on data from 1996 (Bulger et al, 2000), of which 39% is in Virginia. Less than 7% of all the streams *by number* in the Southern Appalachian Mountain Initiative region had ANC < 0 µeq L^{-1}, mostly in Virginia or West Virginia; about 11% had ANC of 20 µeq L^{-1} or less all in Virginia or West Virginia (Webb, 2004). In contrast, the median ANC for all SAMI streams was 172 µeq L^{-1} L^{-1}. As an alternative to focusing on number of streams or stream segments, Figure 15 depicts the stream length distribution in the SAMI region by ANC class (SAMI, 2002). Of the total stream length in the SAMI region, less than 2% *by length* had ANC < 0 µeq L^{-1}, and less than 7 percent had ANC < 20 µeq L^{-1}.

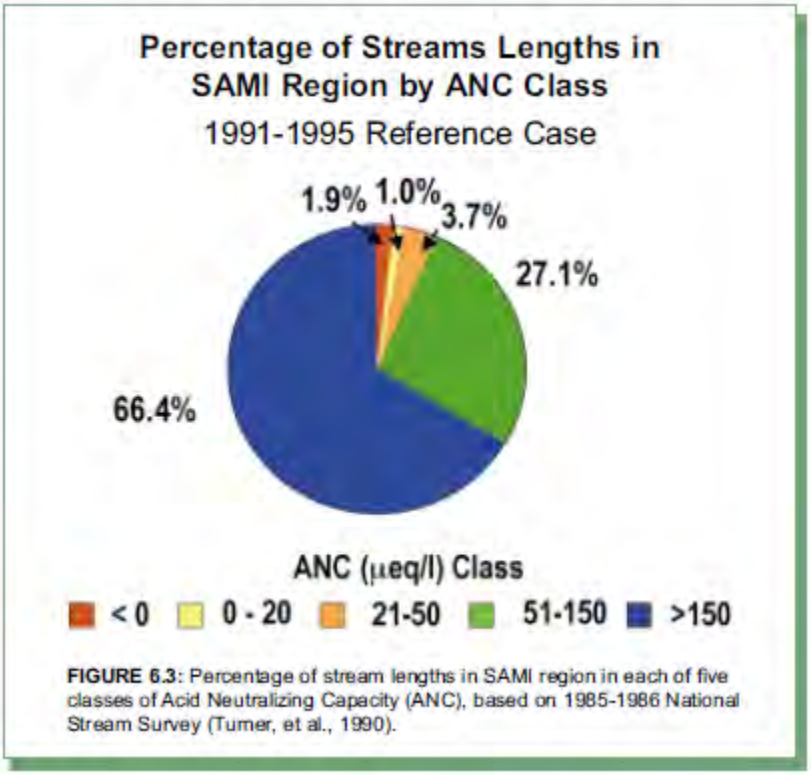

Figure 15: Reproduction of Figure 6.3 from Southern Appalachian Mountain Initiative (SAMI) Final Report, 2002 (ftp://narsto.esd.ornl.gov/pub/SAMI/SAMI_CD2/SAMI_reports/)

Out of the 758 waterbodies with ANC data in Ecoregion 8.4.1 Ridge and Valley, which includes the Shenandoah National Park, 18% (*by number*) had ANC values less than 50 μeq L^{-1}, 10% had ANC < 20 μeq L^{-1}, and 4% percent had ANC < 0 μeq L^{-1}. A total of 458 waterbodies had sufficient data to compute critical loads in this region. Detailed investigations have been conducted in the Shenandoah National Park, which has about 90 small streams, many of which have supported native brook trout (Sullivan et al, 2008). A total of 14 streams with different underlying bedrock types were examined. The five streams with siliclastic bedrock had median ANC values less than 20 μeq L^{-1}. Additional discussion of the effect of bedrock on weathering and ANC is presented in the next section. The comparison of numbers of streams to the number used by EPA show that a small percentage of waterbodies were sampled, and of those, a much smaller percent were acid-sensitive. Inclusion of data from intensively-studied known acid-sensitive systems such as headwater streams in the Shenandoah National Park has a disproportionate effect on the AAI distribution and hence the AAI selected for this ecoregion.

Summary of Comments on Regionalization and Data Representativeness

There are several concerns with the selection of Level III ecoregions by EPA. These ecoregions were defined based on a combination of factors, but appear to be overly influenced by factors related to climate, elevation, and vegetation. This approach was not based primarily on factors that have been shown to be important predictors of potential effects from acid deposition including presence of at least

0.1% carbonate rocks, soil thickness and bedrock type. The Level III ecoregions are overly broad, combine disparate areas, and even include areas separated spatially by about 25 miles. Because of this design, many ecoregions include numerous non-sensitive waterbodies in a given ecoregion. In addition, there was no screening process to eliminate waterbodies that were affected by other anthropogenic sources besides atmospheric deposition, such as acid-mine drainage, sewage treatment plants, and industrial discharges. The EPA had planned to drop waterbodies with sulfate concentrations greater than 400 mg L^{-1}, but this was not done for the Final PA Document. Sulfate concentrations in some waterbodies were quite high, as shown in Table 1, and most likely were influenced by factors other than acid deposition.

The EPA used water quality data sets available from past research, which had been directed toward systems known or expected to be sensitive to acid deposition. A random survey designed to characterize all waterbodies in a given ecoregion was not the norm for these investigations. Thus, the data in a given ecoregion were often dominated by known highly sensitive waterbodies, such as the well-studied waterbodies in the Adirondacks and Blue Ridge area of Virginia that were chosen for research due to their high sensitivity. For example, the percent of lakes that have lost one or more fish species in the Adirondacks due to acidification is small based on lake area (1.5-3%) and a small fraction of the total number of lakes without fish due to all causes (EPRI, 1989)**.** This is important, because the EPA's proposed approach to developing a future Secondary NAAQS for NOx and SOx relies on selection of either the 70th or 90th percentile critical load in acid-sensitive ecoregions or the 50th percentile in non-sensitive ecoregions to calculate the AAI. The EPA's distinction between acid-sensitive and non-sensitive ecoregions is based on having greater than 5% of waterbodies with ANC < 200 µeq L^{-1} and greater than 1% of waterbodies with ANC < 100 µeq L^{-1}. These criteria are highly subjective and given the lack of data representativeness of underlying datasets, they could result in ecoregions being classified as acid-sensitive even though there are a small number of waterbodies that are truly sensitive to acid deposition. (The previous section summarized the problems with using ANC as a universal indicator of ecosystem viability.)

It is also important to recognize that a distinction must be made between "acidic" waterbodies and "acidified" waterbodies, i.e., not all waterbodies that are "acidic" are so primarily by the impacts of acid deposition; this and other important factors determining the water chemistry and modeling of water chemistry are covered in the subsequent section.

Critical Load Calculations: Steady State Assumptions and Application of Simple Aquatic Models

Acid-Base Chemistry

A brief discussion of acid-base chemistry is in order. For natural waters, the Brønstead theory for acids and bases serves well. A Brønstead acid is a molecule that donates hydrogen ions (protons) to solution. A Brønstead base accepts hydrogen ions from solution. Strong acids readily donate almost all of their

hydrogen ions to solution. Weak acids only donate a small proportion of their hydrogen ions. Strong acids are most influential in general, but weak acids present in natural waters can shift pH by as much as 2–3 units on the pH scale. Strong and weak bases behave in an analogous fashion.

At any time, the concentration of hydrogen ions free in solution is determined by the amounts and the interplay of the strong and weak acids and bases in solution. Essentially the strong acids are always dissociated—their hydrogen ions are free in solution; the weak acids are dissociated to varying degrees depending on the quantity of hydrogen ions already in solution. The strong and weak bases behave in a like fashion.

Calculating the pH of Mixtures of Water or Waters of Changing Composition

When a liter solution with a 10 mg L^{-1} of chloride is mixed with a liter with a 20 mg L^{-1} chloride one can readily calculate the resulting chloride concentration—it is just the average concentration, 15 mg L^{-1}. Because the hydrogen ions freely dissociate and reassociate with bases, no such simple mass balance applies when mixing two waters with different hydrogen ion concentrations. For example when mixing one liter natural water samples with hydrogen ion concentration of 10 µeq L^{-1} and 1 µeq L^{-1}, the resulting hydrogen ion concentration is rarely the average of the two (i.e., 5.5 µeq L^{-1}), nor is it the average pH of the mixed initial hydrogen ion concentrations, $pH = -\log_{10}((10^{-5} + 10^{-6}) / 2) = 5.3$. In fact, additional information about the two samples is needed.

We need to know for both samples the total amount of strong acid or base present (ANC) and the amount of weak acids and bases present. For the weak acids and bases we also need to have estimates of their relative strengths as acids or bases. This is usually quantified by equivalent dissociation equilibrium constants (K_a or K_b for acids and bases, respectively). With this information, free hydrogen concentrations can be readily calculated using mathematical simulation codes such as ILWAS, pHCALC, MAGIC, PnET-BGC, ALCHEMI or various geochemical codes (Goldstein et al, 1984, 1985; Gherini et al, 1985; Cosby et al, 1985a-c; Baker and Gherini in ALSC, 1990; Chen et al, 2004). Alternatively one can calculate pH or Al_i from nomographs such as shown in Figure 16 for H^+-ion concentration.

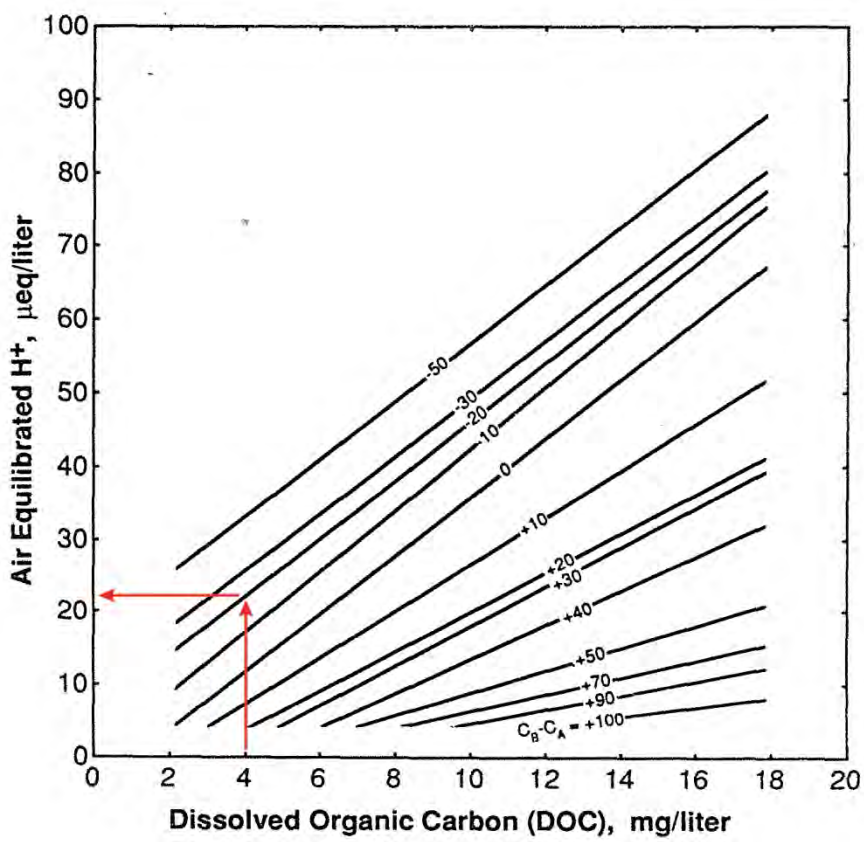

Figure 16: Air-equilibrated hydrogen ion concentration versus DOC over a range of C_B-C_A values. This plot can be used to determine H+ concentration and thus pH given C_B-C_A ANC and DOC. This set of curves was developed from over 6000 data points from the ALSC investigation. For the example above, using values of DOC = 4 mg L^{-1} and $C_B - C_A$ = -20 µeq L^{-1} , the nomograph yields a value of pH ≈ $-\log_{10}(20 \times 10^{-6})$ = 4.7. (Munson, et al. 1990).

Processes Influencing Acidification of Soils and Waterbodies

The EPA's development of a standard to protect waterbodies from acidification is based on a modified form of the conceptual Steady-State Water Chemistry (SSWC) model (Henriksen and Posch, 2001) whose simplicity can make it seem attractive to use in establishing a standard with such widespread applicability. However, surface water acidification is dependent on the interaction of a wide variety of complex processes. These include deposition processes (wet and dry and occult deposition via cloud and fog interception), hydrologic processes that determine where water flows (Figure 17), and biogeochemical processes that influence the acid-base chemistry of water flowing through a basin. The interaction of all of these processes determines water quality (Munson and Gherini, 1991a). A representation as simple as the SSWC model cannot capture that complexity and will produce an inaccurate representation of surface water response to changes in acidic deposition.

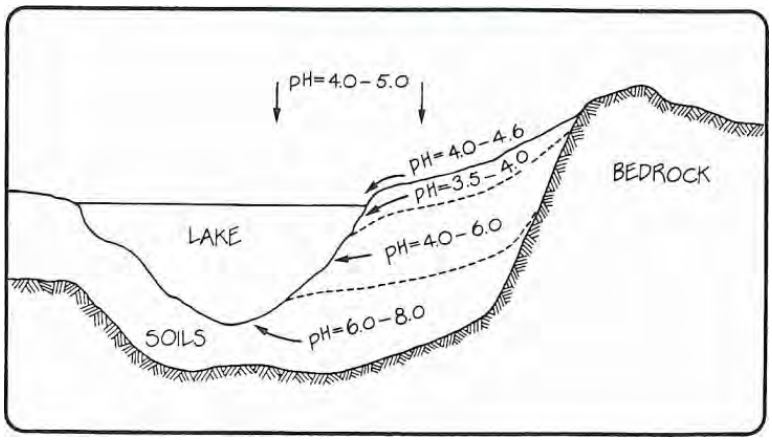

Figure 17: Changes in Soil Solution pH with Vertical Distance through the Soil Profile for an Adirondack Lake Watershed (after Gherini et al, 1985). Solution in the upper soil horizons is often more acidic than the incident precipitation or throughfall. As one moves down the soil profile more alkaline solution is encountered. The amount of water moving laterally through the soil horizons strongly influences the acidity of surface waters, and this lateral routing can change. Large amounts of water from storms and snow melt can overwhelm the lateral flow carrying capacity of the lower layers and back up lateral flow into the upper layers, resulting in more acidic surface waters.

The assumptions of the SSWC model, as described in the Final PA Document (EPA, 2011), include several key over simplifications. Among these are overly simplistic representations of ion exchange; a lack of detailed sulfur process (i.e., no sulfide oxidation, sulfate uptake, no permanent sulfate fixation, no sulfate reduction, and no sulfate adsorption-desorption); and the assumption that the hydrology is simple with only downward infiltration through the soil profile.

These assumptions are not in general appropriate for watersheds or areas affected by acid-mine drainage. In addition, variable flow paths occur when the infiltration rate is higher (e.g. after storms) than the underlying soil flow carrying capacity when the mineral soil layers become saturated, forcing lateral flow through the upper, highly-acidic organic horizons. Flow paths also change when the soil is frozen and nitrate builds up in the soil interstices and snow pack, contributing to acidic runoff when the snow melts.

The basis of the EPA's approach based on the Aquatic Acidification Index is the estimation of the critical loads (EPA, 2011). The equation for the critical load of waterbody is:

$$CL = ([BC]_0^* - ANC_{lim})\, Q + N_{eco} \qquad \text{Equation 2}$$

where Q is the annual run-off rate of the waterbody and ANC_{lim} is the ANC level targeted by the critical load (the ANC limit believed to be protective of biota in the ecosystem). An important parameter in this equation is the preindustrial (or pre-acidification) base cation input BC_0^*. BC_0^* is a key parameter in calculating critical loads and is defined in the Final PA document as follows:

$$BC_0^* = BC_w + BC_{dep}^* - BC_u = BC_t - BC_i \qquad \text{Equation 3}$$

- BC_{dep}^* = *Non-anthropogenic* deposition of base cations
- BC_w = Average weathering production of base cations
- BC_u = Net long-term average uptake of base cations by the biomass

- BC_t = Present-day BC levels
- BC_i = BC input due to ion exchange

For calculation of the term BC_0^* EPA staff proposed two different calculation methods, the Model of Acidification of Groundwater in Catchments (MAGIC) and the Henriksen f-factor approach. EPA identified in its early drafts of the Policy Assessment Documents that MAGIC would be the preferred approach for calculating the value of BC_0^*. (Comments on the MAGIC model were provided in EPRI's Comments on the Second PA Document and its presentations to the CASAC Review Panel.) However, in the development of the Final Policy Assessment Document, EPA defaulted to using the Henriksen f-factor approach (due to data limitation) in all its final analyses of the AAI and the proposed approach for a future Secondary NAAQS for NOx and SOx.

A detailed comparison and evaluation of the Henriksen f-factor approach to empirical data is presented later. At this moment, it is important to note that instead of estimating the physical and biogeochemical processes affecting BC_0^* (deposition, weathering, uptake and ion exchange), the Henriksen f-factor approach estimates values of BC_0^* using using the following equation:

$$[BC_0]^* = [BC]_t - [BC]_i = [BC]_t - F \times ([SO_4^{2-}]_t - [SO_4^{2-}]_0 + [NO_3^-]_t - [NO_3^-]_0) \qquad \text{Equation 4}$$

where

$F = \sin\left(\frac{\pi}{2}\ [BC]_t/S\right)$, where S = 400 µeq L^{-1} (value for Norway, Brakke et al., 1990 as referenced in EPA, 2011)

$[SO_4^{2-}]_0 = 15 + 0.16 \times [BC]_t$ (µeq L^{-1}, equation for Ontario, Canada, Henriksen et al., 2002, as referenced in EPA, 2011)

$[NO_3^-]_0 = 0$ (assumed)

and the subscript $_t$ = today; Subscript $_0$ = preindustrial/preacidification. Before presenting an evaluation of Henriksen f-factor approach, we will first discuss the importance of the key physical and biogechemical processes that are not represented mechanistically in such an approach. This discussion will emphasize how the individual processes fail to align with a steady-state assumption and thus the chief premise of the critical load calculations is not satisfied. The evaluation of the Henriksen f-factor approach will also demonstrate with empirical data that this methodology is inappropriate for broader application and illustrates that systems in common regions behave quite differently and fail to show any trends towards steady state.

The final term, N_{eco}, represents nitrogen uptake by ecosystem. EPA proposes two different calculation methods, both of which are also too simplistic. These methods were addressed in detail in EPRI Comments on Second Draft PA Document. An additional analysis of nitrogen uptake in ecosystems is provided in the subsequent section.

Base Cation Deposition

EPA's approach in the Final PA Document is to employ the Henriksen f-factor approach rather than estimate the individual processes affecting base cation supply. One of these processes is base cation deposition. There are at least some data available for wet deposition of base cations from the National Atmospheric Deposition Program (NADP, 2010) and for dry deposition estimates from the CASTNET dry deposition network (EPA, 2009). Further, it has been shown previously (by Chen et al, 1983 and Lindberg et al, 1986) that actual deposition to forested ecosystems can be increased considerably by the forest canopy (enhanced collection of dry deposition).

Although the input of all base cations impact a waterbody, the supply of base cations that is utilized in Equation 3 is limited to the non-anthropogenic deposition of base cations is difficult to estimate. Sampling methodologies do not separate anthropogenic flux from non-anthropogenic flux, and anthropogenic flux of base cations is ill-defined at best. Base cation inputs originating from a cement plant would clearly be anthropogenic, but it is unclear whether dust generated from nearby dirt roads is considered anthropogenic or non-anthropogenic. The challenge of source classification is further complicated by the inability of sensors to distinguish anthropogenic from non-anthropogenic cation sources. Estimates of anthropogenic inputs versus non-anthropogenic inputs can be determined, but the basis for the calculations is unclear and the applicability of any calculation scheme nationwide would be questionable due to differing processes occurring in different regions. These issues illustrate that even for the component of BC_0^* with the most reliable data for a detailed derivation, the uncertainties are large. Furthermore, the steady-state methodology proposed by EPA assumes that base cation deposition rates remain constant, although as shown in Figure 18, this is not always the case.

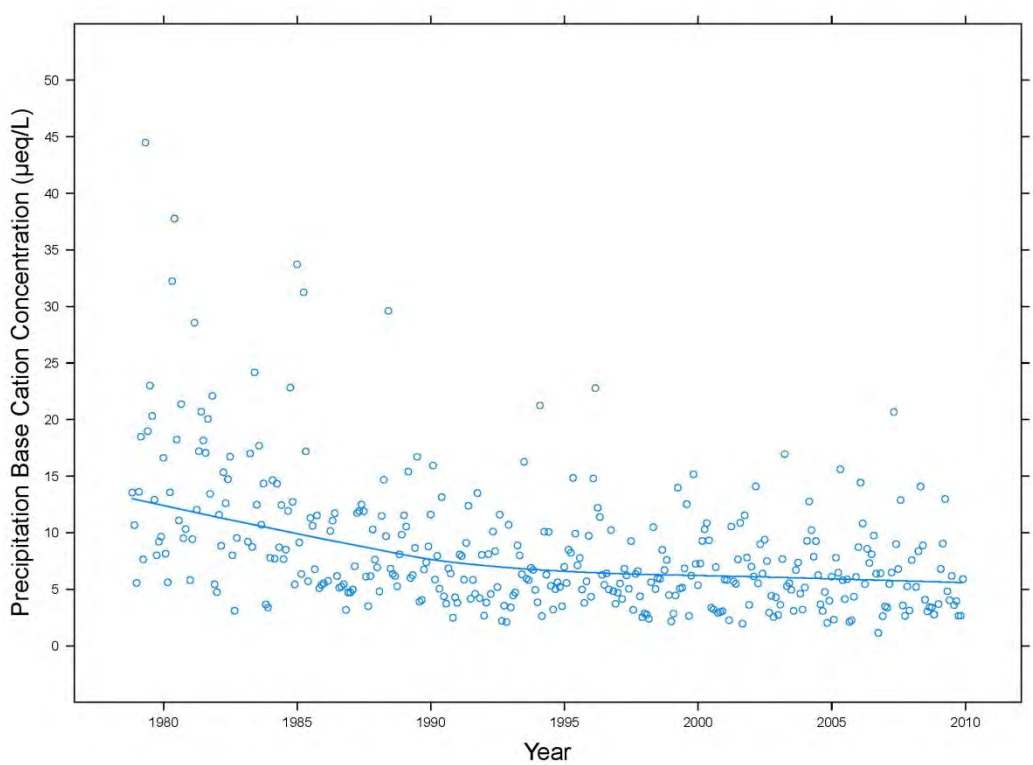

Figure 18: Example of Base Cations in Precipitation at NADP Site NY20.

Base Cation Uptake

Base cation uptake in forest soils is another process affectly base cation supply in waterbodies. Base cation uptake is a highly variable process that is influenced by a wide range of natural processes, including land management practices. The U.S. Forest Service (USFS) has data on vegetation characteristics for most parts of the country, including areas that are thought to be sensitive to acidic deposition. However, the uptake rate changes over time. For example, Figure 19 shows the response to clear cutting of two watersheds in the Hubbard Brook Experimental Forest (Likens et al, 1994). In Watershed 2, growth was suppressed for three years following clear cutting. In Watershed 5, regrowth was allowed to progress immediately after clear cutting. Note that the rate of calcium uptake in Watershed 5 doubled in years 4 to 8 in comparison to years 1 to 3, and in Watershed 2 uptake went from zero during years 1 to 3 (due to a land management practice - growth suppression) to over 2 kmol/ha during years 4 to 8. The results of this analysis demonstrate three important points:

1. Changes in uptake occur in response to perturbations
2. Uptake rates can change over time
3. Uptake rates can vary substantially even in watersheds that are physically close together and have similar characteristics, as reflected in the differences in uptake in the two watersheds during the years 4 to 8 time period.

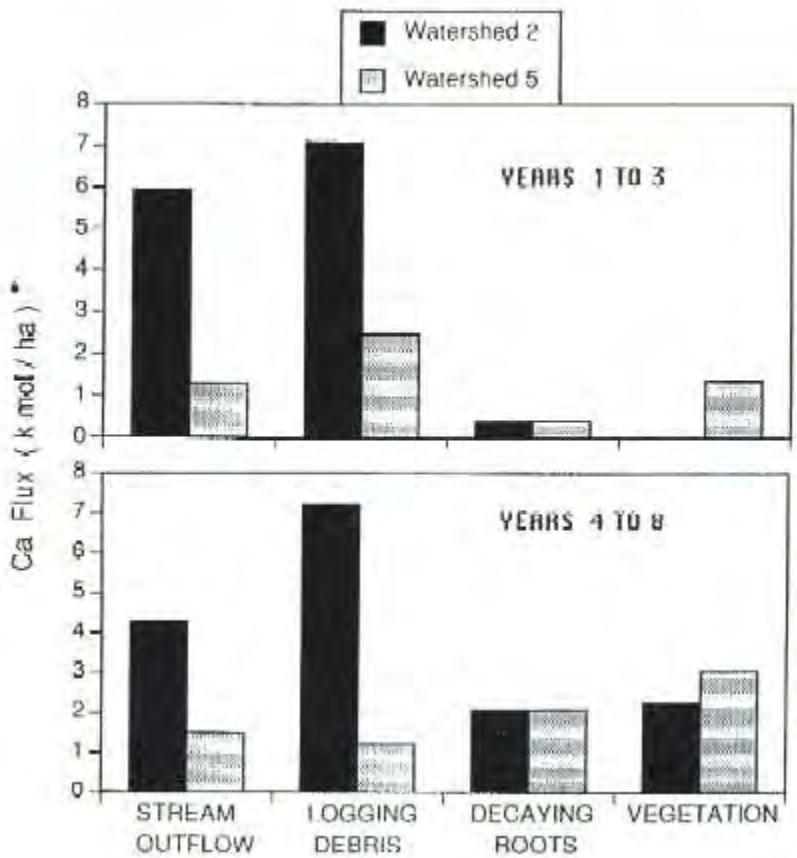

Figure 19: Response of Watersheds in Hubbard Brook Experimental Forest to Clear Cutting (Likens et al, 1994).

Variability in uptake within a region is further illustrated using the results of the Integrated Lake-Watershed Acidification Study (ILWAS) of lakes in the Adirondacks (Goldstein et al, 1984). Woods, Panther, and Sagamore Lakes are located in close physical proximity, receive nearly identical deposition loads, and have similar soil and geologic characteristics. Woods Lake is acidic; Panther is alkaline; and Sagamore is in-between. During a three-year study, over 600,000 data points were generated to evaluate the processes influencing the acid-base characteristics of the three lake-watershed systems. A dynamic mechanistic simulation model developed as part of the study, the ILWAS model, was applied to the lakes to evaluate their response to changes in acidic deposition (Gherini et al, 1985). Figure 20 shows the simulated contribution of various processes to the observed ANC in Woods and Panther Lakes. As indicated, plant growth has a much larger impact on the surface water characteristics of Woods Lake than Panther Lake (Munson and Gherini, 1991b). In spite of the significant similarities between the two systems in terms of proximity and acidic inputs, the impact of uptake by vegetation is considerably different. Thus a simplistic treatment of base cation uptake may be inappropriate.

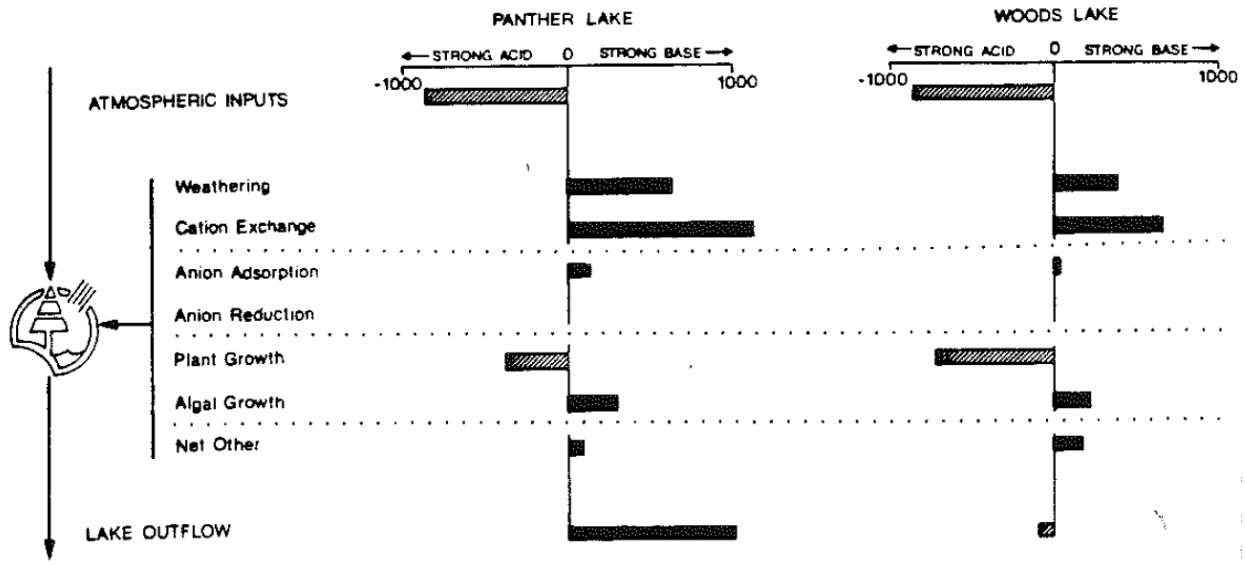

Figure 20: Contribution of Various Processes to the Observed ANC in Woods and Panther Lakes (Based on ILWAS Model Simulations). Note the large difference in acid generation due to plant growth between the two systems. Units are eq ha^{-1} y^{-1} (Munson et al, 1987).

The EPA tries to circumvent these issues by assuming that **"***steady-state conditions exist."* The assumption of steady state is a large over-simplification. Ecological processes are never at a truly steady-state condition (Sullivan et al, 2009). Climatic variations, fires, forest blowdown, perturbations by biota (e.g., beaver activity and insect infestations) and even processes that take place over geologic time scales (e.g., glaciation) all cause deviations from steady-state conditions. Ion uptake varies considerably depending on the forest successional stage, which is typically characterized as rapid uptake to support early growth, followed by slower maintenance uptake, and finally minimal uptake when the forest is in decline. Perturbations impose large variations in uptake by changing this general successional pattern.

Base Cation Weathering

Mineral weathering is a slow process that adds base cations (and thus ANC) to solutions in specific stoichiometric ratios (April and Newton, 1985; Munson and Gherini, 1991a, 1991b and 1993). The rate of weathering has been reported to have a fractional dependence on hydrogen ion concentration ranging from 0.0 to 0.8 (Bloom, 1988; Schnoor and Stumm, 1984; Drever and Hurcomb, 1986). This is the type of formulation that is included in models such as PROFILE (Warfvinge and Sverdrup, 1992) and ILWAS (Gherini et al, 1985). Although EPA ultimately relied only on the Henriksen f-factor approach for calculating BC_0*, it is important to note that weathering in the MAGIC model—which EPA identified as a preferred method for estimating BC_0*, and thus could be employed in future assessment— is not tied to any specific minerals, and instead is adjusted on an ion-by-ion basis. The impact of this type of formulation is that weathering estimates generated by MAGIC have little or no relationship to the minerals that exist in watershed soils. This is a highly under-constrained condition with the potential to introduce large errors in weathering estimates.

An additional concern is the high spatial variability of weathering rates. For example, data indicate that weathering rates vary substantially within the Adirondacks (April et al, 1986). Weathering inputs in the western Adirondacks are dominated by amphiboles (hornblende). In the eastern Adirondacks, however, mineral weathering inputs are controlled by a calcium-rich anorthosite. In addition, there are regions within the Adirondacks with calcite minerals, e.g. Windfall Pond in the Big Moose basin of the western Adirondacks (Newton et al, 1987). There are lakes in the eastern and western Adirondacks with similar surface water characteristics, but the actual weathering rates and weathering products in the two systems could be substantially different because there are distinctly different minerals controlling weathering inputs.

Another example of the difference in weathering is seen in data for Virginia streams. Figure 21 illustrates variability in calcium leaching in specific stream watersheds as a function of silica, where higher concentrations are indicative of more intense weathering. These differences are due to bedrock geology and groundwater flow rates. The effect of bedrock geology is clearly seen in Figure 22 which shows cation leaching for three rock types in Virginia: basaltic, granitic, and siliclastic. The importance of bedrock geology and flow rate on surface water quality and ANC is discussed in detail elsewhere (Webb, 2004).

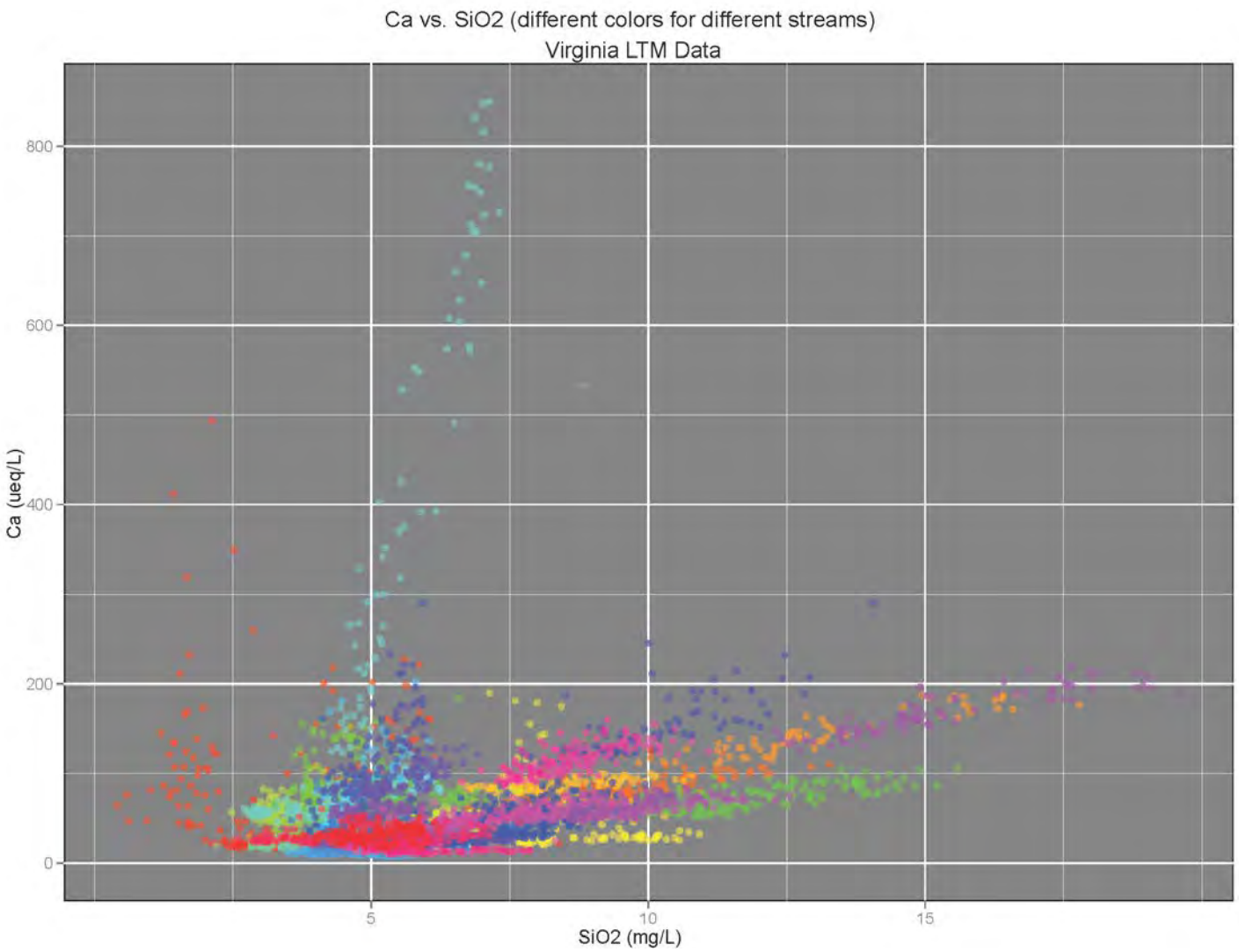

Figure 21: Calcium versus Silica Concentrations in Virginia Streams. Different colors represent different streams.

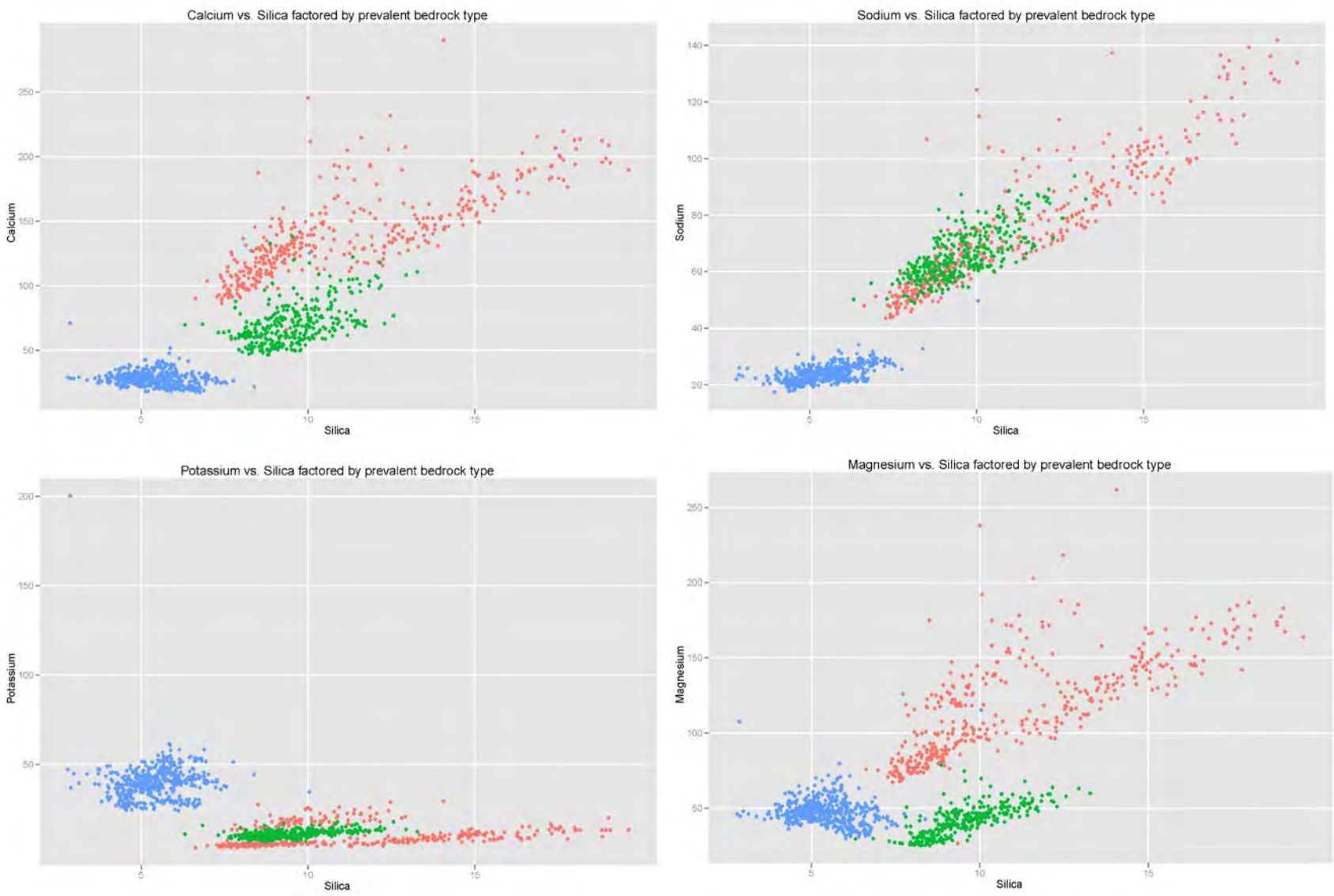

Figure 22: Base Cations versus Silica for Three Bedrock Types in Virginia Streams. Red is for streams draining Basaltic regions, green is for granitic streams, and blue is for siliclastic streams. Cation concentrations are in µeq L^{-1}; silica is in mg L^{-1}.

Cation Exchange

The base cation supply to surface water systems includes inputs from deposition, organic matter mineralization, mineral weathering, and cation exchange. In the Henriksen f-factor approach used by EPA, the contribution of cation exchange to surface water base supply is subtracted from the calculation of BC_0* (see Equations 3 and 4). EPA's justification for this assumption is that present-day base cation concentrations are higher than the steady-state preindustrial concentrations. However, as stated previously, ecological processes are never at a truly steady-state condition (Sullivan et al, 2009). In effect, EPA does not consider base cations from the ion exchange complex as a renewable source of base cations.

Climatic variations can lead to soil drying and precipitation of salts. Upon rewetting, these salts can re-dissolve and influence the movement of cations onto or off of the exchange complex. Forest blowdown can lead to warming of soils and rapid decay of organic matter, releasing acidic compounds that can drive exchange reactions. Insect infestations can have a similar impact. Beaver activity in a watershed can lead to inundation of soils and deposition of reduced sulfur species. Upon drying, these species can re-oxidize to generate acids that promote ion exchange. Soil formation processes themselves (e.g., podsolization) can produce acidic species that alter soil exchange properties. The supposition that ecosystems existed in some form of steady state prior in the past prior to industrialization or could be brought to steady state in the future has no technical basis. This error is compounded by the notion that we have an understanding of the historic chemical characteristics of watershed components across the nation. Measurements of these characteristics simply do not exist on a historical basis, let alone on a nationwide basis. Theoretical constructs of past acid-base characteristics of surface waters can be attempted, but, in the end they are nothing more than speculation.

Something tangible that we do have for some systems are data collected since the late 1970s. Early research on acid deposition effects was hampered by the fact that there was no change in signal with respect to acid inputs. However, we now have seen a change in deposition to use as a test of our theoretical understanding of the response of ecosystems to changes in acidic inputs. The response to that change integrates the influence of all of the processes that contribute to surface water characteristics, including cation exchange. It would seem prudent to base a standard on available observations rather than speculations about pre-industrial conditions.

One region that has data reflecting the response of surface waters to the decrease in deposition acidity is the Adirondacks. Changes in lake chemistry for 16 lakes sampled from 1982 through 2004 and for 48 lakes sampled from 1992 through 2004 are shown in Figure 23 (Driscoll et al, 2007). Focusing on the lakes with the longer sampling period (1982 – 2004), all 16 lakes show statistically significant decreases in sulfate concentration, the sulfate plus nitrate concentration, and base cation concentrations. This observation suggests that many of the base cations in solution were induced by acidic inputs. With regard to ANC, only 11 of the 16 lakes have statistically significant changes, with a relatively small mean value of 0.76 $\mu eq\ L^{-1}\ y^{-1}$. Similar results are seen when evaluating the larger data set (48 lakes) as well. If these observations apply broadly, they imply that even with additional decreases in acid inputs, large increases in ANC are unlikely because base cation concentrations will decrease as well. An important

research objective should be to understand the extent to which future reductions in SOx and NOx will have on ANC, H^+-ion, and Al_{im} concentrations; this and other recommendations are stated in EPRI's main comments. These comments and observations underscore the point made by Sullivan et al. (2009) in an analysis of streams in Virginia and West Virginia where they said,

> "*Some acidified lakes and streams are not projected to recover to critical criteria values even if deposition is reduced to zero because they were not that high to begin with*."

The complexity embodied in the observed data cannot be captured by the simple approach proposed to estimate critical loads. Cation exchange is an important process in determining the response to changes in deposition inputs, and its influence should be included in future assessments of acidic waterbodies. Moreover, the differentiation between "acidic" and "acidified" waterbodies should be more than a discussion of perceived "semantics". It is important to understand the differentiation between naturally acidic waterbodies and those that are acidic due to anthropogenic influences.

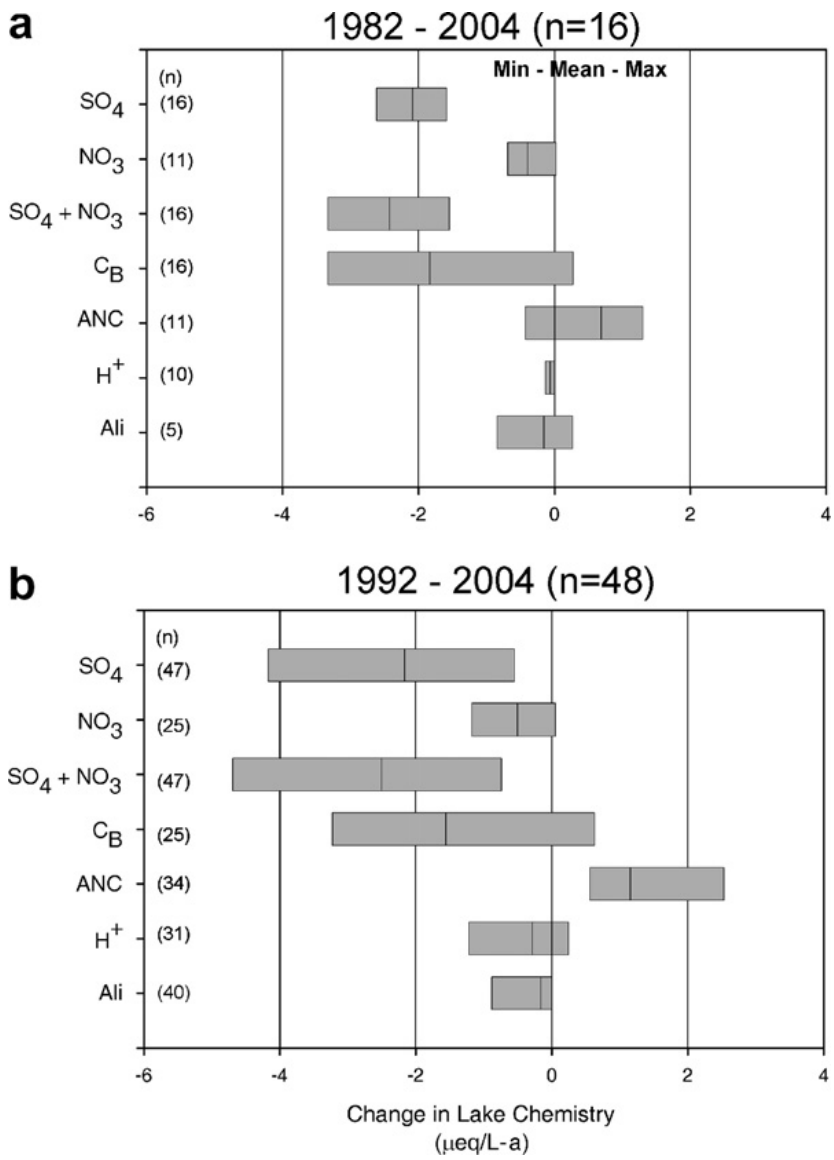

Figure 23: Mean Rates of Change in Solute Concentrations in 16 Lakes from 1982–2004 (a) and 48 Lakes from 1992–2004 (b) of the Adirondack Long-Term Monitoring (ALTM) program (Driscoll et al, 2007). Minimum, mean, and maximum changes in concentrations and number of lakes showing significant trends are shown. All values are in µeq L^{-1} y^{-1}, except for concentrations of inorganic monomeric aluminum (Al_i) which is expressed in µmol L^{-1} y^{-1}.

With specific regard to the longevity of cation exchange, studies have indicated that soils in the northeastern U.S. have adequate sorbed base cations to continue to buffer acid inputs for anywhere from 50 to 200 years (Schnoor and Stumm, 1984) to as many as several hundred years (Gherini et al, 1985; Munson and Gherini, 1991a). Any assessment or analysis, let alone a methodology proposed for a national standard, should not ignore a process that has the potential to continue to influence surface water acid-base characteristics for extended time periods such as these.

The processes described above (deposition, hydrologic processes, and chemical responses) cause changes to C_B and C_A, and thus to ANC. To evaluate the interaction of these processes and determine the

net effect on ANC in a waterbody, researchers use two approaches: one simple and the other complex. The simple method is use of the "f" factor as implemented in the proposed methodology. The complex approach is to use process-based, mathematical simulation models such as ILWAS, which have more data requirements but provide more information on why a particular response to changes in deposition occurred in a given waterbody.

The "f" Factor

The f-factor was introduced in the previous section. Henriksen et al (1984) proposed the f-factor as a simple method to predict how surface waters would respond to changes in atmospheric deposition. Regional surface waters—and even national surface waters—would be assumed to respond similarly to changes in deposition acidity as described in Equation 4. The "f" factor can be restated as follows (using similar nomenclature as above):

$$f = \Delta\Sigma C_B / \Delta\Sigma C_A \qquad \text{Equation 5}$$

The f term is simply the change in the total base cation concentration per change in the total strong acid anion concentrations.

The f-factor was believed to range from 0.0 to 1.0. At 0.0 the base cation concentrations did not change with any changes in the concentration of the strong acid anions. In other words the base supply rate from the hydrologic basin would remain constant and thus be independent of the amount of acid input i.e., the base cations in solution were not induced or brought into solution by the acid anion inputs. Initial thinking assumed natural water base input remained constant. Decreases in strong acid inputs would then create a one-to-one decrease in ANC.

At f-factor values of 1.0, the base cation concentrations would change in a one-to-one ratio with changes in strong acid anion inputs. Thus, for example, decreases in strong acid anions would be accompanied by one to one decreases in base cation concentrations. Implicitly, the base cations in solution were essentially due to the strong acid anion inputs. Thus, no changes would be encountered in surface water ANC values for even large decreases in deposition acidity.

Of course the typical problems with ratios prevail. For example even small changes in acid anion concentrations could yield very large values of the f-factor, as the value of the denominator, $\Delta\Sigma C_A$, approaches zero.

Since the f-factor approach was first proposed it has received considerable attention. Use of the f-factor approach is relatively easy. The large computer codes and extensive data requirements of the mathematical acid rain models (e.g., ILWAS, MAGIC, or PnET-BGC) would not be required. One just selects f-factor parameters (i.e., the parameters ***S***, $[SO_4^{2-}]_0$ and $[NO_3^-]_0$, as described below Equation 4) for the waterbody or groups of waterbodies of interest and then the response to decreasing or increasing deposition acidity is uniquely determined. When the f-factor approach was first proposed, little long-term data were available to test the concept that a waterbody or groups of waterbodies would respond as indicated by an f factor.

Evaluation of "f" Factor Approach

Now several years have passed since large reductions in SO_2 and NOx emissions. In areas with sulfate adsoption, surface waters have experience almost proportional decreases in sulfate concentrations.[1] One can test the f-factor approach by using actual water quality data and calculating actual f-factor values for individual waterbodies/regions.

Critical Loads have been defined as the amount of acid deposition a hydrologic basin can receive without its surface water ANC dropping below a specified value. As a part of calculating a critical load, the EPA attempts to quantify the pre-industrial base supply rate (BC_0*) to the waterbody using Henriksen f-factor approach within a steady-state water chemistry modeling framework. To be effective the f factor should be representative of the water bodies involved and stay constant over time to satisfy the steady-state assumption. At the very least, the f-factor should be robust and show consistency in its behavior over time and within any a determine region.

Two regions in the U.S. have been the sites of most acid deposition effects research and public attention: Adirondack lakes and Virginia streams.

Adirondacks

If the f-factor approach is valid, it should predict the change in total base cation concentrations that have occurred since the large reduction in SOx and NOx emissions since 1990. EPA's analysis suggests that an appropriate value for the f-factor in the Adirondacks ranges from 0.2 to 0.3, a value close to previous representative values (0.2 to 0.4) for other regions of Norway, Sweden, U.S. and Canada (Henriksen, 1984).

We now use data collected over about twenty years in the Adirondacks to test the validity of the f factor. First we will calculate f-factors for the 44 Adirondack lakes in EPA's database used in the REA and PA documents. These values are summarized in the histogram presented in Figure 24. The lake values of f-factors vary widely from the 0.2 to 0.3 value selected by EPA for the Adirondacks. We found a median value of about 0.6, and a range of about -0.2 to 2.4.

[1] Large reductions have occurred in NOx emissions as well, but as noted in the next section and in previous comments, nitrogen is taken up to a large extent by most ecosystems.

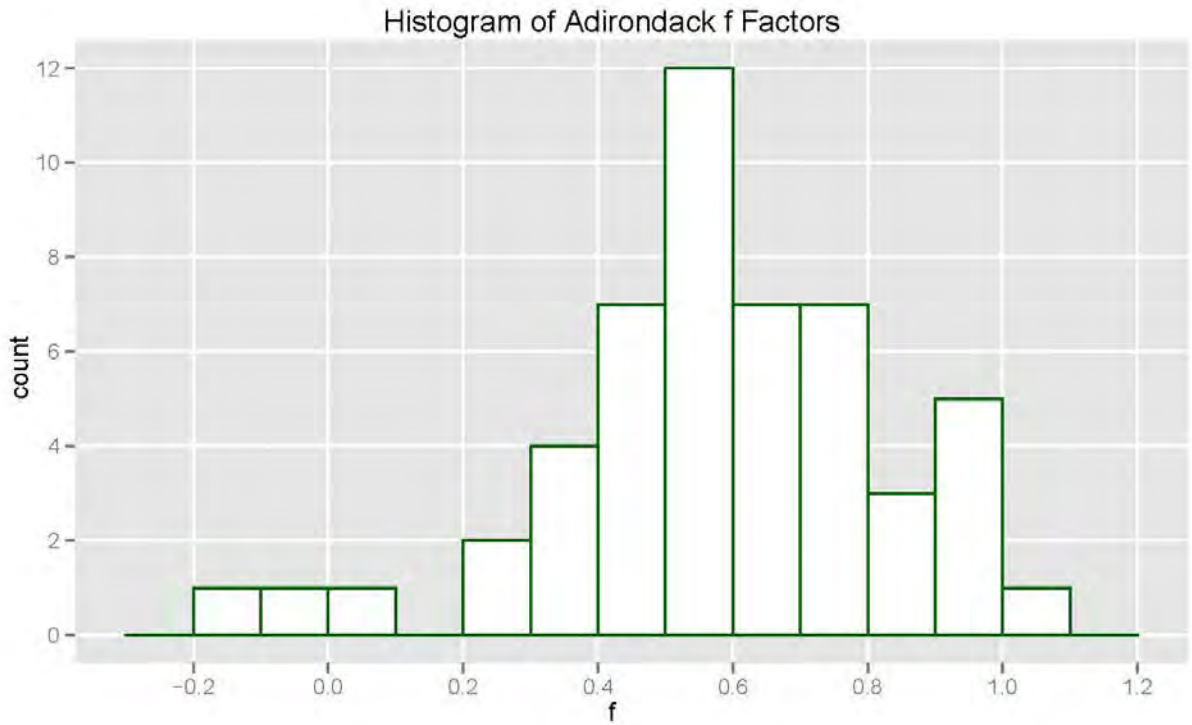

Figure 24: Distribution of f-Factor Values for the 44 Adirondack LTM lakes. The lake values of the f-factor vary widely from the 0.2 to 0.3 range estimated by EPA for the Adirondacks. We found the median value to be about 0.6 (full range not shown).

Now we examine whether the values have remained constant for the Adirondack water bodies over time. We calculate the values of f-factor for the individual lakes in the first and second halves of their data records (typically 9 years each). We find the values have not remained constant, but have fluctuated widely, both up and down as shown in Figure 25a and Figure 25b; moreover, there is no trend in the direction of the fluctuations. These results raise concerns over the validity of using f-factor values and of the steady-state assumption used as the basis for the proposed methodology.

a. Scatter plot of f-factor changes from first to second half of Adirondack LTM data set.

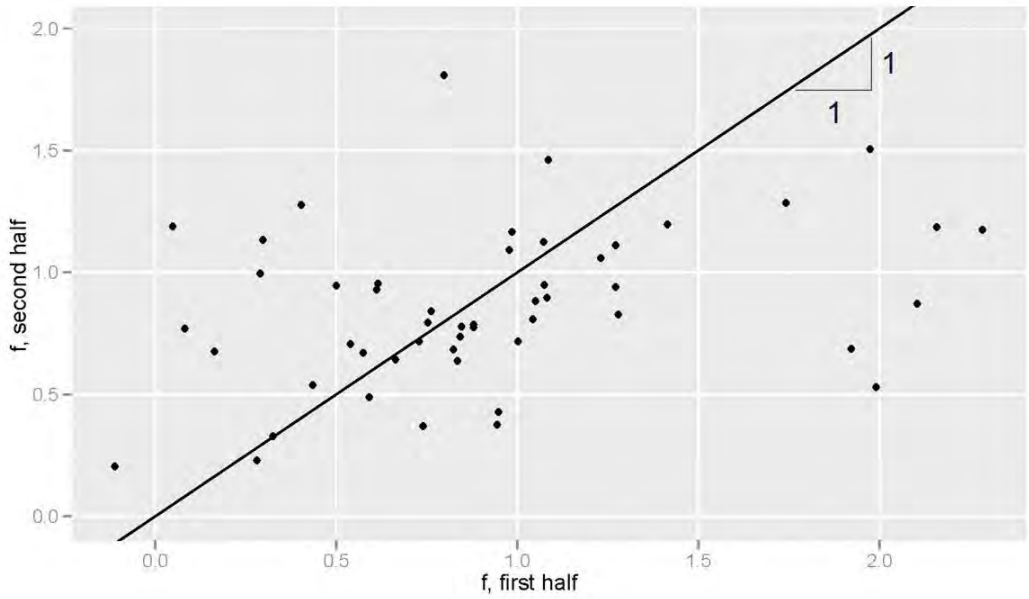

b. Direction of f-factor changes from first to second half of Adirondack LTM data set.

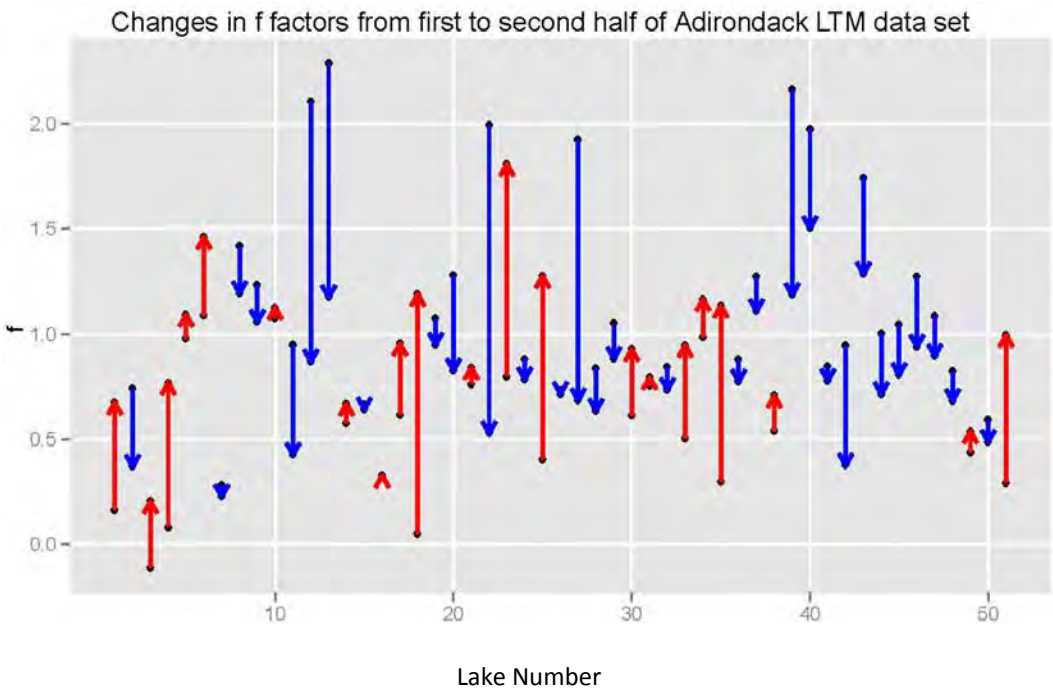

Figure 25: Changes in f-factors from First to Second Half of Adirondack LTM Data Set: a) as Scatter Plot, and b) as Arrows for Direction Change. Colored arrows show direction of change from initial 9-year period to second 9-year period. Red arrows indicate f-factors that increased in value and blue indicate those that decreased. The f values have fluctuated widely from lake to lake and with time.

Figure 26 is an alternate rendition of the data in Figure 25. Figure 26 also includes the Virginia data, which has an even larger spread of f-factors.

a)

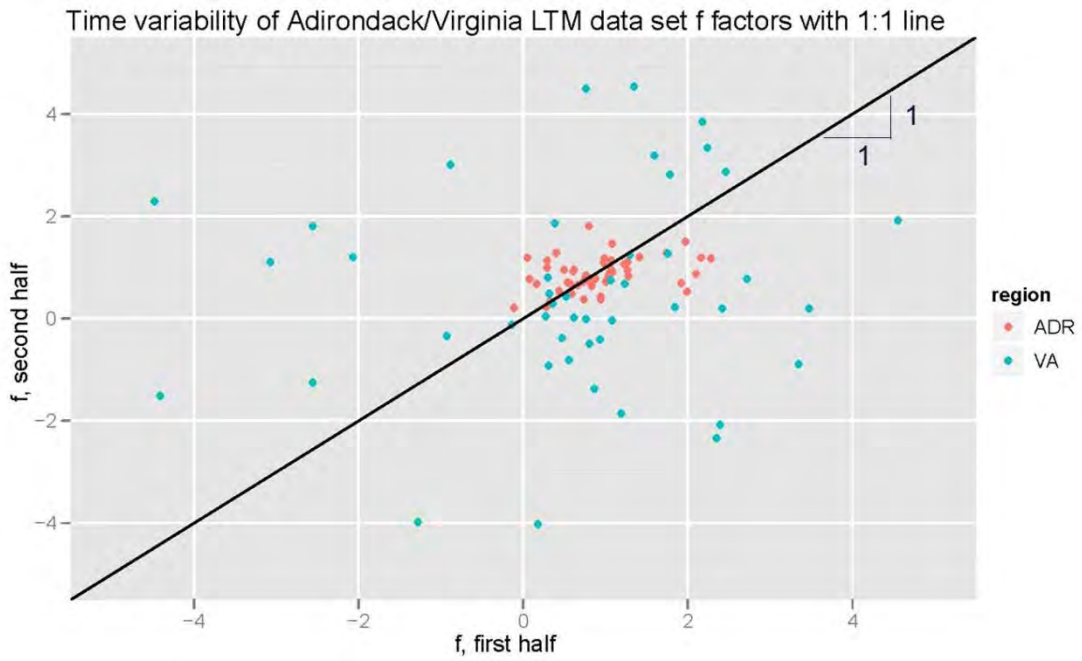

b)

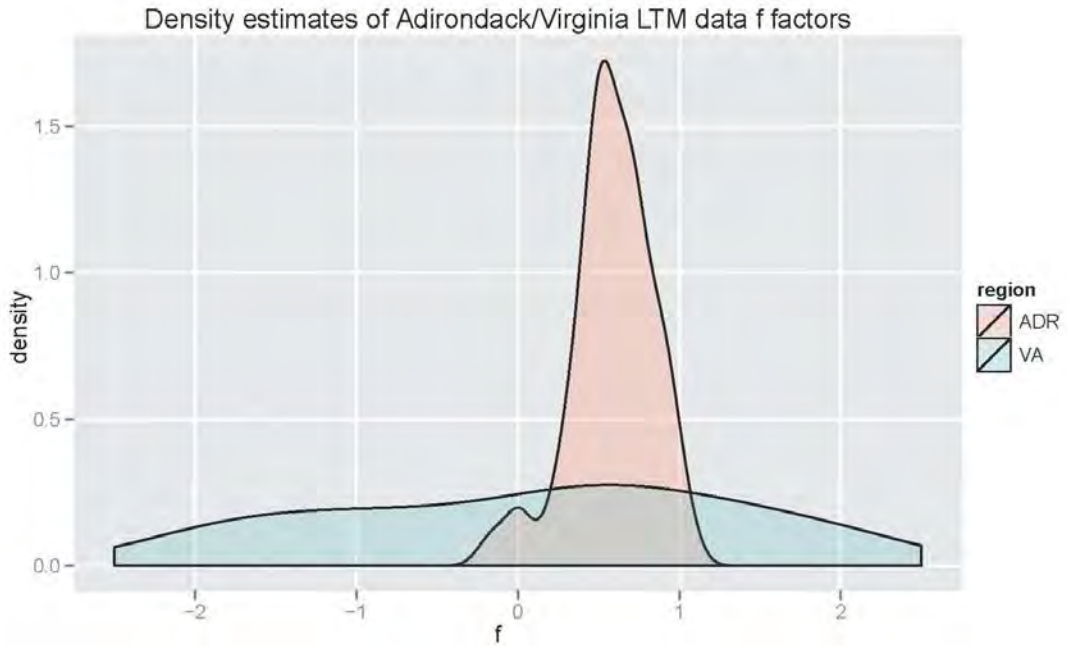

Figure 26: Comparison of f-factors over Time for Both the Adirondacks and Virginia: a) as Scatter Plot and b) as Density Plot.

Virginia Systems

We now evaluate in detail the f factor for the Virginia water bodies, mostly streams. Figure 27 and Figure 28 show the calculated f values. Noting the differences in the axes scales, we can see the values for the f-factor vary more widely than those for the Adirondacks. Sulfate adsorption by Virginia soils yielded very small changes in aqueous sulfate concentrations, and thus very small changes in the denominator of the f factor, i.e., $\Delta\Sigma C_A$, the change in total strong acid ions. In some cases, this results in very large f factors, e.g., -25.1 to 35.2. Small changes in the numerator also resulted in some very small values of the f factor. The median was 0.56 for the 72 streams.

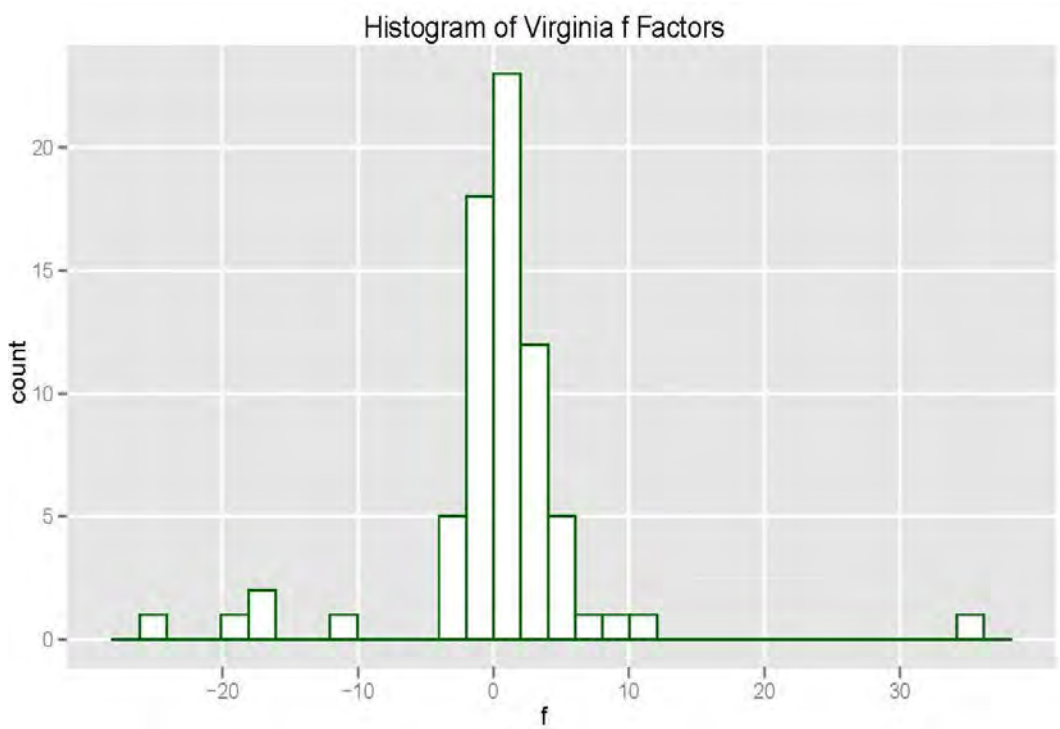

Figure 27: Distribution of f-Factor Values for the Virginia Trout Streams. The stream values of f vary widely from -25.1 to 35.2. The median value was about 0.56.

a)

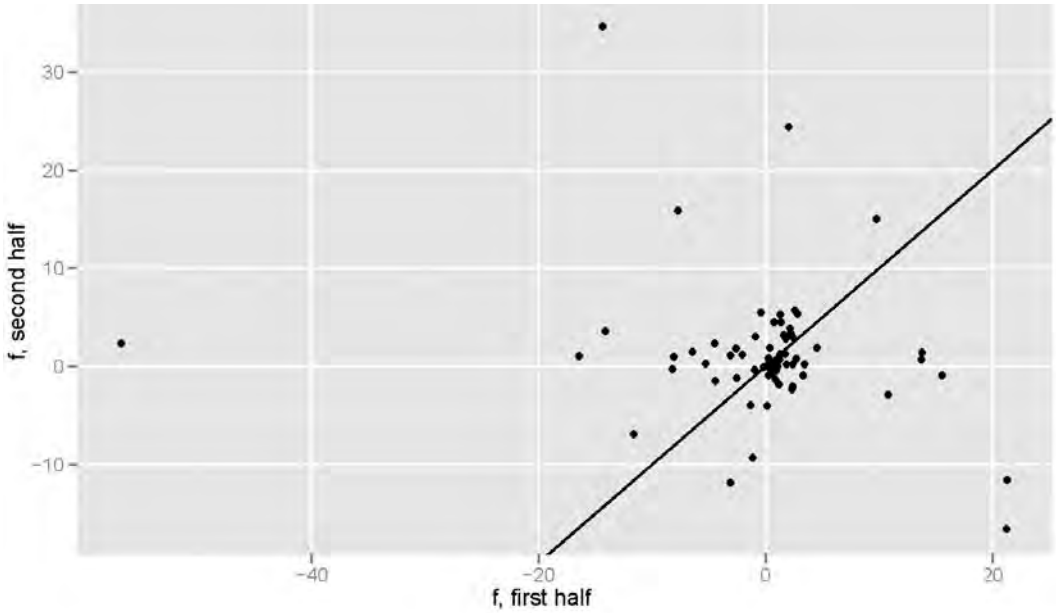

b)

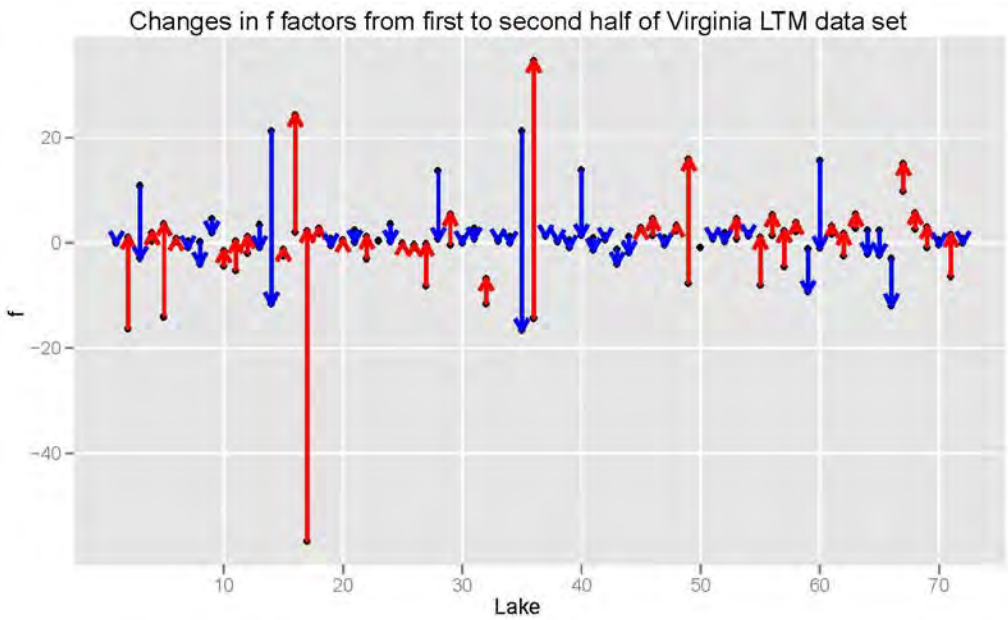

Figure 28: Changes in f-Factors from First to Second Half of Virginia Trout Streams Data Set: a) as Scatter Plot, and b) as Arrows Showing Direction of Change. Colored arrows show direction of change from initial half of data set to second half of data set. Red arrows indicate f factors that increased and blue indicate those that decreased. Note the changes in scale from Figures 25a and 25b.

Understanding System Response to Reductions in Deposition

As explained previously, the response of surface waters, including terrestrial systems, to decreases in deposition, depends on two things:

1) How the base cation supply from the terrestrial system changes with changing acid deposition input. Specifically, to what extent do soil mineral weathering and ion exchange reactions add more or less base cation to solution in response to increases and decreases in acid inputs?
2) The extent to which sulfate is removed from deposition by adsorption-desorption reactions with basin soils and (to a lesser extent) the loss of sulfate by biologically mediated sulfate reduction reactions ($SO_4^{2-} + 8\ e^- + 10\ H^+ \rightarrow H_2S + 4\ H_2O$).[2]

Many researchers mistakenly believed that the base cation supply rate would remain fairly constant and thus decreases in sulfate would result in a one-to-one increase in ANC.

We again focus on the two U.S. regions with the most data, the Adirondacks, and Virginia. These regions have also been the sites of the most research. Other areas have yielded interesting and important process insights, but have produced less data relative to these two.

Adirondacks

More acid deposition research and monitoring has been conducted in the Adirondacks than anywhere else in the United Staes. The Adirondacks is a mountainous region, encompassing about 6 million acres within the Adirondack Park boundary, located in upstate New York. The Adirondacks contains over 3,000 lakes with surface areas greater than one hectare. EPRI's original ILWAS project and its daughter project RILWAS were conducted here with a nine university team doing field and laboratory research: J. Galloway, University of Virginia; C. Schofield, Cornell University; G. Henderson of State University of New York; R. April, Colgate University; R. Newton, Smith College; Chris Cronan, Dartmouth University and University of Maine; A. J. Johannes. E. Altwicker, and N. Clesceri, Rensselaer Polytechnic University; C. Driscoll, Syracuse University; and J. Peters and D. Troutman, US Geological Survey.

C. Chen, S. Gherini, R.J.M. Hudson and J. Dean of Tetra Tech developed the ILWAS model for predicting the response of surface waters to changes in deposition acidity. R.A. Goldstein of EPRI managed the four-year investigation that collected over 600,000 data points for three lake-watershed systems and collected extensive data on several more hydrologic basins. The research produced over 40 peer reviewed papers. Major findings of the research include the importance of alkalinity (ANC) as a useful concept for predicting surface water acid-base behavior[3] and the importance of hydrologic flow path through watershed soils in determining lake response to acid deposition. In shallow soils, most of the precipitation and snow melt moved laterally through acidic soil layers. This resulted in less acid neutralization and lower ANC surface waters. Deeper, more alkaline soils yielded higher alkalinities (Goldstein et al., 1984).

The Adirondacks was also the site of the large ALSC sponsored systematic sampling of 1469 lakes. Analysis of the resulting data indicated that less than approximately 1.5 to 3 percent of the lakes were acidic from atmospheric deposition (ALSC, 1990) The results of field monitoring by EPA, EPRI, and others

[2] As noted in the next section and in previous comments, nitrogen is taken up to a large extent by most ecosystems.
[3] Although a useful concept, it is the application of ANC alone as a universal indicator of ecosystem sustainability for aquatic biota that raises serious scientific concerns as noted earlier. In particular, the use of single ANC level as an appropriate "ecological indicator" without consideration of other variables and stressors is inadequate.

in the Adirondacks has produced a recent 16 year set of lake data for 44 lakes. During this period there have been large reductions in NOx and SOx emissions and ensuing deposition fluxes.

For the Adirondack lakes, after large reductions in SOx and NOx emissions, sulfate water concentrations decreased an average of 34 µeq L^{-1} but experienced only a 5 µeq L^{-1} average increase in ANC (Figure 29). Some have claimed there must be a delay in the magnitude of the ANC increase due to sulfate adsorption-desorption by the soils. But measurements of adsorption-desorption properties in these systems and mass balances on sulfate showed sulfate adsorption-desorption to be minimal. The Adirondacks were glaciated less than 10,000 years ago leaving behind tills with very small amounts of sulfate adsorbing sesquioxides (See Sidebar 2 for simulations of sulfate adsorption behavior in both the Adirondacks and the southern Appalachians.)

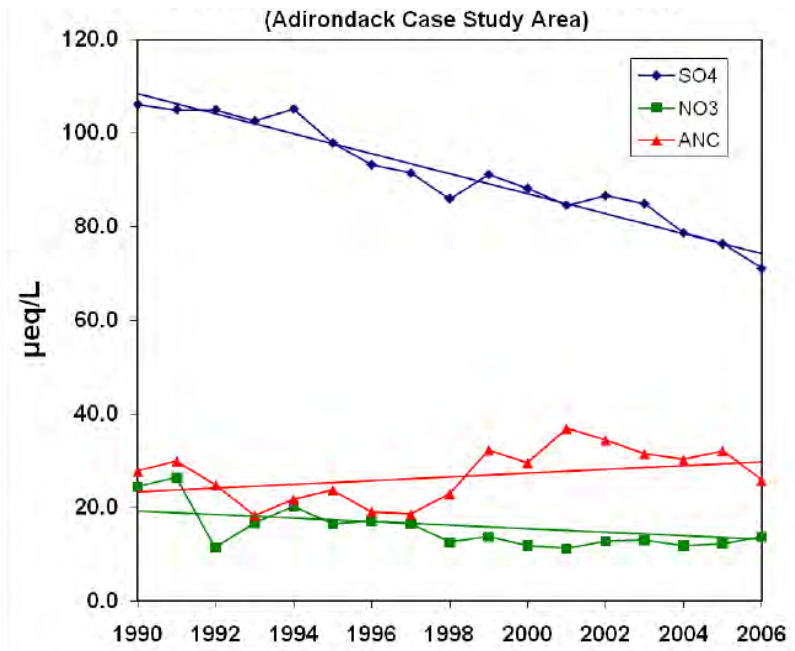

Figure 29: Annual Average Trends (1990-2006) in 44 Adirondack LTM Lakes for Sulfate, Nitrate, and Acid Neutralizing Capacity (EPA, 2009).

Sidebar 2: Sulfate Adsorption-Desorption by Soils

Hydrologic Routing Model

We prepared a simple hydrologic routing model to evaluate any lag due to flow routing and sulfate adsorption-desorption by soils. First, we simulated a case for conditions encountered in the Southern Appalachinans, where sulfate adsorption is large in the sesquioxide-laden soils, and then we examined an Adirondack basin.

Lag Simulation

As a check of how the concentration of the strong acid anion sulfate in a hydrologic basin might respond to decreasing sulfate deposition, we constructed a simple model of water routing in the basin. The principle of mass balance requires that for both the soil and the water

$$\frac{d(CV)}{dt} = \dot{\text{in}} - \text{out} \qquad \text{(a)}$$

where C is the sulfate concentration and V is the volume of the solution (lake/stream or soil water). First, we define some parameters for our basin. The surface area of the hydrologic basin is A, and the surface areas of the lake/stream and soil respectively are A_l and A_s. The average depth of the lake/stream and soil respectively are d_l and d_s. We denote a soil porosity θ. The bulk density of the soil is ρ. The soil absorbs sulfate reversibly, as quantified by an equilibrium equation

$$C_{soil} = K \cdot C_{solution} \,. \qquad \text{(b)}$$

The volumetric amount of rainfall per year is denoted Q_r and the amount of water leaving the watershed through evapotranspiration per year is Q_e; the net annual water flow through the watershed is taken to be $Q = Q_r - Q_e$.

Now we discuss some simplifying assumptions used in the model. Precipitation falls at a uniform rate both onto the soil and the lake. The lake remains well-mixed at all times. Rain falling onto the soil eventually passes into the lake after a flow-through time,

$$\tau = \frac{V_s}{Q} = \frac{d_s \theta A_s}{Q} \,. \qquad \text{(c)}$$

Conceptually, the water is moving in a plug-flow fashion through the soil as shown in Figure S-1, starting at the border of the watershed and ending in the lake. In reality, some precipitation will fall on the soil near the lake and not have to traverse the whole pathway, but the plug flow simplification made here will conservatively overestimate the lag in the system.

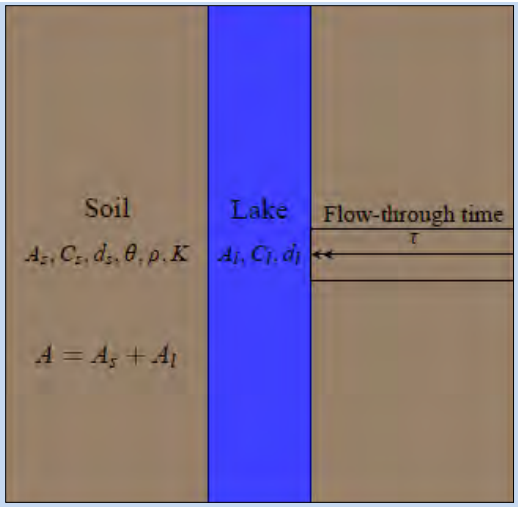

Figure S-1: The watershed.

Water flows out from the lake such that all volumes remain constant at all times. The flow of sulfate is shown below.

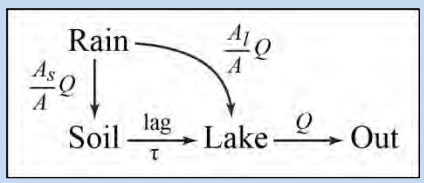

At the beginning of the simulation, the precipitation, soil, and lake have all reached a steady state with sulfate concentration, C_0. From there, the deposition flux decreases linearly, stopping at the value, $\frac{C_0}{2}$.

If $C_r, C_s,$ and C_l denote the sulfate concentrations in the precipitation, soil solution, and lake/stream, respectively, then, from equation (a), the system is governed by the differential equations

$$\frac{d(C_l V_l)}{dt} = (d_l A_l)\frac{dC_l}{dt} = \frac{A_l}{A} \cdot Q \cdot C_r(t) + \frac{A_s}{A} \cdot Q \cdot C_s(t-\tau) - Q \cdot C_l(t), \quad \text{(d)}$$

$$R_d \cdot \frac{d(C_s V_s)}{dt} = R_d(d_s \theta A_s)\frac{dC_s}{dt} = \frac{A_s}{A} \cdot Q \cdot C_r(t) - \frac{A_s}{A} \cdot Q \cdot C_s(t), \quad \text{(e)}$$

$$\frac{dC_r}{dt} = -m. \quad \text{(f)}$$

The R_d in the second equation is a consequence of equation (b): the change in concentration of the soil solution is retarded by a factor of $R_d = 1 + \frac{K_\rho}{\theta}$ due to reversible sulfate adsorption.

Southern Appalachian Mountains

We now run two examples with parameter values representing a typical basin for the Southern Appalachian Mountains, a region of moderate sulfate adsorption and the Adirondacks, a region of minimal sulfate adsorption. The values of the physical parameters for the basin representing the Southern Appalachian Mountains are $C_0 = 150\mu eq/L$ (high, but for comparison purposes), $A = 50ha$, $A_s = 0.98A$, $A_l = 0.02A$, $\theta = 0.25$, $d_l = 0.2m$, $d_s = 1m$, $Q_r = 1m\ ha/y$, $Q_e = \frac{1}{2}Q_r$, $K = 5$, and $\rho = 1.6m^3/kg$. As shown in Figure S-2, after the precipitation sulfate achieves 90% of its eventual total decrease, it takes the surface water concentration about 33 years to reach the same level.

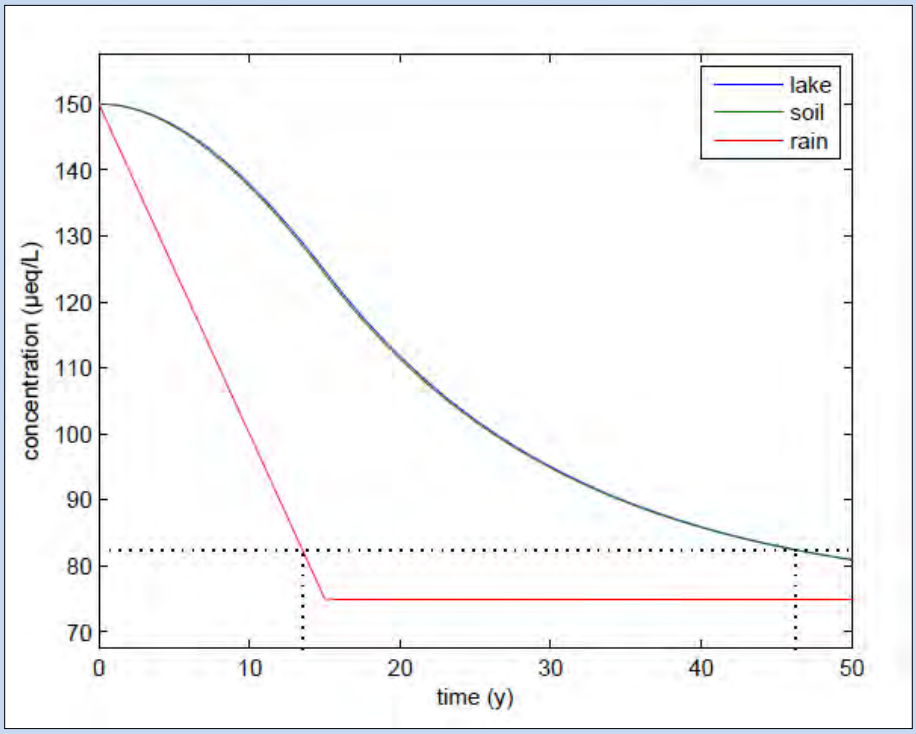

Figure S-2. Lake, soil, and precipitation sulfate concentrations in a basin representative of the Southern Appalachians Mountains. In this system with *significant* sulfate adsorption a lag of about 33 years exists before the surface water concentrations catch up (90 percent) to the change in sulfate deposition.

Adirondacks

To represent a basin in the Adirondacks, we used the parameter values $C_0 = 150\mu eq/L$, $A = 25ha$, $A_s = 0.80A$, $A_l = 0.20A$, $\theta = 0.25$, $d_l = 1.5m$, $d_s = 0.3m$, $Q_r = 1m\ ha/y$, $Q_e = \frac{1}{2}Q_r$, $K = 0.005$, and $\rho = 1.6m^3/kg$. Here, it only takes the lake about 0.82 year to reach 90% of the sulfate concentration reduction (see Figure S-3).

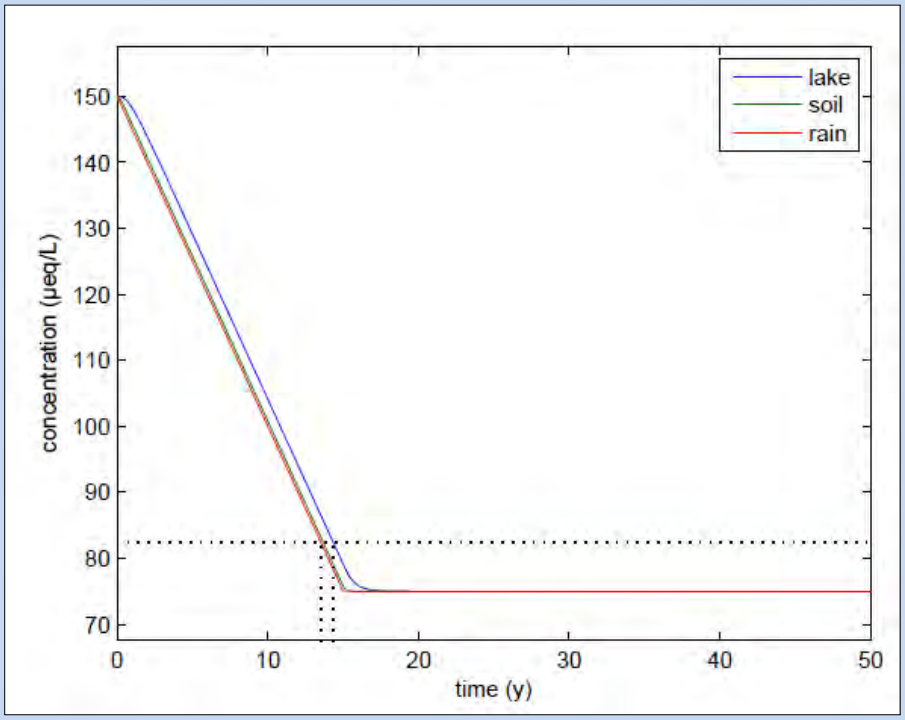

Figure S-3. Lake, soil, and precipitation sulfate concentrations in a basin representative of the Adirondack Mountains. In this system with minimum sulfate adsorption a lag of only 0.82 years exists before the lake concentrations catch up (90 percent) to a change in sulfate deposition.

Using field data for selection of the parameters and modeling, we have demonstrated that in the minimally-sulfate adsorbing basins of the Adirondacks, particularly in basins with thin soils (low ANC surface waters), lag times are very short at best. Thus, the results of sulfate deposition reductions will be manifested quickly, without a lag. Conversely, in basins with deeper soils and soils that strongly adsorb sulfate, the lag times can be 20 to 30 years or more.

Virginia Trout Streams

These water bodies are mostly small streams located predominantly in the mountainous western part of the state of Virginia, in the Shenandoah region (including Shenandoah National Park). Quarterly data are available from 1987 through 2008. These data were provided to EPRI by EPA in April 2011.

Using the acid-base theory discussed earlier we can examine what occurred in the Virginia Trout Streams. Again we used best fit linear curves of the actual data. The overall sulfate concentration decreased by only 2 µeq L^{-1} over the 21 years, nitrate decreased by 2 µeq L^{-1}, and ANC increased by 9 µeq L^{-1}. The increases in ANC were small, largely because the decrease in strong acid anion concentration was only about 4 µeq L^{-1}, This was also illustrated in the 16-year trends plotted by EPA in the Policy Assessment document, reproduced her as Figure 30 . This decrease would have been larger, except for the very small decrease in sulfate due to sulfate adsorption-desorption. Unlike the Adirondacks, this area was never glaciated. The soils and bedrock in western Virginia are some of the oldest in the U.S. and contain highly weathered material including the sesquioxides that provide ideal sites for sulfate adsorption and desorption.

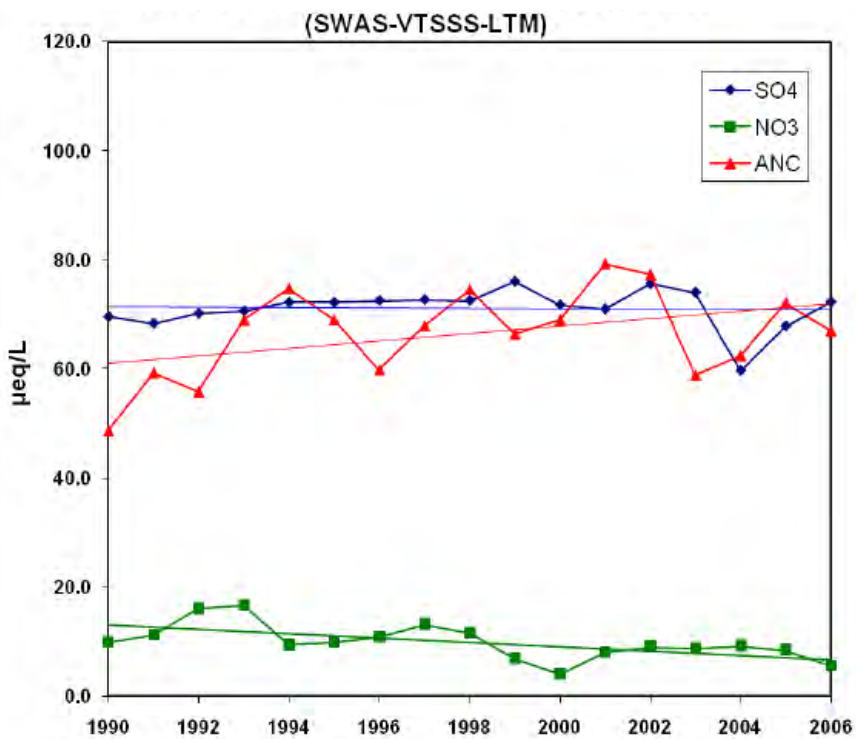

Figure 30: Annual Average Trends (1990-2006) in VTSSS LTM-monitored Streams for Sulfate, Nitrate, and Acid neutralizing Capacity (EPA, 2009).

These observations underscore the importance of additional research to understand the potential for additional acidification under current emissions and future emissions trends. Moreover, one must also evaluate the potential for recovery in these systems and corresponding response times so that we can properly adjust our expectations of recovery.

Atmospheric Nitrogen Deposition and Inorganic Nitrogen Fluxes in Ecosystems

The proposed approach to estimating critical loads considers sulfate and nitrate equally able to cause acidity, but then adds complexity to allow for some uptake of nitrate by vegetation and to consider the effect of ammonia deposition. The acidifying effect of nitrate is small compared to sulfate, since about 85 percent of nitrate is taken up by vegetation. To further assess this general observation, we looked at nitrogen behavior in detail. (EPRI comments to the second Policy Assessment Document also include additional discussion on nitrogen cycling in ecosystems.) In this section, we have analyzed various data sets. They confirm the finding that most nitrate is used by vegetation, and thus does not contribute to acidification of waterbodies.

The study of elemental cycles, both at the ecosystem level and globally, is a firmly established scientific discipline. Because of its importance as a plant nutrient, the cycle of nitrogen (N) has been intensively studied. The N cycle is complex, involving a multiplicity of oxidation states and resulting occurrences of N as a positive or negative ion in solution, in a variety of gases, and as a constituent of organic matter (Canfield et al, 2010). Alteration of the N cycle by man has been identified as a serious environmental issue (Galloway et al, 2003; Vitousek et al, 1997). Flux of dissolved inorganic N (DIN) from terrestrial ecosystems (DIN_{out}: primarily NO_3^-), resulting from atmospheric deposition (DIN_{in}: NO_3^- and NH_4^+), has been considered to be an important contributor to acidification of linked aquatic systems (Vitousek et al, 1997). The basis of this concern is the nitrogen saturation hypothesis, positing that additions of N to terrestrial ecosystems in excess of biological requirements will result in DIN leaching (Aber et al, 1988, 1999). Changes in DIN in linked aquatic systems conceptually fit the hypothesis (Stoddard, 1994).

Because N is commonly deficient or limiting in terrestrial ecosystems, any leaching loss is said to indicate a N-saturated ecosystem. Many authors have reported that DIN_{out} increases sharply at about 10 kg ha^{-1} y^{-1} DIN_{in}. For example, Driscoll et al (1989) suggested that data from sites primarily in eastern North America indicated N leaching at wet deposition greater than 400 mol ha^{-1} y^{-1} (5.6 kg ha^{-1} y^{-1}). If total atmospheric N deposition, including both wet plus dry, ranges from about 1.5 to 2 times wet deposition (Boyer et al, 2002), then this is equivalent to ~ 11 kg ha^{-1} y^{-1} total deposition. Analysis of those data and additional data led Stoddard (1994) to conclude that ~ 300 equiv ha^{-1} y^{-1} (4.2 kg ha^{-1} y^{-1}) of wet deposition was a "threshold value" (~ 8.5 kg ha^{-1} y^{-1} total deposition), above which substantial N leaching might begin to occur. Similarly, Aber et al (2003) reported a steep increase in N leaching (they used the termed "threshold") at total N deposition above about 7 kg ha^{-1} y^{-1} at low elevation sites (base of watersheds) in the northeastern U.S.; they inferred that was equal to 9 to 13 kg ha^{-1} y^{-1} deposition for the entire watershed. Based on data from 31 forested sites throughout the Northern Hemisphere, Johnson (1992) concluded that N inputs in excess of the requirement for vegetation increment resulted in a nearly 1:1 relationship between the excess N and DIN_{out}; the average N requirement in the 26 studies for which data were available was 10 kg ha^{-1} y^{-1}.

In data compilations from Europe, elevated DIN_{out} is rare below 10 kg N ha^{-1} y^{-1} in throughfall (a surrogate for wet plus dry deposition) (Dise and Wright, 1995; Gundersen et al, 1998; Kristensen et al, 2004; MacDonald et al, 2002; Nilsson et al, 1998). Above that input, rates of DIN_{out} exceed 5 kg ha^{-1} y^{-1}.

These observations have led to the suggestion that a "threshold" for elevated DIN_{out} occurs at about 10 kg ha^{-1} y^{-1} DIN_{in} in both Europe and North America (Gunderson et al, 2006).

By the same criterion that defines N saturation, virtually all terrestrial ecosystems are also calcium-, magnesium, and potassium-saturated. Although those elements are essential plant nutrients, they also leach from terrestrial ecosystems, sometimes in excess of inputs. This leaching even occurs in ecosystems that are considered to have base cation deficiency. Although DIN does leach from some terrestrial systems, their developmental history, including disturbances, affect the magnitude of leaching. For example, Bernhardt et al (2005) discuss the linkage between DIN_{out} and a variety of factors, including a severe drought, severe insect defoliation, soil freezing, a severe ice storm, and floods, all in the context of a single "undisturbed" watershed at Hubbard Brook, New Hampshire. Similarly, in their review of the literature, Ito et al (2005) cite many factors that influence N retention or loss from watersheds, including hydrology, vegetation type, land-use history, wetland cover, N-fixing plants, and hydraulic residence time.

The issue of N leaching from terrestrial to aquatic systems has regulatory importance. The Final Policy Assessment document stressed the importance of N_{eco} (the amount of atmospheric N deposition that is effectively retained by terrestrial ecosystems) because it *does not* contribute to aquatic acidification. If N_{eco} is large, DIN deposition would not have a significant effect on aquatic acidification. Conceptually, N inputs to a terrestrial system (DIN_{in}) are equal to the sum of N_{eco} and DIN_{out}.

The purpose of this study was to explore DIN_{in} and DIN_{out} data from past or existing studies. The first objective was to document the spatial and temporal variation in those data, but especially in DIN_{out}. The second objective was to examine the $DIN_{in} - DIN_{out}$ relationship, and especially the presence or absence of a threshold of increased leaching beyond about 10 kg ha^{-1} y^{-1} DIN_{in}.

Methods

Data Sets

Three different datasets were used. Data were obtained from published literature, personal communication, and datasets available on the Internet. In some cases, data were derived directly from tables within reports, and in other cases data were extracted from figures. Analysis was restricted to data from watersheds in the U.S., and concentrated on DIN, not on other forms of N such as dissolved organic N. The first dataset consisted of input-output budgets for DIN for eight forested watersheds. The relatively small watersheds, all termed control or reference watersheds, are located throughout the U.S. (Table 6). They are all considered to be free from recent anthropogenic vegetation disturbance, but some anthropogenic disturbance is likely for nearly all watersheds in the continental United Sates. This group will be referred to as the *intensive* dataset.

Table 6: Details of Watershed Data from the Intensive Sites

State	Dates	Area (ha)	Location	Watershed	Data Source
AK	1986, 2001–2003	520	Poker Creek	C2	Jones et al. 2005
ME	1988–2008	11	Bear Brook	EB	Fernandez 2010[a]
MN	1980–2007	9.2	Marcell	S2	Sebestyen 2010[b]
NC	1979–2007	13	Coweeta	WS18	Knoepp 2010[c]
NH	1979–2001	13	Hubbard Brook	W-6	Bernhardt et al. 2005
OR	1980–2009	8.5	Andrews	WS9	Johnson and Fredriksen 2010
TN	1991–2002	38.4	Walker Branch	W Branch	Mulholland 2004
WV	1982–2003	39	Fernow	WS4	Adams 2010[d]

[a] Dr. Ivan J. Fernandez, University of Maine, personal communication, 17 October 2010
[b] Dr. Stephen D. Sebestyen, USDA Forest Service, personal communication, 3 November 2010
[c] Dr. Jennifer D. Knoepp, USDA Forest Service, personal communication,16 November 2010
[d] Dr. M.B. Adams, USDA Forest Service, personal communication, 28 October 2010

The second dataset was obtained primarily from published reports, and also included data from other watersheds that lay in the same study area(s) as the intensive dataset. The result was an eclectic group (Table 7). Some data were multi-year summaries of a suite of watersheds. For example, Campbell et al (2004) summarized input-output budgets for DIN for 24 small watersheds at 15 locations in the northeastern United States. Similarly, Kane et al (2008) investigated long-term and seasonal patterns of N imports and exports across biomes using data from 15 watersheds from 9 National Science Foundation-funded Long Term Ecological Research sites in North America. Other studies were focused on small geographic areas, either multi-year (e.g., annual N input-output budgets for 52 lake-containing watersheds in the Adirondack region from 1998 to 2000 – Ito et al, 2005) or single-year (e.g., 13 forested catchments in the headwaters of the Upper Susquehanna River – Goodale et al, 2009). These data will be referred to as the *extensive* dataset.

Table 7: Data Sources Included in the Extensive Dataset

State	Watersheds	Data Source
AK	2	Jones et al. 2005
CA	7	Meixner and Fenn 2004
CA	6	Riggan et al. 1994
MD	8	Groffman et al. 2004
NC	2	Brookshire et al. 2010
NC	1	Knoepp 2010 [a]
NH	25	Goodale et al. 2000
NY	13	Goodale et al. 2009
NY	2	Lovett et al. 2000
NY	52	Ito et al. 2005
OR	6	Johnson and Fredriksen 2010
OR	27	Compton et al. 2003
PA, MD, WV	9	Williard et al. 1997
WV	7	Adams 2010 [b]
Varied	24	Campbell et al. 2004
Varied	30	Driscoll et al. 1989
Varied	13	Kane et al. 2008

[a] Dr. Jennifer D. Knoepp, USDA Forest Service, personal communication,16 November 2010
[b] Dr. M.B. Adams, USDA Forest Service, personal communication, 28 October 2010

The third data set was from the United States Geological Survey National Water-Quality Assessment Program (USGS 2010). Data include annual N inputs from a variety of nonpoint sources, including wet atmospheric deposition, and N outputs, including DIN, from 499 stream sites in 51 major river basins and aquifer systems, with watersheds ranging in size from 2.3 to 220,000 km^2 and a median size of 1190 km^2. This will be referred to as the *USGS* dataset.

Atmospheric Deposition

All the data included measurements of DIN_{out}, but their treatment of DIN_{in} varied. Some reports simply did not include those data. In other cases, DIN_{in} was wet deposition reported from a co-located National Atmospheric Deposition Program/National Trends Network (NADP/NTN) monitoring site. In other cases, precipitation was assumed to have a constant DIN concentration and volume was estimated by a model (Goodale et al, 2000). In others, modeling was used to estimate both concentration and volume (Ito et al, 2005). In yet others, concentration was measured at one location and volume at multiple locations (Swank and Vose, 1997). Total deposition (wet and dry) was estimated by throughfall (Adams et al, 1997), in some cases weighted by canopy cover (Meixner and Fenn, 2004). For some data, estimates of wet and dry deposition were based on a nearby U.S. EPA Clean Air Status and Trends Network site and the National Oceanic and Atmospheric Administration's Atmospheric Integrated Research Monitoring Network (Goodale et al. 2009).

To place all data on a common basis, we retrieved annual wet N deposition data from the NADP/NTN website (NADP, 2010). We used the NADP/NTN data for the year(s) and from station(s) nearest the

watershed with reported DIN_{out} to estimate DIN_{in}. Dry deposition is not included, and is assumed to be about equal to wet deposition (Boyer et al, 2002). There can also be elevation-related differences in volume of precipitation (Goodale et al, 2000) and potentially in concentration, resulting in greater deposition at higher elevations compared to valleys (the location of most NADP stations). As a result, the DIN_{in} used in this analysis is assuredly an underestimate of atmospheric N inputs. Because N retention is calculated as the difference between DIN_{in} and DIN_{out}, underestimation of DIN_{in} will also lead to underestimation of retention.

Data Screening

To calculate spatial and temporal variability, all applicable data were used. Some data were eliminated in the examination of the $DIN_{in} - DIN_{out}$ relationship. All of the data in the intensive dataset were used (171 pairs of input-output data), but in the extensive and USGS datasets, cases where DIN_{out} was greater than DIN_{in} (there was apparent net production of N in the system) were eliminated. Most of these cases were explicable, including the effects of post-fire erosion (Riggan et al, 1994), loss of N stored in discontinuous permafrost (Jones et al. 2005), N-fixing species in the watershed (Compton et al. 2003), and additional N inputs via urban and agricultural fertilization (Groffman et al, 2004). In the USGS dataset, other nonpoint sources of N, including farm and non-farm fertilizer and manure, potentially obscured any relationship between atmospheric deposition and DIN_{out}. For that dataset, only observations from watersheds where greater than 1/3 of the N inputs were from wet atmospheric deposition were used. If wet and dry depositions are about equal, then half the N input to these watersheds is from the atmosphere. After screening, the extensive dataset contained 474 input-output pairs of data, and the USGS dataset contained 97 pairs.

After removal of the 8 cases where DIN_{out} was greater than DIN_{in} in the intensive dataset, the screened data were aggregated into a *combined* dataset. Because the data came from varied sources, there may be some duplication for specific watersheds, but it is unlikely that exactly the same time periods would be duplicated. There is a bias in the data toward the eastern and especially the northeastern U.S. (Table 6 and Table 7) as a reflection of the research interests and funding of scientists in that region.

Statistical Analysis

All statistical analyses were conducted using SYSTAT (2007). A subset of data from small watersheds falling in close proximity of one another for a single year of observation was used to determine spatial variation. This included data from Goodale et al (2000), Goodale et al (2009), Ito et al (2005), and Compton et al (2003), all of whom presented data from multiple small watersheds for a single year. Data for multiple years from multiple watersheds within experimental forests were available for H.J Andrews Experimental Forest (Johnson and Fredriksen 2010), the Fernow Experimental Forest (Dr. M.B. Adams, USDA Forest Service, personal communication, 28 October 2010), the Coweeta Experimental Forest (Dr. Jennifer D. Knoepp, USDA Forest Service, personal communication, 16 November 2010; Brookshire et al. 2010), and Poker Creek (Jones et al. 2005). Variation in DIN_{out} for the single year of observation was computed for the former set; variation in DIN_{out} due to differences among watersheds, holding year constant, was calculated for the experimental forests. Both estimates of variation were used to determine a pooled standard deviation (SD) and coefficient of variation (CV = standard deviation divided

by the mean). Temporal variation in DIN_{out} as inter-annual variation within watersheds in the intensive dataset was calculated and used to determine pooled SD and CV (Table 6).

The relationships between DIN_{in} and DIN_{out} were examined for the intensive dataset, the extensive dataset, the USGS dataset, and the combined dataset. Linear regression

$$DIN_{out} = A + DIN_{in} \times B \qquad \text{Equation 6}$$

and nonlinear regression were used. In the latter case, both the power function

$$DIN_{out} = A \times DIN_{in}^{\ B} \qquad \text{Equation 7}$$

(e.g., Dubrovsky et al, 2010) and the exponential function

$$DIN_{out} = A \times \exp(DIN_{in} \times B) \qquad \text{Equation 8}$$

(e.g., Castro et al, 2001) have been used to represent relationships between DIN_{in} and DIN_{out}, and were used in this analysis. In all cases, the parameters *A* and *B* were determined by least-squares techniques.

To determine the robustness of the estimated parameters for the combined dataset, 50 sets of 500 observations each were randomly selected—in each case about 70% of the total—and the relationship between DIN_{in} and DIN_{out} for each of those sets was described by the power function.

Results and Discussion

Variation

The DIN_{out} data were highly variable in both space and time. The pooled SD between small watersheds falling in close proximity for a single year of observation was about 2.1 kg ha^{-1} y^{-1}. Mean DIN_{out} ranged over an order of magnitude, from 0.05 to over 13 kg ha^{-1} y^{-1} (Table 8). Because of this wide range, the CV may be a better overall basis for comparison. The pooled CV of DIN_{out} was 0.96, nearly equal to the mean.

This high spatial variation is not surprising. The CVs in the data from the experimental forests were higher than those from single years of observation (Table 8). In these forests, the watersheds have been subjected to varying experimental treatments and were located in a variety of landscape positions with different microclimates and vegetation. The results illustrate that "average" DIN_{out}, even for a very small geographic area, is highly variable. Based on this spatial variation, for any single year over 350 observations would be required to estimate DIN_{out} within 10% of the mean at the 95% confidence interval for watersheds within a proximate area.

Table 8: Summary Statistics for Watersheds used to Evaluate Spatial Variation in DIN_{out}.

State	Watersheds	Mean	SD[a]	CV[b]	Data Source
		kg ha^{-1} y^{-1}	kg ha^{-1} y^{-1}		
AK	3	0.73	0.49	0.67	Jones et al. 2005
NC	4	0.25	0.30	1.21	Knoepp 2010[e]; Brookshire et al. 2010
NH	25	0.82	0.63	0.77	Goodale et al. 2000
NY	13	0.36	0.15	0.42	Goodale et al. 2009
NY	52	2.37	1.09	0.46	Ito et al. 2005
OR	7	0.05	0.16	3.35	Johnson and Fredriksen 2010
OR	27	13.67	0.92	0.07	Compton et al. 2003
WV	8	4.84	8.19	1.69	Adams 2010[f]
All	139	4.02[c]	2.07[d]	0.96[d]	

[a] Standard deviation among watersheds
[b] Coefficient of variation among watersheds
[c] Mean of all watersheds
[d] Pooled value
[e] Dr. Jennifer D. Knoepp, USDA Forest Service, personal communication,16 November 2010
[f] Dr. M.B. Adams, USDA Forest Service, personal communication, 28 October 2010

Temporal (inter-annual) variation in $DIN_{out,}$ based on the intensive dataset from small reference watersheds, was also high (Table 9). The SD varied more than an order of magnitude, from less than 0.1 to more than 1 kg ha^{-1} y^{-1}, with a pooled SD of 0.75 kg ha^{-1} y^{-1} and a pooled CV of 0.72 (Table 9). Average DIN_{in} (wet) ranged from less than 1 to more than 6 kg ha^{-1} y^{-1} in this dataset (Table 9), and its inter-annual variation is about the same as that of DIN_{out}; a pooled SD of 0.84 kg ha^{-1} y^{-1} (Table 9). However, because of the higher means for DIN_{in}, its pooled CV is only about one-third that of DIN_{out}; 0.21 (Table 9).

Table 9: Summary Statistics for Watersheds used to Evaluate Inter-annual Variation in DIN_{out} and DIN_{in}.

State	Years	DIN_{in}				DIN_{out}			
		Mean	Median	SD[a]	CV[b]	Mean	Median	SD[a]	CV[b]
		kg ha^{-1} y^{-1}	kg ha^{-1} y^{-1}	kg ha^{-1} y^{-1}		kg ha^{-1} y^{-1}	kg ha^{-1} y^{-1}	kg ha^{-1} y^{-1}	
AK	4	0.26	0.24	0.09	0.35	0.76	0.75	0.24	0.31
ME	21	3.60	3.57	1.06	0.29	0.60	0.28	0.77	1.27
MN	25	3.95	3.85	0.60	0.15	0.27	0.21	0.18	0.64
NC	29	4.55	4.57	0.80	0.18	0.10	0.09	0.04	0.41
NH	23	5.11	5.08	0.76	0.15	1.30	1.03	0.95	0.73
OR	30	0.93	0.89	0.23	0.25	0.04	0.02	0.03	0.90
TN	12	5.12	5.27	0.80	0.16	0.27	0.25	0.07	0.28
WV	22	6.50	6.38	1.30	0.20	5.08	5.29	1.51	0.30
All	171	4.03	4.23	0.84[c]	0.21[c]	1.15	0.23	0.75[c]	0.72[c]

[a] Standard deviation
[b] Coefficient of variation
[c] Pooled value

The high inter-annual variation in DIN_{out} may not be surprising because of the many known and unknown causal factors cited in the Introduction, but it is important to note its magnitude at about three-fourths of the mean for small, undisturbed control watersheds. Expansion of that population to the broader range of terrestrial watersheds will certainly increase the variation. This high variation also has significant implications for estimation of N_{eco}. The pooled CV of the difference between DIN_{in} and DIN_{out} (= N_{eco}), using formulae for propagation of variance, is about 0.7, and direct computation from the data yields a pooled CV of similar magnitude (0.6). Even if data are averaged over 3- or 5-year periods to reduce variability, the variation remains at about 30% of those averages. A 95% confidence interval of retention, based on this pooled CV, would span a wide range (0.4 times the mean to 1.6 times the mean – a fourfold range). Based on existing data, watershed input-output budgets for DIN have high uncertainty.

Functional Relationships

All three functional forms explained similar amounts of the variation (30 to 40%) in the relationships between DIN_{in} and DIN_{out} (Table 10). The shape of both nonlinear functions is similar, and because the power function explained slightly more of the variation, passed through the origin (therefore, if DIN_{in} = 0, DIN_{out} = 0), and because it can assume a near-linear shape, it will be emphasized in the discussion. One reason for the relatively low explanatory powers of the relationships is that the data include both spatial and temporal variability. Because temporal variability was quantified in the intensive dataset, it can be mathematically removed from that system. If the variation due to inter-annual fluctuations is subtracted, the power function explains over half of the remaining variation (0.58) between DIN_{in} and DIN_{out} in that dataset.

Table 10: Linear or Nonlinear Solutions to Functions Relating DIN_{in} (independent variable) to DIN_{out} (dependent variable).

Dataset	Function	*A*[a]	*B*[b]	R^2	n	$MSE^{½}$ [c]
Intensive	**Linear**	-1.043	0.544	0.32	171	1.57
Extensive	**Linear**	-0.297	0.327	0.31	474	1.18
USGS	**Linear**	-0.588	0.341	0.34	97	2.25
Combined	**Linear**	-0.399	0.343	0.34	734	1.42
Intensive	**Power**	0.018	2.689	0.43	171	1.44
Extensive	**Power**	0.119	1.464	0.32	474	1.18
USGS	**Power**	0.110	1.381	0.35	97	2.24
Combined	**Power**	0.168	1.256	0.35	734	1.42
Intensive	**Exponential**	0.171	0.413	0.41	171	1.48
Extensive	**Exponential**	0.283	0.278	0.30	474	1.20
USGS	**Exponential**	0.591	0.136	0.34	97	2.27
Combined	**Exponential**	0.583	0.144	0.29	734	1.49

[a] Parameter *A* in Eq. [6], [7], or [8
[b] Parameter *B* in Eq. [6], [7], or [8]
[c] Square root of residual mean square error, equal to standard error of estimate in a linear model

The parameters and hence the shape of the relationships for the extensive dataset, the USGS dataset, and the combined dataset were similar; the latter similarity is not surprising because it was an inclusive dataset (Table 10). However, the relationship for the intensive dataset differed, and DIN_{out} increased sharply beyond about 5 kg ha^{-1} y^{-1} wet deposition, related to the higher *B* parameter (Table 10). The 95% confidence intervals of that *B* do not overlap those from any of the other datasets, although the *B*s in the latter group overlap one-another. Examination of those data indicated that the shape of the function was strongly influenced by data from Watershed W-6 at Hubbard Brook, NH (Bernhardt et al. 2005), and from Watershed WS4 at Fernow Experimental Forest, WV (Dr. M.B. Adams, USDA Forest Service, personal communication, 28 October 2010). In a comprehensive analysis of water chemistry data from more than 300 small (generally < 250 ha) forested watersheds throughout the U. S., Ice and Binkley (2003) found highest DIN concentrations from hardwood forests of New Hampshire, mixed hardwood forests in West Virginia, and alder-dominated forests in Oregon. These correspond to the DIN_{out} – DIN_{in} data in the intensive dataset from Bernhardt et al (2005) and Adams (Dr. M.B. Adams, USDA Forest Service, personal communication, 28 October 2010), and in the extensive dataset from Compton et al. (2003), respectively.

These data appear to be outliers to the national patterns. The data from Compton et al (2003) are assuredly affected by presence of N-fixing red alder (*Alnus rubra* Bong.) in those watersheds. Reasons for higher flux from the other two locations are more speculative. In the case of the New Hampshire forests, the dominance of sugar maple (*Acer saccharum* Marshall) in those forests is likely to be a causal factor. In a review of the literature, Lovett and Mitchell (2004) report that forest stands dominated by sugar maple tend to have high rates of nitrification and nitrate leaching to surface waters. The mixed hardwood forests in West Virginia, including the Fernow site, have historically received some of the highest levels of atmospheric N deposition in the U.S. (Adams et al, 2004), and these chronic additions may have influenced N leaching. However, the composition of these forests have been profoundly changed by the demise of American chestnut (*Castanea dentata* (Marsh.) Borkh.) due to chestnut blight (*Cryphonectria parasitica*) during the first half of the 20th century. Chestnut was a major component of those forests (Adams et al, 2006), and its virtual elimination and replacement by other tree species undoubtedly profoundly changed nutrient cycling in those forests.

The larger number of observations in the combined dataset overwhelms the influence of those unique watersheds in affecting the shape of the relationship (Table 10). A visual inspection of the combined relationship shows that it is nearly linear, with approximately 75% retention of wet deposition up to 8 kg ha^{-1} y^{-1} wet deposition (Figure 31). If dry deposition is approximately equal to wet deposition, then 85% of total deposition is retained. To place this in context, the frequency distribution of average DIN_{in} for the period 2004 to 2008 for all NADP/NTN stations in the eastern forested U.S shows a near-normal distribution with mean = 4 kg ha^{-1} y^{-1} and 97% of the observations less than 6 kg ha^{-1} y^{-1} (Figure 32). During that same period, DIN_{in} declined at a significant rate of 0.13 kg ha^{-1} y^{-2} ($F(1,95) = 24.4$, *prob.* = 0.0).

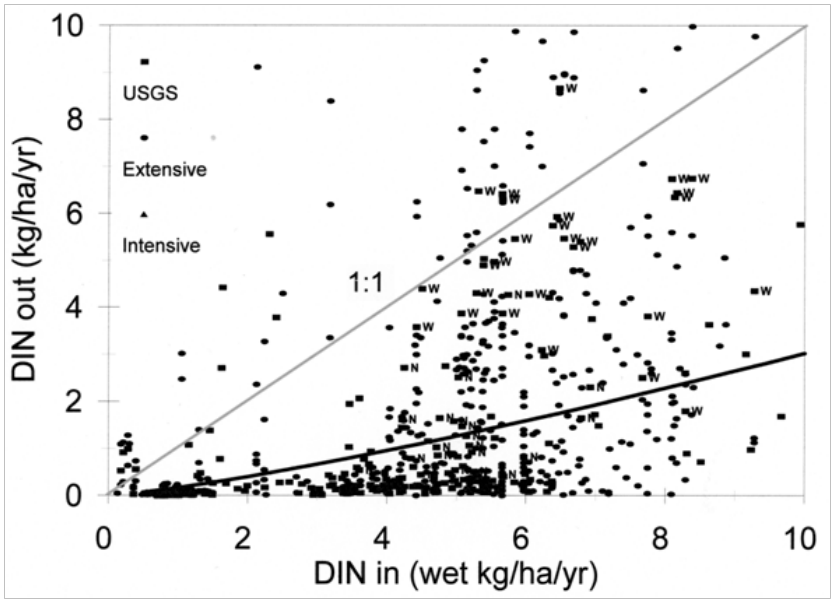

Figure 31: Relationship between DIN_{in} and DIN_{out}, Described by the Power Function, for the Combined Dataset. Points above the 1:1 line indicate net production of DIN in the watershed, and were not used in the regression. Observations that influenced the shape of the function for the intensive dataset from watersheds W-6 at Hubbard Brook, NH (=N) and WS4 at Fernow Experimental Forest, WV (=W) are also indicated. Detailed statistics in Table **10**.

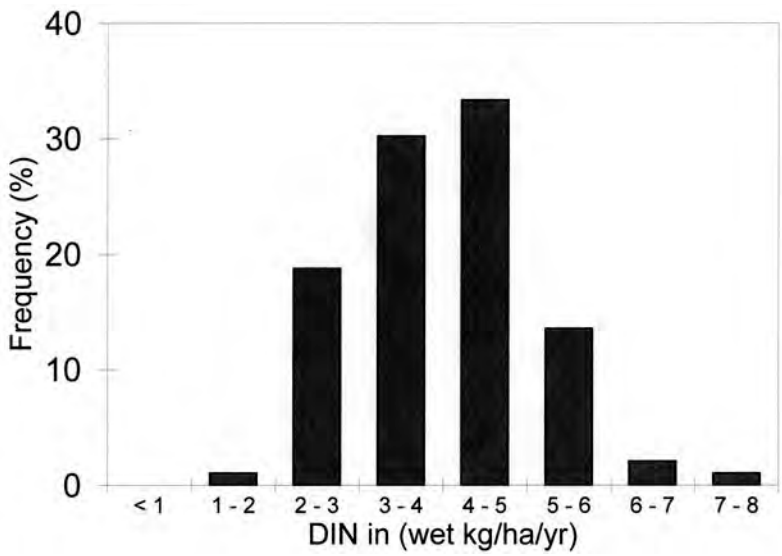

Figure 32: Frequency Distribution of Average DIN_{in} for the Period 2004 to 2008 for all NADP/NTN Stations in the Eastern Forested U.S. (AL, CT, DE, FL, GA, KY, MA, MD, ME, NC, NH, NJ, NY, PA, SC, TN, VA, VT, WV) (96 stations, 468 observations).

Determination of parameters for descriptive relationships between observed variables are fraught with difficulties related to the uncertainty in the variables (described earlier), the representativeness of the dataset, and, especially in the case of nonlinear relationships, statistical vagaries such as initial estimates in the iterative nonlinear estimation procedure. Based on the results of the analysis of the 50 randomly-selected datasets, the estimated parameters in the power function for the combined dataset (Table 10) were robust. Mean values for *A* (0.164) and *B* (1.278) over the 50 datasets were both very similar to the overall estimates (Table 10), and both means had low CVs (0.20; 0.08, respectively). The two parameters from the 50 datasets were linearly related (R^2= 0.96, *prob.* = 0.0). Importantly, the estimated retention

of DIN_{in} using the parameters determined for the combined dataset (Table 10) or the pairs of parameters from the random datasets with minimum *A* and maximum *B* or with maximum *A* and minimum *B* was very similar over the realistic range of wet deposition (Table 11).

Table 11: Estimated retention of DIN_{in} using either parameters determined from the combined dataset or the pair of parameters with minimum *A* and maximum *B* or that with maximum *A* and minimum *B* from the random datasets.

Deposition ($kg\ ha^{-1}\ y^{-1}$)		Combined Data		Minimum *A*, Maximum *B*		Maximum *A*, Minimum *B*	
		A	B	A	B	A	B
		0.168	1.256	0.100	1.551	0.264	1.007
		Proportional Retention					
Wet	Total[a]	of wet	of total	of wet	of total	of wet	of total
1	2	0.83	0.92	0.90	0.95	0.74	0.87
2.5	5	0.79	0.89	0.83	0.92	0.73	0.87
5	10	0.75	0.87	0.76	0.88	0.73	0.87
7.5	15	0.72	0.86	0.70	0.85	0.73	0.87
10	20	0.70	0.85	0.64	0.82	0.73	0.87

[a] assuming wet and dry deposition are equal

The analysis presented here does not support the concept of thresholds with respect to the relationship between DIN_{in} and DIN_{out}, at least at realistic levels of DIN_{in}. The relationship for the combined dataset, based on over 700 input-output budgets for DIN for watersheds around the U.S., indicate a nearly linear retention of over 85% of wet plus dry DIN_{in} (Table 10, Figure 31). Our results are surprisingly similar to those from the analysis of the USGS data by Dubrovsky et al. (2010). They reported that N flux from watersheds increased with increasing N inputs, regardless of land use. Analysis of the accompanying log-log figure indicates a linearized logarithmic fit to the data (indicated by the asymmetrical confidence intervals), with the best-fit line a power function with $A = 0.15$ and $B = 1$ (equivalent to a linear function with intercept of 0 and slope of 0.15). Stream flux of N is about 15% of N inputs; a retention of 85%. However, in the USGS data stream flux includes both dissolved DIN and organic (Kjeldahl) N, and N inputs, from all nonpoint sources, is predominantly from non-atmospheric sources (median = 22.8 kg $ha^{-1}\ y^{-1}$) compared to that from atmospheric wet deposition (median = 3.9 kg $ha^{-1}\ y^{-1}$). Our results estimate nearly exactly the same retention (Table 11), but in our case the dominant or only source of N to watersheds is atmospheric deposition.

Over half the input-output observations in the combined dataset indicate more than 95% (90% wet) and over two-thirds indicate more than 90% (80% wet) retention of DIN_{in}. When the observations are compared to the functional relationship (Figure 31), over 85% of the observed DIN_{out} is either less than or falls within the range of the predicted $DIN_{out} \pm MSE^{½}$. These watersheds span a wide geographic range and size (from < 10 to > 30 x 10^5 ha).

Summary

An examination of large and diverse data from published literature, personal communication, and web sites, indicates two characteristics of DIN flux from terrestrial watersheds. First, it is highly variable in both space and time. Even averages over multiple sites or years have high uncertainty. The second characteristic is that terrestrial ecosystems retain a very high proportion of atmospheric N deposition. The near linearity of the relationship between wet DIN_{in} and DIN_{out} at current levels of deposition provides no evidence of a 10 kg ha^{-1} y^{-1} threshold leading to significant flux. Retention of 85% to 95% or more of DIN_{in} by terrestrial watersheds calls into question the importance of DIN as a contributor to acidification of aquatic systems except in a few very rare cases. The nitrogen saturation hypothesis may not fully explain N behavior in terrestrial ecosystems.

Atmospheric Models and Model Evaluation

The conceptual design of the new secondary NAAQS proposed by EPA is presented in a simplified form in Figure 33 (Figure 7-1 in the Policy Assessment Document), which consists of three main components: (1) linkage between ecological indicators and ecological effects; (2) linkage between an ecological indicator and atmospheric deposition; and (3) linkage between deposition and ambient air indicators.

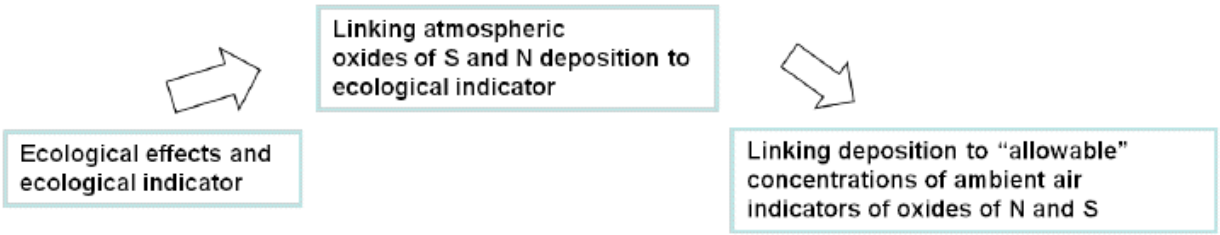

Figure 33: Conceptual design of the form of an aquatic acidification standard for oxides of nitrogen and sulfur (EPA, 2011).

To link atmospheric deposition to the ecological indicator, ANC (middle blue box in Figure 33), EPA proposed to use ecosystem acidification models that quantify the relationship between deposition of nitrogen and sulfur and the resulting ANC in surface waters based on an ecosystem's inherent generation of ANC and ability to neutralize nitrogen deposition through biological and physical processes.

The linkage between deposition and ambient concentrations of NOy and SOx (right blue box in Figure 33) introduces a new quantity termed as Transference Ratio (T) which is defined as the ratio of total wet and dry deposition to concentration:

$$\mathrm{TSO_X} = \frac{\mathrm{Dep(SO_X)}}{[\mathrm{SO_X}]}$$

$$\mathrm{TNO_Y} = \frac{\mathrm{Dep(NO_Y)}}{[\mathrm{NO_Y}]}$$

where $\mathrm{Dep(SO_X)}$ and $\mathrm{Dep(NO_Y)}$ are the annual total wet and dry deposition of SOx or NOy, respectively, and $[\mathrm{SO_X}]$ and $[\mathrm{NO_Y}]$ are the annual average concentrations of ambient SOx or NOy, respectively. EPA proposed to use EPA's Community Multiscale Air Quality (CMAQ) modeling system to calculate these Transference Ratios. We have evaluated different chemical transport models for their ability to accurately estimate the components of these transference ratios. We also evaluated the variability in the estimates of the ratios within ecoregions or case-study areas *and* across different modeling systems, simulations (different meteorology and/or different emissions), and model configuration (e.g., grid resolution).

Modeling Databases and Monitoring Networks

Modeling Databases

Several chemical transport model simulation outputs were selected for a rigorous model performance evaluation for depositions and ambient concentrations of oxides of sulfur and nitrogen. A model simulation needs to meet two conditions to be included in the performance evaluation: (1) since the new secondary NAAQS considered by EPA is based on annualized depositions and ambient concentrations, the modeling period should cover at least a year; (2) both the concentration and deposition outputs should be available. Since many of the historical model runs were performed to address concentration-related issues (e.g., ozone, $PM_{2.5}$ and regional haze SIPs), the deposition outputs were not archived in several past modeling databases.

Table 12 summarizes the modeling datasets included in this study. The compiled datasets show variations in the model, emission/meteorological modeling year and grid resolution used.

Chemical Transport Models

A brief description for each of the chemical transport models used in this study is given here.

CAMx

The Comprehensive Air Quality Model with Extensions (CAMx) modeling system is a state-of-science 'One-Atmosphere' photochemical grid model capable of addressing ozone, particulate matter (PM), visibility and acid deposition at regional scale for periods up to one year (ENVIRON, 2010). CAMx is a publicly available open-source computer modeling system for the integrated assessment of gaseous and particulate air pollution. Built on today's understanding that air quality issues are complex, interrelated, and reach beyond the urban scale, CAMx is designed to (a) simulate air quality over many geographic scales, (b) treat a wide variety of inert and chemically active pollutants including ozone, inorganic and organic $PM_{2.5}$ and PM_{10} and mercury and toxics, (c) provide source-receptor, sensitivity, and process analyses and (d) be computationally efficient and easy to use. The US EPA has approved the use of CAMx for numerous ozone and PM State Implementation Plans (SIPs) throughout the US and has used this model to evaluate regional mitigation strategies including those for recent regional rules (e.g., CAIR, NOx SIP Call, CSAPR, etc.).

CMAQ

EPA's Models-3/Community Multiscale Air Quality (CMAQ) modeling system is also 'One-Atmosphere' photochemical grid model capable of addressing ozone, particulate matter (PM), visibility and acid deposition at regional scale for periods up to one year (Byun and Ching, 1999). The CMAQ modeling system was designed to approach air quality as a whole by including state-of-the-science capabilities for modeling multiple air quality issues, including tropospheric ozone, fine particles, toxics, acid deposition, and visibility degradation. CMAQ was also designed to have multi-scale capabilities so that separate models were not needed for urban and regional scale air quality modeling. The CMAQ modeling system contains three types of modeling components: (a) a meteorological module for the description of atmospheric states and motions, (b) an emission models for man-made and natural emissions that are

injected into the atmosphere, and (c) a chemistry-transport modeling system for simulation of the chemical transformation and fate.

CMAQ-AMSTERDAM

The Advanced Modeling System for Transport, Emissions, Reactions and Deposition of Atmospheric Matter (AMSTERDAM) is a version of CMAQ that incorporates an alternative treatment of aerosol processes and also adds a plume-in-grid (PinG) treatment to simulate the subgrid-scale features associated with pollutant emissions from point sources (Karamchandani et al., 2010). PinG treatment is provided with the Advanced Plume Treatment (APT) option (Karamchandani et al., 2002, 2006), and the embedded reactive plume model is adapted from the Second–order Closure Integrated puff model with Chemistry (SCICHEM) (Karamchandani et al., 2000). Aerosol processes are treated by the Model of Aerosol Dynamics, Reaction, Ionization and Dissolution (MADRID) developed by Zhang et al. (2004).

Meteorological Modeling Years and Emission Scenarios

Simulation outputs for three different meteorological modeling years (2002, 2005 and 2006) are available for the CONUS 36-km modeling domain. Also, the VISTAS modeling datasets include future year emission scenarios for 2009, 2012 and 2018 in addition to the 2002 base year simulation.

Grid Resolutions

Each of the VISTAS and UBAQS modeling includes nested grid simulation with 12-km resolution (while covering a different region) in addition to the 36-km CONUS modeling domain (see Figures 34 and 35). The FCAQTF modeling domain consists of 12-km and 4-km nested grids covering southwestern US and the Four Corners region, respectively, as well as the common 36-km CONUS domain (see Figure 37).

Monitoring Networks

Ambient and deposition monitoring networks used for the model performance evaluation in this study are summarized in Table 13. Note that dry deposition data reported by CASTNET are not “true” measurements, but estimates based on an “inferential model” involving measured air concentrations coupled with species- and location-dependent deposition velocities that reflect local land use and meteorological conditions at each monitoring site. Recently proposed NCore program to provide routine measurements of NOy and SOx is scheduled to fully operational beginning 2011, thus not included in our evaluation.

Table 12: Annual chemical transport model datasets compiled and used for this study.

Study	Model (version)	Emiss/Met Year	Domain (grid resolution)		
			Grid #1	Grid #2	Grid #3
VISTAS[1]	CMAQ (V4.5.1_SOAmods)	2002/2002 2009/2002 2012/2002 2018/2002	CONUS (36 km)[6]	SE US (12 km)[7]	
UBAQS[2]	CMAQ (V4.6)	2005/2005 2006/2006 2012/2005 2012/2006	CONUS (36 km)	UT-CO (12 km)[8]	
EPRI[3]	CMAQ (AMSTERDAM)	2002/2002		E US (12 km)[9]	
General[4]	CAMx (V5.21)	2005/2005 2006/2006	CONUS (36 km)		
FCAQTF[5]	CAMx (V4.51)	2018/2005	CONUS (36 km)	SW US (12 km)[10]	4Corners (4 km)[11]

[1]Visibility Improvements State and Tribal Association of the Southeast (VISTAS) regional haze SIP modeling study (Morris et al., 2009a)
[2]Uinta Basin Air Quality Study (UBAQS) (Morris et al., 2009b)
[3]Electric Power Research Institute (EPRI) project for development and application of the Advanced Modeling System for Transport, Emissions, Reactions and Deposition of Atmospheric Matter (AMSTERDAM) (Karamchandani et al., 2010)
[4]CAMx modeling over the 36-km continental US domain for various applications including Denver SIP modeling study (Morris et al., 2008)
[5]Four Corners Air Quality Task Force (FCAQTF) modeling study for the Four Corners region (Stoeckenius et al., 2009)
[6]Continental US 36-km modeling domain (see Figure 34)
[7]Southeastern US 12-km modeling domain (see Figure 34)
[8]Utah-Colorado 12-km modeling domain (see Figure 35)
[9]Eastern US 12-km modeling domain (see Figure 36)
[10]Southwestern US 12-km modeling domain (see Figure 37)
[11]Four Corners 4-km modeling domain (see Figure 37)

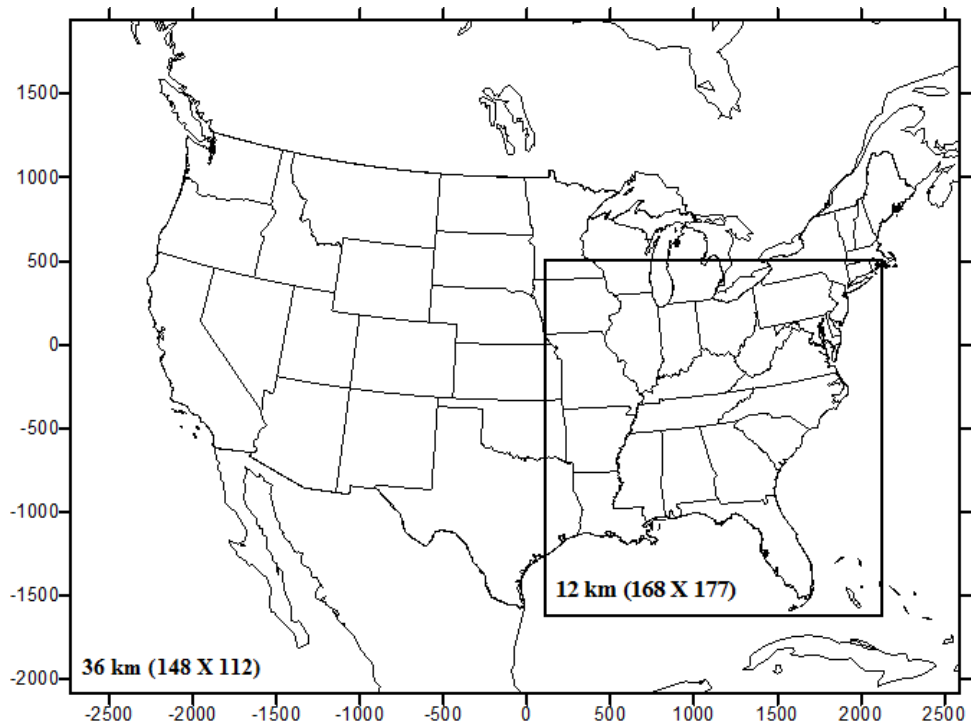

Figure 34: Continental US (CONUS) 36-km and southeastern US (SE US) 12-km modeling domains for the VISTAS regional haze SIP modeling study.

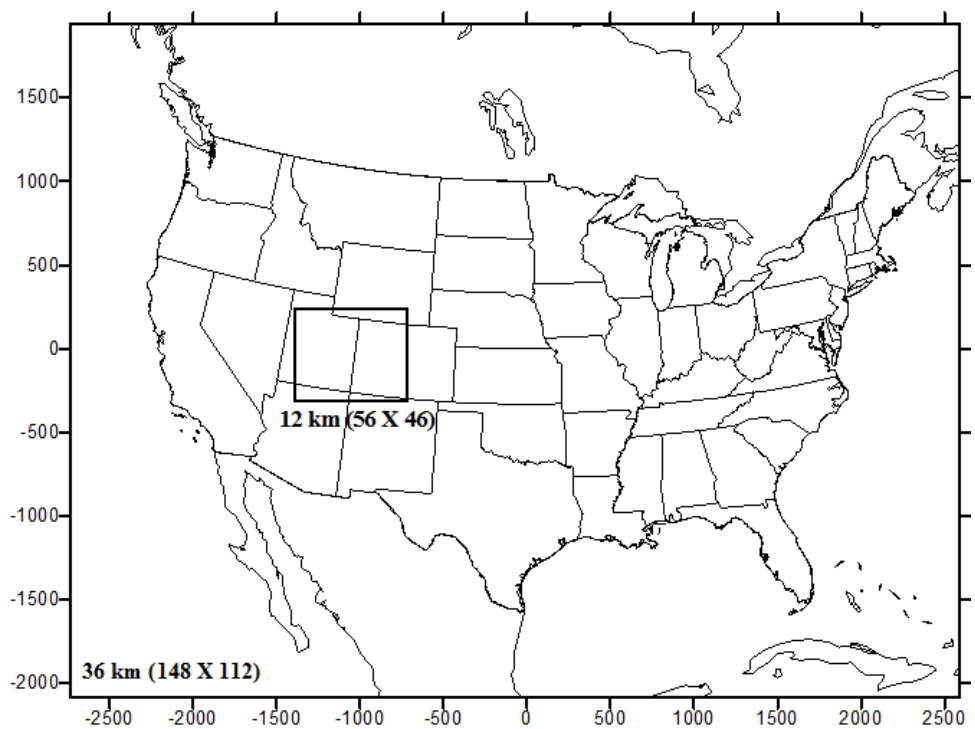

Figure 35: Continental US (CONUS) 36-km and Utah-Colorado (UT-CO) 12-km modeling domains for the UBAQS modeling study.

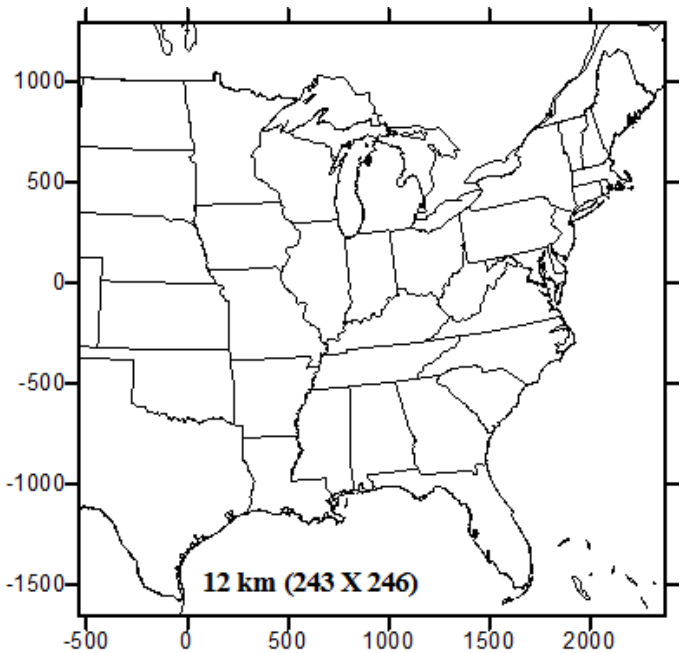

Figure 36: Eastern US (E US) 12-km modeling domain for the EPRI modeling study.

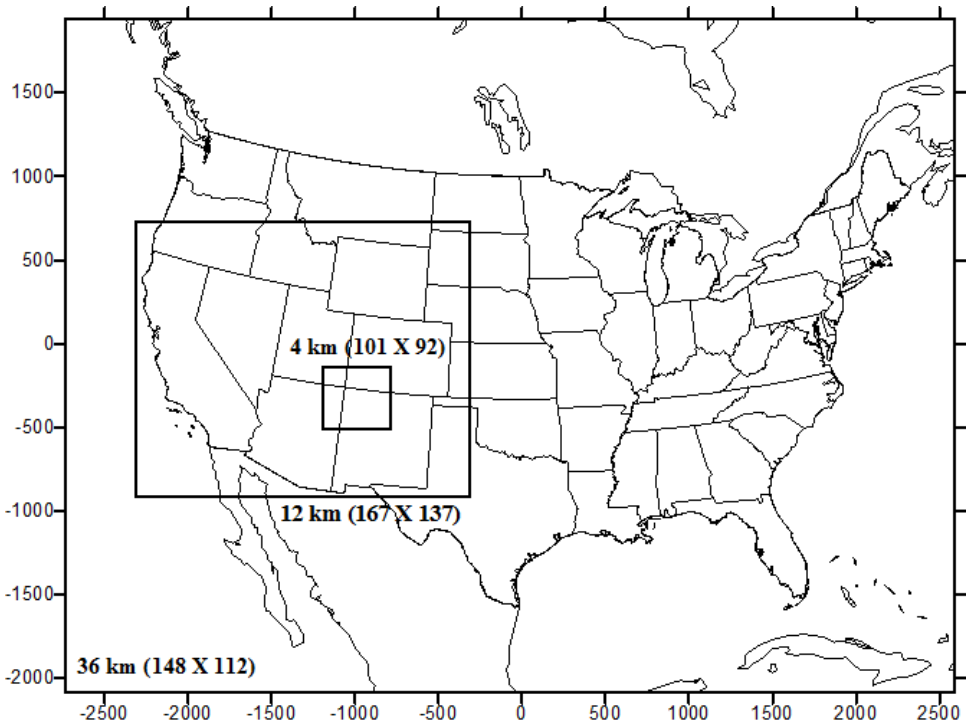

Figure 37: Continental US (CONUS) 36-km, southwestern US (SW US) 12-km, and Four Corners (4Corners) 4-km modeling domains for the FCAQTF modeling study.

Table 13: Overview of ambient and deposition monitoring networks.

Monitoring Network	Chemical Species Measured[1]	Sampling Period	Description
Clean Air Status and Trends Network (**CASTNET**)	Ambient conc. SO_2, HNO_3, particulate SO_4^{2-}, particulate NO_3^- Dry dep. SO_2, HNO_3, particulate NH_4^+, particulate SO_4^{2-}, particulate NO_3^-	Weekly average	Regional long-term monitoring focusing on rural areas; dry deposition fluxes are calculated from measured concentrations and meteorological data using the Multi-Layer Model (MLM); http://java.epa.gov/castnet/
National Atmospheric Deposition Program (**NADP**)	Wet dep. Total sulfate, total nitrate, total ammonium	Weekly average	Long-term monitoring of the acids, nutrients, and base cations in US precipitation; http://nadp.sws.uiuc.edu/
Air Quality System (**AQS**) Aka Aerometric Information Retrieval System (**AIRS**)	Ambient conc. NOy	Hourly average	Ambient concentrations of criteria and hazardous air pollutants at primarily urban sites; http://www.epa.gov/air/data/
Southeastern Aerosol Research and Characterization (**SEARCH**)	Ambient conc. NOy	Hourly average	Eight-station network (4 pairs of urban and rural/suburban stations) in the states of AL, FL, GA and MS; http://www.atmospheric-research.com

[1]Only the species relevant to this study are shown.

Model Performance Evaluation

As mentioned earlier, the proposed new standard in the PAD relies extensively on modeling results rather than monitoring data, therefore, a rigorous evaluation of model performance is crucial. EPA has presented performance evaluation for their CMAQ modeling over the continental US modeling domain (the 2002 annual simulation with CMAQ v4.6 and the 2002 through 2005 simulations with CMAQ v4.7) in the REA (EPA, 2009) and the PA (EPA, 2011). It should be noted that EPA's evaluation focused on statistics based on annualized quantities and/or averaged over large regions. Such statistics tend to suffer from compensation errors and may be misleading.

In this study, we conducted more comprehensive model performance evaluation using several annual CMAQ and CAMx simulations for the 36-km CONUS modeling domain, and examined how different statistics affect the performance evaluation results.

Mean Normalized Bias and Error

For the performance statistics, we use mean normalized bias (MNB) and mean normalized error (MNE) defined as follows:

$$\mathrm{MNB} = \frac{1}{\mathrm{N}} \sum \frac{\mathrm{Model} - \mathrm{Observation}}{\mathrm{Observation}}$$

$$\mathrm{NME} = \frac{1}{\mathrm{N}} \sum \frac{|\mathrm{Model} - \mathrm{Observation}|}{\mathrm{Observation}}$$

where N is the number of pairs of modeled and observed quantities matched in time and space. One concern with EPA's performance evaluation is that they primarily focused on annualized quantities (annual average concentrations and annual total depositions) in calculating their performance statistics. Using such annualized quantities is subject to compensation errors due to temporal averaging/aggregation, as shown in Figure 38 and Figure 39. A more rigorous evaluation should use the modeled quantities averaged or aggregated at the native time-resolution of the measurements (i.e., hourly or weekly in this case). Figure 38 compares scatter plots of modeled vs. observed SO_2 concentrations: One with annual average SO_2 concentrations and the other with SO_2 concentrations averaged over CASTNET's native sampling period (a week). Figure 39 compares modeled NO_Y concentrations with measurements at SEARCH monitoring stations.

(a) Annual average SO_2 conc. (µg-S m^{-3})

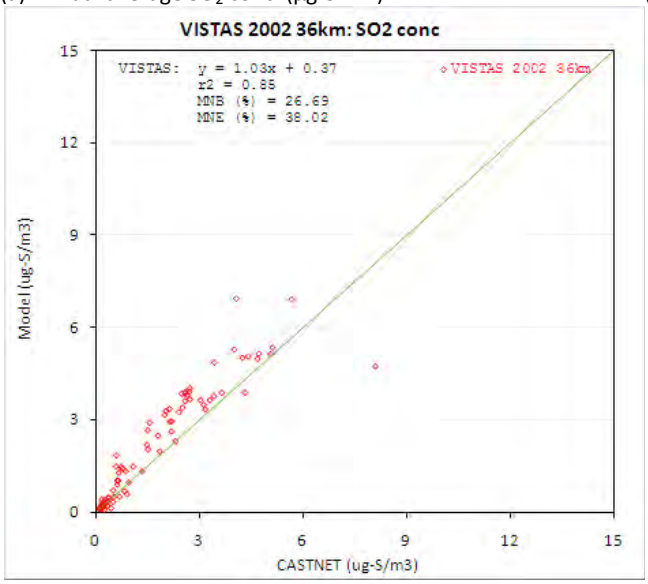

(b) Weekly average SO_2 conc. (µg-S m^{-3})

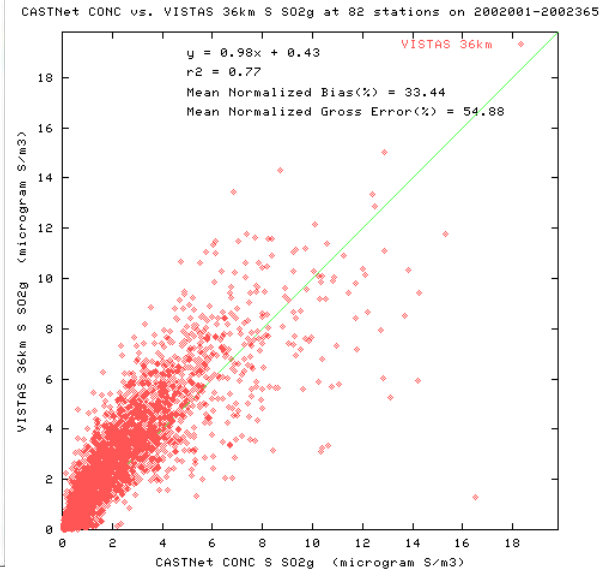

Figure 38: Scatter plots of (a) annual average SO_2 concentrations and (b) weekly average SO_2 concentrations: VISTAS 2002 annual CMAQ simulation vs. CASTNET monitoring data.

(a) Annual average NO_Y conc. (µg-N m^{-3})

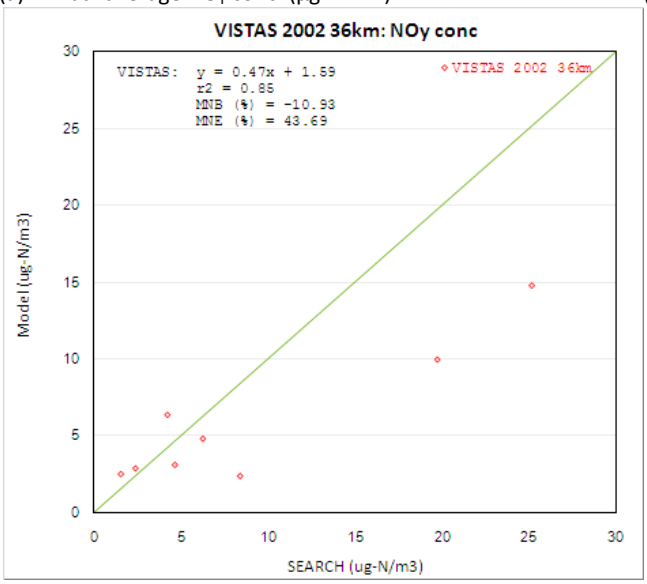

(b) Hourly average NO_Y conc. (µg-N m^{-3})

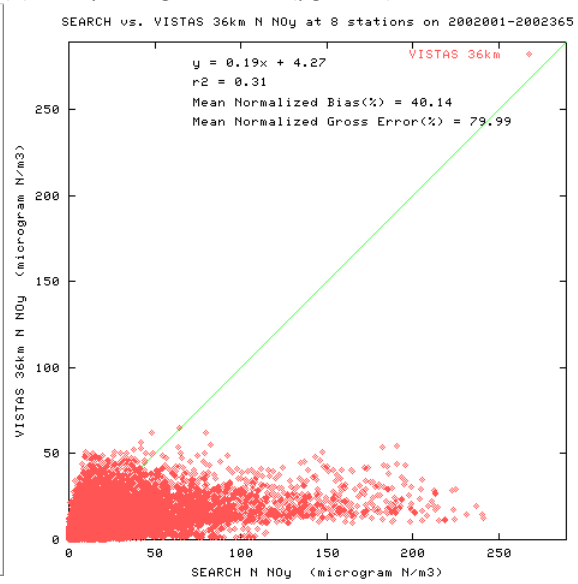

Figure 39: Scatter plots of (a) annual average NO_Y concentrations and (b) hourly average NO_Y concentrations: VISTAS 2002 annual CMAQ simulation vs. SEARCH monitoring data.

Figures 40 through 53 compare model performance statistics (MNB and MNE) for annualized quantities vs. those with the native time-resolution of the measurements (scatter plots corresponding to these bar charts are given in Appendices C1 and C2). In most cases, the biases and errors with weekly or hourly quantities (ambient concentrations or depositions) are poorer than those with annualized quantities reflecting the effect of error compensation. In general, model performance for ambient concentrations

is relatively better than model performance for deposition fluxes, with dry deposition flux model performance being especially poor. As noted earlier, CASTNET's dry deposition data is not "true" measurements, but estimates based on an "inferential model" involving measured air concentrations coupled with species- and location-dependent deposition velocities that reflect local land use and meteorological conditions at each monitoring site. Therefore, the performance evaluation results for dry deposition should be taken with this caveat in mind. However, the large discrepancies between CMAQ-predicted dry depositions and CASTNET estimates indicate significant uncertainties in dry deposition modeling and an urgent need to develop techniques to accurately measure dry deposition fluxes of NOy, SOx and NHx species.

The models also exhibit particularly poor performance for wet depositions of total ammonium (defined as NH_3 and particulate NH_4^+). As EPA has noted in the PA (EPA, 2011), modeling ammonia deposition is a difficult task due to complexity of ammonia deposition processes (e.g., bi-directional flux of ammonia) and relatively large uncertainty in the ammonia emission inventory. EPA has attempted to improve CMAQ model performance for depositions, for example, by adjusting the CMAQ model output based on precipitation data generated by the Parameter-elevation Regressions on Independent Slopes Model (PRISM) or by incorporating a bi-directional ammonia flux algorithm in CMAQ (EPA, 2011). However, these corrections should be evaluated in a more comprehensive and thorough fashion.

(a) MNB (%)

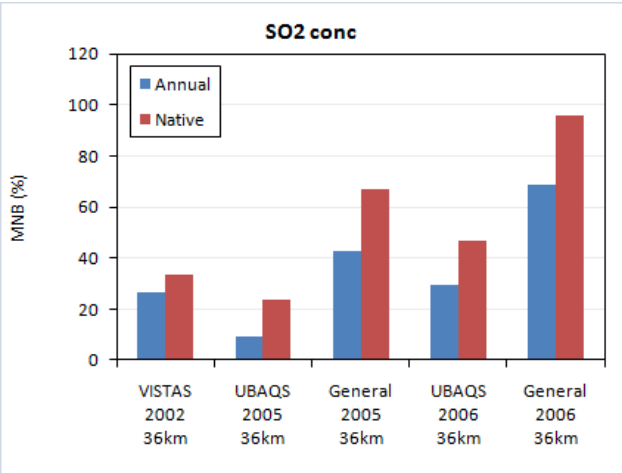

(b) MNE (%)

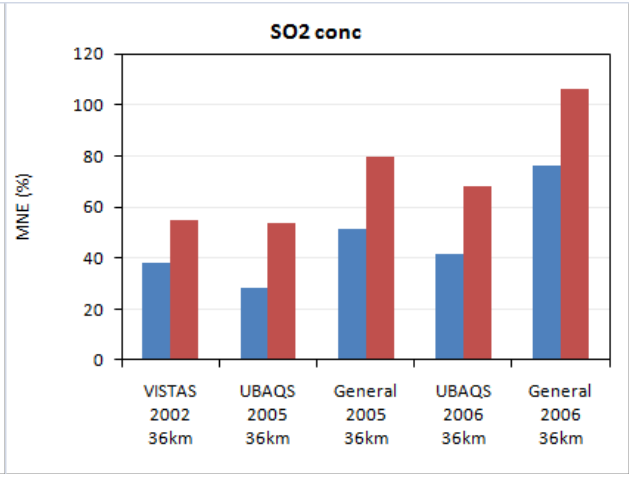

Figure 40: Mean normalized bias (MNB) and mean normalized error (MNE) for modeled SO_2 concentrations at CASTNET stations using annual average or native sampling time-resolution (weekly average).

(a) MNB (%) (b) MNE (%)

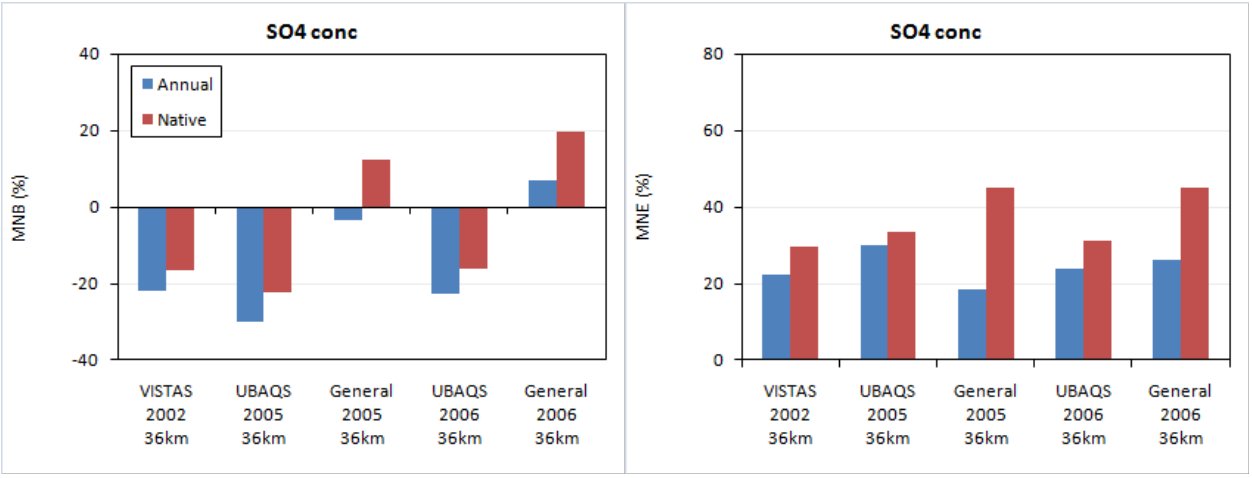

Figure 41: Mean normalized bias (MNB) and mean normalized error (MNE) for modeled particulate SO_4 concentrations at CASTNET stations using annual average or native sampling time-resolution (weekly average).

(a) MNB (%) (b) MNE (%)

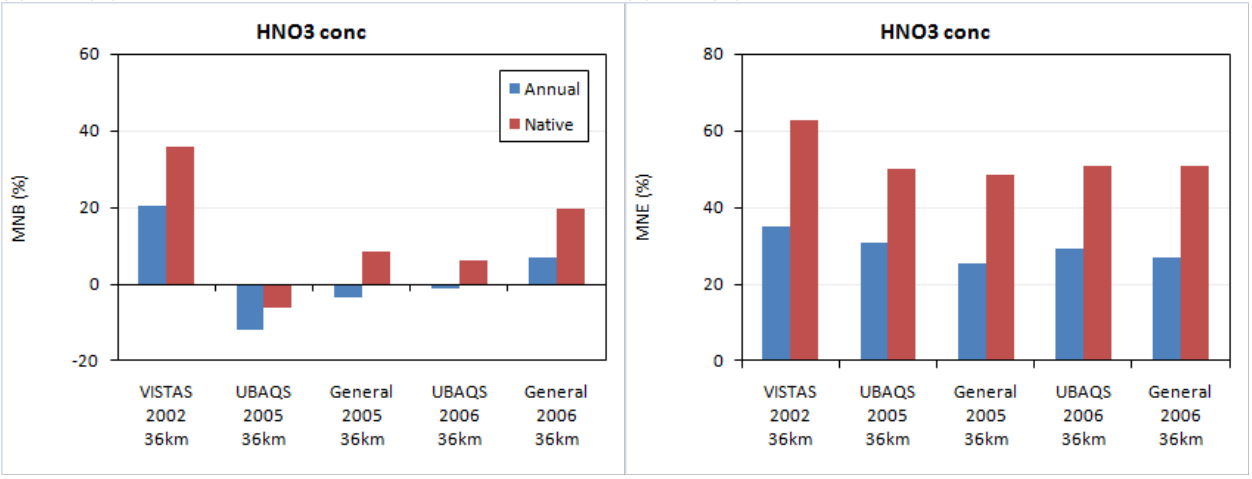

Figure 42: Mean normalized bias (MNB) and mean normalized error (MNE) for modeled HNO_3 concentrations at CASTNET stations using annual average or native sampling time-resolution (weekly average).

(a) MNB (%) (b) MNE (%)

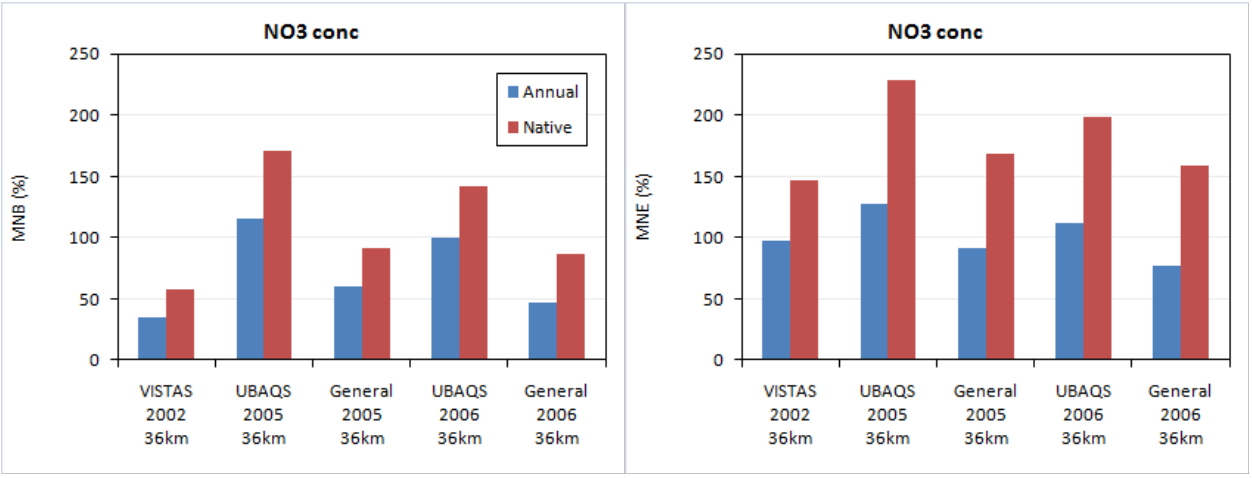

Figure 43: Mean normalized bias (MNB) and mean normalized error (MNE) for modeled particulate NO_3 concentrations at CASTNET stations using annual average or native sampling time-resolution (weekly average).

(a) MNB (%) (b) MNE (%)

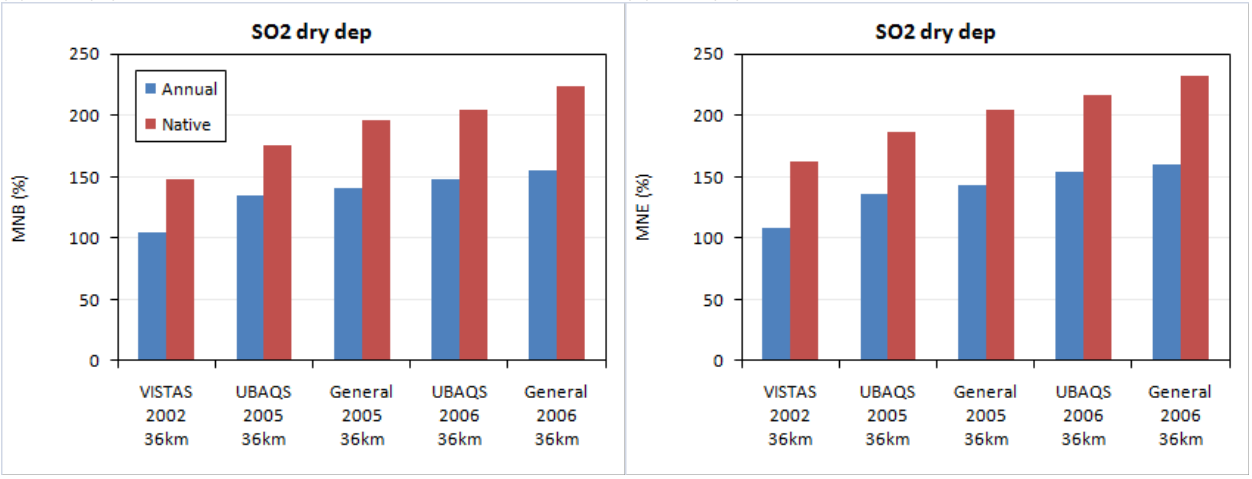

Figure 44: Mean normalized bias (MNB) and mean normalized error (MNE) for modeled SO_2 dry depositions at CASTNET stations using annual total or native sampling time-resolution (weekly total).

(a) MNB (%) (b) MNE (%)

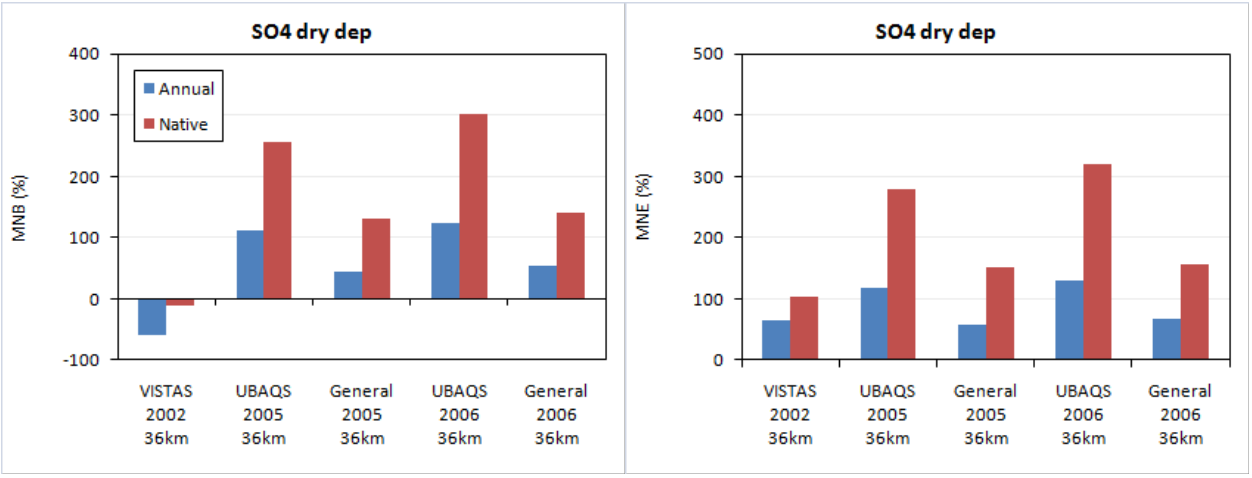

Figure 45: Mean normalized bias (MNB) and mean normalized error (MNE) for modeled particulate SO_4 dry depositions at CASTNET stations using annual total or native sampling time-resolution (weekly total).

(a) MNB (%) (b) MNE (%)

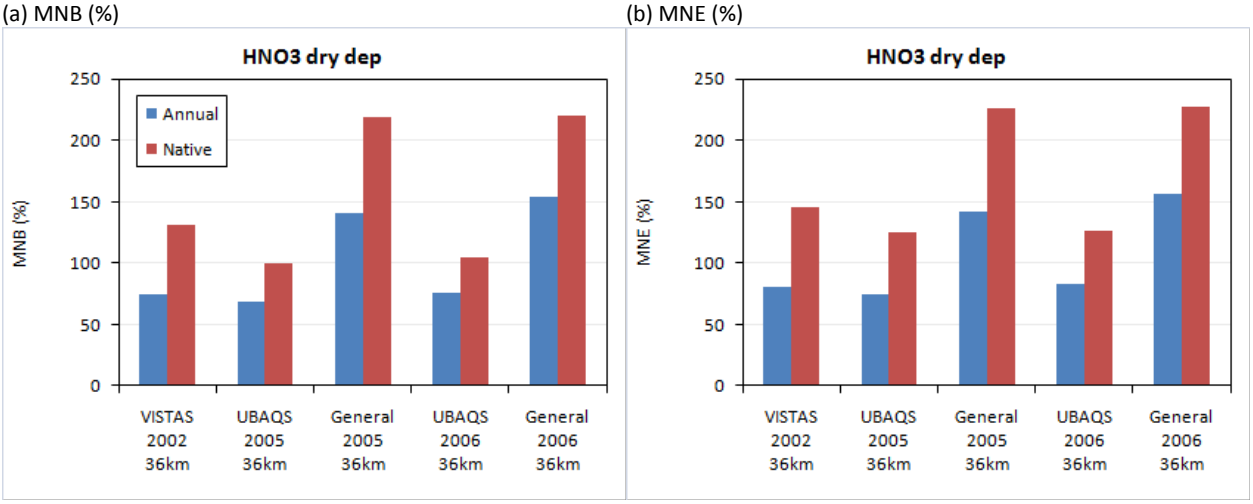

Figure 46: Mean normalized bias (MNB) and mean normalized error (MNE) for modeled HNO_3 dry depositions at CASTNET stations using annual total or native sampling time-resolution (weekly total).

(a) MNB (%) (b) MNE (%)

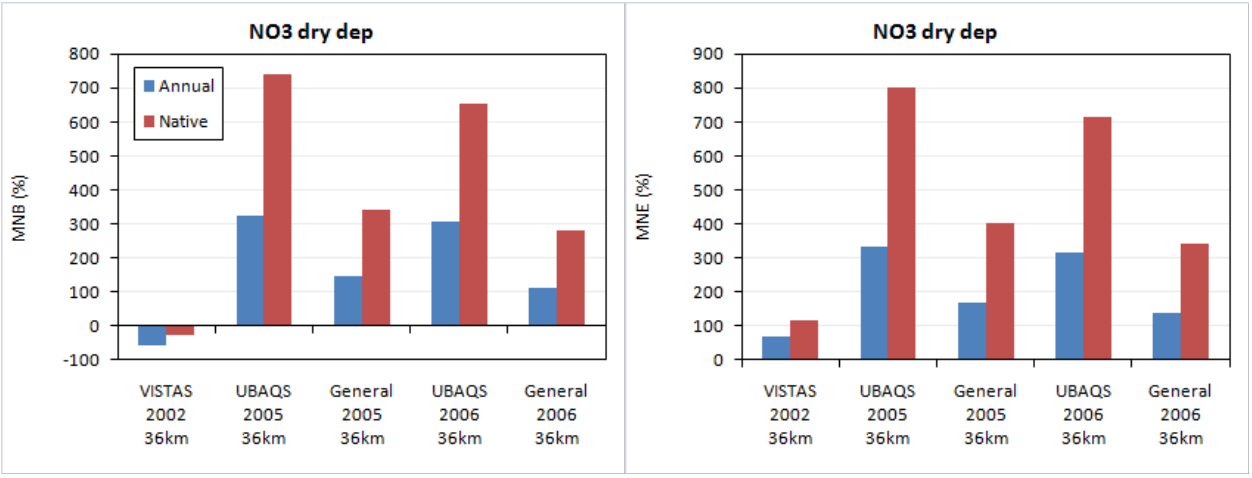

Figure 47: Mean normalized bias (MNB) and mean normalized error (MNE) for modeled particulate NO_3 dry depositions at CASTNET stations using annual total or native sampling time-resolution (weekly total).

(a) MNB (%) (b) MNE (%)

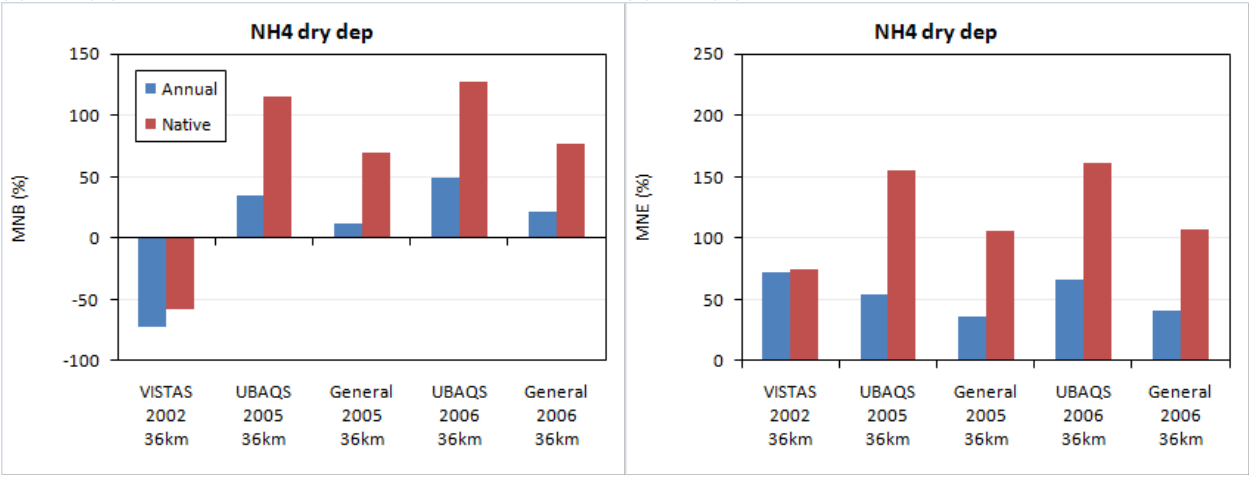

Figure 48: Mean normalized bias (MNB) and mean normalized error (MNE) for modeled particulate NH_4 dry depositions at CASTNET stations using annual total or native sampling time-resolution (weekly total).

(a) MNB (%) (b) MNE (%)

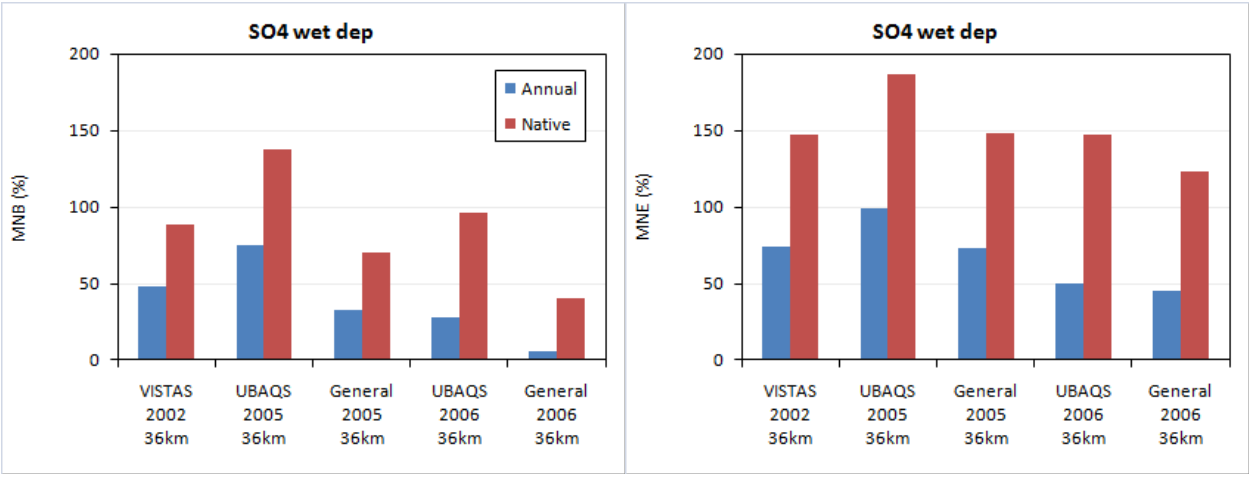

Figure 49: Mean normalized bias (MNB) and mean normalized error (MNE) for modeled total SO_4 wet depositions at NADP stations using annual total or native sampling time-resolution (weekly total).

(a) MNB (%) (b) MNE (%)

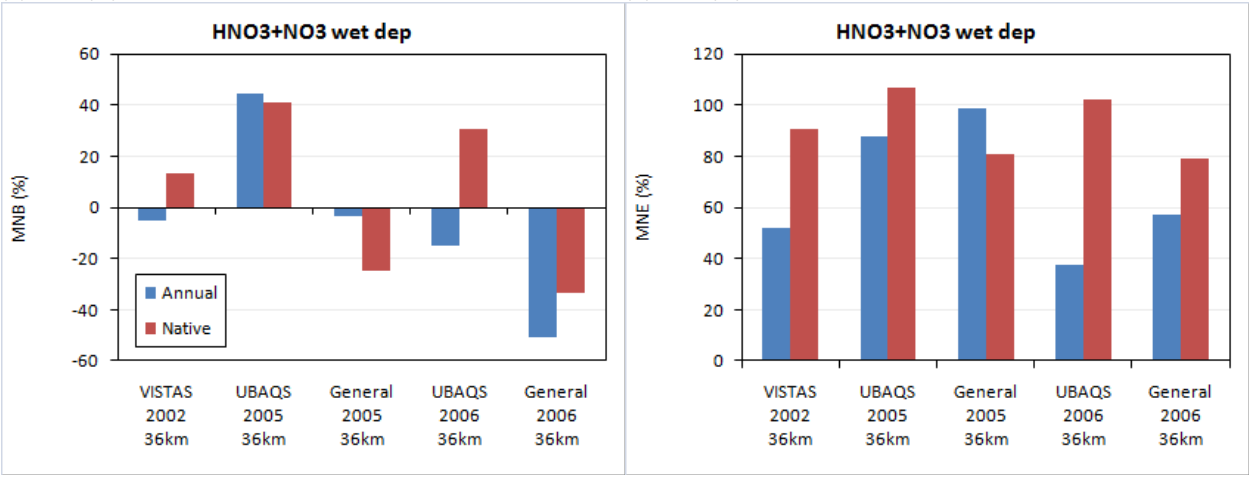

Figure 50: Mean normalized bias (MNB) and mean normalized error (MNE) for modeled total NO_3 wet depositions at NADP stations using annual total or native sampling time-resolution (weekly total).

(a) MNB (%) (b) MNE (%)

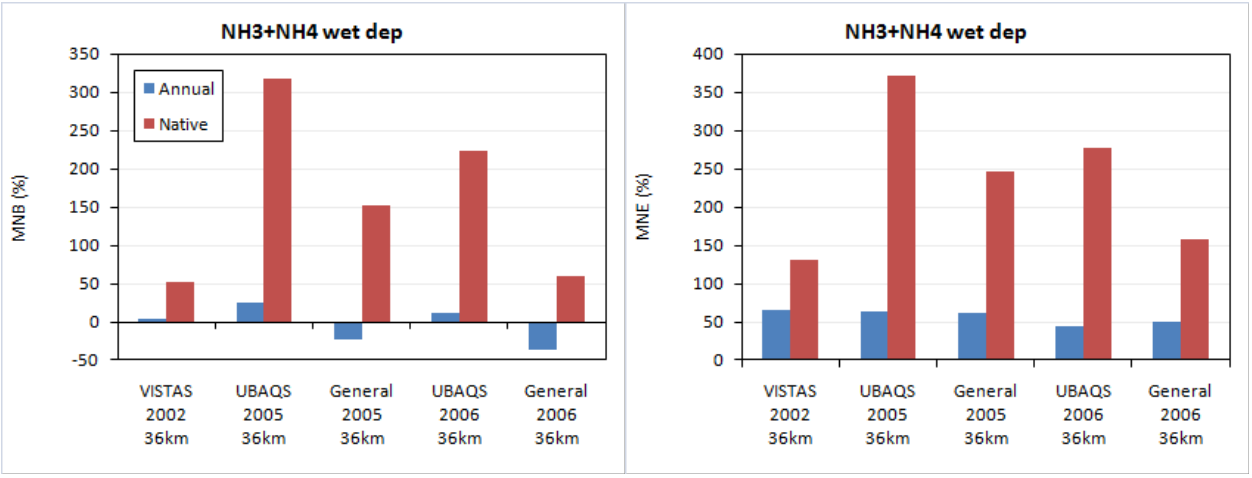

Figure 51: Mean normalized bias (MNB) and mean normalized error (MNE) for modeled total NH_4 wet depositions at NADP stations using annual total or native sampling time-resolution (weekly total).

(a) MNB (%) (b) MNE (%)

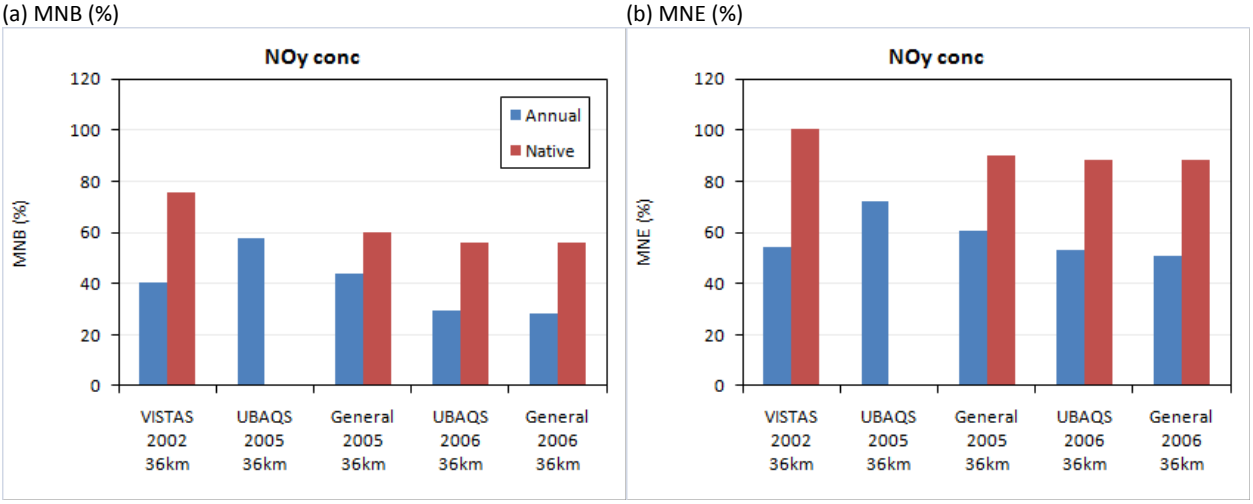

Figure 52: Mean normalized bias (MNB) and mean normalized error (MNE) for modeled NO_Y concentrations at AQS stations using annual average or native sampling time-resolution (hourly average).

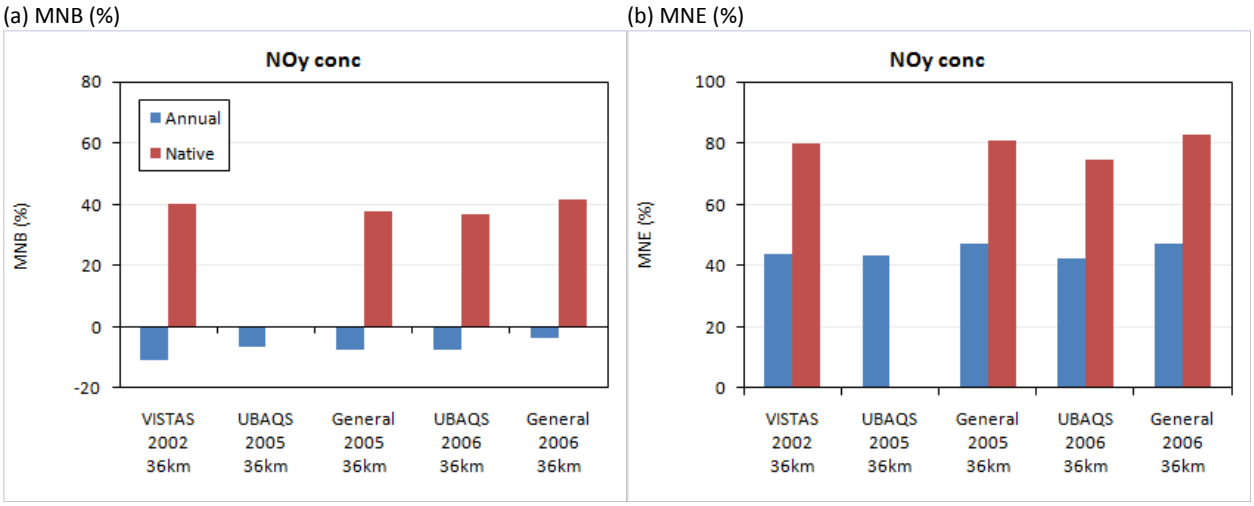

Figure 53: Mean normalized bias (MNB) and mean normalized error (MNE) for modeled NO_Y concentrations at SEARCH stations using annual average or native sampling time-resolution (hourly average).

Spatial Maps of Model Performance Statistics

Another concern with EPA's performance evaluation is related to spatial aggregation. Figure 54 shows examples of EPA's comparison plots of modeled and observed monthly average concentrations and monthly total wet deposition fluxes (Figures 1.2-15 and 1.2-21 in the REA). Although these plots are designed to show temporal patterns of model performance, averaging across large regions (Figure 54 shows concentrations and depositions averaged over monitoring sites across the eastern US) would fail to reveal spatial variations in model performance because areas of overestimation and underestimation can compensate each other. Figure 55 shows spatial maps of MNB and MNE of CMAQ-predicted weekly average SO_4^{2-} concentrations along with CASTNET measurements (the contours are generated by Kriging interpolation of values at the monitoring stations). The model underestimates SO_4 concentrations in most areas while exhibiting overestimations in certain regions. Spatial variation of the model performance is more obvious in Figure 56 which shows similar maps to Figure 55 but for CMAQ-modeled and NADP-observed SO_4^{2-} wet depositions. Temporal averaging also affects this spatial variation. Figure 57 compares spatial maps of MNB calculated using weekly total and annual total SO_4 wet depositions. Using annualized quantities lessens level of the model overestimations in eastern US and even changes sign of the biases in certain areas in central US (from overestimation to underestimation). Spatial maps for complete sets of sulfur and nitrogen species are given in Appendix D1 (for absolute concentrations and deposition), Appendix D2 (for MNB and MNE using annualized concentrations and deposition), and Appendix D3 (for MNB and MNE using concentrations and deposition fluxes with native temporal resolutions of the measurements).

(a) SO_4 concentration (μg m^{-3})

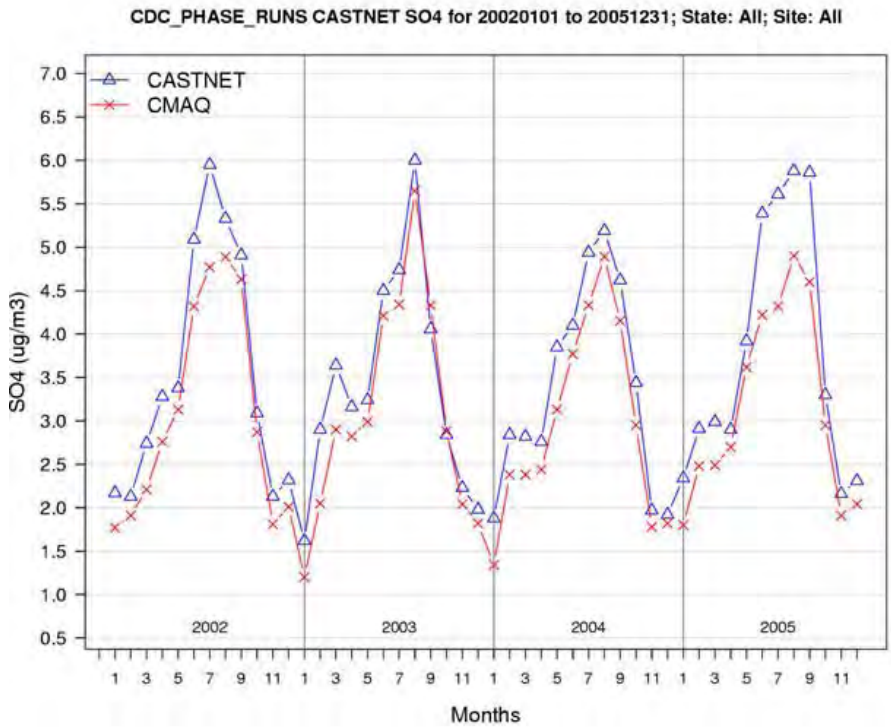

(b) SO_4 wet deposition (kg ha^{-1})

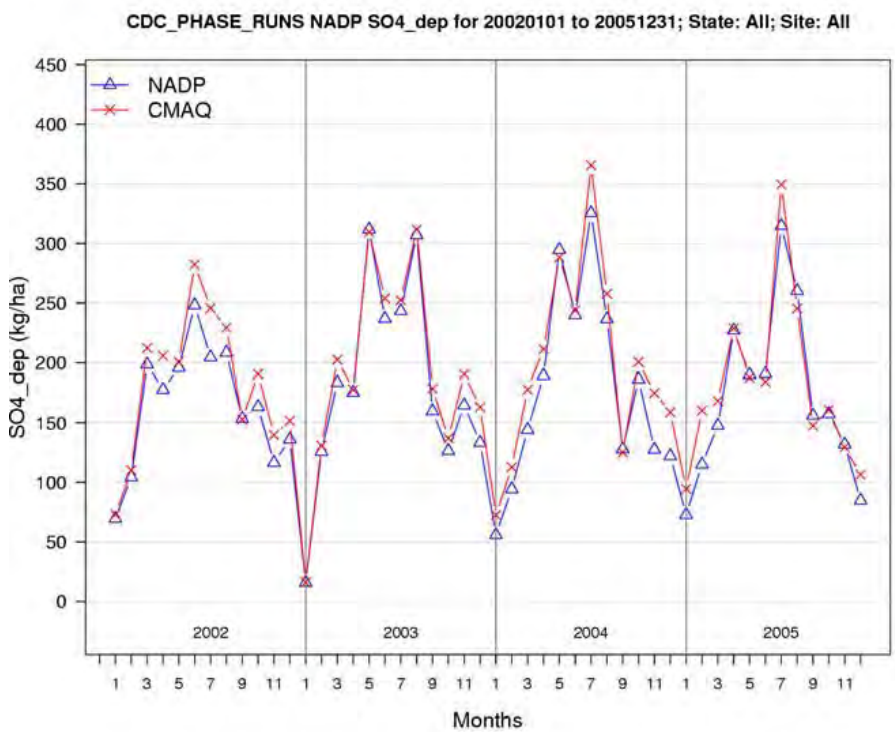

Figure 54: Monthly time-series plots of observations and CMAQ-predictions averaged over the eastern US modeling domain: (a) Monthly average SO_4 concentrations at CASTNET stations; (b) monthly total SO_4 wet depositions at NADP stations (EPA, 2009).

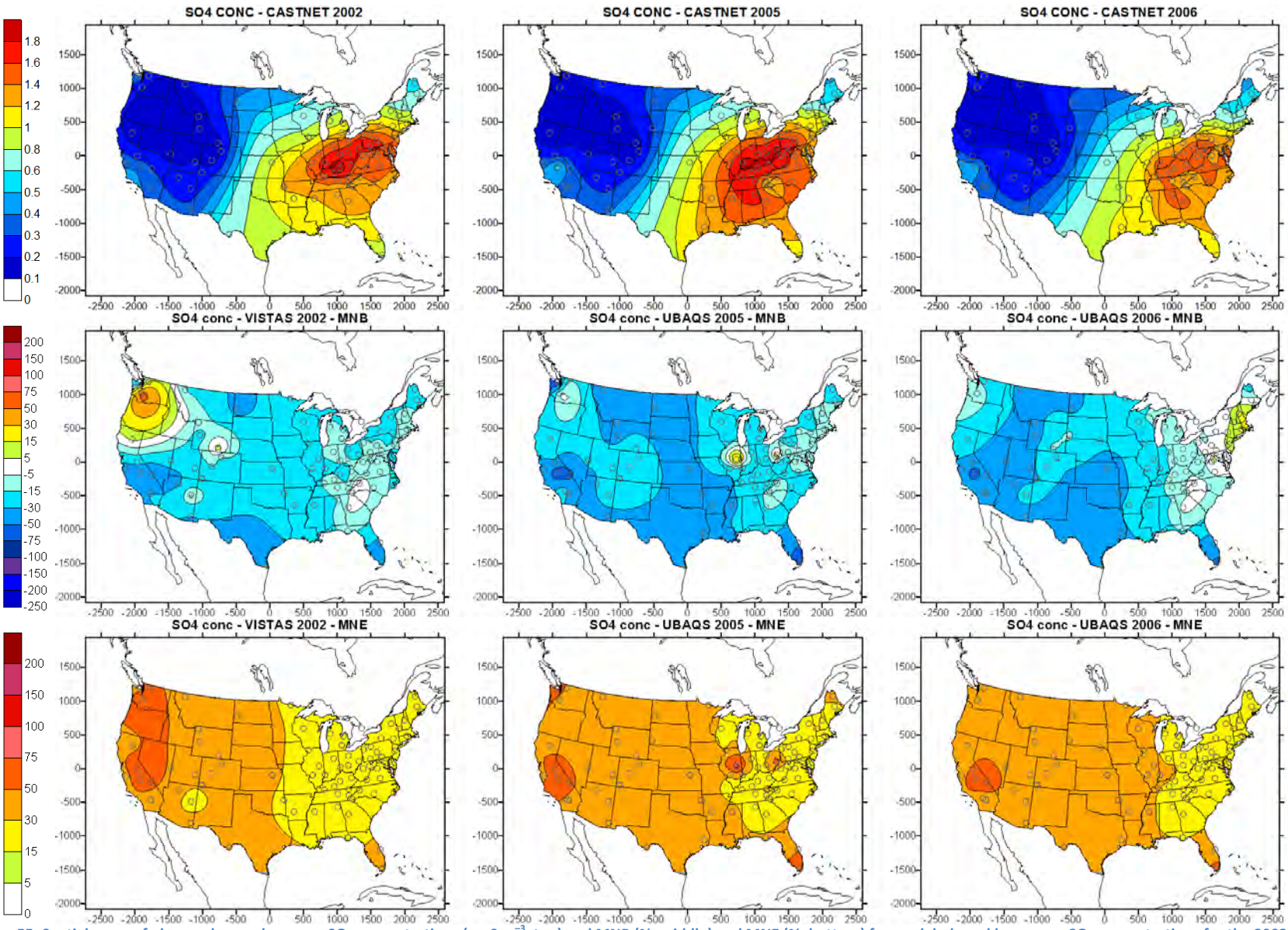

Figure 55: Spatial maps of observed annual average SO_4 concentrations (μg-S m^{-3}; top) and MNB (%; middle) and MNE (%; bottom) for modeled weekly average SO_4 concentrations for the 2002 (left), 2005 (center) and 2006 (right) modeling years. Contours are created using Kriging interpolation of values at CASTNET stations (circle markers).

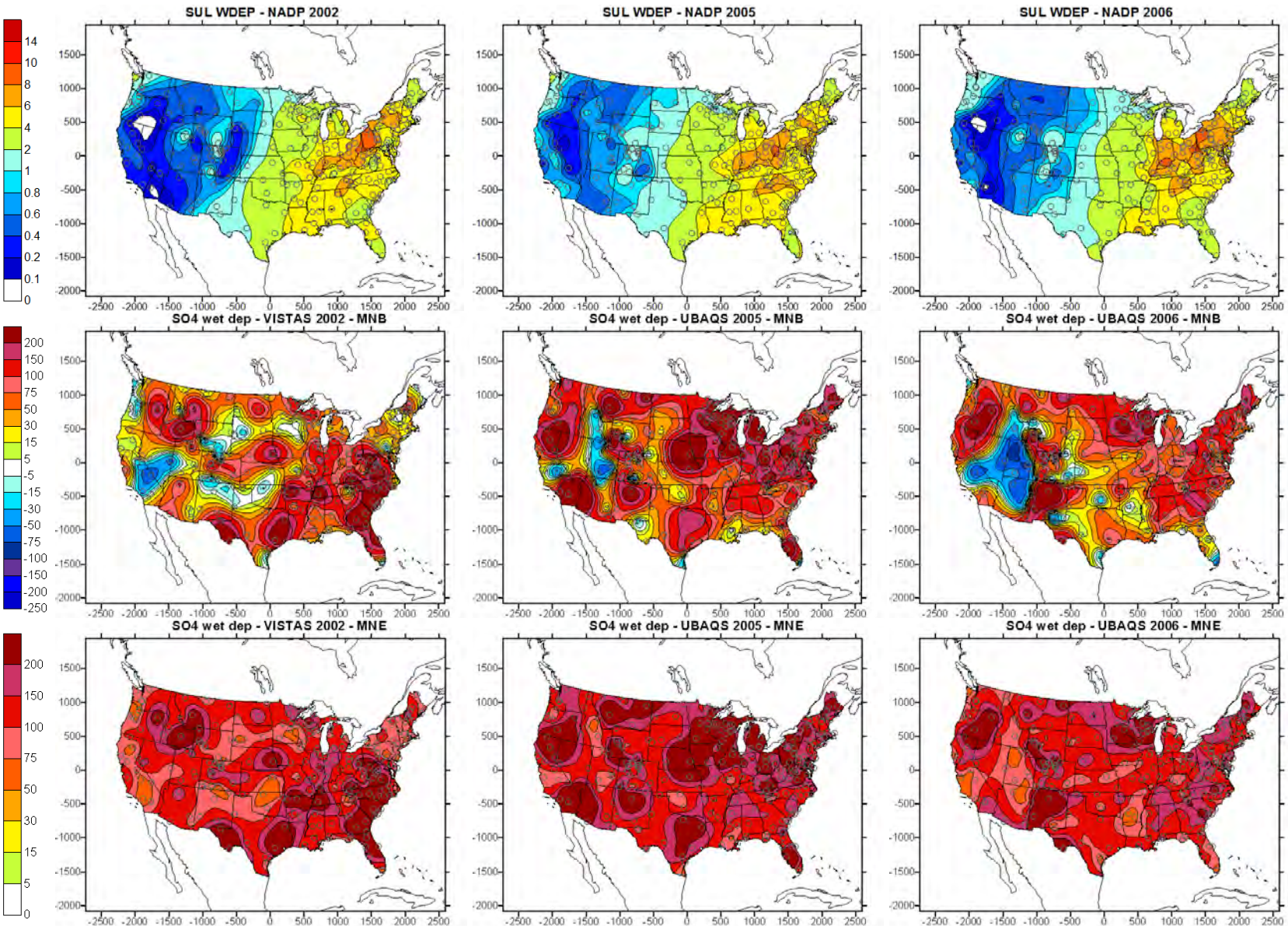

Figure 56: Spatial maps of observed annual total SO_4 wet depositions (kg-S/ha/yr; top) and MNB (%; middle) and MNE (%; bottom) for modeled weekly total SO_4 wet depositions for the 2002 (left), 2005 (center) and 2006 (right) modeling years. Contours are created using Kriging interpolation of values at NADP stations (circle markers).

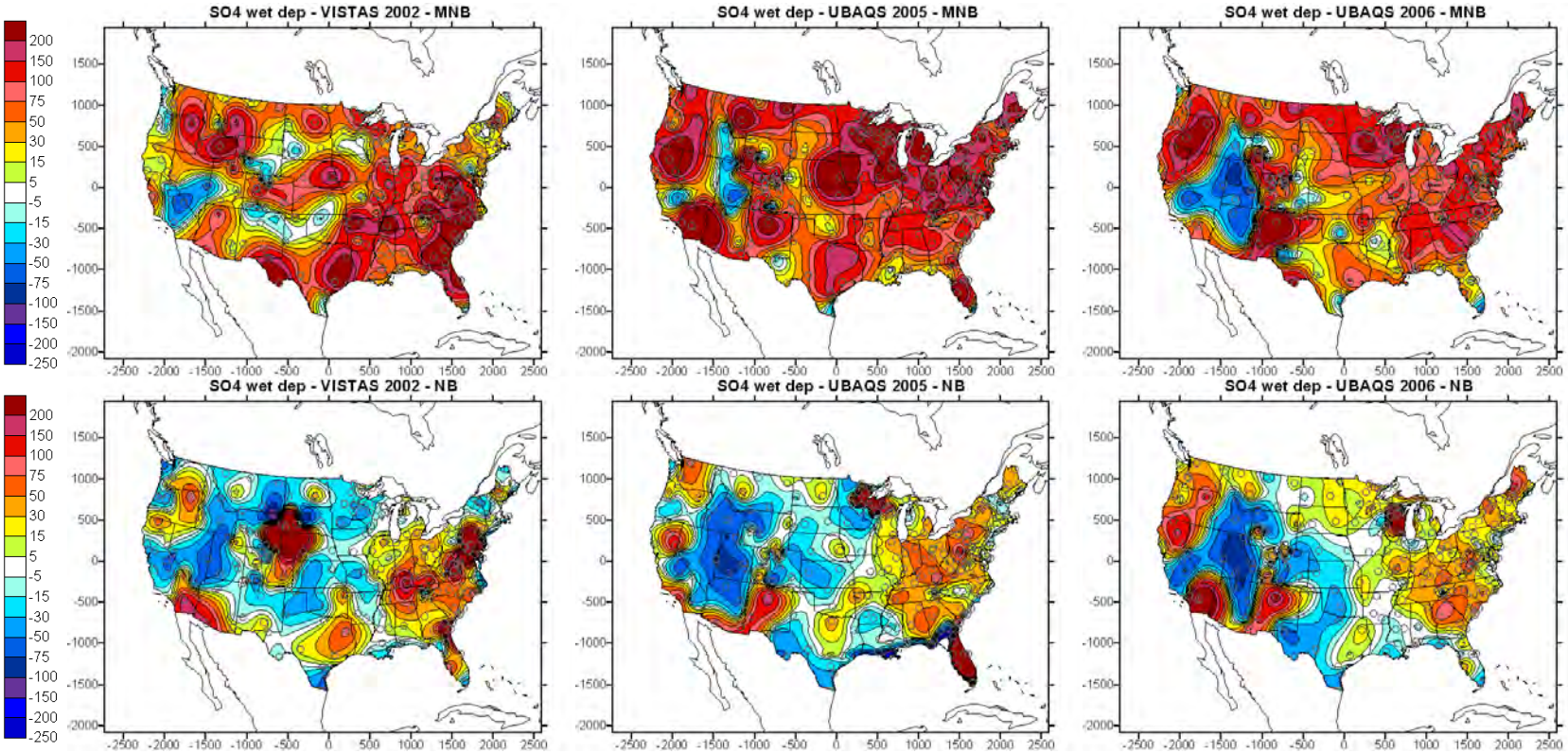

Figure 57: Spatial maps of mean normalized bias (MNB) for modeled SO_4 wet depositions using weekly total (top) and annual total (bottom) deposition values from the VISTAS 2002 (left) and UBAQS 2005 (center) and 2006 (right) CMAQ simulations. Contours are created using Kriging interpolation of values at NADP stations (circle markers).

Variability in Transference Ratios and Reduced Nitrogen Deposition Estimates Estimated from Atmospheric Models

As described earlier, EPA has proposed to use the Transference Ratios to link the air quality indicator (ambient concentrations of SOx and NOy) with acidifying deposition into an ecosystem. The Transference Ratios, TSO_X and TNO_Y, are calculated from model simulations by dividing annual total depositions of SOx and NOy by annual average SOx and NOy concentrations, respectively, for each grid cell and then aggregating all grid cells in the area of interest, and are key parameters in determining the Aquatic Acidification Index (AAI). Another key parameter in the AAI formulation is total reduced nitrogen loading (LNH_X) which is also based on model simulations. EPA suggested that these parameters are sufficiently stable across time and space based on the CMAQ modeling results over the Adirondacks and Shenandoah case study areas. In this study, we conducted more comprehensive analysis by including variety of annual model simulations and examining variability in these parameters over various regions in US.

To examine variability in TSO_X, TNO_Y, and LNH_X, we calculated these parameters using compiled set of annual chemical transport model simulations (see Table 12 for the list of annual simulations used) over various regions in US including the Adirondacks and Shenandoah case study areas.

We first focused our analysis on the two case study areas that have been extensively studied by EPA for their review of the secondary SO_X and NO_X NAAQS (Figure 58). Variability in TSO_X, TNO_Y and LNH_X is displayed by utilizing the "box and whisker" plot. Figure 59 illustrates how to read a box and whisker plot. Figure 60 presents variability in the TSO_X, TNO_Y, and LNH_X values across the grid cells within each case study area calculated by all the model simulations considered in this study. Both TSO_X and TNO_Y vary considerably. At Adirondacks, the TSO_X values range from 0.56 to 2.6 cm s^{-1} (varying by a factor of ~5) and TNO_Y from 0.24 to 1.7 cm s^{-1} (varying by a factor of ~7). TSO_X and TNO_Y at Shenandoah show similar variability: The TSO_X values spans from 0.35 to 1.5 cm s^{-1} (by a factor of ~4) and TNO_Y from 0.22 to 1.2 cm s^{-1} (by a factor of ~5). The LNH_X values show even higher variability: At Shenandoah, LNH_X changes its value by a factor of 23.

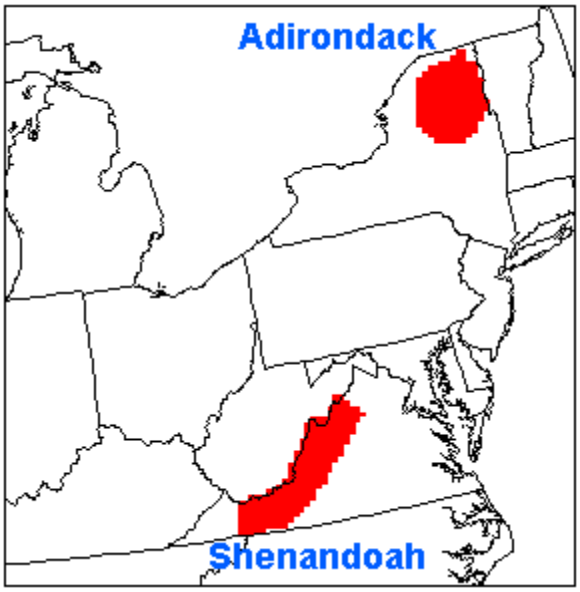

Figure 58: Regions used for analysis of variability in TSO_X, TNO_Y and LNH_X. The Adirondack region includes 18 grid cells in a 36-km modeling grid and 164 cells in a 12-km grid. The Shenandoah region has 23 cells in a 36-km grid and 207 cells in a 12-km grid.

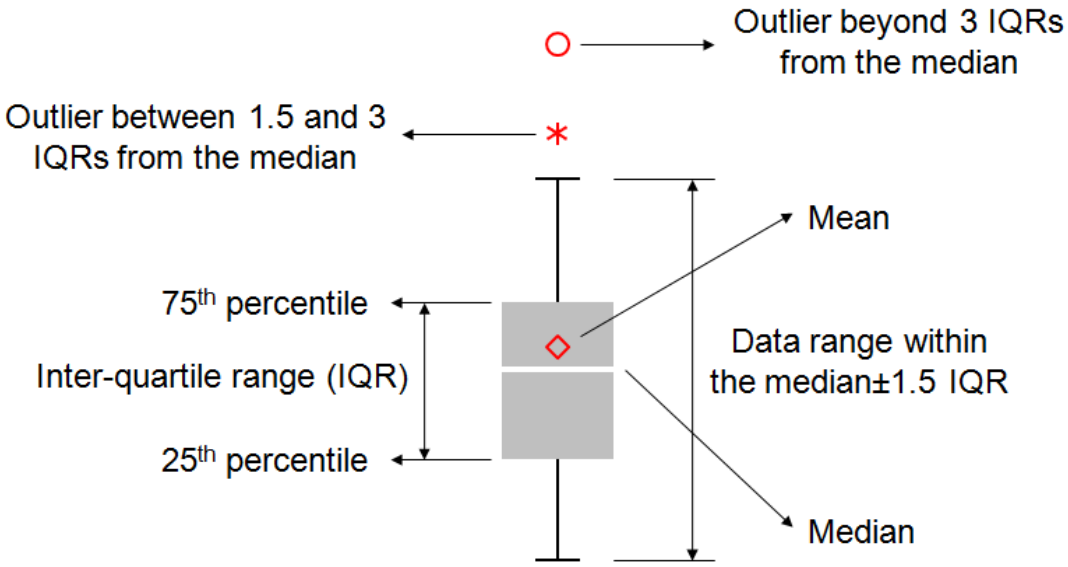

Figure 59: Illustrative diagram of a box and whisker plot. The inner quartiles of each data sample are represented by a stack of two gray boxes, separated at the median by a thin line. The height of the gray boxes together makes up the interquartile range (IQR). The range of data falling within 1.5 IQRs of the median is represented by whiskers. Any outliers that fall between 1.5 and 3 IQRs from the median are represented by asterisk markers, while any outliers falling beyond 3 IQRs from the median are represented by circular markers. The average of each sample is represented by a diamond marker.

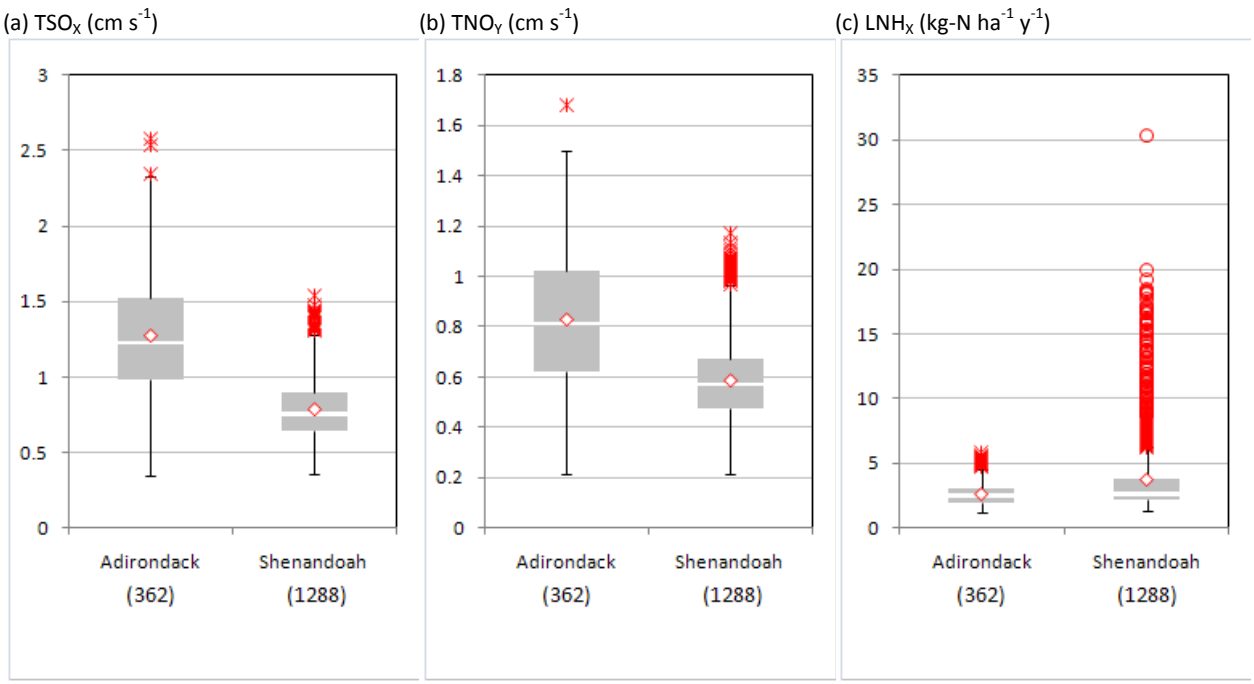

Figure 60: Box and whisker plots for variability of (a) TSO_X, (b) TNO_Y, and (c) LNH_X across all the grid cells at each case study area and all the model simulations. The number in parentheses represents the number of each sample data.

Figures 61 to 63 show spatial variability in TSO_X, TNO_Y, and LNH_X at each of the two case study areas for each annual model simulation. A comparison of model simulations of the same meteorological modeling year but with different emission scenarios (VISTAS 2002 vs. 2009 vs. 2012 vs. 2018; UBAQS 2005 vs. 2012met05; UBAQS 2006 vs. 2012met06) shows that emission changes *alone* have minor impacts on the TSO_X and TNO_Y variability while emission reductions slightly increase the LNH_X variability. The impact of different meteorological modeling years on the TSO_X and TNO_Y is more complex. The mean TSO_X slightly increased from 2005 to 2006 of the UBAQS simulations at Adirondacks, but slightly decreased at Shenandoah. Choice of chemical transport model appears to have the largest influence on variability. The CMAQ V4.6 (UBAQS) model shows higher TSO_X than the CAMx V5.21 (General) at both Adirondacks and Shenandoah. TNO_Y is slightly higher with CMAQ V4.6 than CAMx at Adirondacks, but slightly lower at Shenandoah. CMAQ-AMSTERDAM (EPRI) tends to estimate higher TSO_X and TNO_Y with greater variability than the CMAQ V4.5.1_SOAmods code used for VISTAS. Comparing VISTAS 2002 with UBAQS 2005 or 2006 shows combined impact of using different meteorological modeling years (2002 vs. 2005 or 2006) and different models (CMAQ V4.5.1_SOAmods vs. CMAQ V4.6), and TSO_X, TNO_Y, and LNH_X from the VISTAS simulation are generally lower than those from the UBAQS simulation. In general, the simulations with a fine grid (12 km) show higher variability in TSO_X, TNO_Y, and LNH_X than those with a coarse grid (36 km) at these case study areas. In addition to the two case study areas, we have extended our analysis to include four new regions: Virginia, Wisconsin, Florida Panhandle, and Ecoregion 9.3.4 (as defined by EPA's Omernik classifications; Omernik, 1987). The results for these additional regions are given in Appendix E.

(a) Adirondacks

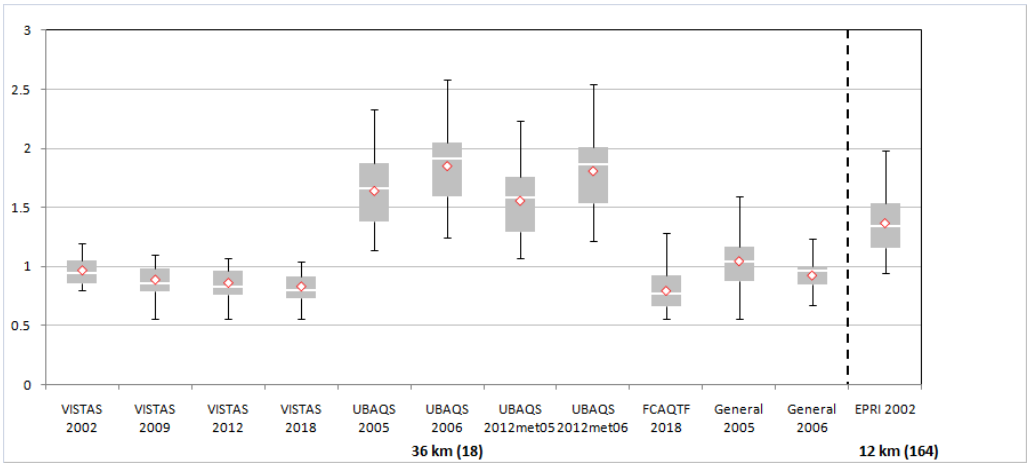

(b) Shenandoah

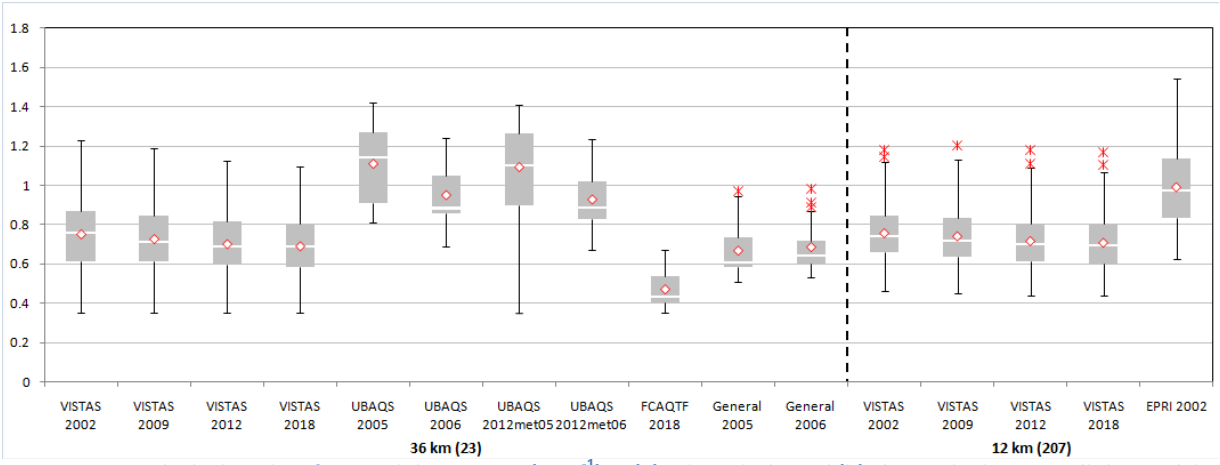

Figure 61: Box and whisker plots for variability in TSO_X (cm s^{-1}) at (a) Adirondacks and (b) Shenandoah across all the model simulations. The number in parentheses represents the number of each sample data.

(a) Adirondacks

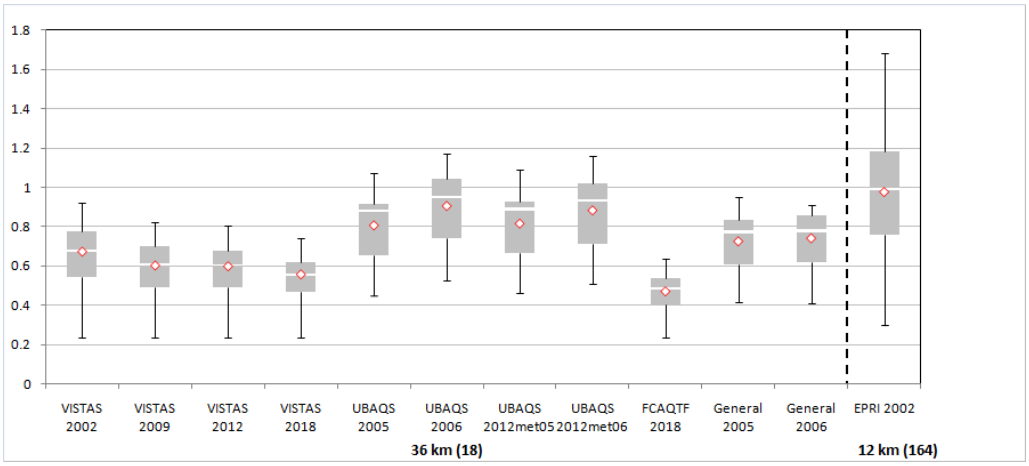

(b) Shenandoah

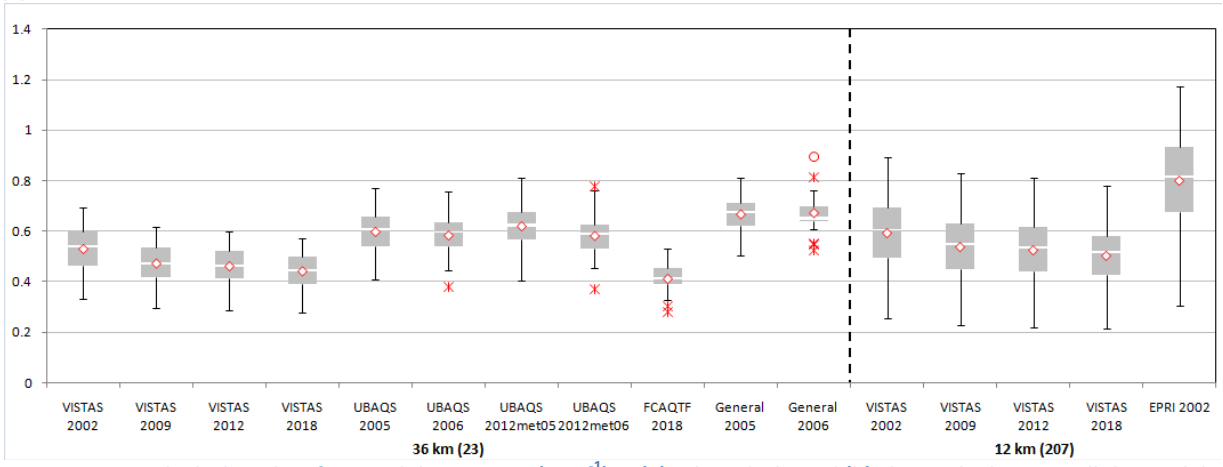

Figure 62: Box and whisker plots for variability in TNO_Y (cm s^{-1}) at (a) Adirondacks and (b) Shenandoah across all the model simulations. The number in parentheses represents the number of each sample data.

(a) Adirondacks

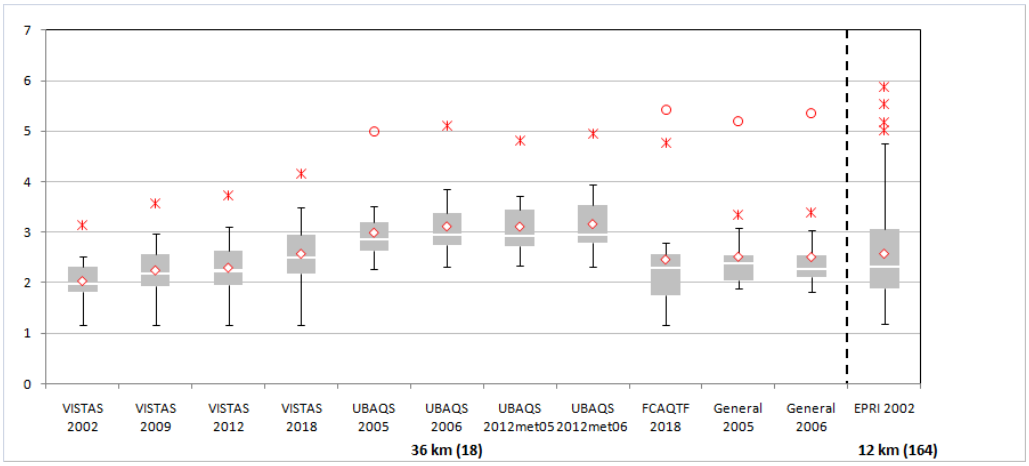

(b) Shenandoah

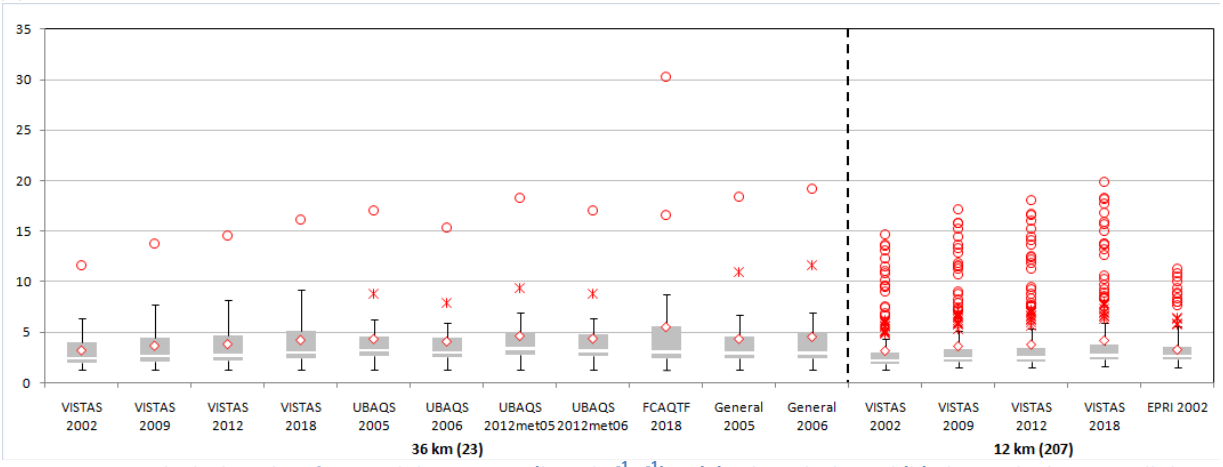

Figure 63: Box and whisker plots for variability in LNH_X (kg-N ha^{-1} y^{-1}) at (a) Adirondacks and (b) Shenandoah across all the model simulations. The number in parentheses represents the number of each sample data.

We also looked at variability in these parameters at several Class I areas: Olympic NP (OLYM1); Mount Rainier NP (MORA1); Yosemite NP (YOSE1); Grand Canyon NP (GRCA2); Glacier NP (GLAC1); Yellowstone NP (YELL2); Rocky Mountain NP (ROMO1); Mesa Verde NP (MEVE1); Great Smoky Mountains NP (GRSM1). Unlike the Adirondacks and Shenandoah areas discussed above, these Class I areas are each represented as a single grid cell (at the corresponding IMPROVE monitoring sites), therefore, only the variability across the model simulations are shown in Figure 64. Again, TSO_X, TNO_Y, and LNH_X show large variability. TSO_X spans from 0.2 to 1.8 cm/s with higher variability at Mount Rainier NP, Yellowstone NP, and Rocky Mountain NP. The TNO_Y values range from 0.2 to 0.9 with higher variability at Yosemite NP, Yellowstone NP, and Rocky Mountain NP. The LNH_X values also display a wide range of variability.

In conclusion, the choice of different modeling systems, simulations (different meteorology and/or different emissions), and model configuration (e.g., grid resolution) can make a large difference in the calculated TSO_X, TNO_Y and LNH_X parameters. This suggests that these parameters are not stable (as assumed in EPA's proposed approach), and such variability can potentially introduce significant uncertainty in the definition of the new secondary SO_X and NO_Y standards proposed by EPA in the Final Policy Assessment Document.

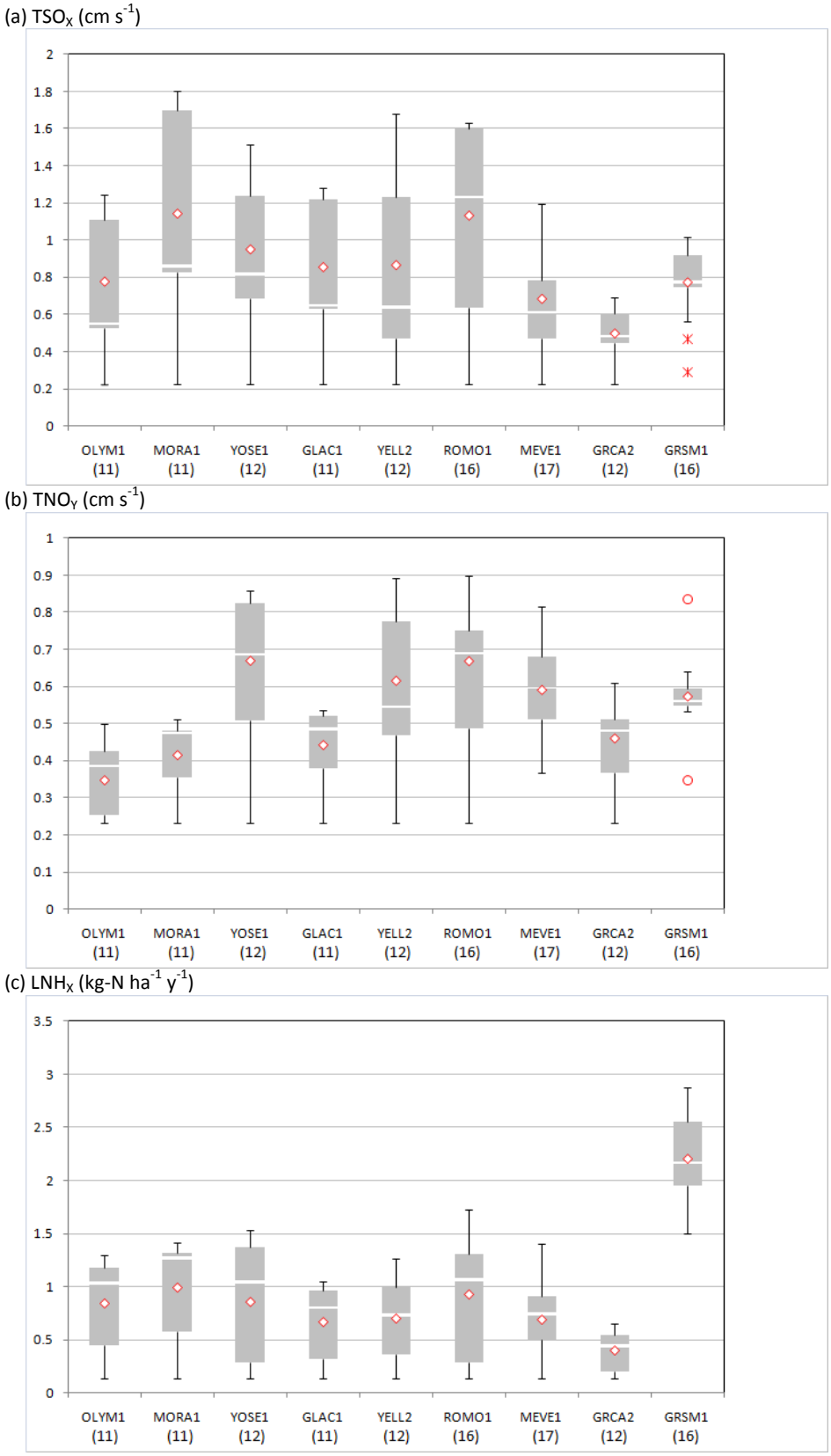

Figure 64: Box and whisker plots for variability in (a) TSO_X, (b) TNO_Y and (c) LNH_X across all the model simulations at each IMPROVE site. The number in parentheses represents the number of each sample data.

References for Appendix A

Aber, J., W. McDowell, K. Nadelhoffer, A. Magill, G. Berntson, M. Kamakea, S. McNulty, W. Currie, L. Rustad, and I. Fernandez. 1998. Nitrogen saturation in temperate forest ecosystems. Bioscience 48:921–934.

Aber, J.D., K.J. Nadelhoffer, P. Steudler, and J.M. Melillo. 1989. Nitrogen saturation in northern forest ecosystems. Bioscience 39: 378–386.

Aber, J.D., C.L. Goodale, S.V. Ollinger, M-L. Smith, A.H. Magill, M.E. Martin, R.A. Hallett, and J.L. Stoddard. 2003. Is nitrogen deposition altering the nitrogen status of northeastern forests? Bioscience 53:375–389.

Adams, M.B., D.R. DeWalle, and J.L. Hom, (eds.). 2006. The Fernow watershed acidification study. Springer. Dordrecht, Netherlands. 279 p.

Adams, M.B., P.J. Edwards, J.N. Kochenderfer, and F. Wood. 2004. Fifty years of watershed research on the Fernow Experimental Forest, WV: effects of forest management and air pollution on hardwood forests. P. 391-396. In First interagency conference on research in the watersheds (KG. Renard, S.A. McElroy, W.J. Gburek, H.E. Canfield, and R.L. Scott, eds.) 2003 October 27-30, Benson, AZ. U.S.D.A. Agricultural Research Service, Southwest Watershed Research Center, Tucson, AZ.

Adams, M.B., T.R. Angradi, and J.N. Kochenderfer. 1997. Streamwater and soil solution responses to 5 years of nitrogen and sulfur additions at the Fernow Experimental Forest, West Virginia. Forest Ecology and Management 95:79–91.

Adirondack Lakes Survey Corporation (ALSC), 1990. An Interpretive Analysis of Fish Communities and Water Chemistry, 1984-1987. ALSC, c/o the New York State Department of Environmental Conservation, Ray Brook, NY 12977. Project Coordinators J. Baker and S. Gherini.

April, R.H., and R.M. Newton. 1985. Influence of geology on lake acidification in the ILWAS watersheds. Water Air and Soil Pollution, 26:373 – 386.

April, R.H., R.M. Newton and L.T. Coles. 1986. Chemical weathering in two Adirondack watersheds: Past and present day rates. Geological Society of America Bulletin, 97:1232 - 1238.

Bailey, R.G., P.E. Avers, T. King, W.H. McNab, eds. 1994. Ecoregions and subregions of the United States (map and unit descriptions). Washington D.C,: U.S. Geological Survey. Scale 1:7,500,999. Prepared for the USDA Forest Service.

Bailey, R.G., 1995. Descriptions of the Ecoregions of the United States (2nd Edition). Miscellaneous Publication No. 1391, Map-scale 1:7,500,000, U.S. Department of Agriculture, Forest Service. 108 p.

Bailey, R.G., 1998. Ecoregions Map of North America: Explanatory Note. Misc. Pub. No. 1548. Washington, D.C.: USDA Forest Service. 10 pp., with separate map at 1:15,000,000 in cooperation with The Nature Conservancy and the U.S. Geological Survey.

Bailey, R.G., 2004. Changing Ecoregional Map Boundaries. Technical Note dated Feb. 12, 2004 from USDA Forest Service, Inventory & Monitoring Institute. Available from http://www.fs.fed.us/rm/analytics/publications/changing_ecoregional_map_boundaries2.pdf.

Baker and Gherini, 1990: See ALSC, 1990.

Bernhardt, E.S., G.E.Likens, R.O. Hall, Jr., D.C. Buso, S.C. Fisher, T.M. Burton, J.L. Meyer, W,M, McDowell, M.S. Mayer, W.E. Bowden, S.E.G. Findlay, K.H. MacNeale, R.S. Stelzer, and W.H. Lowe. 2005. Can't see the forest for the stream? In-stream processing and terrestrial nitrogen exports. Bioscience 55: 219-230.

Bloom, P.R. 1988. ALBIOS: Dissolution kinetics of minerals. Annual Report to the Electric Power Research Institute, Palo Alto, CA

Boyer, E.W., C.L. Goodale, N.A. Jaworski, and R.W. Howarth. 2002. Anthropogenic nitrogen sources and relationships to riverine nitrogen export in the northeastern U.S.A. Biogeochemistry 57/58:137–169.

Brakke, D.F., A. Henriksen, and S.A. Norton, 1990. A variable F-factor to explain changes in base cation concentrations as a function of strong acid deposition. Verh. Int. Verein. Limnol. 24: 146-149.

Brookshire, J., S. Gerber, J.R. Webster, J.M. Vose, and W.T. Swank. 2010. Direct effects of temperature on forest nitrogen cycling revealed through analysis of long term watershed records. Global Change Biology DOI: 10.1111/J.1365-2486.2010.02245.x

Bryce, S.A., J.M. Omernik, and D.P., Larsen, 1999. Ecoregions: A geographic framework to guide risk characterization and ecosystem management. Environmental Practice, Journal of the National Association of Environmental Professionals 1(3):142-155.

Bulger, A.J., B.J. Cosby, and J.R. Webb. 2000. Current, reconstructed past, and projected future status of brook trout (Salvelinus fontinalis) streams in Virginia. Ca, J. Fish. Aquatic Sci. 57: 1515-1523.

Bulger, A.J., Cosby, B.J,. Dolloff, C.A., Eshleman, K.N., Webb, J.R., Galloway, J.N. 1996. SNP:FISH Shenandoah National Park: Fish in Sensitive Habitats. Project Final Report. Vol. 1. http://www.nps.gov/nero/science/FINAL/Shen%20Fish/Shen%20Fish.htm

Byun, D.W. and J.K.S. Ching (1999) Science Algorithms of the EPA Models-3 Community Multiscale Air Quality (CMAQ) Modeling System. US Environmental Protection Agency, Research Triangle Park, NC, EPA/600/R-99/030, http://www.epa.gov/asmdnerl/CMAQ/CMAQscienceDoc.html.

Campbell, J.L., J.W. Hornbeck, M.J. Mitchell, M.B. Adams, M.S. Castro, C.T. Driscoll, J.S. Kahl, J.N. Kochenderfer, G.E. Likens, J.A. Lynch, P.S. Murdoch, S.J. Nelson, and S.B Shanley. 2004. Input-output budgets of inorganic nitrogen for 24 forested watersheds in the northeastern united states: a review. Water Air and Soil Pollution 151: 373-396.

Canfield, D.E., A.N. Glazer, and P.G. Falkowski. 2010. The evolution and future of Earth's nitrogen cycle. Science 330:192-196.

Castro, M.S., C.T. Driscoll, T.E. Jordan, W.G. Reay, W.R. Boynton, S.P. Seitzinger, R.V. Styles, and J.E. Cable. 2001. Contributions of atmospheric deposition to the total nitrogen loads to thirty-four estuaries on the Atlantic and Gulf coasts of the United States. p. 77-90. In Nitrogen loading in coastal water bodies: and atmospheric perspective. (R.M. Valigura, R.B. Alexander, M.S. Castro, H. Greening, T. Meyers, H. Paerl, and R.E. Turner, eds). Coastal and Estuarine Studies, American Geophysical Union, Washington, DC.

Chen, C.W., R.J.M. Hudson, S.A. Gherini, J.D. Dean, and R.A. Goldstein, 1983. Acid Rain Model: Canopy Module. Journal of Environmental Engineering Vol. 109, No. 3, p. 585-603.

Chen, L., C. T. Driscoll, S. Gbondo-Tugbawa, M. J. Mitchell, and P. S. Murdoch. 2004. The application of an integrated biogeochemical model (PnET-BGC) to five forested watersheds in the Adirondack and Catskill regions of New York. Hydrological Processes 18:2631-2650. (The pNet-BGC model is available from the following Website: http://www.ecs.syr.edu/faculty/driscoll/personal/PnET%20BGC.asp).

Compton, J.E., M. R Church, S.T. Larned, and W.E . Hogsett. 2003. Nitrogen export from forested watersheds in the Oregon Coast Range: the role of N_2-fixing red alder. Ecosystems 6: 773-785.

Cosby, B.J., R.F. Wright, G.M. Hornberger, and J.N. Galloway. 1985a. Modelling the effects of acid deposition: Assessment of a lumped parameter model of soil water and streamwater chemistry. Water Resources Research 21:51–63.

Cosby, B.J., R.F. Wright, G.M. Hornberger, and J.N. Galloway. 1985b. Modelling the effects of acid deposition: Estimation of long-term water quality responses in a small forested catchment. Water Resources Research 21:1591–1601.

Cosby B.J., G.M. Hornberger, J.N. Galloway, and R.F. Wright. 1985c. Time scales of catchment acidification: a quantitative model for estimating freshwater acidification. Environ Sci. Technol, 19, 1144-1149

Dise, N.B. and R.F. Wright. 1995. Nitrogen leaching from European forests in relation to nitrogen deposition. For. Ecol. Mgmt. 71:153-161.

Drever, J.I., and D.R. Hurcomb. 1986. Neutralization of atmospheric acidity in an alpine drainage basin by chemical weathering in the North Cascade Mountains. Geology, 14:221 – 224.

Driscoll, C.T., D.A Schaefer, L.A. Molot, and P.J Dillon. 1989. Summary of North American data. p. 6-1 - 6-45. In The role of nitrogen in the acidification of surface waters. (J.L. Malanchuk and J. Nilsson, eds.). Nordic Council of Ministers, Kobenhavn, Miljrapport 1989:92.

Driscoll, C.T., K.M. Driscoll, K.M. Roy, and J. Dukett. 2007. Changes in the chemistry of lakes in the Adirondack region of New York following declines in acidic deposition. Applied Geochemistry, 22:1181–1188

Dubrovsky, N.M., K.R.Burow, G.M. Clark, J.M. Gronberg, P.A. Hamilton, K.J. Hitt, D.K. Mueller, M.D. Munn, B.T. Nolan, I.J. Puckett, M.G. Rupert, T.M. Short, N.E. Spahr, L.A.Sprague, and W.G. Wilber. 2010. The quality of our nation's waters—Nutrients in the nation's streams and groundwater, 1992-2004: U.S. Geological Survey Circular 1350, 174 p.

Dupont, J., T.A. Clair, C. Gagnon, D.S. Jeffries, J.S. Kahl, S.J. Nelson, and J.M. Peckenham, 2005. Estimation of Critical Loads of Acidity for Lakes in Northeastern United States and Eastern Canada. Environmental Monitoring and Assessment 109:275-291. DOI: 10.1007/s10661-005-6286-x.

ENVIRON (2010) User's Guide – Comprehensive Air-quality Model with extensions, Version 5.30. ENVIRON International Corporation, Novato, CA, http://www.camx.com.

EPA: See US Environmental Protection Agency.

Electric Power Research Institute (EPRI), 1989. Acid Rain Research Results An Environmental Briefing – July 1989. Report No. EN 3006.7 89, 16 pp.

Galloway, J.N, J.D. Aber, J.W. Erisman, S.P. Seitz1inger, R.W. Howarth, E.B. Cowling, and B.J. Cosby. 2003. The nitrogen cascade. BioScience 53(4):341-356.

Gherini, S.A., L. Mok, R.J.M. Hudson, G.F. Davis and R.A. Goldstein. 1985. The ILWAS Model: Formulation and application. Water, Air, and Soil Pollution. 26:425-459.

Goldstein, R.A., S.A. Gherini, C.W. Chen, L. Mok, and R.J.M. Hudson. 1984. Integrated Acidification Study (ILWAS): A Mechanistic Ecosystem Analysis. Phil. Trans. Royal Society London B. 305:409-425.

Goldstein, R.A., C.W. Chen and S.A. Gherini. 1985. The Integrated Lake-Watershed Acidification (ILWAS) Study: Summary. Water, Air, and Soil Pollution. 26:327-337.

Goodale, C. L., S.A. Thomas, G. Fredriksen, E.M. Elliott, K.M. Flinn, T.J. Butler, and M.T. Walter. 2009. Unusual seasonal patterns and inferred processes of N retention in forested headwaters of the Upper Susquehanna River. Biogeochemistry 93:197-218.

Goodale, C.L., J.D. Aber, and W.H. McDowell. 2000. The long-term effects of disturbance on organic and inorganic nitrogen export in the White Mountains, New Hampshire. Ecosystems 3:433–450.

Gran, G. 1952. Determination of the equivalence point in potentiometric titrations. ANALYST: Int. Congr. Anal. Chem. 77:661 - 671

Groffman, P.M., N.L. Law, K.T. Belt, L.E. Band, and G.T. Fisher. 2004. Nitrogen fluxes and retention in urban watershed ecosystems. Ecosystems 7:393-403.

Gundersen, P., Callesen, I., and de Vries, W. 1998. Nitrate leaching in forest ecosystems is controlled by forest floor C/N ratio. Environ. Pollut. 102: 403-407.

Gundersen, P., I.K. Schmidt, and K. Raulund-Rasmussen. 2006. Leaching of nitrate from temperate forests–effects of air pollution and forest management, Environ. Rev. 14:1-57.

Hargrove and Hoffman, 1999. Using multivariate clustering to characterize ecoregion borders. Computers in Science and Engineering, 1: 18-25.

Hargrove and Hoffman, 2004. The potential of multivariate quantitative methods for delineation and visualization of ecoregions. Environmental Management, 34, S39-S60.

Hargrove and Hoffman, 2009. Index to National Ecological Observatory Network (NEON) Domain Development and Presentation "Why 20 NEON Domains". http://www.geobabble.org/~hnw/neon/neonindex/ Maps of the NEON Domains and other information were accessed from http://www.neoninc.org/domains/overview.

Henriksen, A., 1984. Changes in base cations concentrations due to freshwater acidification. Verh. International. Verein. Limnol., 22:692-698.

Henriksen, A., Dillon, P.J., Aherne, J. 2002. Critical loads of acidity for surface waters in south-central Ontario, Canada: regional application of the Steady-State Water Chemistry (SSWC) model. Can. J. Fish. Aquat. Sci. 59: 1287-1295.

Ice, G. and D. Binkley. 2003. Forest streamwater concentrations of nitrogen and phosphorus. Journal of Forestry, January/February:21-28.

Ito, M., M.J. Mitchell, C.T. Driscoll, and K.M. Roy. 2005. Nitrogen input-output budgets for lake-containing watersheds in the Adirondack region of New York. Biogeochemistry 72: 283-314.

Johnson, D.W. 1992. Nitrogen retention in forest soils. Journal Environmental Quality 21:1-12.

Johnson, S. and R. Fredriksen. 2010. Long-term stream chemistry concentrations and fluxes: Small watershed proportional samples in the Andrews Experimental Forest. Forest Science Data Bank, Corvallis, OR. [Database]. Accessed 25 October 2010 from.http://andrewsforest.oregonstate.edu/data/abstract.cfm?dbcode=CF002.

Jones, J.B., K.C. Petrone, J.C. Finlay, L.O. Hinzman, and W.R. Bolton. 2005. Nitrogen loss from watersheds of interior Alaska underlain with discontinuous permafrost. Geophysical Research Letters 32: L02401, DOI: 10.1029/2004GL021734.

Kane, E.S., E.F. Betts, A.J. Burgin, H.M. Clilverd, C.L. Crenshaw, J.B. Fellman, I.H. Myers-Smith, J.A. O'Donnell, D.J. Sobota, W.J. Van Verseveld and J.B. Jones. 2008. Precipitation control over inorganic nitrogen import-export budgets across watersheds: a synthesis of long-term ecological research. Ecohydrology 1:105-117.

Karamchandani, P., C. Seigneur, K. Vijayaraghavan, S.Y. Wu. 2002. Development and application of a state–of–the–science plume–in–grid model. Journal of Geophysical Research D: Atmospheres, 107, art. No. 4403.

Karamchandani, P., K. Vijayaraghavan, R. Bronson, S.-Y. Chen, and E.M. Knipping. 2010. Development and application of a parallelized version of the Advanced Modeling System for Transport, Emissions, Reactions and Deposition of Atmospheric Matter (AMSTERDAM): 1. Model performance evaluation. Atmos. Poll. Res., 1, 260—270, doi: 10.5094/APR.2010.033.

Karamchandani, P., K. Vijayaraghavan, S.-Y. Chen, C. Seigneur, E.S. Edgerton. 2006. Plume–in–grid modeling for particulate matter. Atmospheric Environment, 40, 7280–7297.

Karamchandani, P., L. Santos, I. Sykes, Y. Zhang, C. Tonne, and C. Seigneur. 2000. Development and evaluation of a state–of–the–science reactive plume model. Environmental Science and Technology, 34, 870–880.

Keller, A.E and T.L. Crisman, 1990. Factors Influencing Fish Assemblages and Species Richness in Subtropical Florida Lakes and a Comparison with Temperate Lakes. Can, J, Fish Aquatic Science, Vol. 47, p. 2137-2146.

Kristensen, H.L., Gundersen, P., Callesen, I., and Reinds, G.J. 2004. Relationships between soil nitrate concentrations and environmental factors. Ecosystems, 7: 180-192.

Likens, G. E., C. T. Driscoll, D. C. Buso, T. G. Siccama, C. E. Johnson, D. F. Ryan, G. M. Lovett, T. Fahey and W. A. Reiners. 1994. The biogeochemistry of potassium at Hubbard Brook. Biogeochemistry, 25:61-125, http://www.hubbardbrook.org/research/longterm/whole_tree/w5_overview/w5-tim.htm

Lindberg, S.E., G.M. Lovett, D.D. Richter, and D.W. Johnson, 1986. Atmospheric Deposition and Canopy Interactions of Major Ions in a Forest. Science Vol. 231, No. 4734, p. 141-145.

Lovett, G.M. and M.J. Mitchell. 2004. Sugar maple and nitrogen cycling in the forests of eastern North America. Frontiers of Ecology and the Environment 2(2):81-88.

Lovett, G.M., K.C. Weathers, and W. Sobczak. 2000. Nitrogen saturation and retention in forested watersheds of the Catskill Mountains, NY. Ecol. Appl. 10:73–84.

MacDonald, J.A., Dise, N.B., Matzner, E., Armbruster, M., Gundersen, P., and Forsius, M. 2002. Nitrogen input together with ecosystem nitrogen enrichment predict nitrate leaching from European forests. Glob. Chang. Biol. 8: 1028-1033.

Mayer, B., L.I. Wassenaar, J. Chao, L. Rock, K. Hogue, S. Katvala, and B. Promse, 2009. The Impact of Land Use on Sources of Riverine Sulfate, Nitrate, and Chloride in a Large Watershed in Western Canada. Presentation

Meixner, T. and M. Fenn. 2004. Biogeochemical budgets in a Mediterranean catchment with high rates of atmospheric N deposition - importance of scale and temporal asynchrony. Biogeochemistry 70:331-356.

Morris R.E., E. Tai, T. Sakulyanontvittaya, D. McNally, and C. Loomis (2008) Model Performance Evaluation for the June-July 2006 Ozone Episode for the Denver 8-Hour Ozone State Implementation Plan. Final Report prepared for Denver Regional Air Quality Council, Denver, CO, http://www.colorado.gov/airquality/documents/deno308/Denver_2006MPE_DraftFinal_Aug29_2008.pdf.

Morris, R.E., B. Koo, P. Piyachaturawat, G. Stella, D. McNally, C. Loomis, C.-J. Chien, and G. Tonnesen (2009a) Technical Support Document for VISTAS Emissions and Air Quality Modeling to Support Regional Haze State Implementation Plans. Final Report prepared for Visibility Improvement State and Tribal Association of the Southeast, Swannanoa, NC, http://www.metro4-sesarm.org/vistas/data/RHR/Modeling/Reports/VISTASII_TSD_FinalReport_3-09.pdf.

Morris, R.E., S. Kemball-Cook, T. Sakulyanonyvittaya, L. Parker, T. Shah, U. Nopmomngcol, and P. Piyachaturawat (2009b) Uinta Basin Air Quality Study (UBAQS) Technical Report. Final Report prepared for Independent Petroleum Association of Mountain States, Denver, CO, http://ipams.org/wp-content/uploads/UBAQS_Final_Report_Jun30_2009.pdf.

Mulholland, P.J. 2004. The importance of in-stream uptake for regulating stream concentrations and outputs of N and P from a forested watershed: evidence from long-term chemistry records for Walker Branch watershed. Biogeochemistry 70: 403-426.

Munson, R.K., S.A. Gherini, M.M. Lang, L.E. Gomez, C.W. Chen, R.A. Goldstein, and D.R. Knauer. 1987. ILWAS Model Applications: Response of Various Surface Waters to Deposition Acidity, in Acid Rain: Scientific and Technical Advances. Selper Publishing, London.

Munson, R.K., S.A. Gherini, K.H. Reckhow, and C.T. Driscoll. 1990. Integrated Analysis of ALSC Chemistry Data. Pages 2–92 to 2–110. In: Adirondack Lakes Survey: An Interpretive Analysis of Fish Communities and Water Chemistry, 1984–87. Adirondack Lakes Survey Corporation, Ray Brook, New York.

Munson, R.K., and S.A. Gherini. 1991a. Processes Influencing the Acid-Base Characteristics of Surface Waters. In: D.F. Charles, ed. Acid Deposition and Aquatic Ecosystems: Regional Case Studies. Springer-Verlag, New York.

Munson, R.K., and S.A. Gherini. 1991b. Hydrochemical Assessment Methods for Analyzing the Effects of Acidic Deposition on Surface Waters. In: D.F. Charles, ed. Acid Deposition and Aquatic Ecosystems: Regional Case Studies. Springer-Verlag, New York.

Munson, R.K. and S.A. Gherini. 1993. Analysis of the mineral acid-base components of acid-neutralizing capacity in Adirondack Lakes. Water Resources Research Vol. 29, No. 4 p. 881–890.

National Atmospheric Deposition Program (NADP). 2010. National Atmospheric Deposition Program/National Trends Network data. http://nadp.sws.uiuc.edu/NADP/.

Newton, R.M., J. Weintraub, and R.H. April. 1987. The relationship between surface water chemistry and geology in the North Branch of the Moose River. Biogeochemistry, 3:21 – 35

Nilsson, S.I., Berggren, D., and Westling, O. 1998. Retention of deposited $NH4^{+}$-N and NO_3^{-}-N in coniferous forest ecosystems in Southern Sweden. Scand. J. For. Res. 13: 393–401.

Omernik, J.M. (1987) Ecoregions of the conterminous United States. Map (scale 1:7,500,0000). Annals of the Association of American Geographers, 77, 118-125, http://www.epa.gov/wed/pages/ecoregions.htm.

Omernik, J.M. and C.F. Powers, 1983. Map Supplement: Total Alkalinity of Surface Waters – A National Map. Annals of the Association of American Geographers, Vol. 73, No. 1. Pp. 133–136.

Omernik, J.M. and G.E. Griffith, 1986. Total Alkalinity of Surface Waters: a Map of the Upper Midwest Region of the United States. Environmental Management, Vol. 10, No. 6, pp. 829–839.

Omernik, J.M. and R.G. Bailey, 1997. Distinguishing Between Watersheds and Ecoregions. Journal of the American Water Resources Association Vol 33, No. 5, p. 935–949.

Omernik, J.M., 1987a. Ecoregions of the conterminous United States. Map (scale 1: 1:7,500,000). Annals of the Association of American Geographers 77:118–125.

Omernik, J.M., 1987b. Perspectives on the Nature and Definition of Ecological Regions. Environmental Management, Vol. 34, Suppl. 1, pp. S27–S38.

Pollman, C.D., T.M. Lee, W.J. Andrews, L.A. Sacks, S.A. Gherini, and R.K. Munson. 1991. Preliminary Analysis of the Hydrologic and Geochemical Controls on Acid Neutralizing Capacity in Two Acidic Seepage Lakes in Florida. Water Resources Research, 27:2321 - 2335.

Riggan, P.J., R.N. Lockwood, P.M. Jacks, C.G. Colver, F. Weirich, L.F. DeBano, and J.A. Brass.1994. Effects of fire severity on nitrate mobilization in watersheds subject to chronic atmospheric deposition. Environ. Sci. Technol. 28:365-379.

Rochelle, B.P. and M.R. Church, 1987. Regional patterns of sulfur retention in watersheds of the eastern US. Water, Air, and Soil Pollution 36(1-2):61-73.

Rochelle, B.P., M.R. Church, and M.B. David, 1987. Sulfur retention at intensively studies sites in the US and Canada. Water, Air, and Soil Pollution 33:73-83.

Schimel, D., M. Keller, and P. Duffy, 2009. The NEON Strategy Enabling Continental Scale Ecological Forecasting, Second Edition. NEON, Inc, Boulder, CO.

Schnoor, J.L. and W. Stumm. 1984. Acidification of aquatic and terrestrial systems. Pages 311 – 338 in W. Stumm, ed. Chemical Processes in Lakes, John Wiley and Sons, New York.

Stoddard, J.L. 1994. Long-term changes in watershed retention of nitrogen: its causes and aquatic consequences. p. 223-284. In: Environmental Chemistry of Lakes and Reservoirs. (L.A. Baker, ed.) Advances in Chemistry Series, No. 237, American Chemical Society, Washington, DC.

Stoeckenius, T.E., C.A. Emery, T.P. Shah, J.R. Johnson, L.K. Parker, and A.K. Pollack (2009) Air Quality Modeling Study for the Four Corners Region. Final Report prepared for New Mexico Environment Department Air Quality Bureau, Santa Fe, NM, http://www.nmenv.state.nm.us/aqb/4C/Documents/FinalRepRev20090806.pdf.

Southern Appalachian Mountain Initiative (SAMI) Final Report, 2002. ftp://narsto.esd.ornl.gov/pub/SAMI/SAMI_CD2/SAMI_reports/

Stumm, W. and J.J. Morgan, 1981. Aquatic Chemistry: An Introduction Emphasizing Chemical Equilibria in Natural Waters. 2nd Edition. John Wiley & Sons, New York, New York.

Sullivan, T.J., J.R. Webb, K.U. Snyder, A.T. Herlihy, and B.J. Cosby, 2007a. Spatial Distribution of Acid-sensitive and Acid-impacted Streams in Relation to Watershed Features in the Southern Appalachian Mountains. Water, Air, and Soil Pollution 182:57-71, DOI 10.1007/s11270-006-9320-x.

Sullivan, TJ; Cosby, BJ; Herlihy, AT; Driscoll, CT; Fernandez, IJ; McDonnell, TC; Boylen, CW; Nierzwicki-Bauer, SA; Snyder, KU. 2007b. Assessment of the Extent to Which Intensively-studied Lakes are Representative of the Adirondack Region and Response to Future Changes in Acidic Deposition. Water, Air and Soil Pollution, 185, 279-291.

Sullivan, T.J., B.J. Cosby, J.R. Webb, R.L. Dennis, A.J. Bulger, and F.A. Deviney, Jr. 2008. Streamwater acid-base chemistry and critical loads of atmospheric sulfur deposition in Shenandoah National Park, Virginia. Environ. Monit. Assess. 137:85-99.

Sullivan, T.J., B.J. Cosby, and T.C. McDonnell. 2009. Aquatic critical loads in Virginia and West Virginia – Results of the Southeast multi-agency critical loads modeling project. National Atmospheric Deposition Program (NADP), Saratoga Springs, NY, October, 2009.

Swank, W.T. and J.M. Vose. 1997. Long-term nitrogen dynamics of Coweeta forested watersheds in the southeastern United States of America. Global Biogeochemical Cycles 11:657-671.

SYSTAT, Inc. 2007. Intelligent software, version 12.0. SYSTAT, Inc., Evanston, IL.

US Environmental Protection Agency (EPA), 2007. Level III Ecoregion Map for the United States. http://www.epa.gov/wed/pages/ecoregions.htm. The Level I, II, III, and IV ecoregion maps were accessed from this link in October 2010 and revised Level III map in May 2011.

US Environmental Protection Agency (EPA), 2008. Integrated Science Assessment for Oxides of Nitrogen and Sulfur Ecological Criteria (Final Report). US Environmental Protection Agency, Washington, D.C., EPA/600/R-08/082F.

US Environmental Protection Agency (EPA), 2009. Risk and Exposure Assessment for Review of the Secondary National Ambient Air Quality Standards for Oxides of Nitrogen and Oxides of Sulfur - Main Document and Appendices - Final Report. US Environmental Protection Agency, Research Triangle Park, NC, EPA-452/R-09-008a.

US Environmental Protection Agency (EPA), 2010. Primary Distinguishing Characteristics of Level III Ecoregions of the Continent United States. July, 2010. US Environmental Protection Agency, Washington, D.C.; Available at http://www.epa.gov/wed/pages/ecoregions/level_iii_iv.htm.

US Environmental Protection Agency (EPA), 2011. Policy Assessment for the Review of the Secondary National Ambient Air Quality Standards for Oxides of Nitrogen and Oxides of Sulfur. US Environmental Protection Agency, Research Triangle Park, NC, EPA-452/R-11-005a.

US Geological Survey (USGS). 2010. National Water-Quality Assessment Program data. http://water.usgs.gov/nawqa/nutrients/pubs/circ1350/. Accessed 15 Oct 2010.

Vitousek, P.M. R.W. Howarth, G.E. Likens, P.A. Matson, D. Schindler, W.H. Schlesinger, and G.D. Tilman. 1997. Human alteration of the global nitrogen cycle: Causes and consequences. Issues in Ecology 1:1-17.

Warfvinge, P. and H. Sverdrup. 1992. Calculating critical loads of acid deposition with PROFILE, a steady-state soil chemistry model. Water Air and Soil Pollution, 63: 119 - 143.

Webb, J.R. 2004. Effects of Acidic Deposition on Aquatic Resources in the Central Appalachian Mountains. Shenandoah Watershed Study Report.

Williard, K.W.J., D.R. DeWalle, P.J. Edwards, and R.R. Schnabel. 1997. Indicators of nitrate export from forested watersheds in the mid-Appalachians, United States of America. Global Biogeochemical Cycles 11:649–56.

Zhang, Y., B. Pun, K. Vijayaraghavan, S.Y. Wu, C. Seigneur, S. Pandis, M. Jacobson, A. Nenes, J.H. Seinfeld (2004) Development and application of the model of aerosol dynamics, reaction, ionization and dissolution. Journal of Geophysical Research D: Atmospheres, 109, art. No. D01202.

Appendix B: Selected Ecoregion Maps

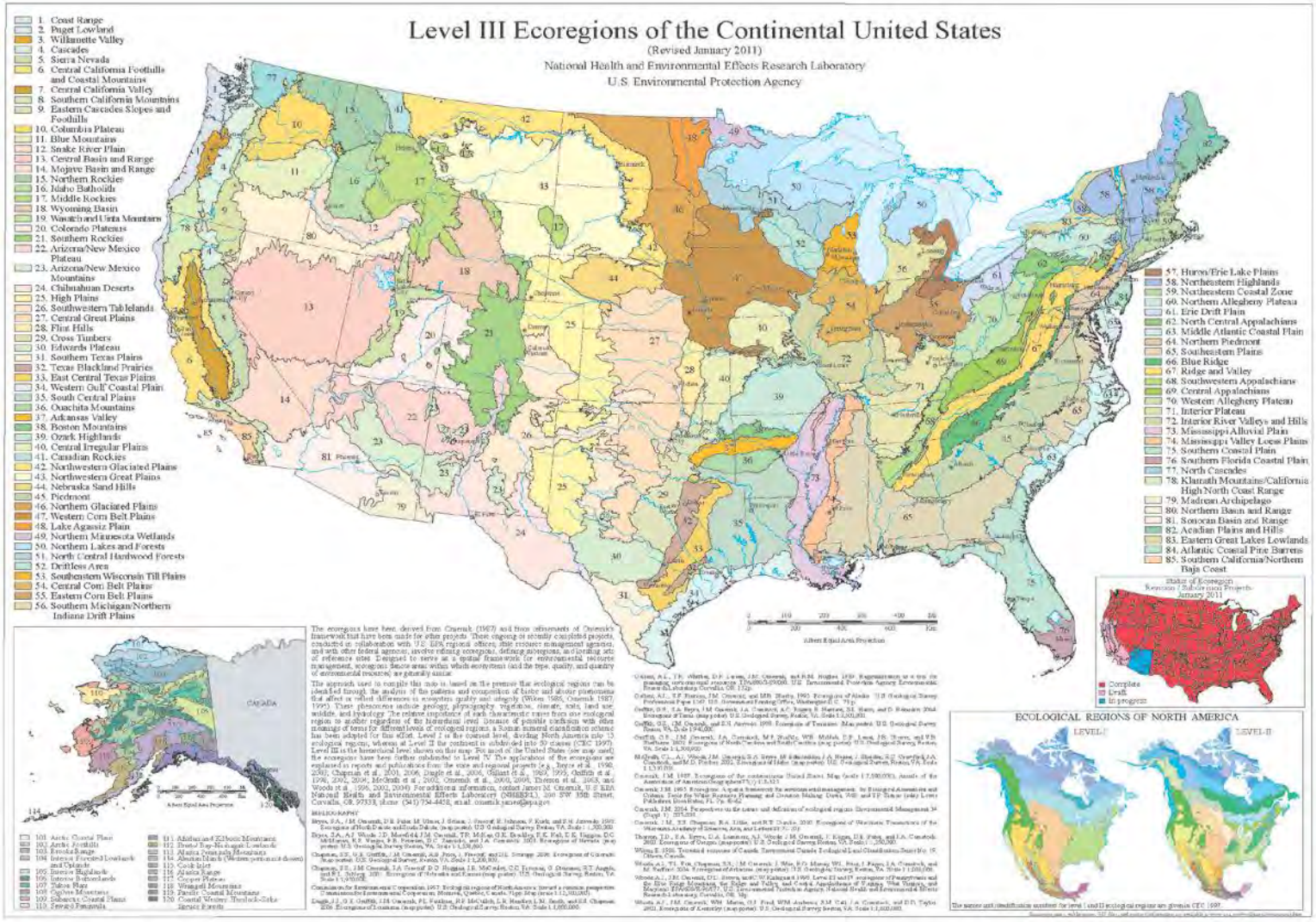

Figure B-1: Level III Ecoregion Map of the Entire US.

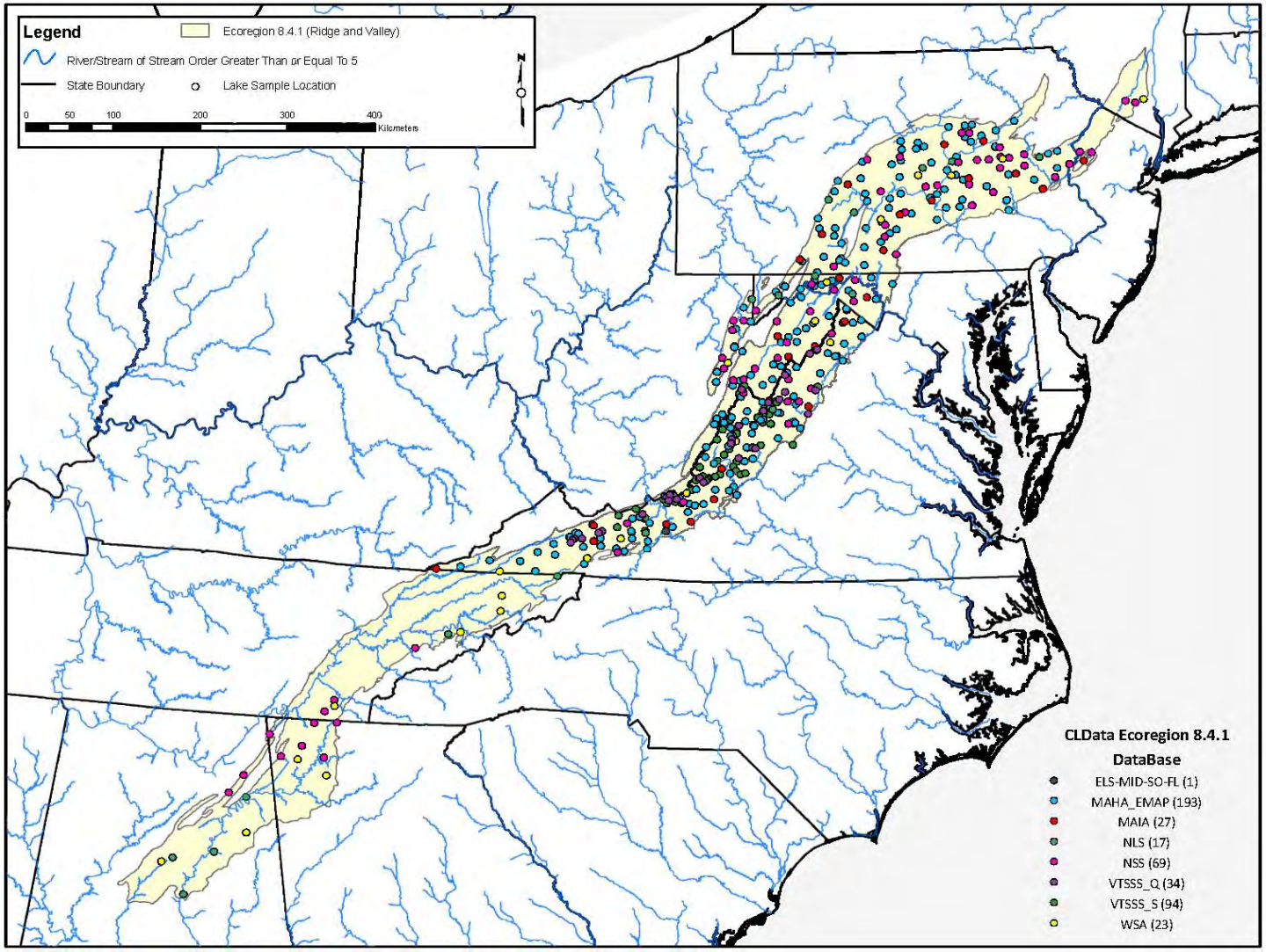

Figure B-2: Data Sets Used by EPA for Ecoregion 8.4.1 Ridge and Valley.

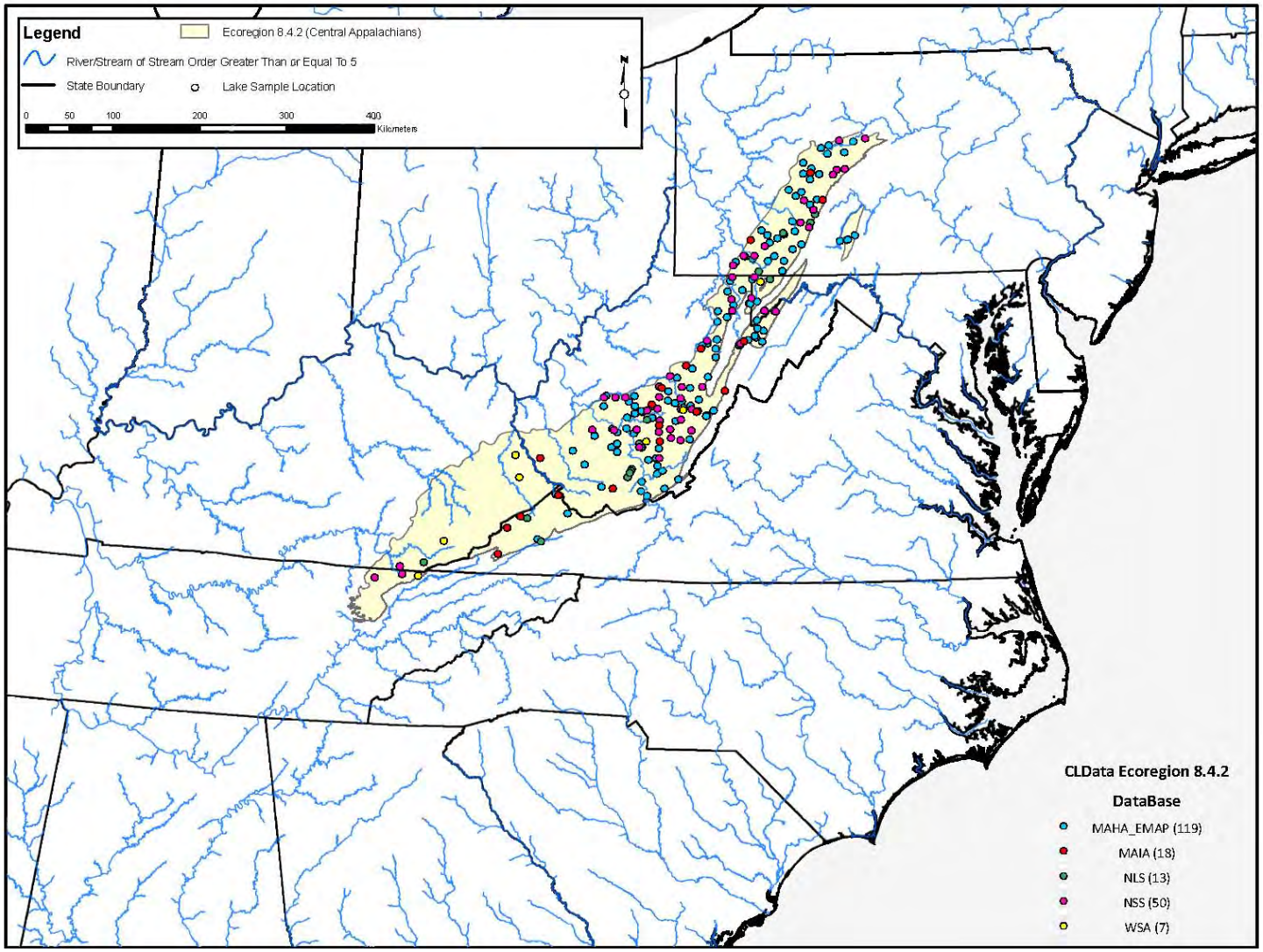

Figure B-2: Data Sets Used by EPA for Ecoregion 8.4.2 Central Appalachians.

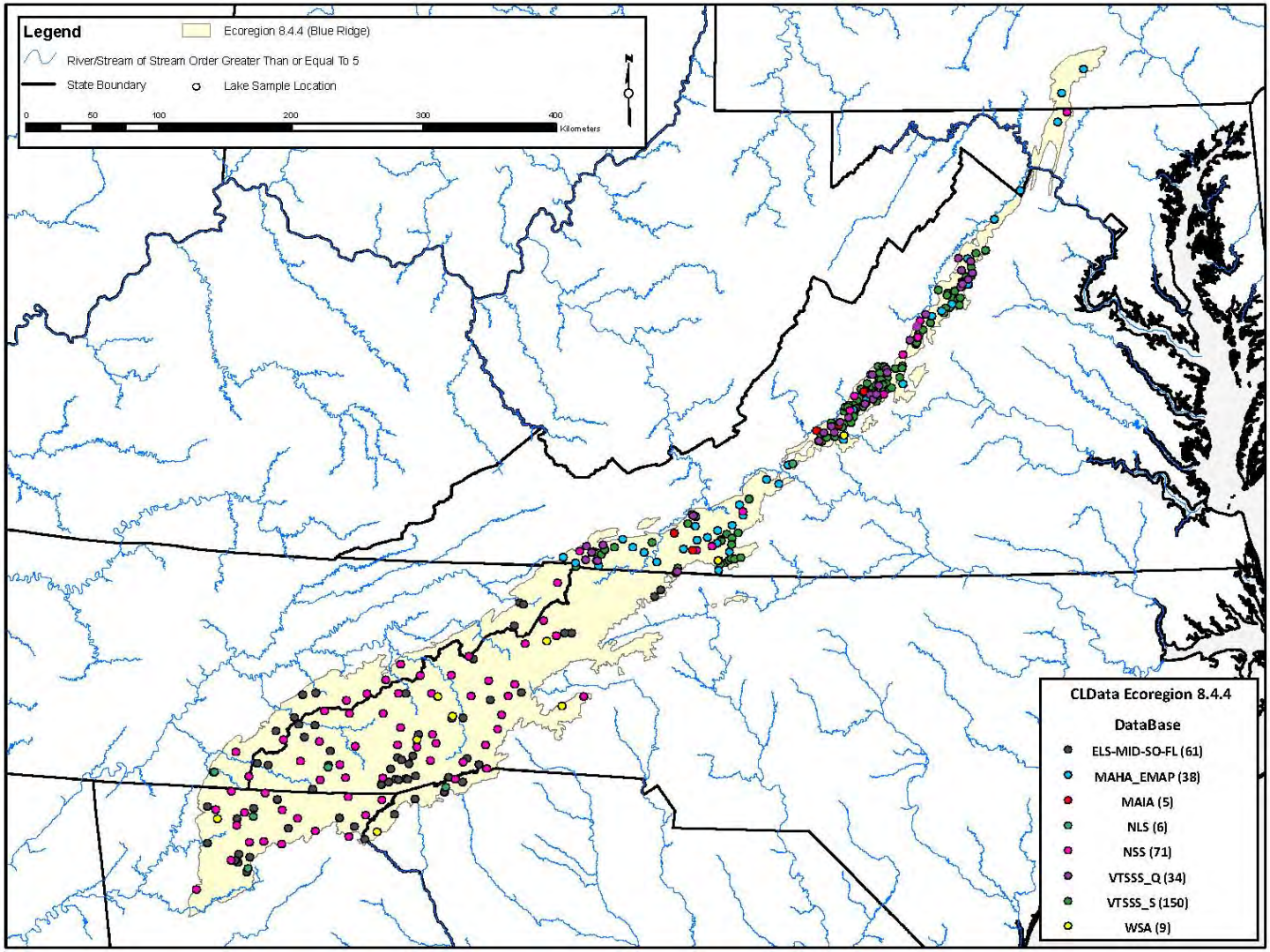

Figure B-4: Data Sets Used by EPA for Ecoregion 8.4.4 Blue Ridge.

Appendix C1: Scatter Plots of Annual Average Concentrations and Annul Total Deposition

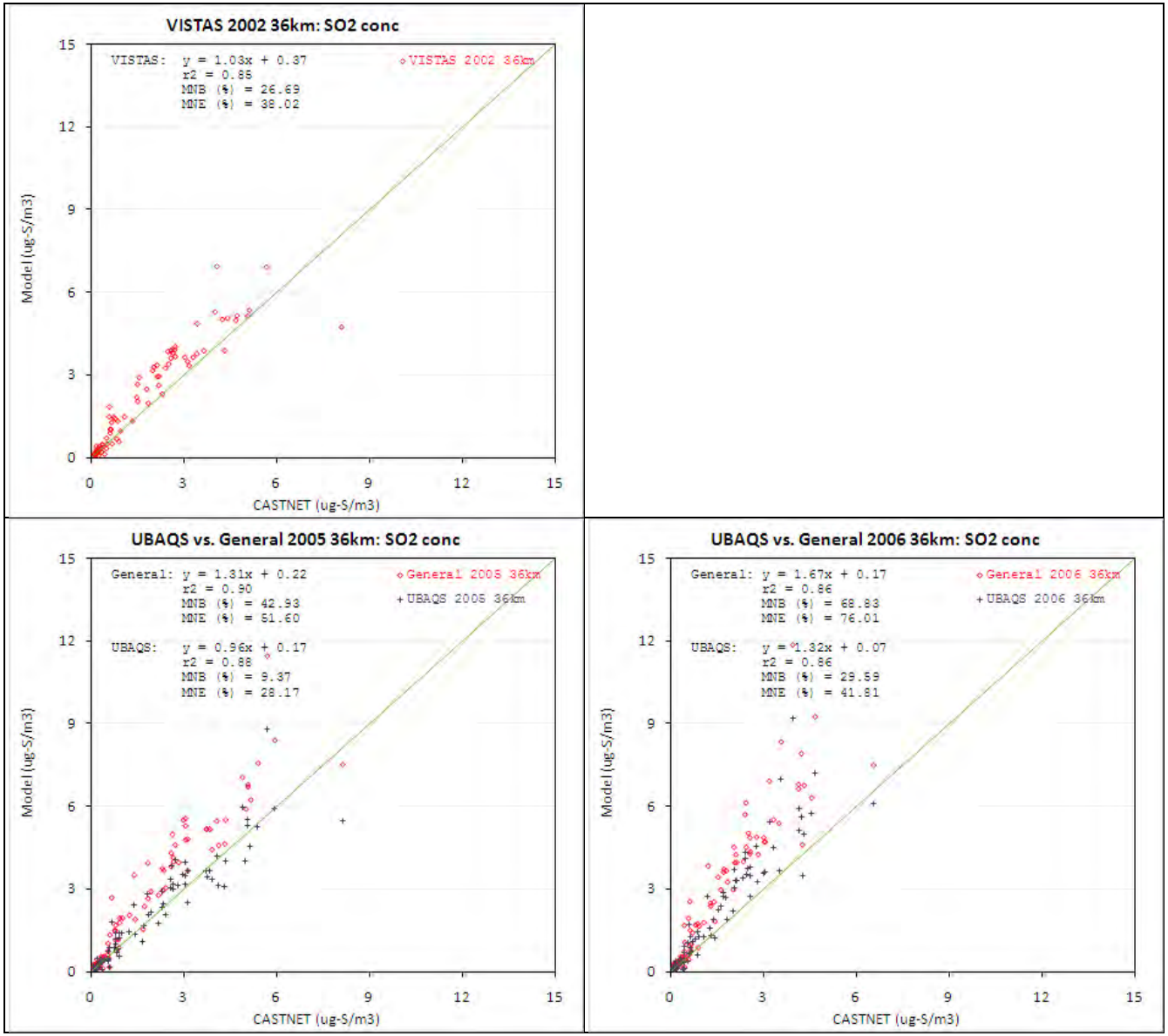

Figure C1-1. Scatter plots of annual average SO_2 concentrations: modeled vs. observed at CASTNET stations.

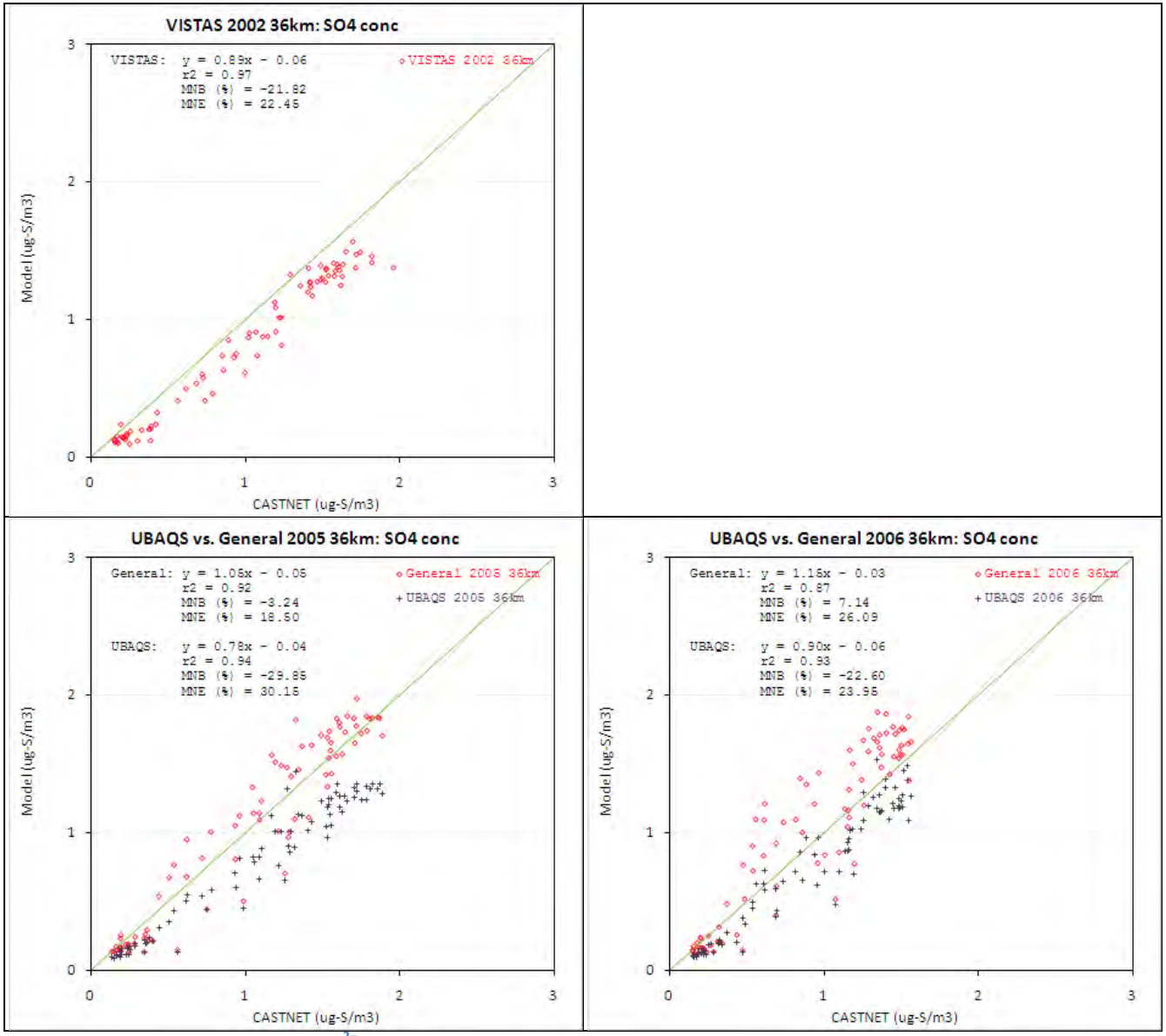

Figure C1-2. Scatter plots of annual average particulate SO_4^{2-} concentrations: modeled vs. observed at CASTNET stations.

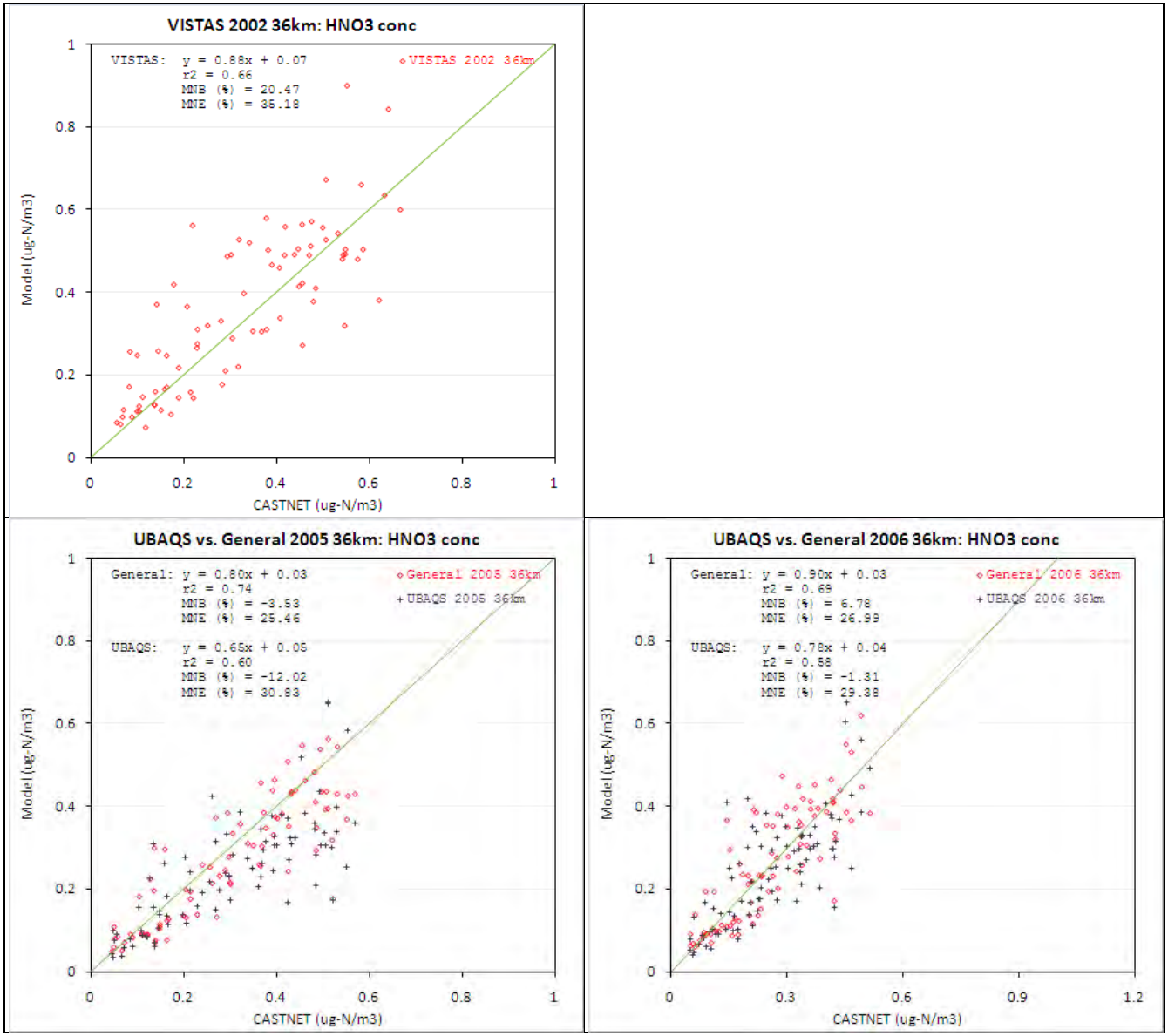

Figure C1-3. Scatter plots of annual average HNO_3 concentrations: modeled vs. observed at CASTNET stations.

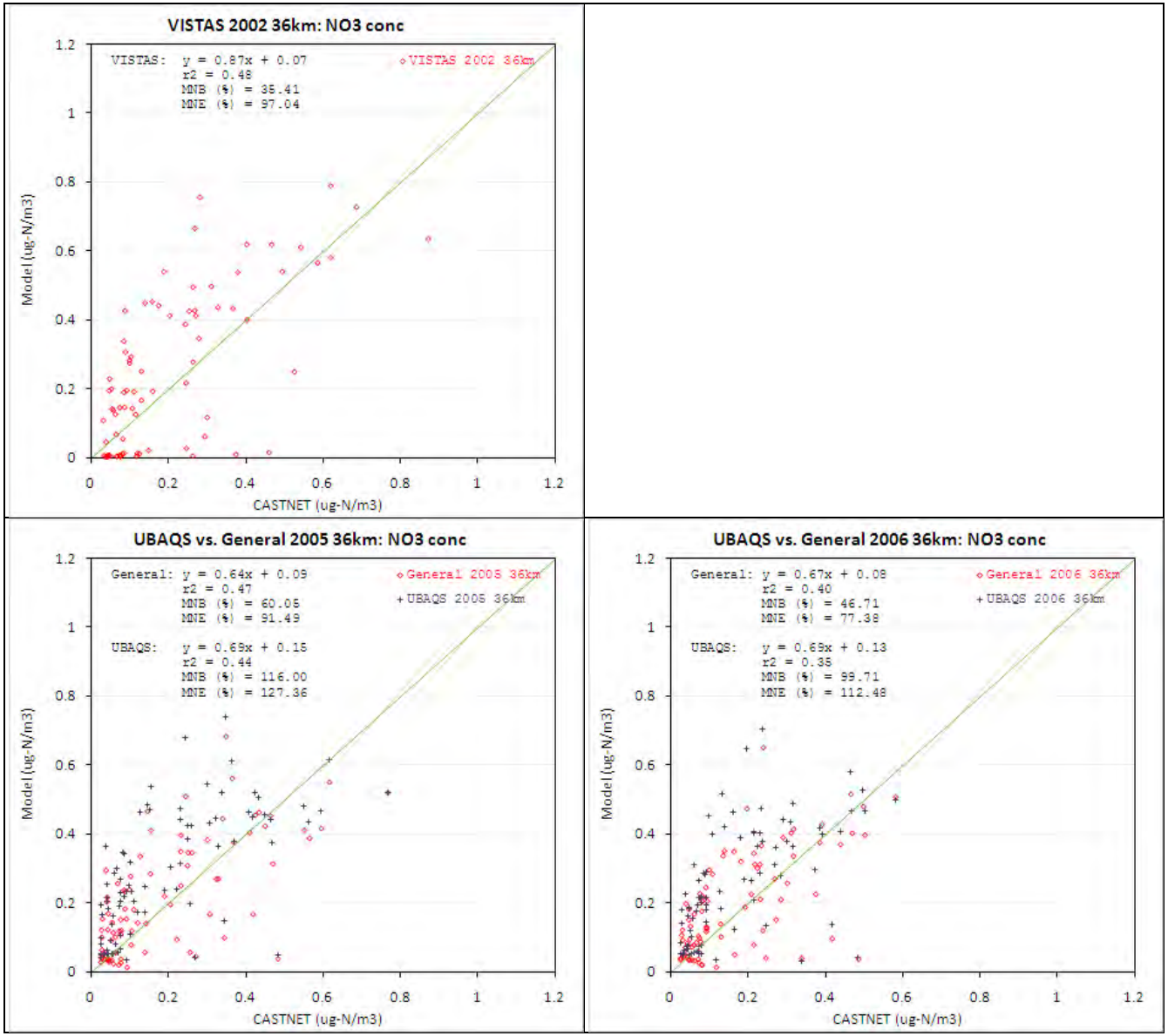

Figure C1-4. Scatter plots of annual average particulate NO_3^- concentrations: modeled vs. observed at CASTNET stations.

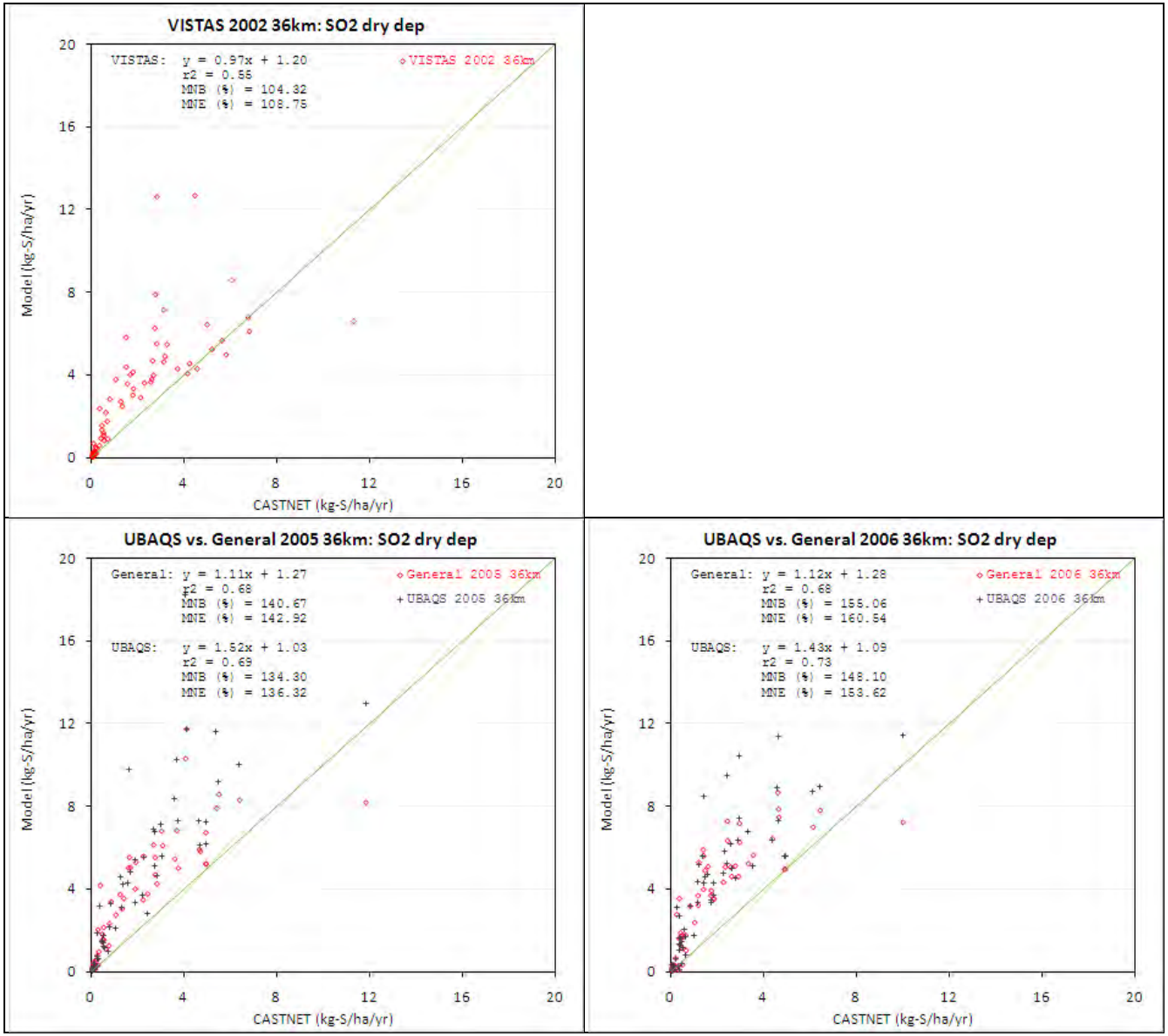

Figure C1-5. Scatter plots of annual total SO_2 dry deposition: modeled vs. observed at CASTNET stations.

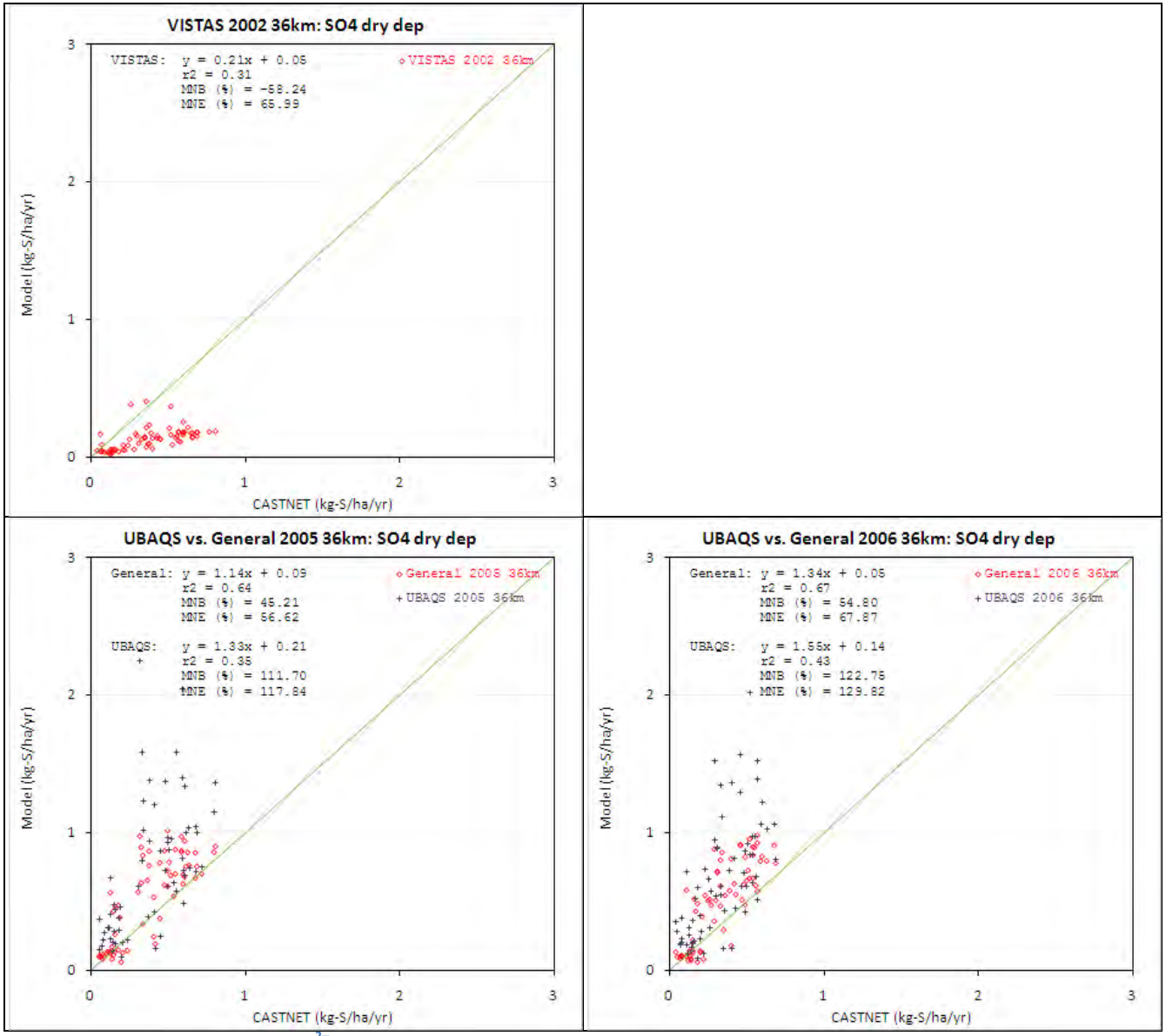

Figure C1-6. Scatter plots of annual total particulate SO_4^{2-} dry deposition: modeled vs. observed at CASTNET stations.

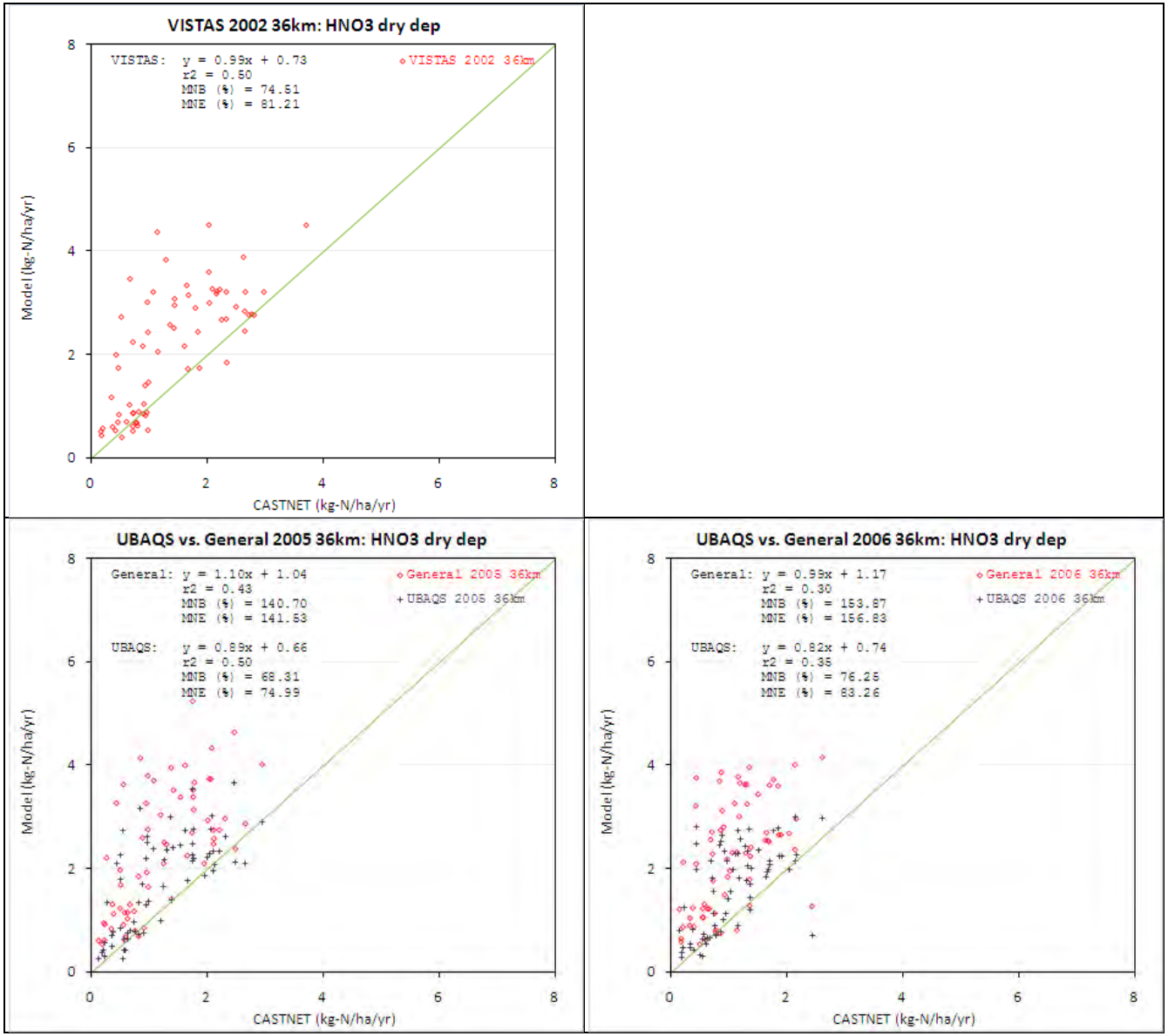

Figure C1-7. Scatter plots of annual total HNO_3 dry deposition: modeled vs. observed at CASTNET stations.

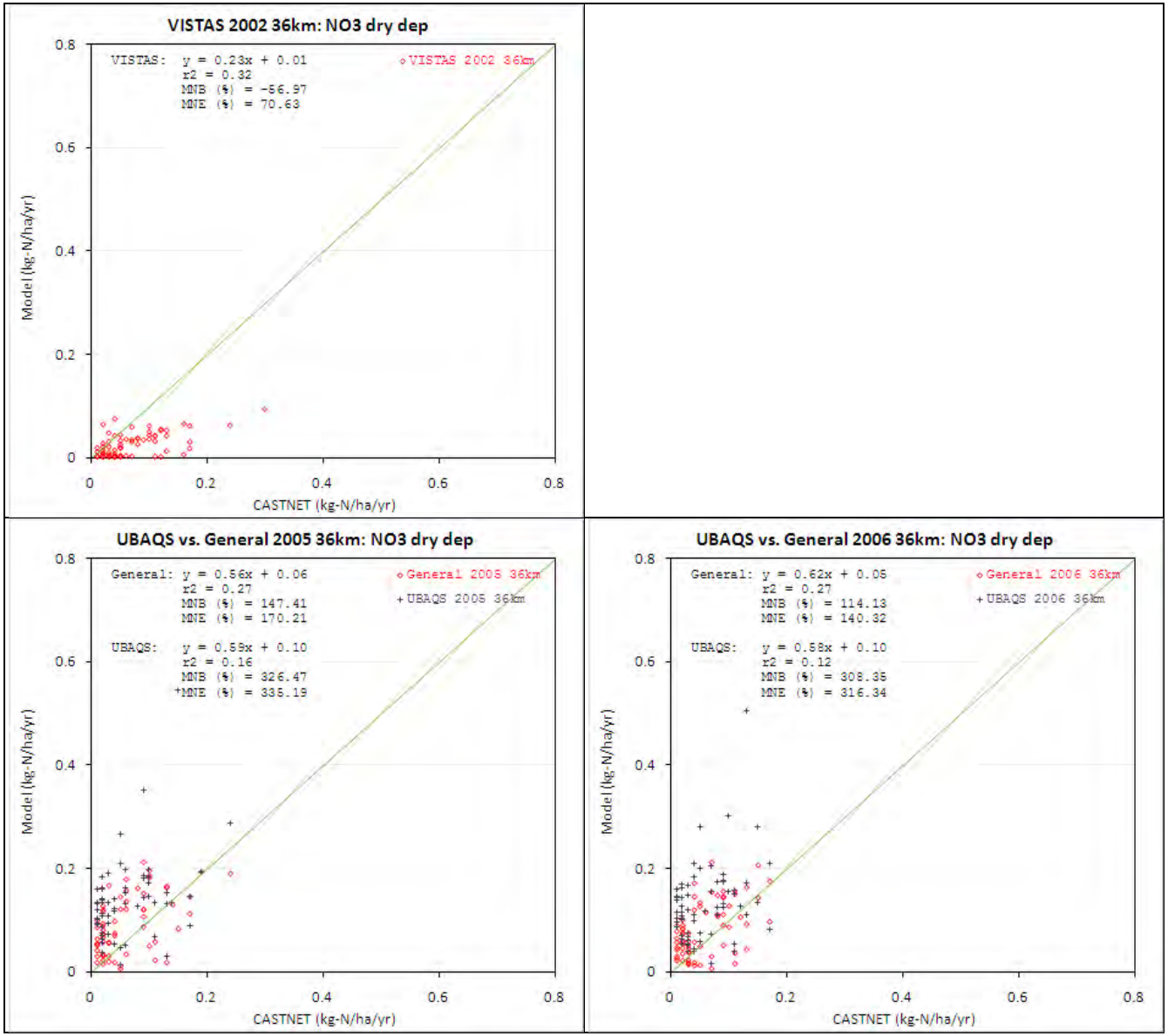

Figure C1-8. Scatter plots of annual total particulate NO_3^- dry deposition: modeled vs. observed at CASTNET stations.

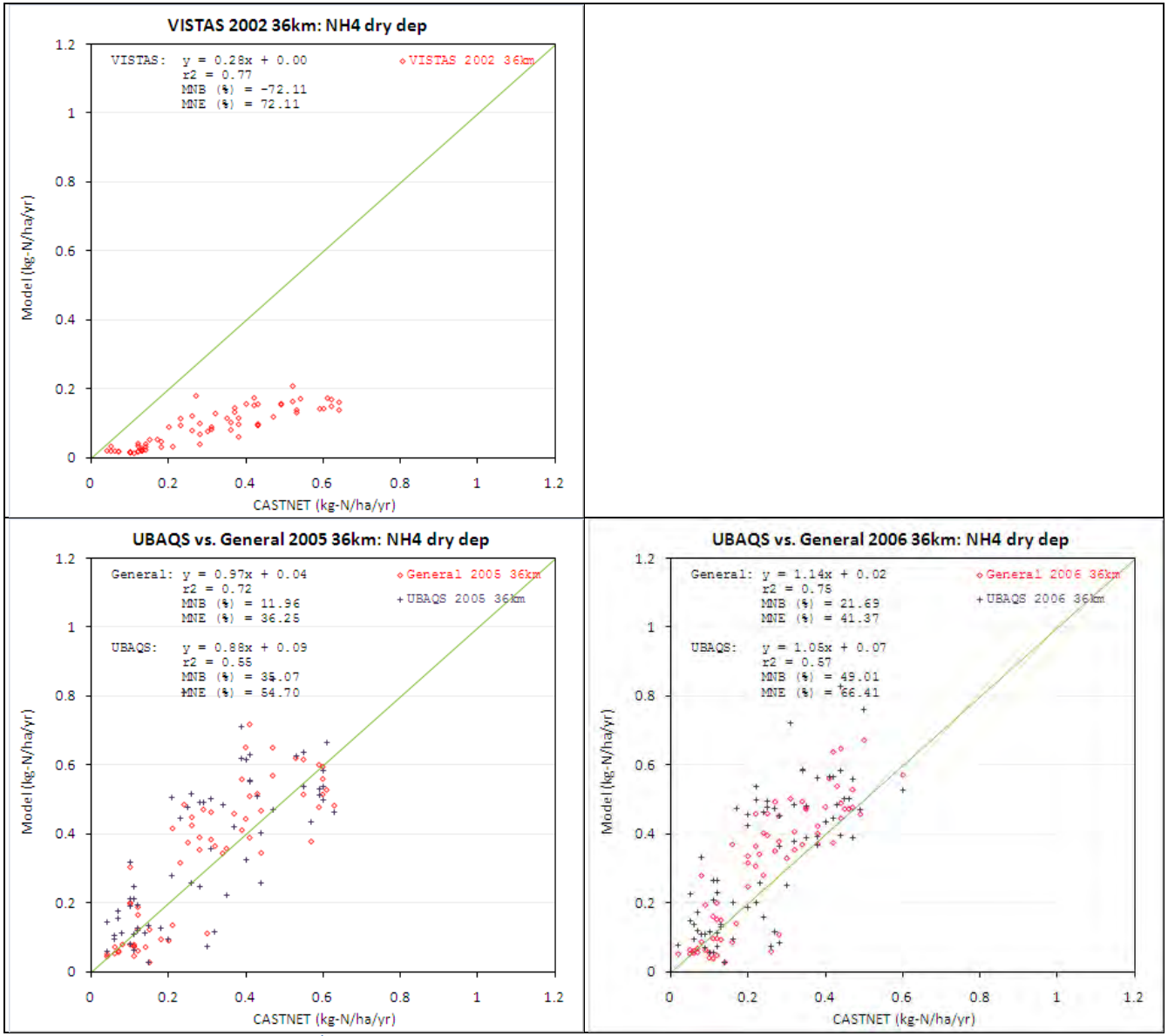

Figure C1-9. Scatter plots of annual total particulate NH_4^+ dry deposition: modeled vs. observed at CASTNET stations.

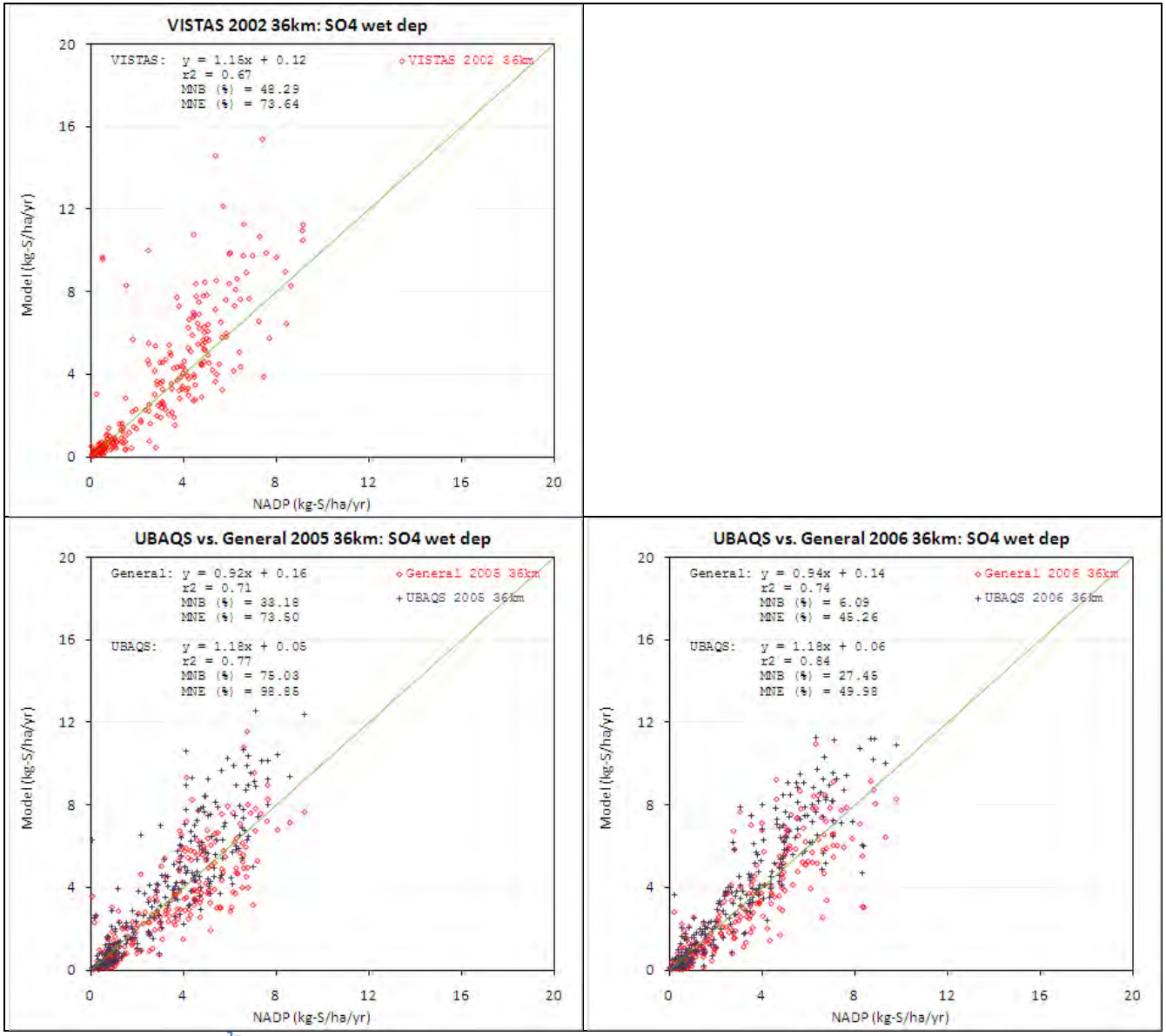

Figure C1-10. Scatter plots of annual total SO_4^{2-} wet deposition: modeled vs. observed at NADP stations.

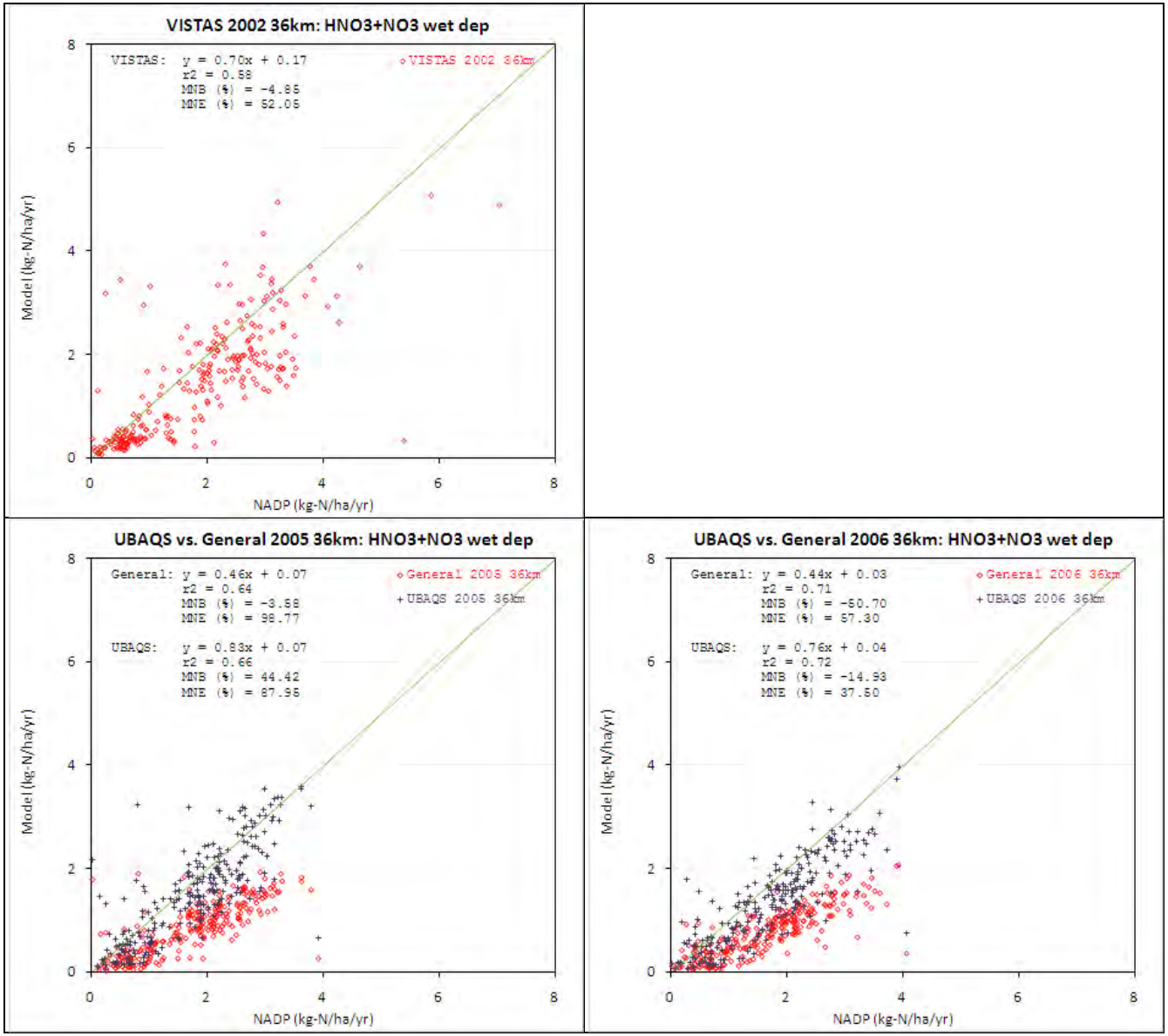

Figure C1-11. Scatter plots of annual total $HNO_3 + NO_3^-$ wet deposition: modeled vs. observed at NADP stations.

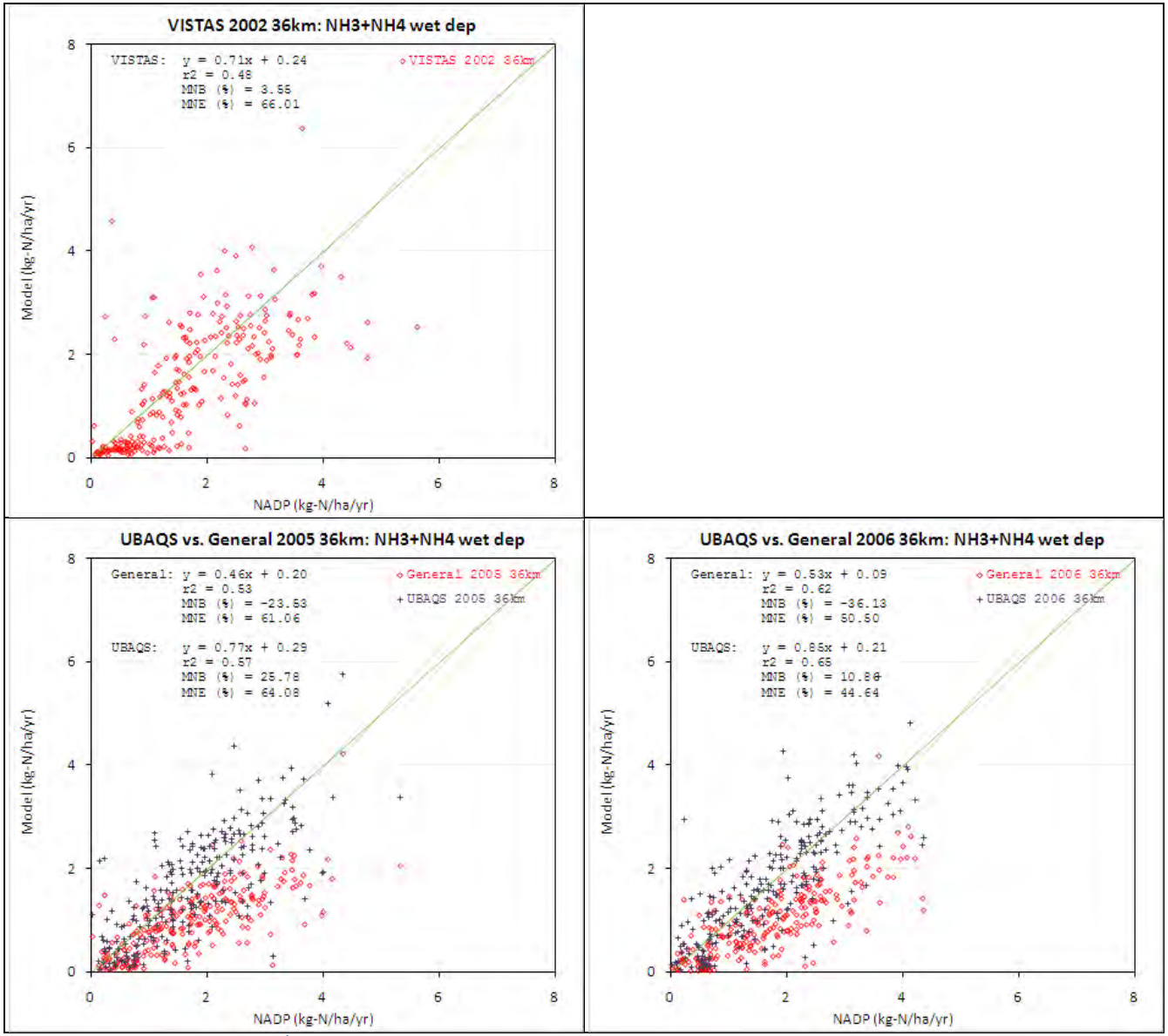

Figure C1-12. Scatter plots of annual total $NH_3 + NH_4^+$ wet deposition: modeled vs. observed at NADP stations.

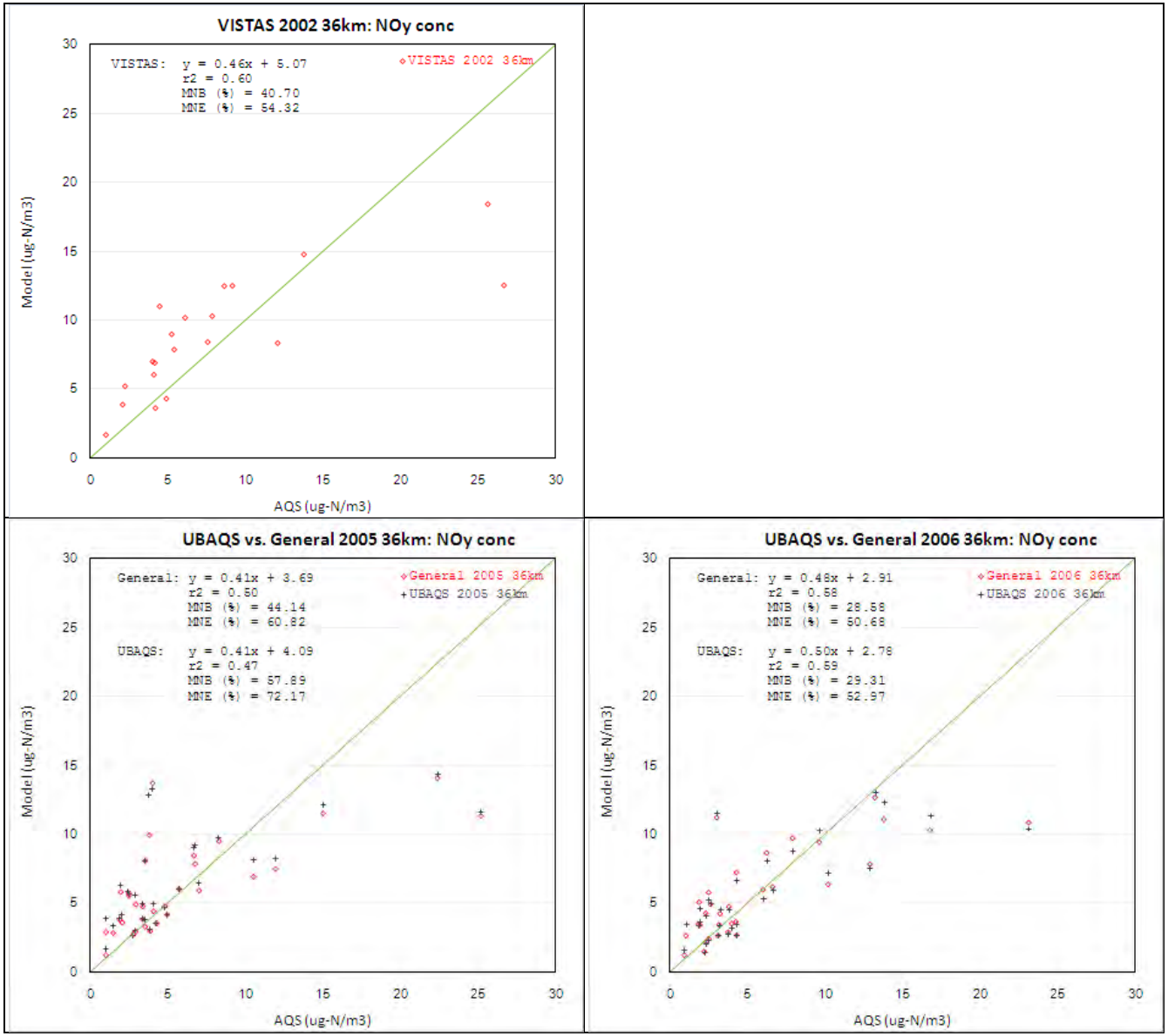

Figure C1-13. Scatter plots of annual average NOy concentration: modeled vs. observed at AQS stations.

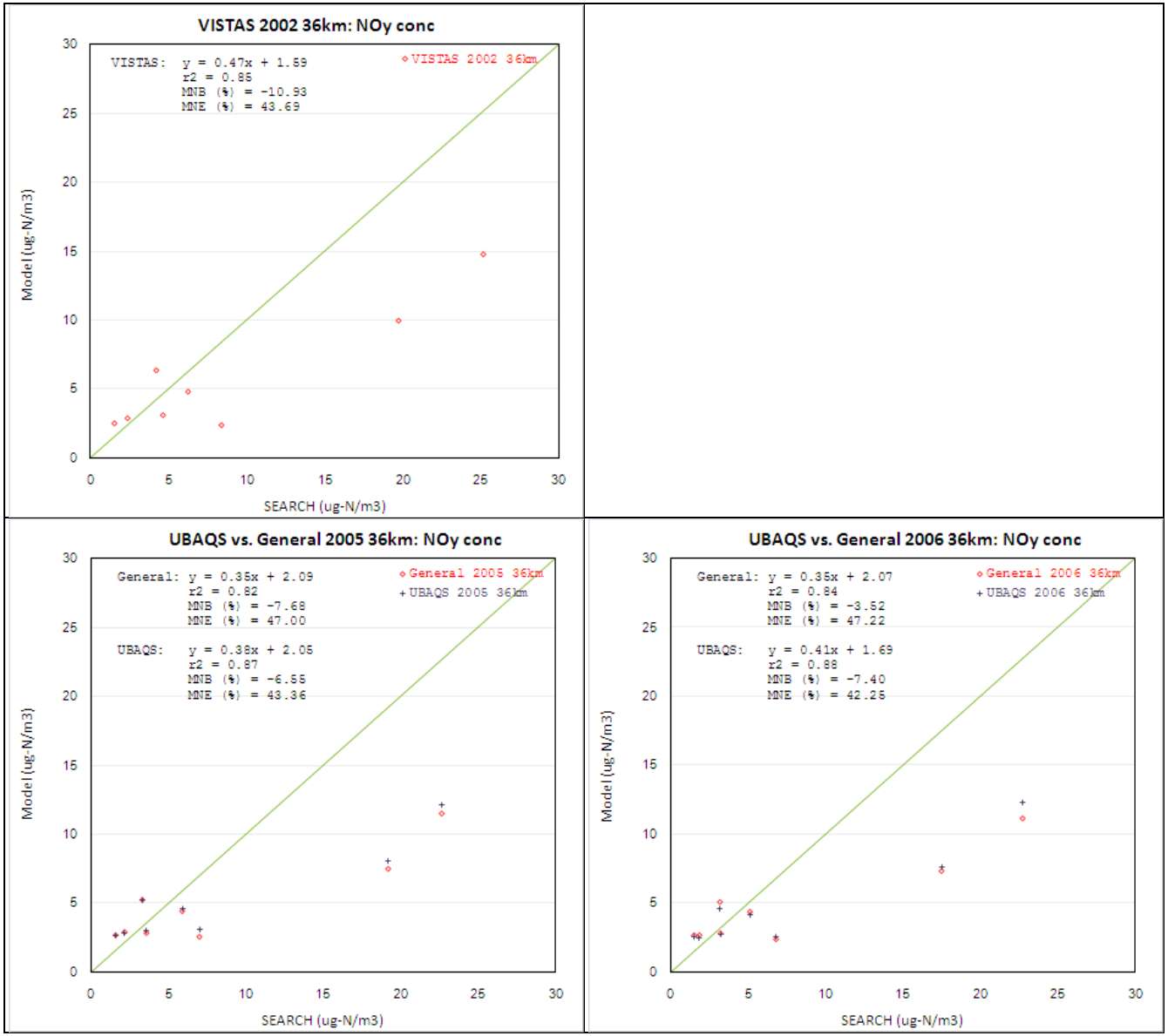

Figure C1-14. Scatter plots of annual average NOy concentration: modeled vs. observed at SEARCH stations.

Appendix C2: Scatter Plots of Concentrations and Deposition with Native Temporal Resolutions of the Measurements

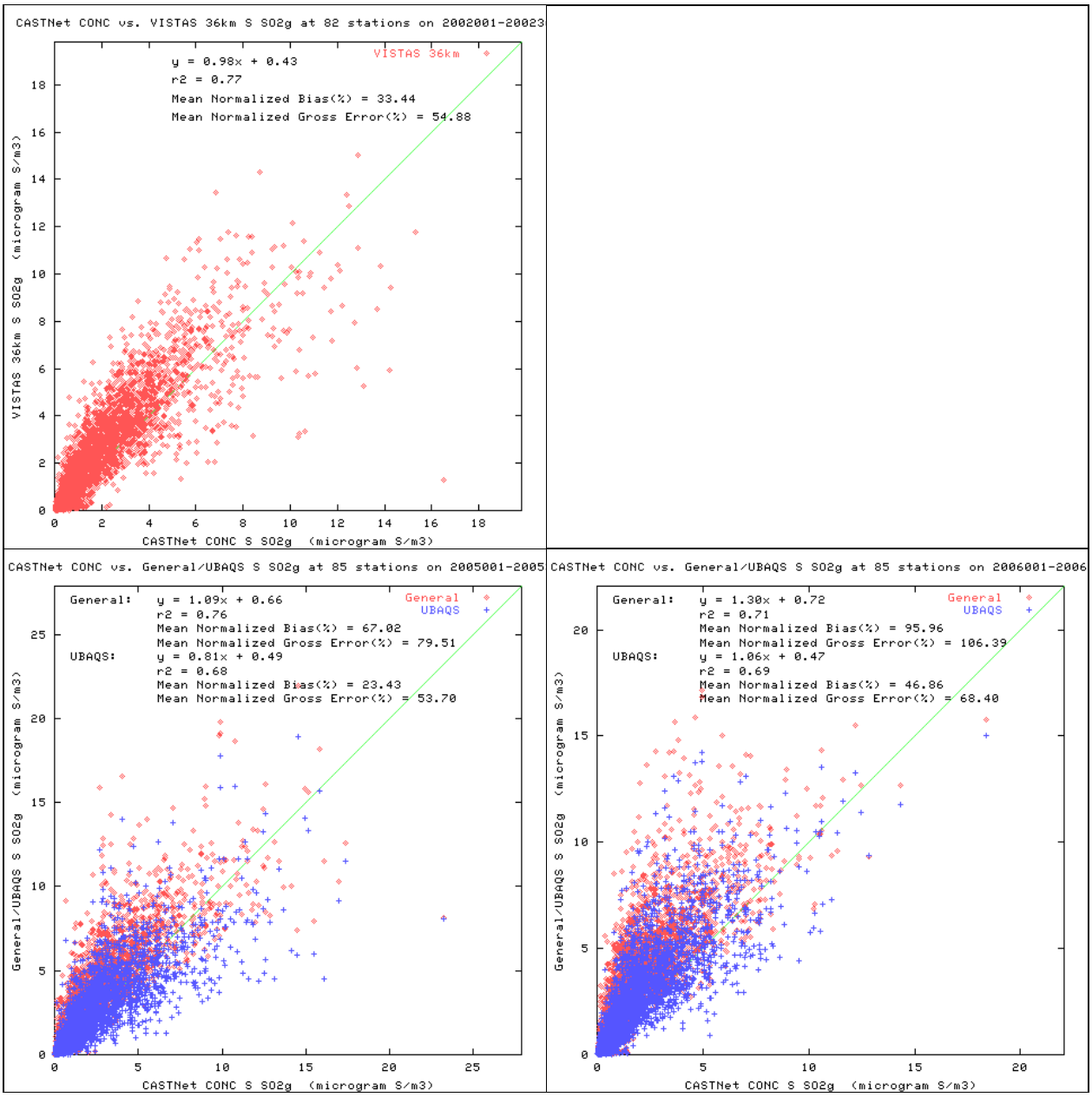

Figure C2-1. Scatter plots of weekly average SO_2 concentrations: modeled vs. observed at CASTNET stations.

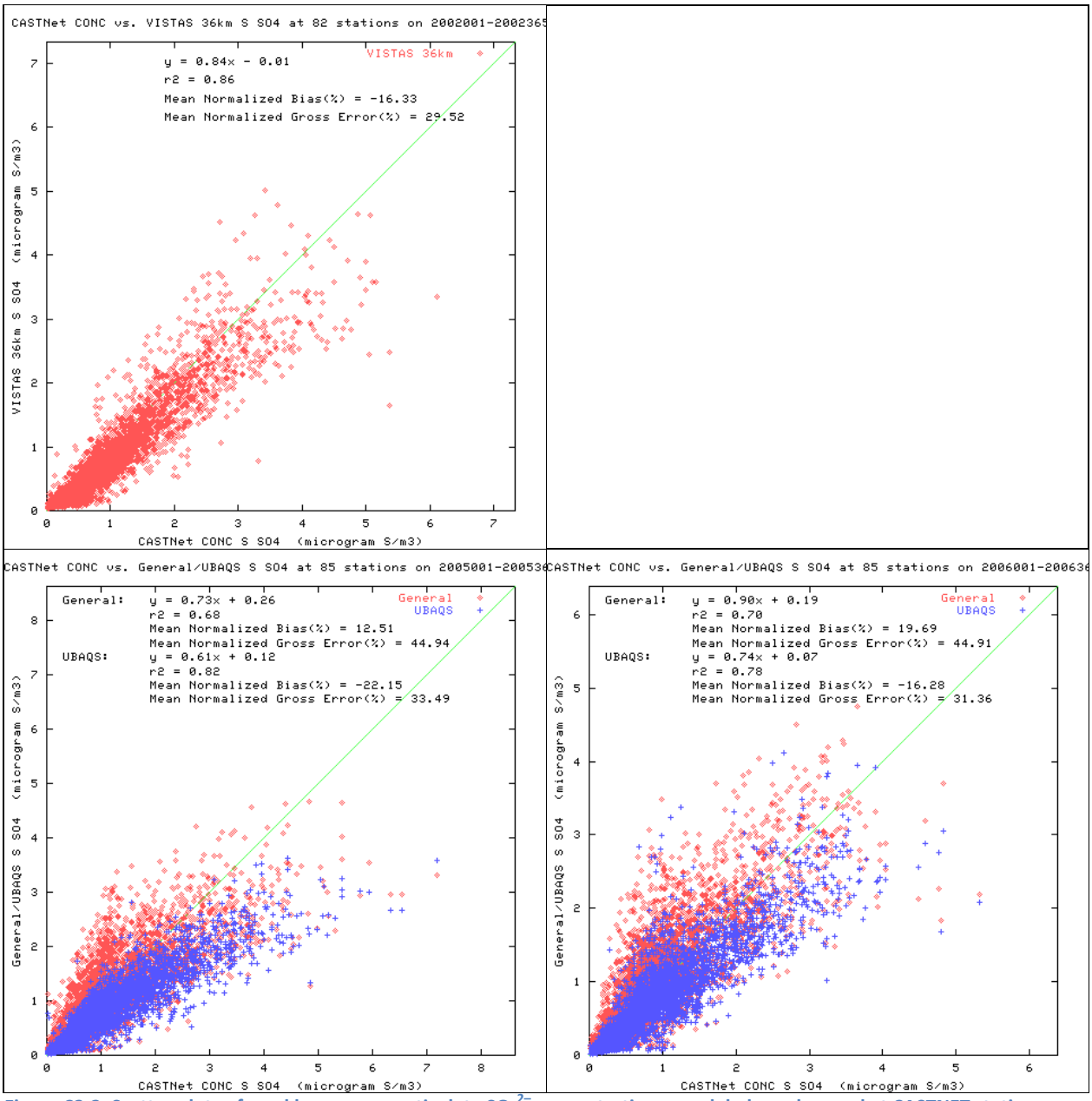

Figure C2-2. Scatter plots of weekly average particulate SO_4^{2-} concentrations: modeled vs. observed at CASTNET stations.

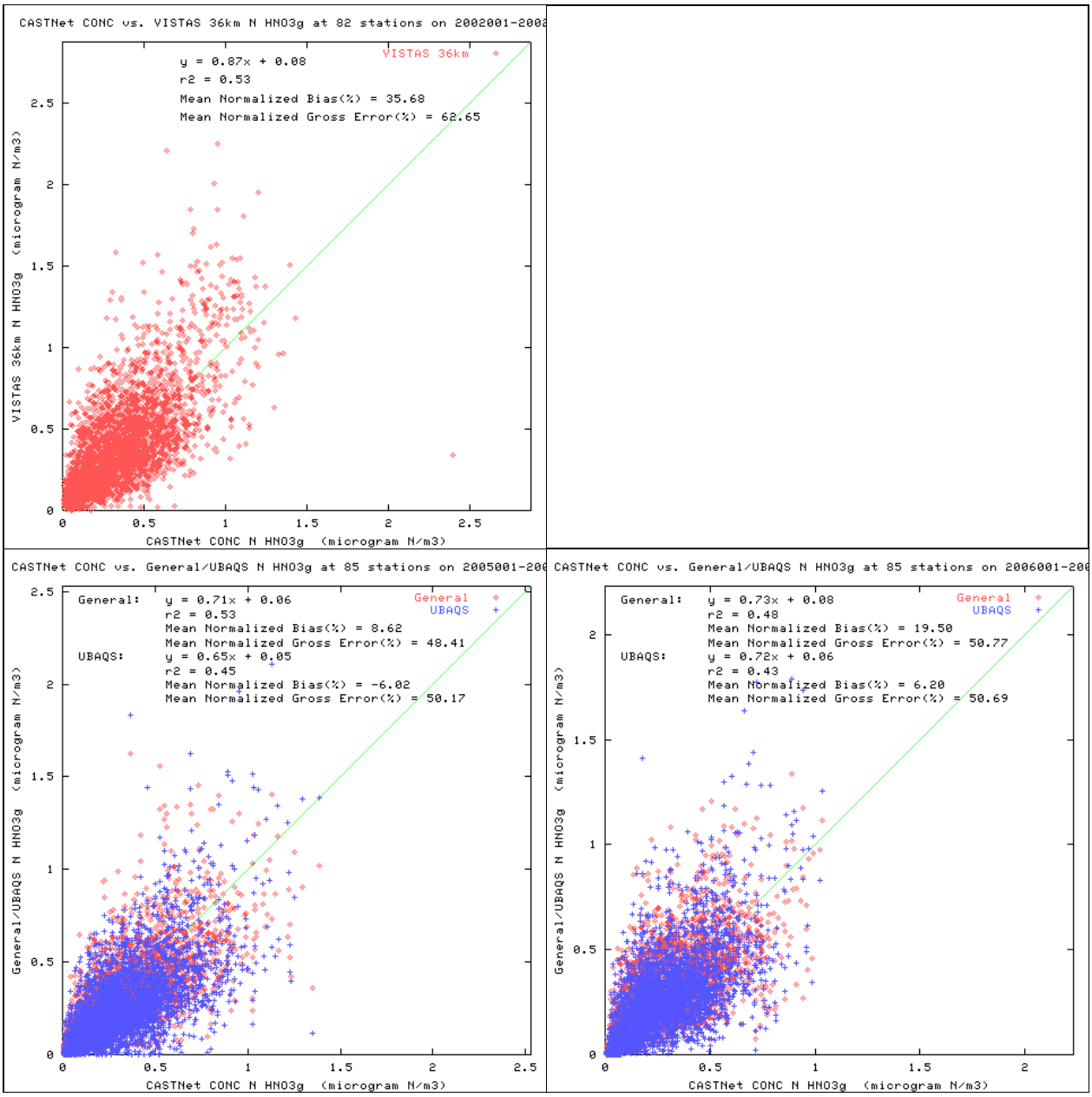

Figure C2-3. Scatter plots of weekly average HNO_3 concentrations: modeled vs. observed at CASTNET stations.

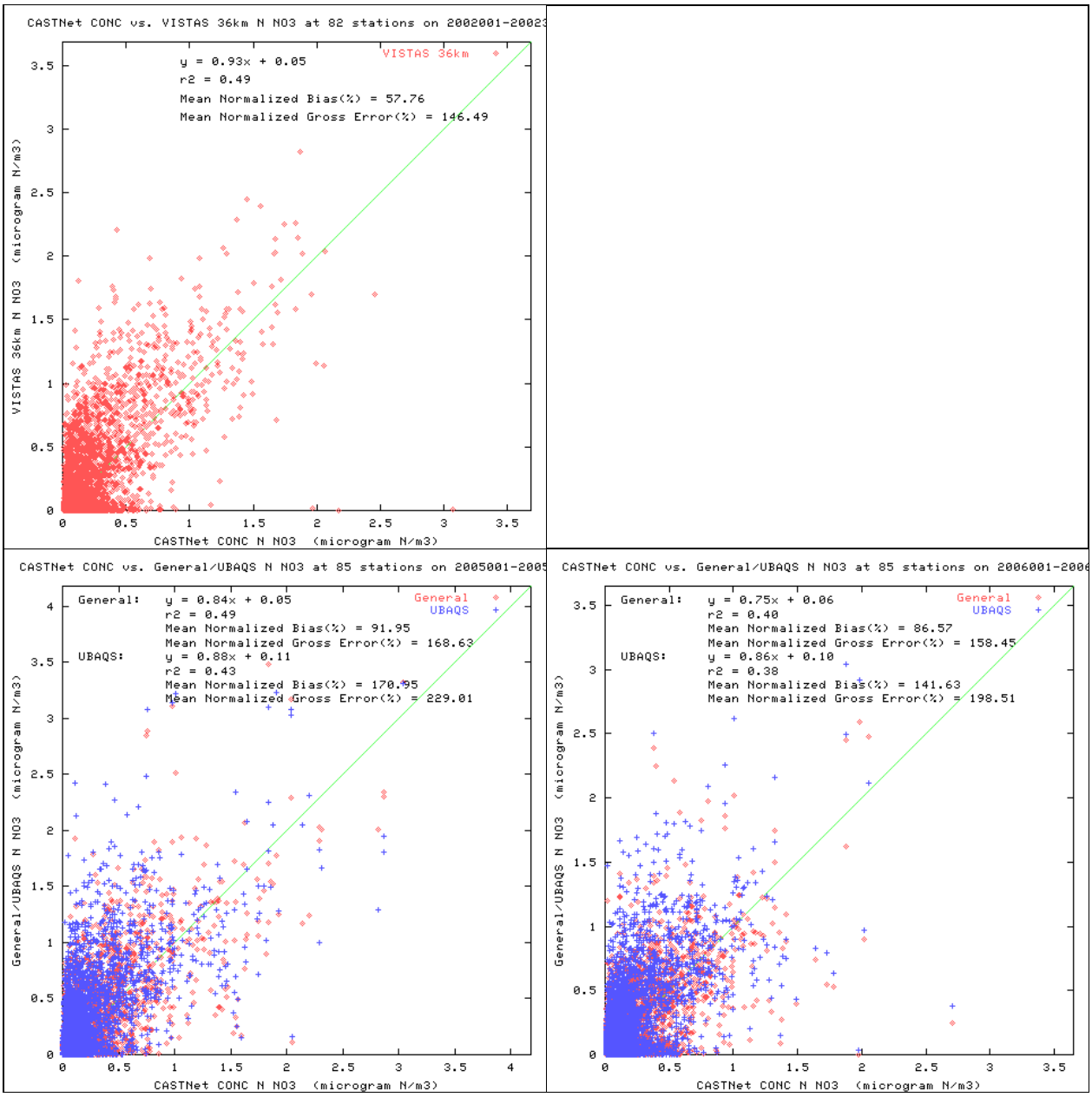

Figure C2-4. Scatter plots of weekly average particulate NO_3^- concentrations: modeled vs. observed at CASTNET stations.

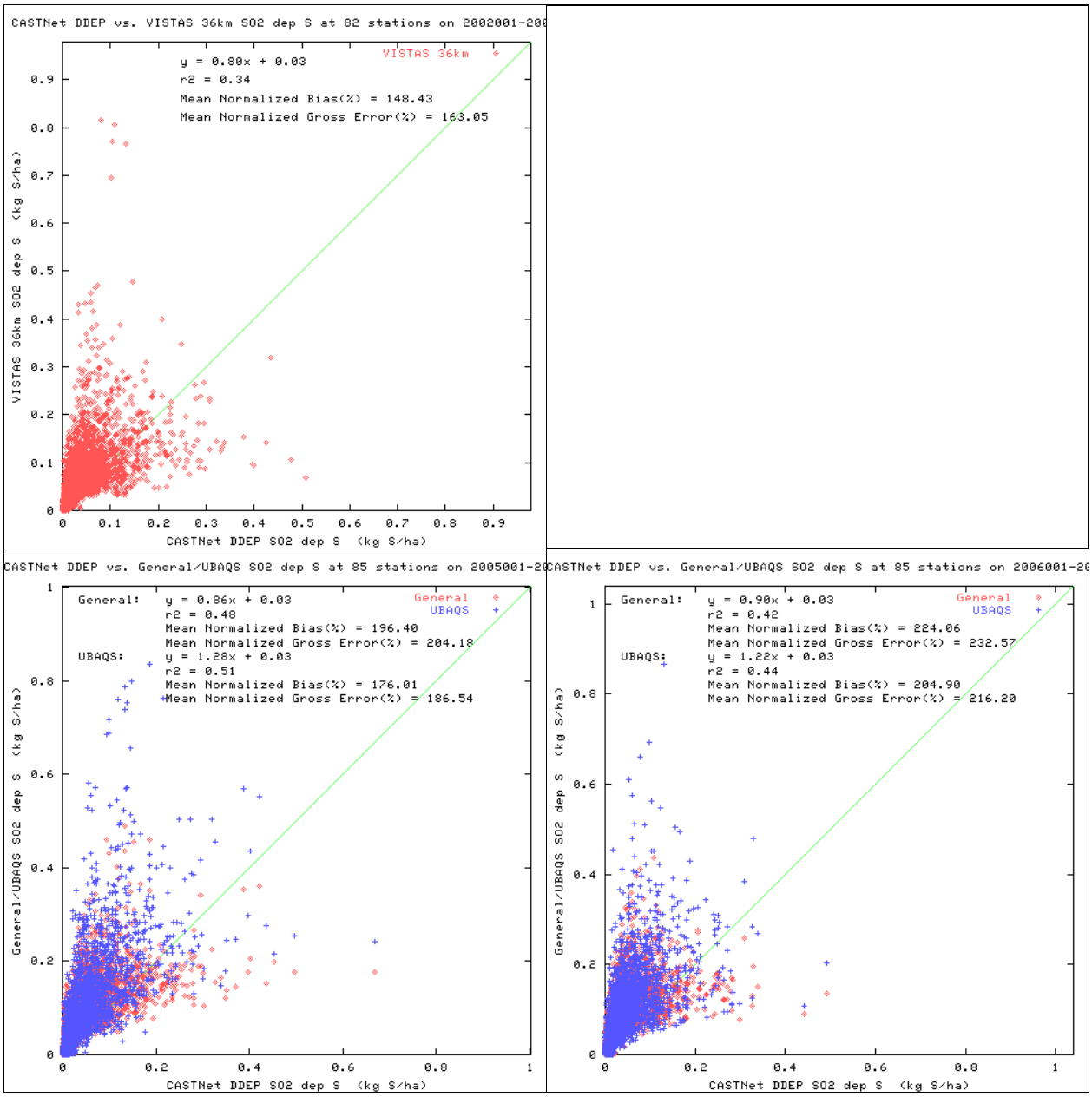

Figure C2-5. Scatter plots of weekly total SO_2 dry deposition: modeled vs. observed at CASTNET stations.

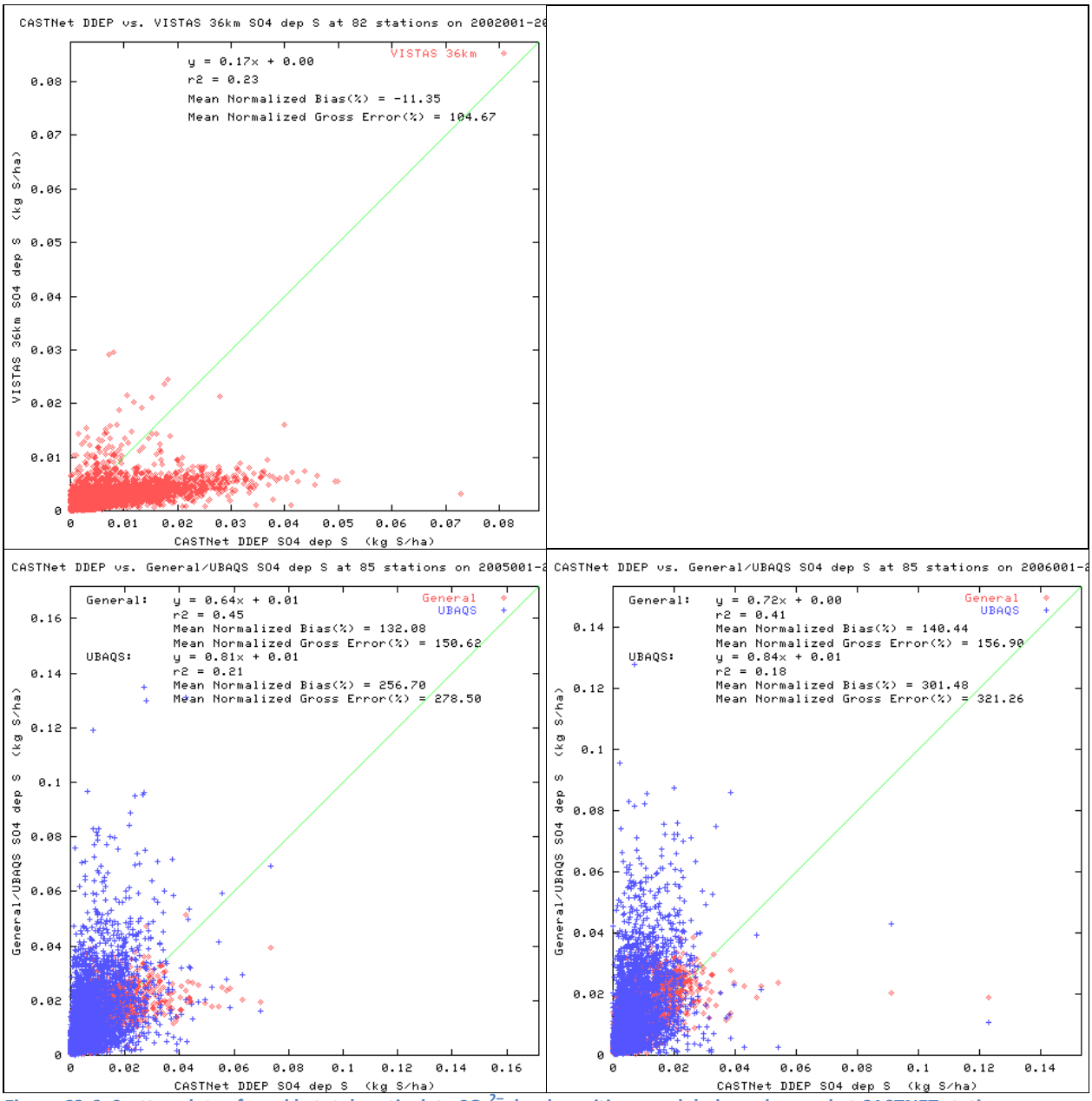

Figure C2-6. Scatter plots of weekly total particulate SO_4^{2-} dry deposition: modeled vs. observed at CASTNET stations.

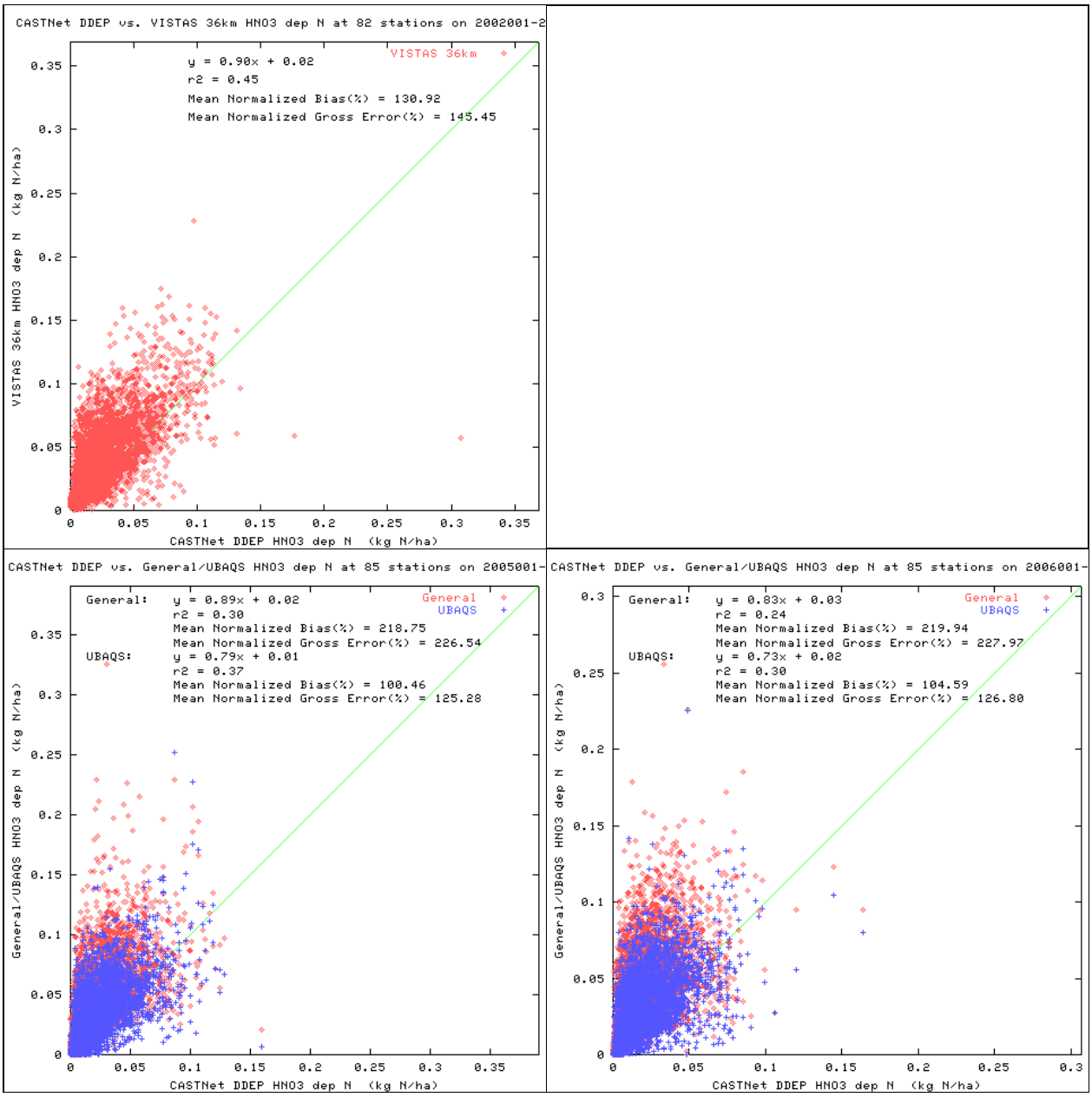

Figure C2-7. Scatter plots of weekly total HNO_3 dry deposition: modeled vs. observed at CASTNET stations.

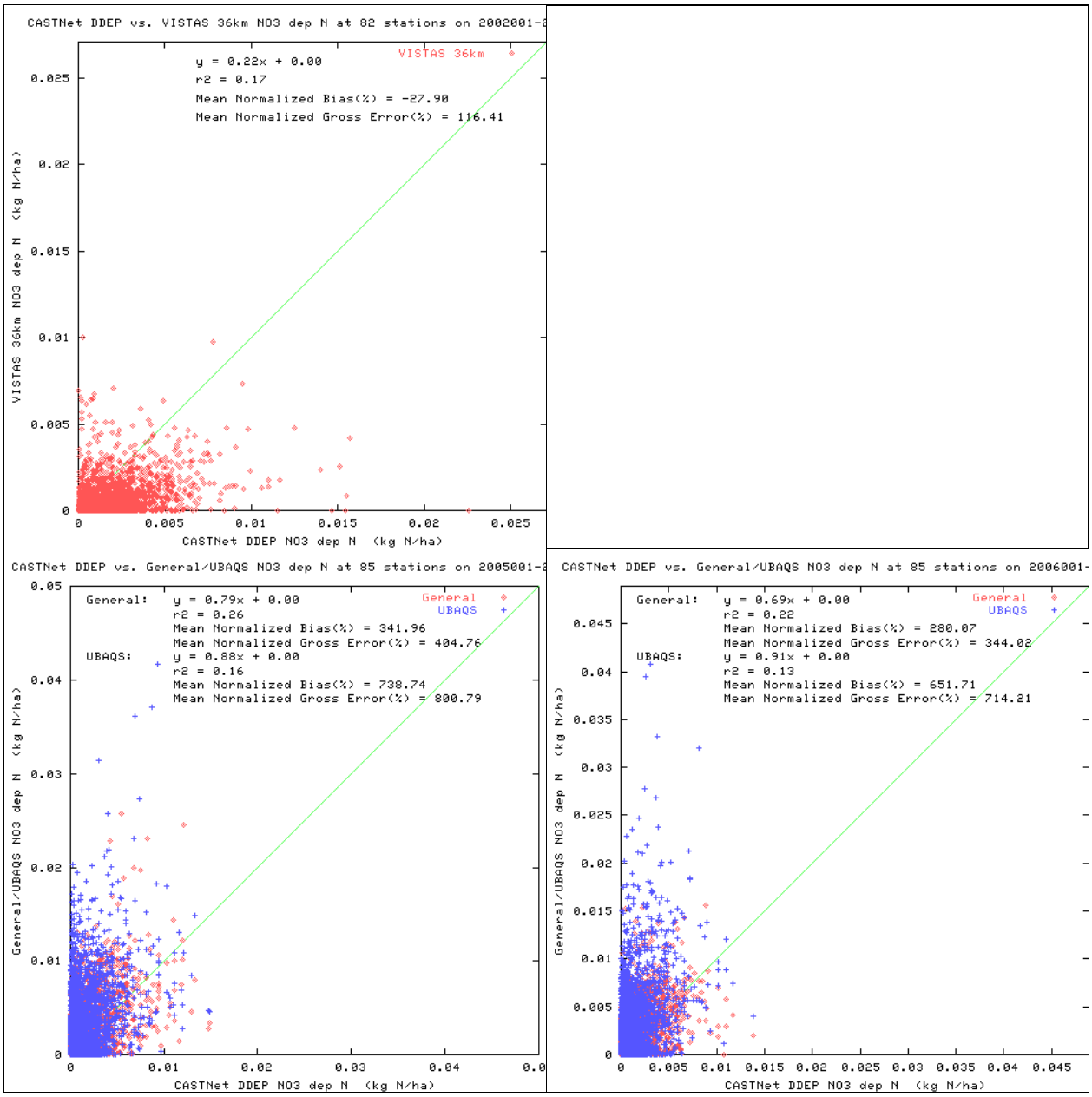

Figure C2-8. Scatter plots of weekly total particulate NO_3^- dry deposition: modeled vs. observed at CASTNET stations.

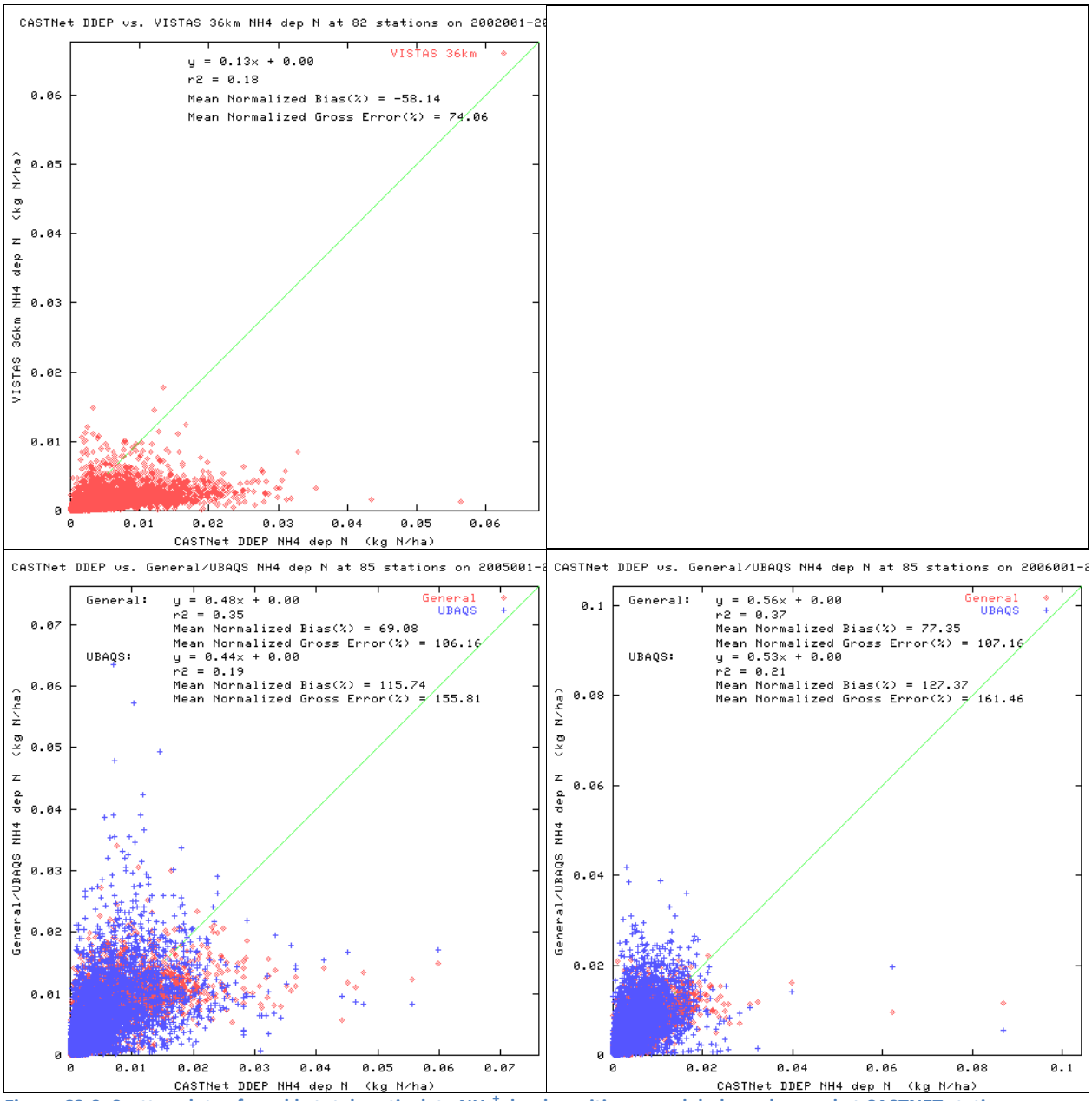

Figure C2-9. Scatter plots of weekly total particulate NH_4^+ dry depositions: modeled vs. observed at CASTNET stations.

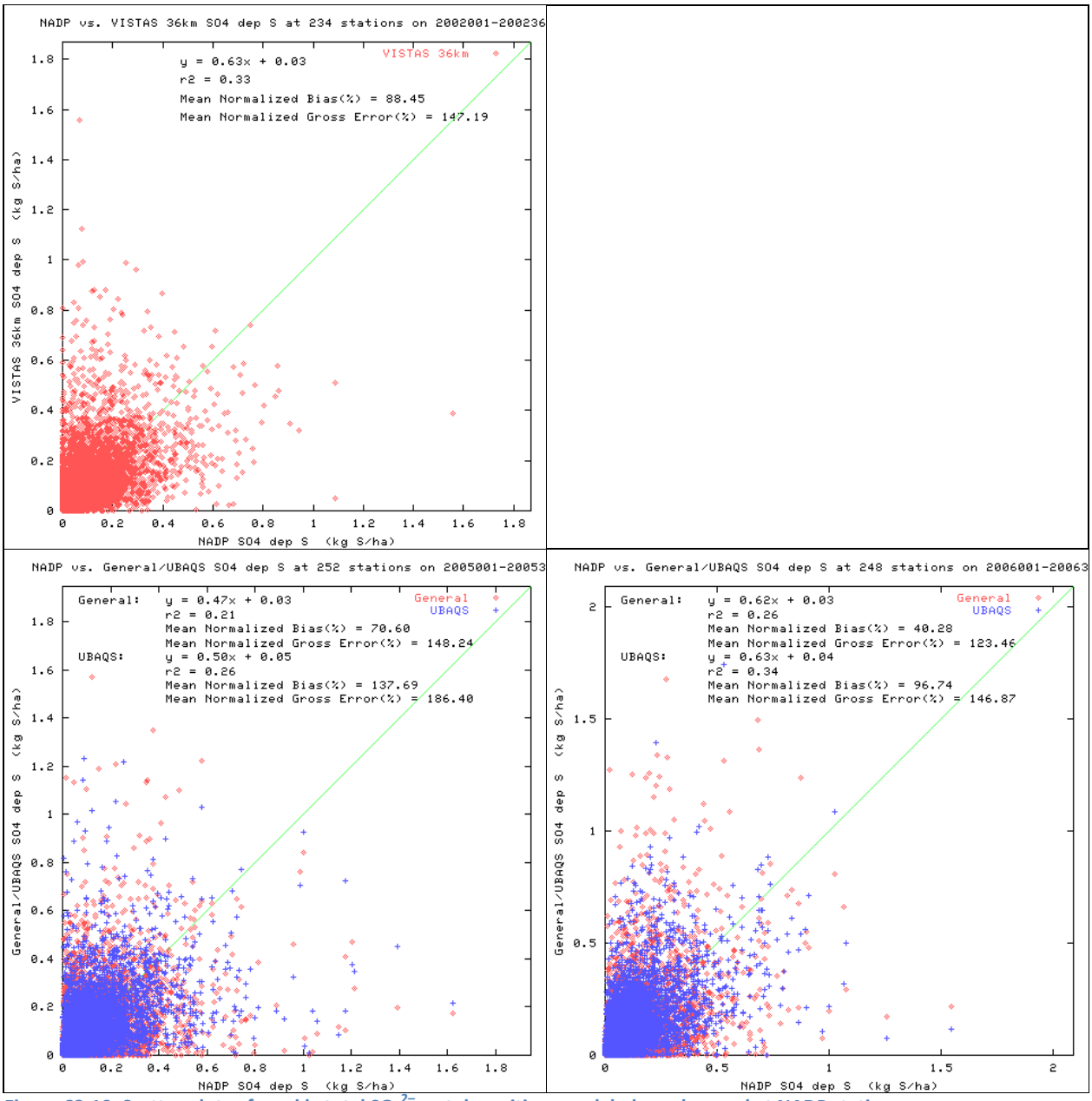

Figure C2-10. Scatter plots of weekly total SO_4^{2-} wet deposition: modeled vs. observed at NADP stations.

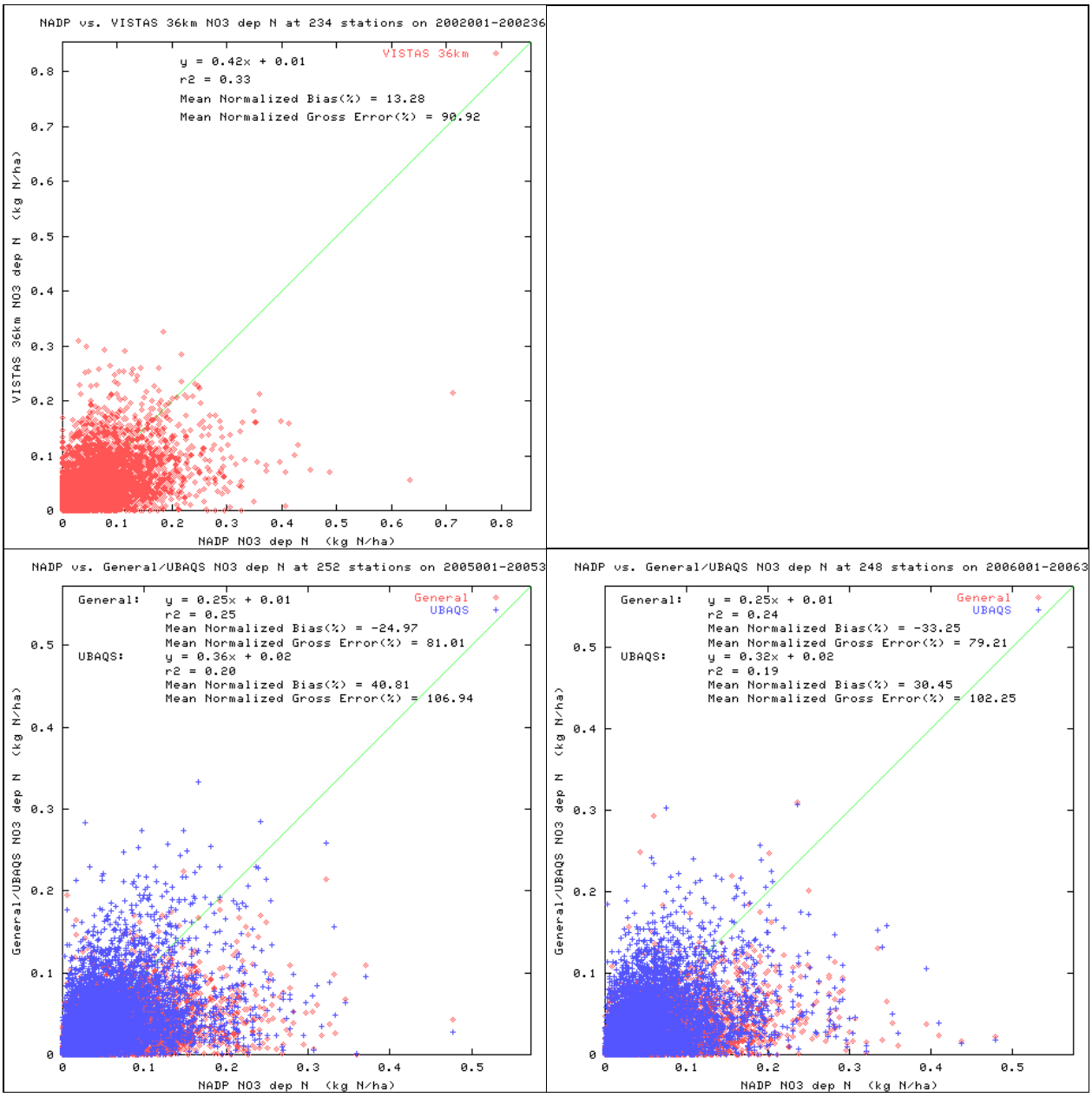

Figure C2-11. Scatter plots of weekly total $HNO_3 + NO_3^-$ wet deposition: modeled vs. observed at NADP stations.

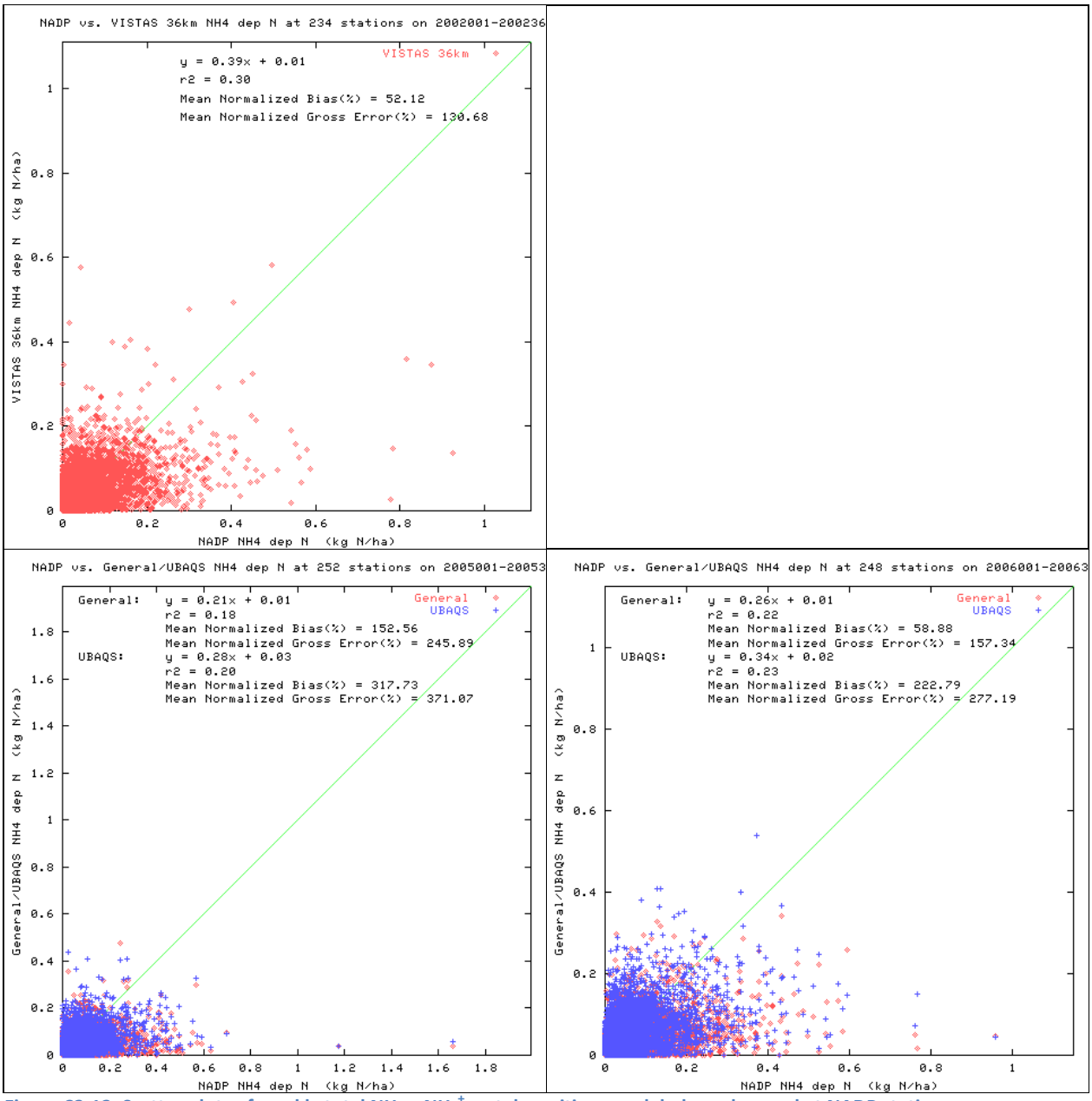

Figure C2-12. Scatter plots of weekly total NH_3 + NH_4^+ wet deposition: modeled vs. observed at NADP stations.

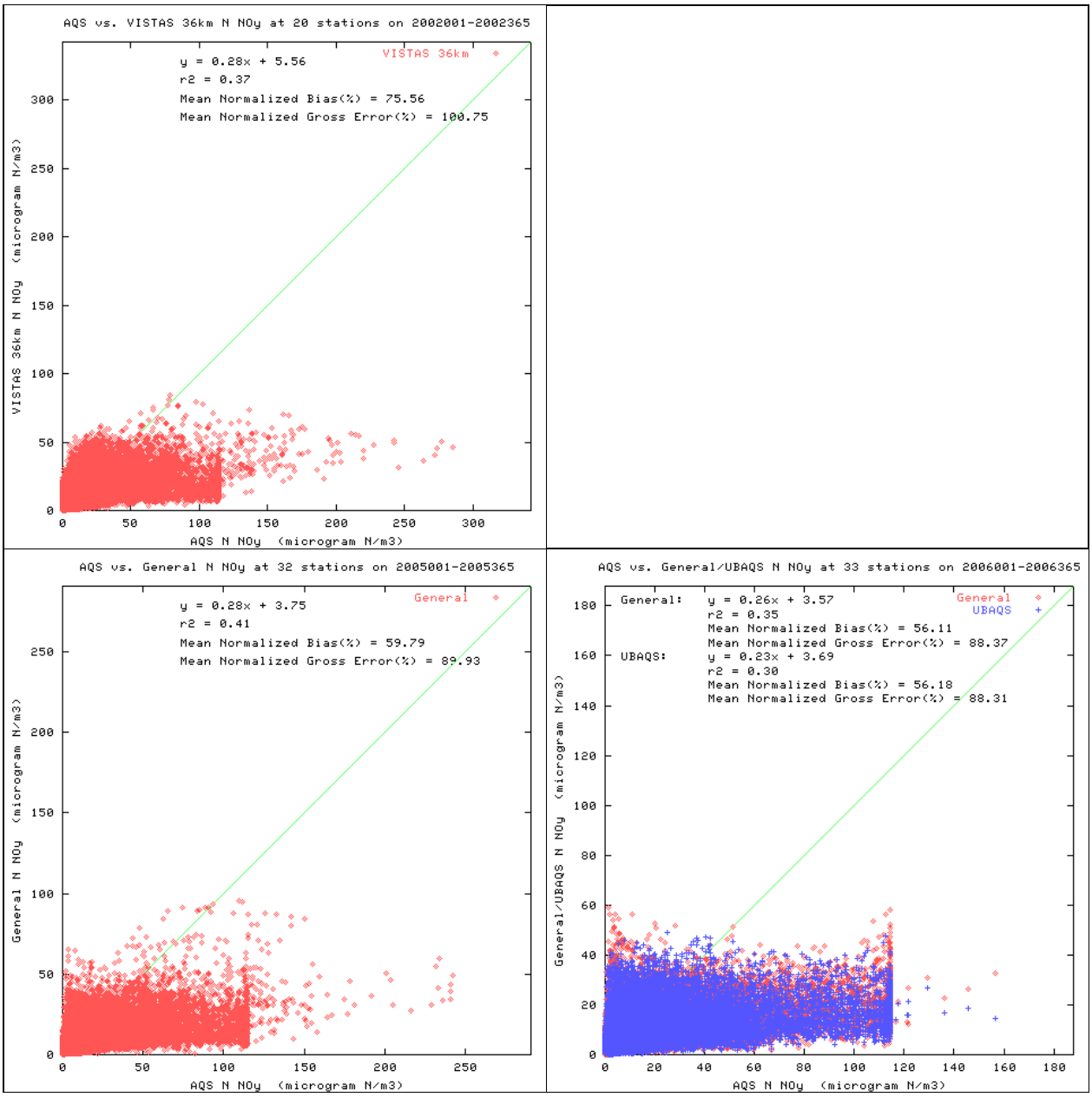

Figure C2-13. Scatter plots of hourly average NOy concentration: modeled vs. observed at AQS stations.

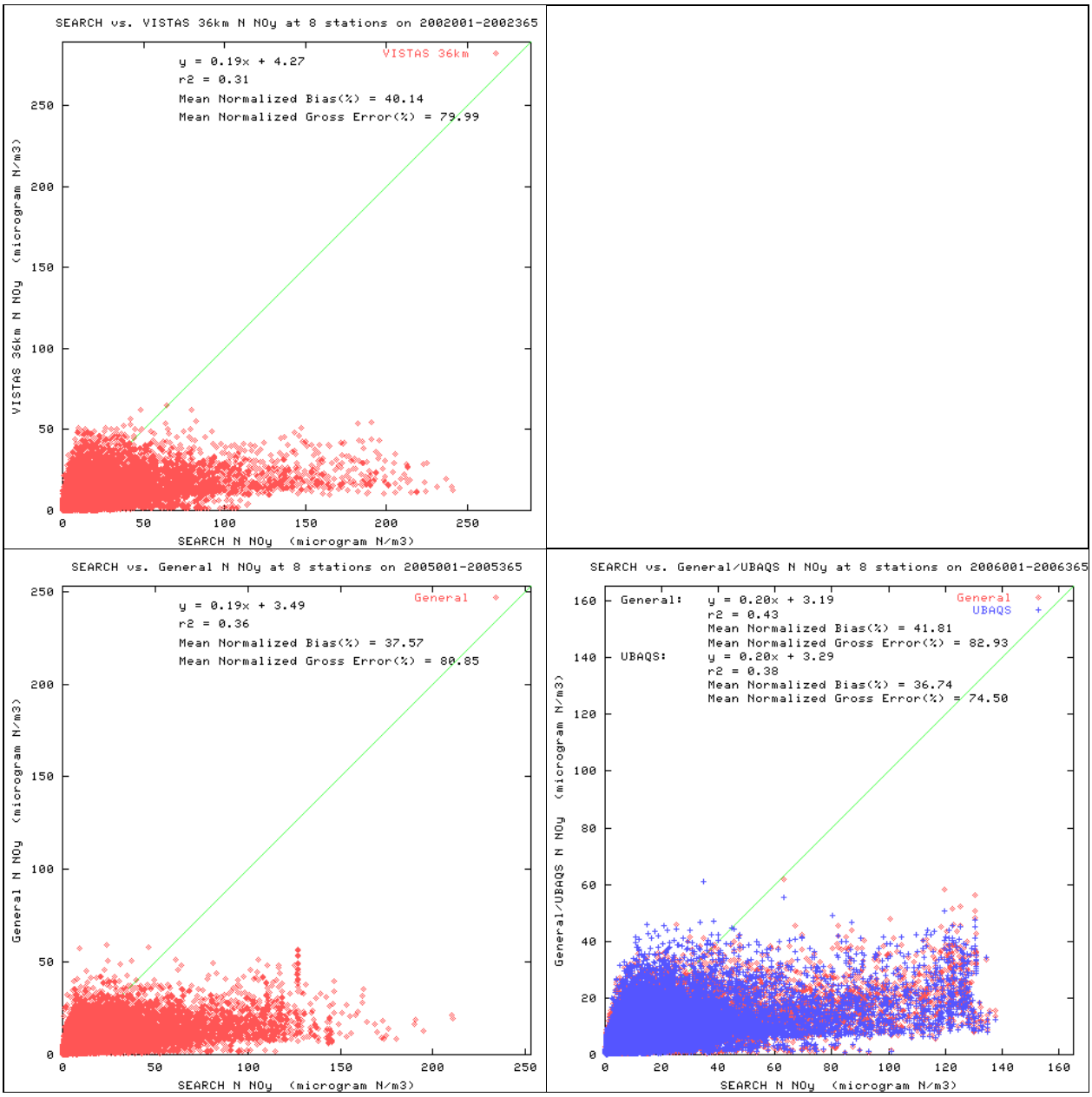

Figure C2-14. Scatter plots of hourly average NOy concentration: modeled vs. observed at SEARCH stations.

Appendix D1: Spatial Maps of Annual Average Concentrations and Annual Total Deposition of SOx, NOy, and NHx

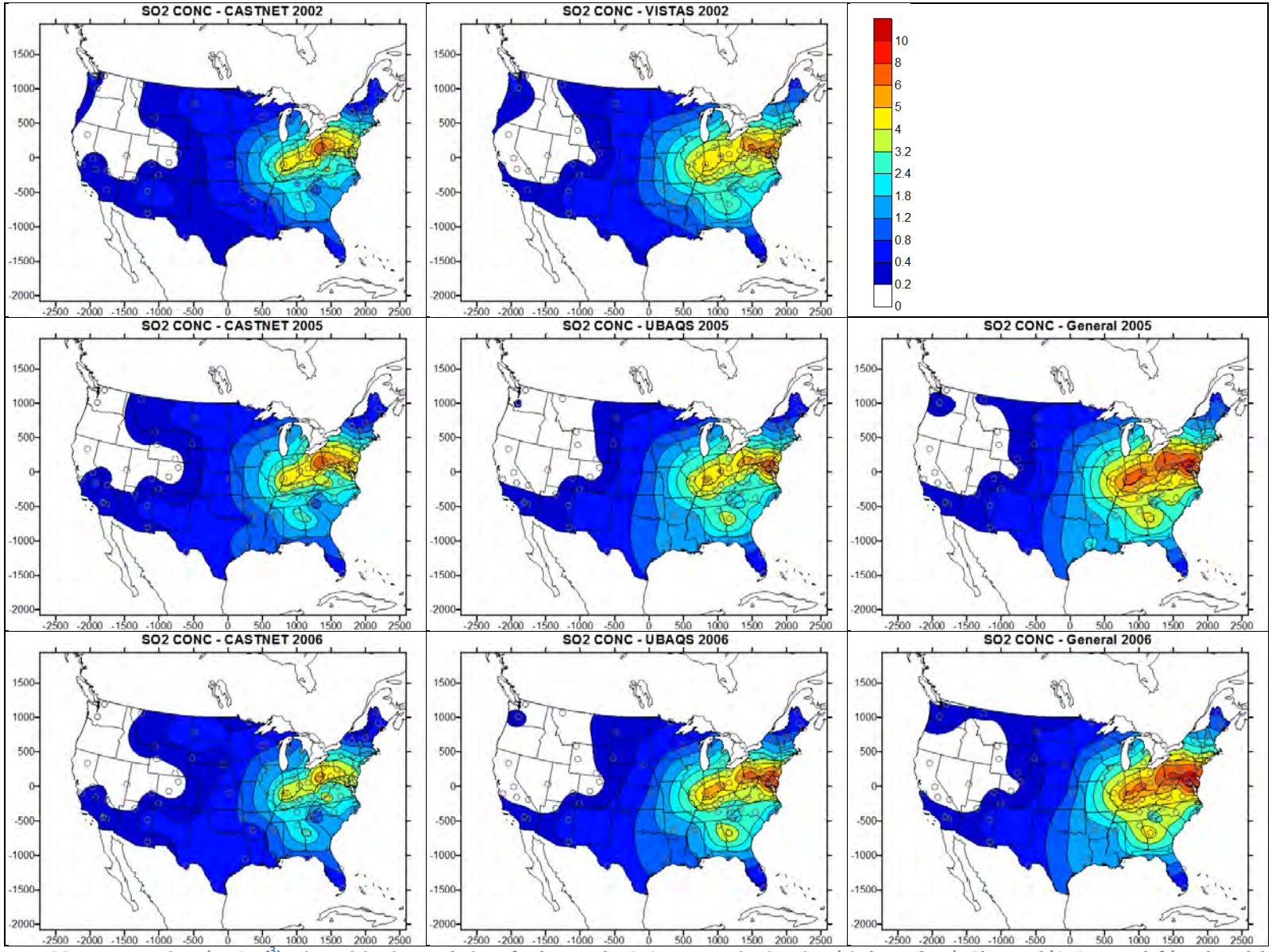

Figure D1-1. SO_2 concentrations (µg-S m^{-3}) using Kriging interpolation of values at the CASTNET monitoring sites (circle markers): Observed (CASTNET – left) and modeled (CMAQ – center; CAMx – right) concentrations for 2002 (top), 2005 (middle) and 2006 (bottom).

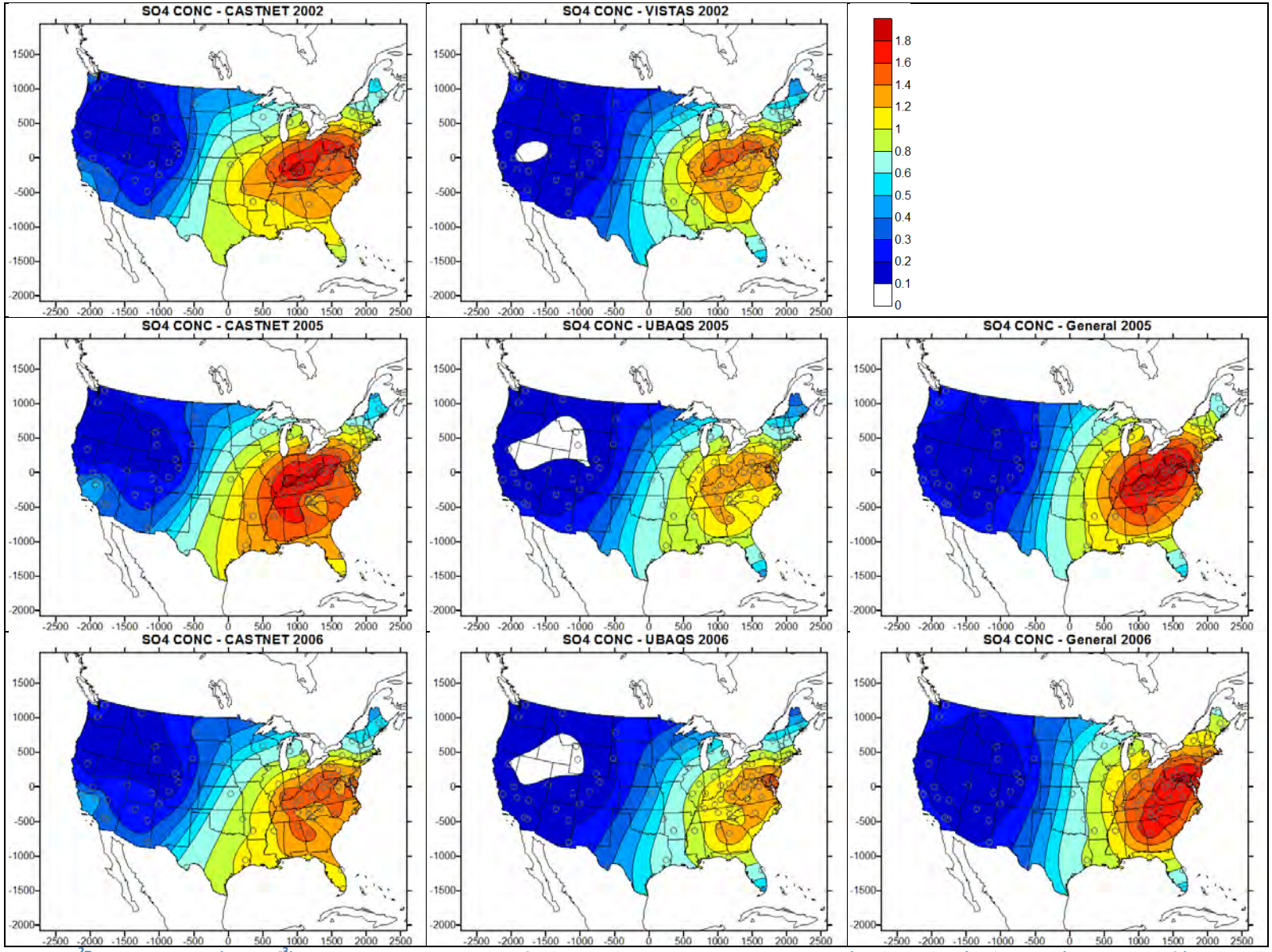

Figure D1-2. SO_4^{2-} concentrations (µg-S m^{-3}) using Kriging interpolation of values at the CASTNET monitoring sites (circle markers): Observed (CASTNET – left) and modeled (CMAQ – center; CAMx – right) concentrations for 2002 (top), 2005 (middle) and 2006 (bottom).

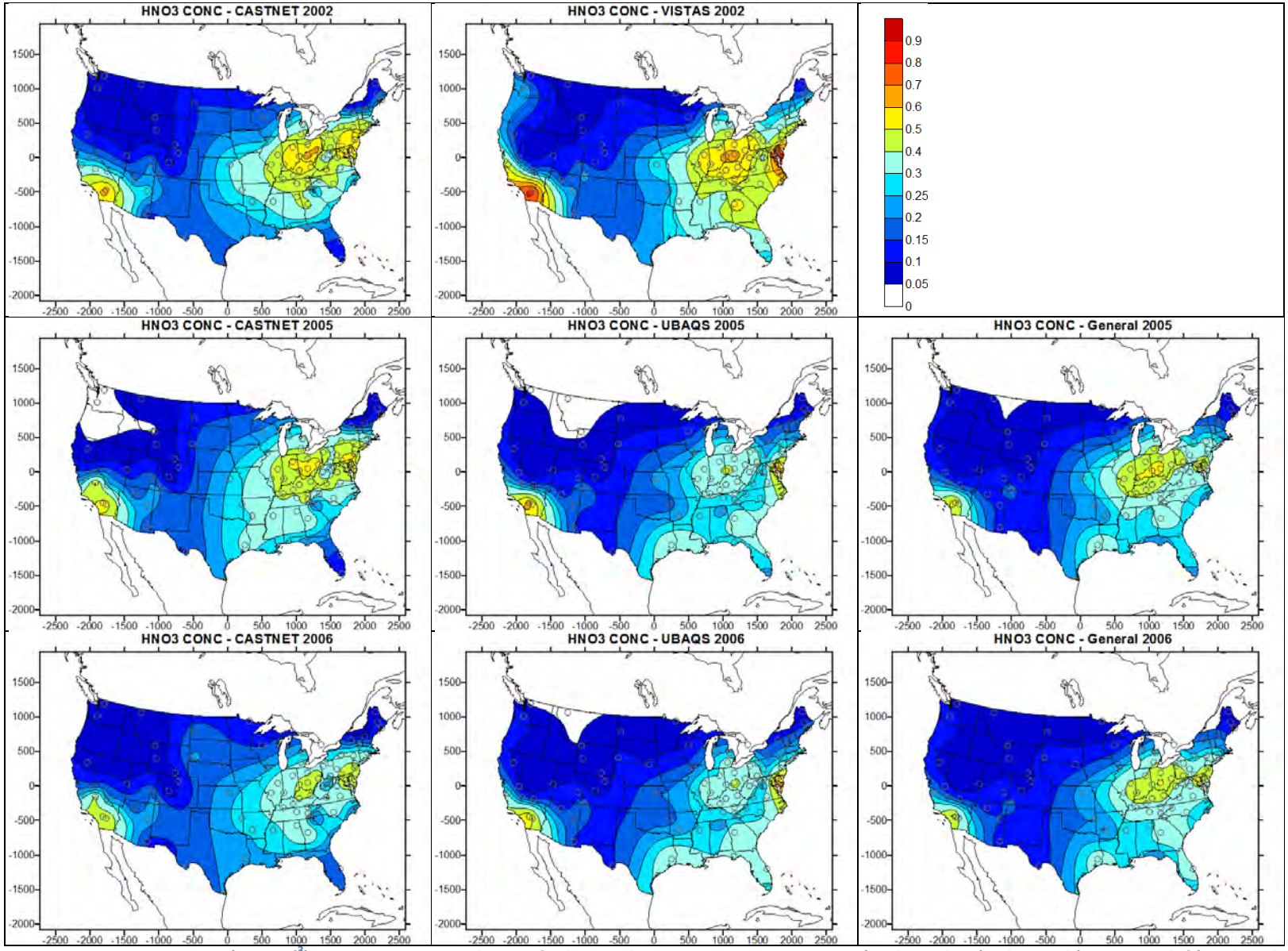

Figure D1-3. HNO_3 concentrations (µg-N m^{-3}) using Kriging interpolation of values at the CASTNET monitoring sites (circle markers): Observed (CASTNET – left) and modeled (CMAQ – center; CAMx – right) concentrations for 2002 (top), 2005 (middle) and 2006 (bottom).

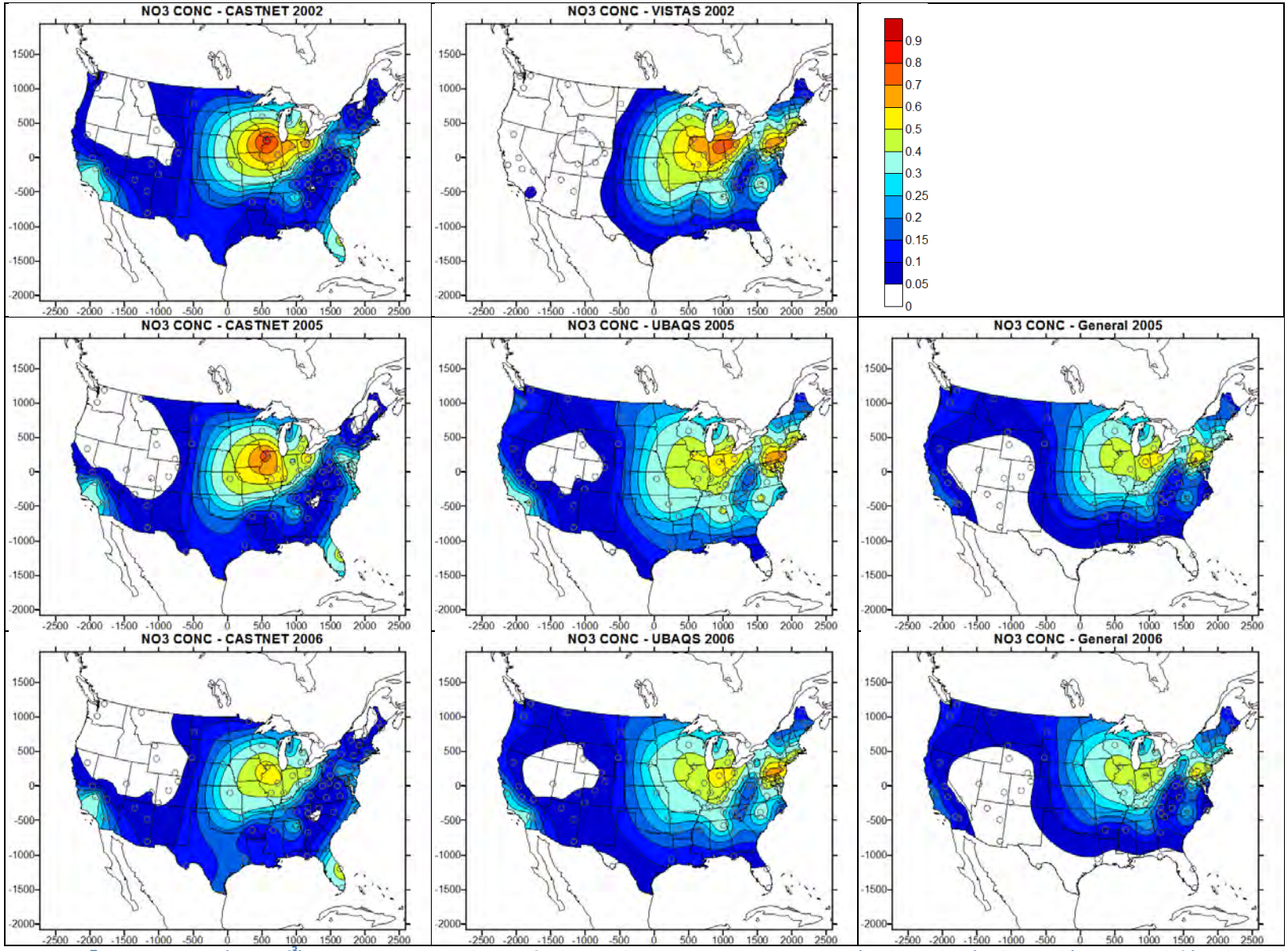

Figure D1-4. NO_3^- concentrations (µg-N m^{-3}) using Kriging interpolation of values at the CASTNET monitoring sites (circle markers): Observed (CASTNET – left) and modeled (CMAQ – center; CAMx – right) concentrations for 2002 (top), 2005 (middle) and 2006 (bottom).

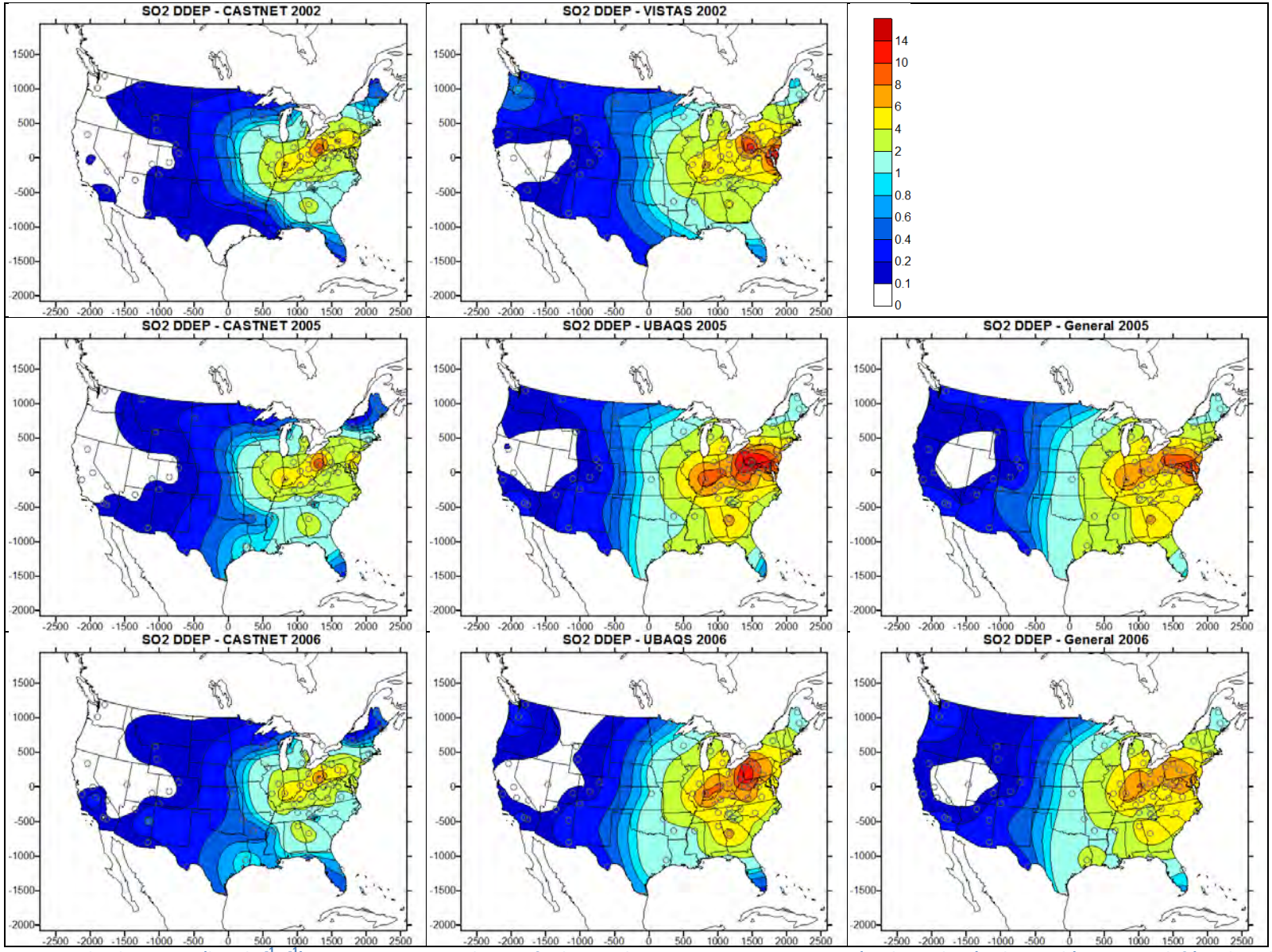

Figure D1-5. SO_2 dry deposition (kg-S ha^{-1} y^{-1}) using Kriging interpolation of values at the CASTNET monitoring sites (circle markers): Observed (CASTNET – left) and modeled (CMAQ – center; CAMx – right) deposition for 2002 (top), 2005 (middle) and 2006 (bottom).

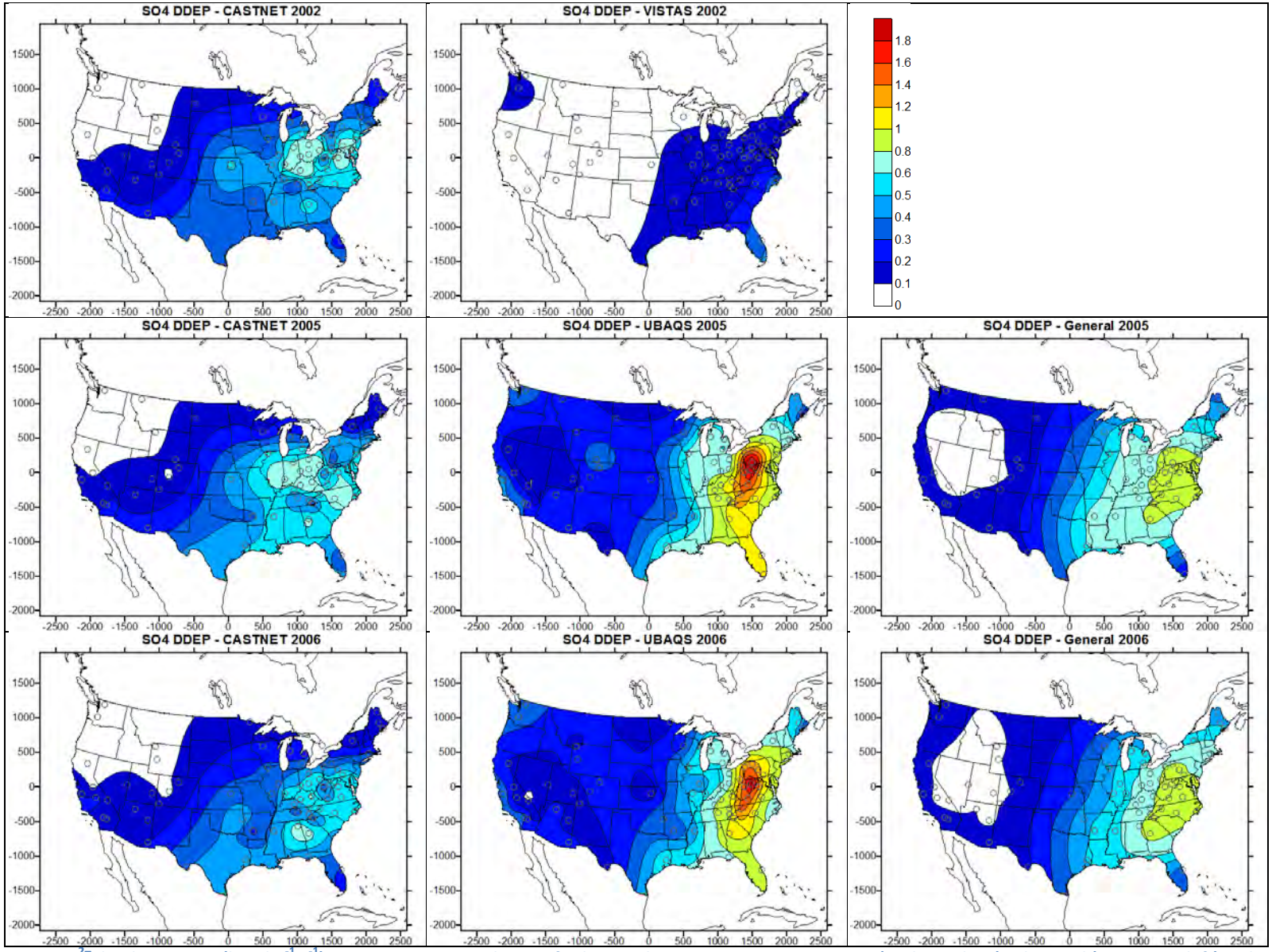

Figure D1-6. SO_4^{2-} dry depositions (kg-S ha^{-1} y^{-1}) using Kriging interpolation of values at the CASTNET monitoring sites (circle markers): Observed (CASTNET – left) and modeled (CMAQ – center; CAMx – right) deposition for 2002 (top), 2005 (middle) and 2006 (bottom).

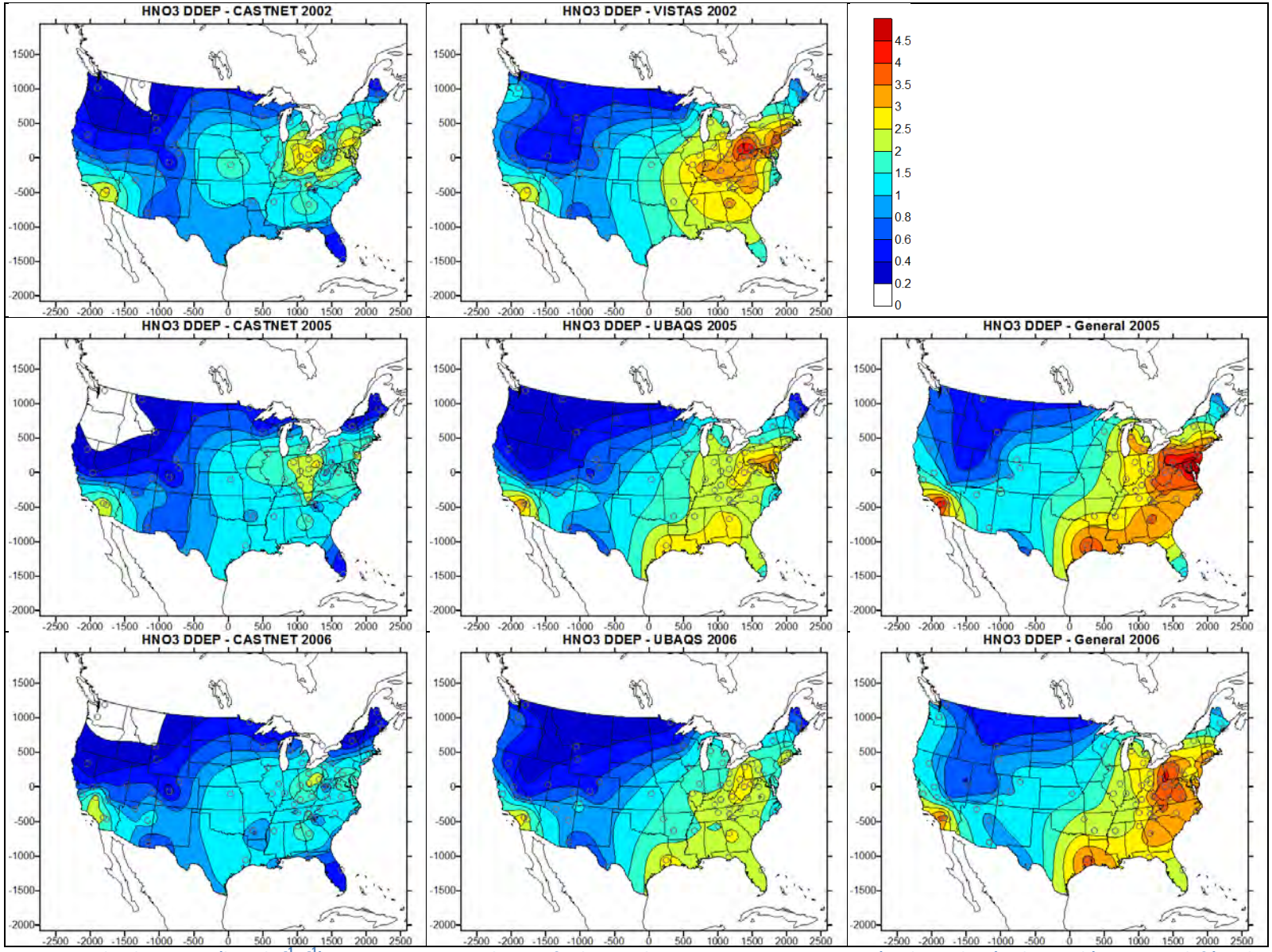

Figure D1-7. HNO_3 dry deposition (kg-N ha^{-1} y^{-1}) using Kriging interpolation of values at the CASTNET monitoring sites (circle markers): Observed (CASTNET – left) and modeled (CMAQ – center; CAMx – right) deposition for 2002 (top), 2005 (middle) and 2006 (bottom).

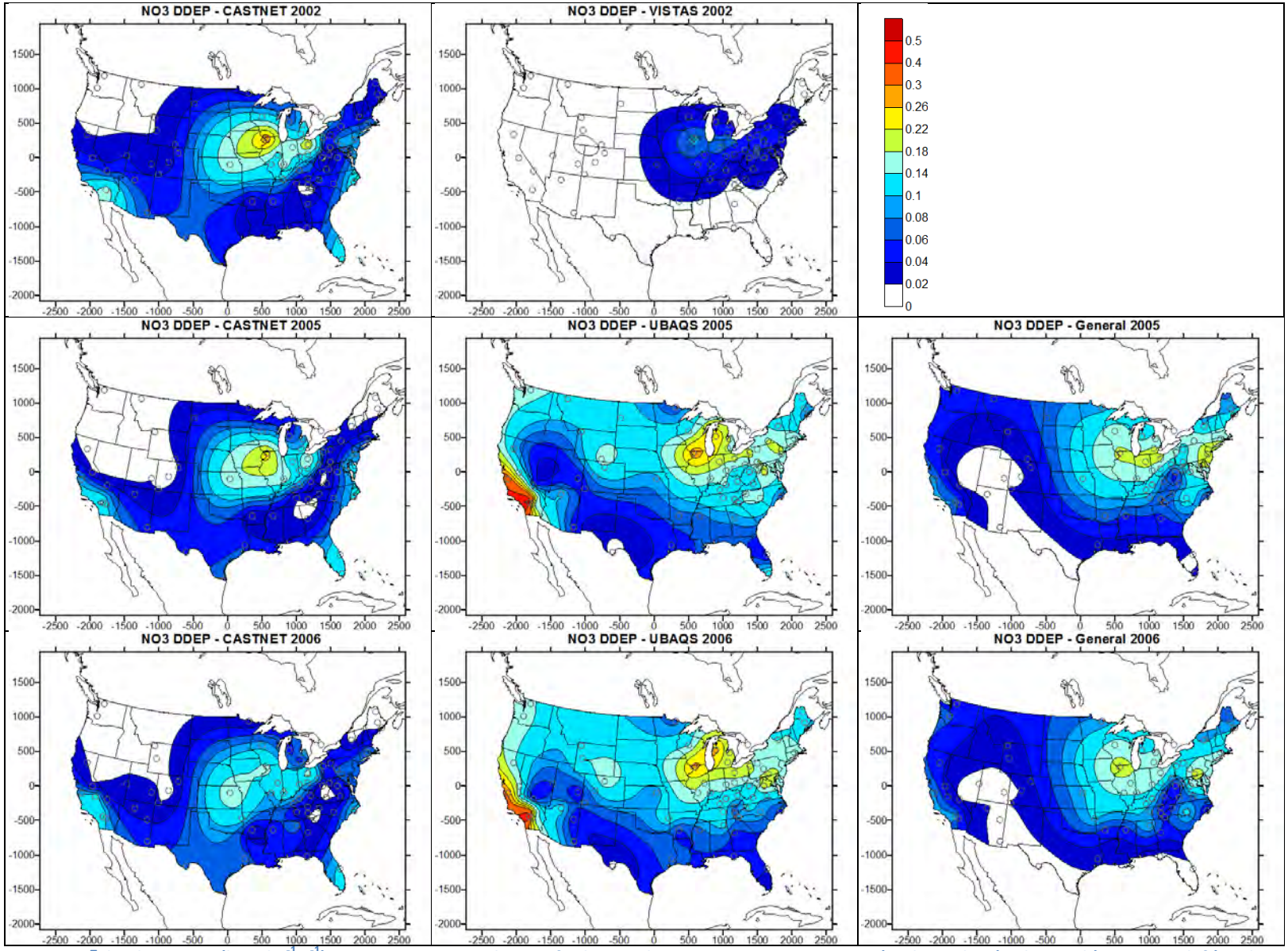

Figure D1-8. NO_3^- dry deposition (kg-N ha^{-1} y^{-1}) using Kriging interpolation of values at the CASTNET monitoring sites (circle markers): Observed (CASTNET – left) and modeled (CMAQ – center; CAMx – right) deposition for 2002 (top), 2005 (middle) and 2006 (bottom).

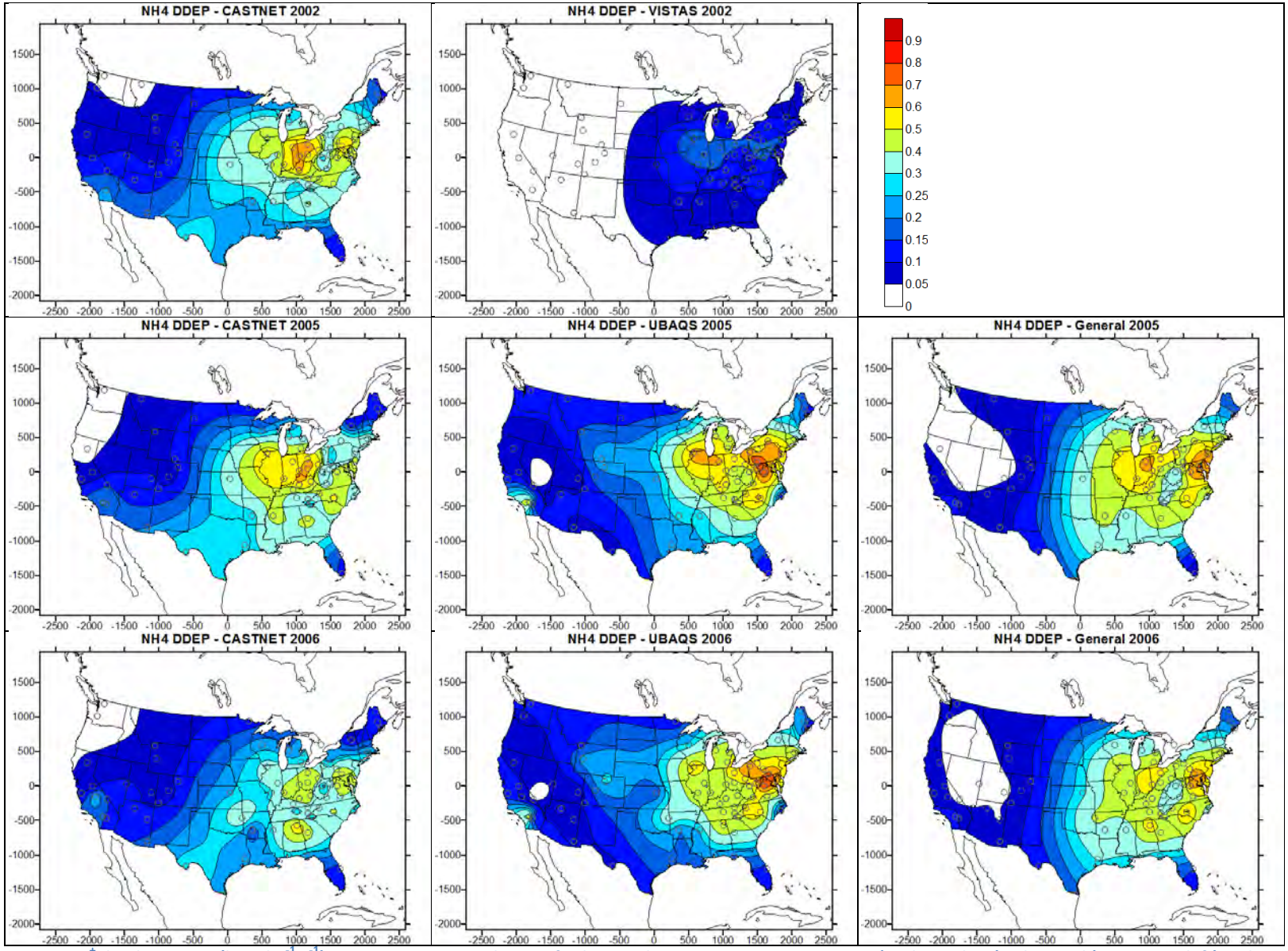

Figure D1-9. NH_4^+ dry deposition (kg-N ha^{-1} y^{-1}) using Kriging interpolation of values at the CASTNET monitoring sites (circle markers): Observed (CASTNET – left) and modeled (CMAQ – center; CAMx – right) deposition for 2002 (top), 2005 (middle) and 2006 (bottom).

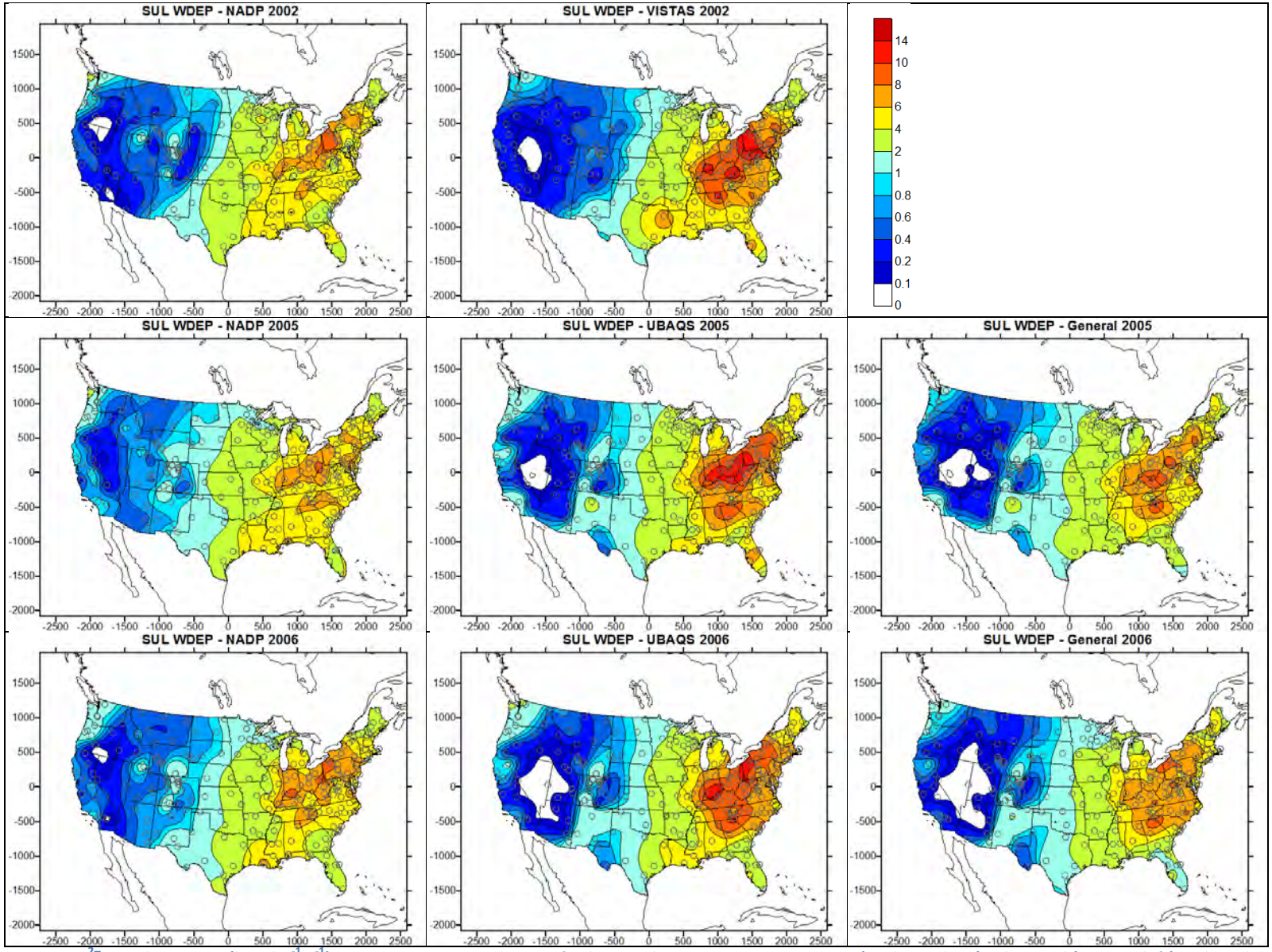

Figure D1-10. SO_4^{2-} wet deposition (kg-S ha^{-1} y^{-1}) using Kriging interpolation of values at the NADP monitoring sites (circle markers): Observed (NADP – left) and modeled (CMAQ – center; CAMx – right) deposition for 2002 (top), 2005 (middle) and 2006 (bottom).

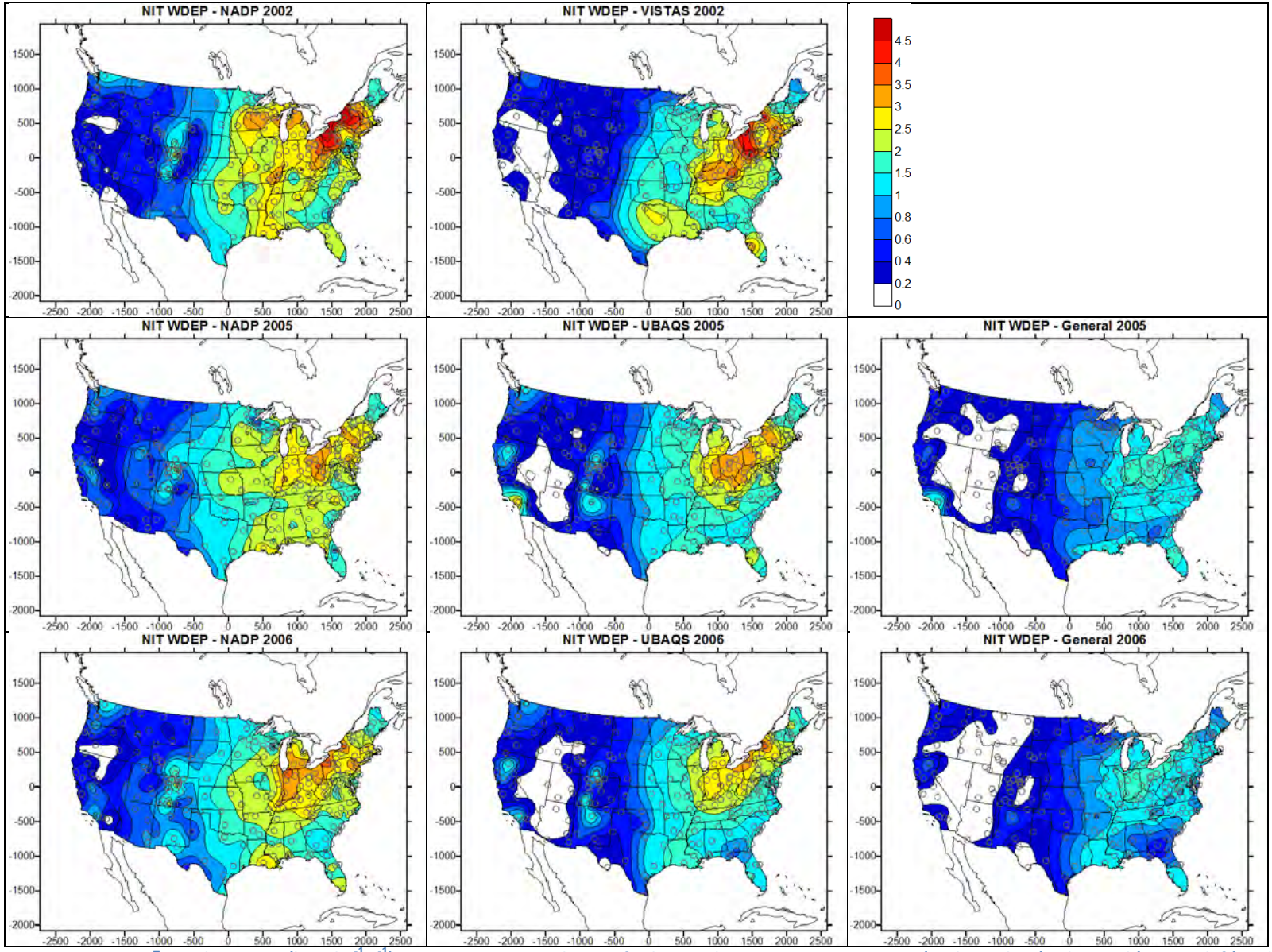

Figure D1-11. $HNO_3 + NO_3^-$ wet deposition (kg-N ha^{-1} y^{-1}) using Kriging interpolation of values at the NADP monitoring sites (circle markers): Observed (NADP – left) and modeled (CMAQ – center; CAMx – right) deposition for 2002 (top), 2005 (middle) and 2006 (bottom).

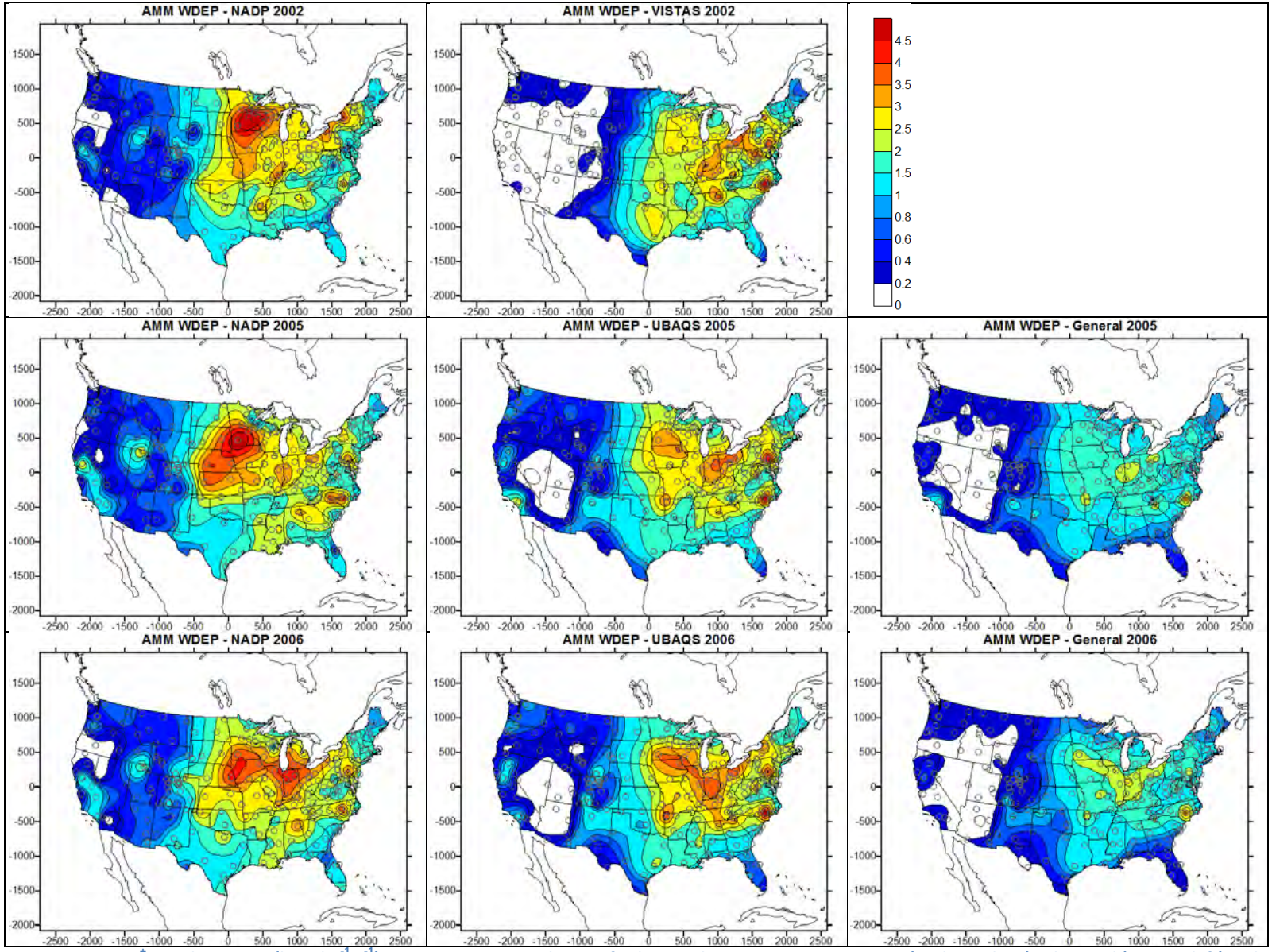

Figure D1-12. NH_3 + NH_4^+ wet deposition (kg-N ha^{-1} y^{-1}) using Kriging interpolation of values at the NADP monitoring sites (circle markers): Observed (NADP – left) and modeled (CMAQ – center; CAMx – right) deposition for 2002 (top), 2005 (middle) and 2006 (bottom).

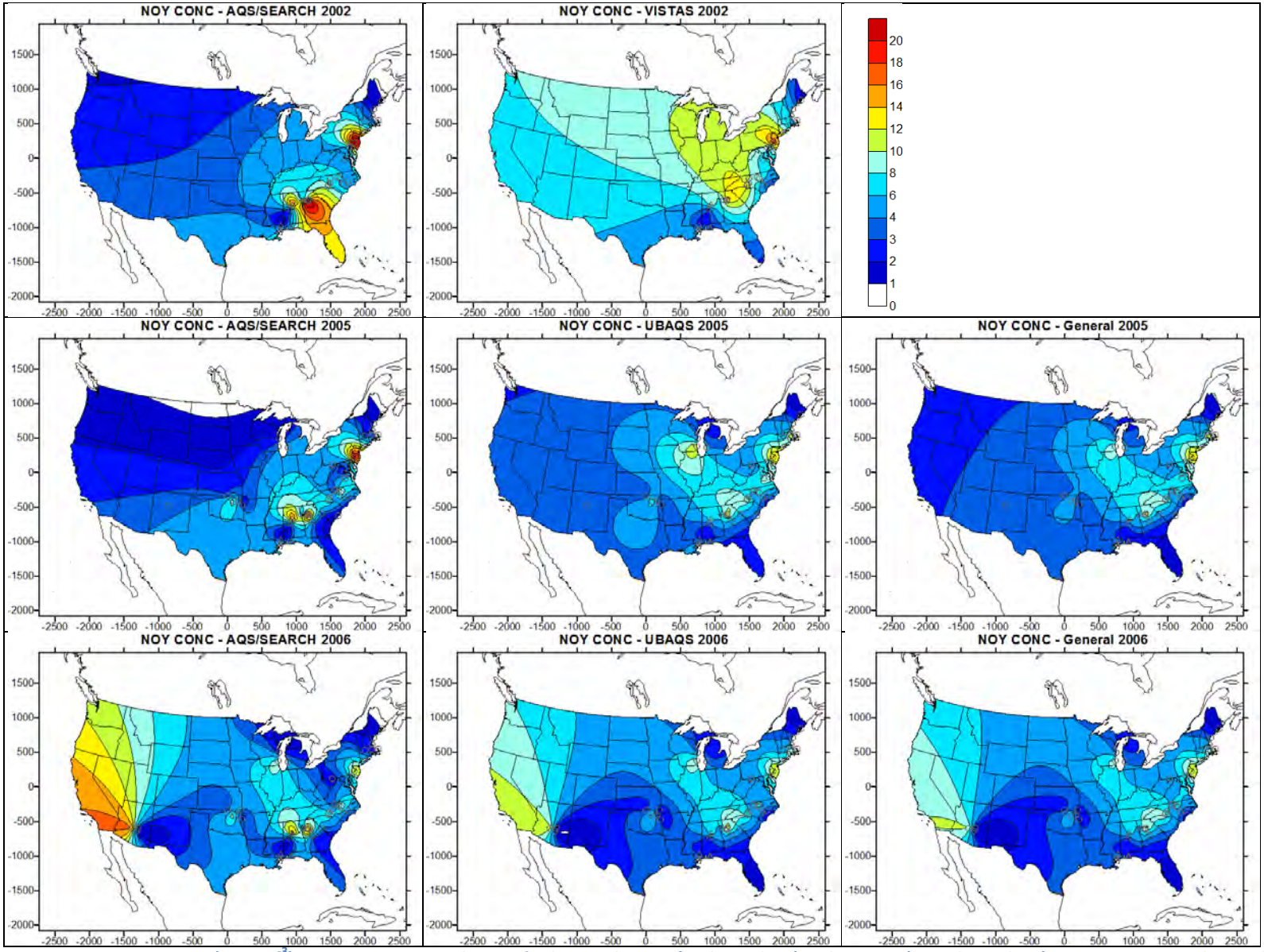

Figure D1-13. NO_y concentrations (µg-N m^{-3}) using Kriging interpolation of values at the AQS (circle markers) and SEARCH (triangle markers) monitoring sites: Observed (AQS & SEARCH – left) and modeled (CMAQ – center; CAMx – right) depositions for 2002 (top), 2005 (middle) and 2006 (bottom).

Appendix D2: Spatial Maps of Mean Normalized Bias and Error for Annual Average Concentrations and Annual Total Deposition of SOx, NOy and NHx

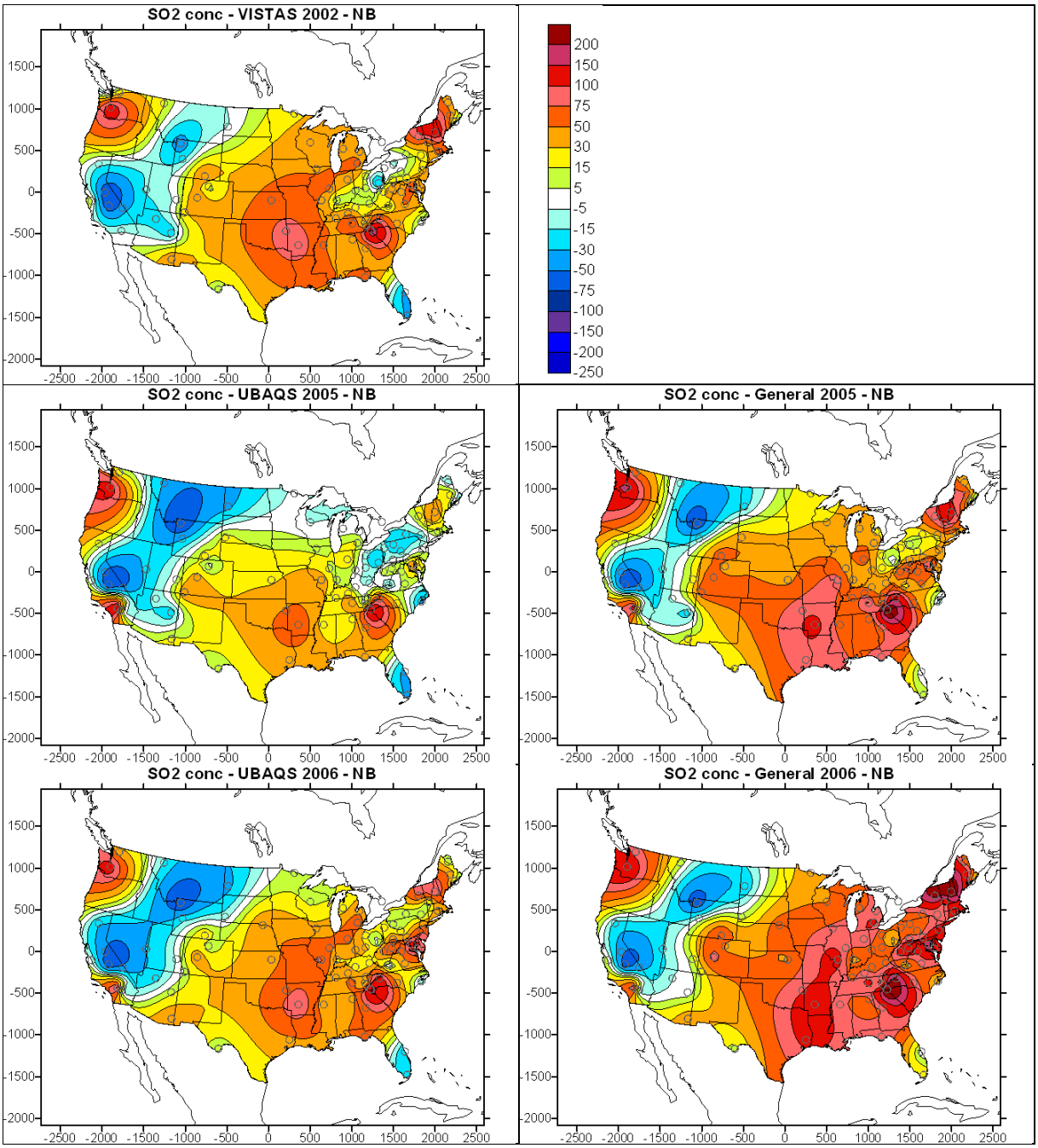

Figure D2-1. Normalized bias (%) of modeled annual average SO_2 concentrations using Kriging interpolation of values at the CASTNET monitoring sites (circle markers): CMAQ (left) and CAMx (right) model simulations for 2002 (top), 2005 (middle) and 2006 (bottom).

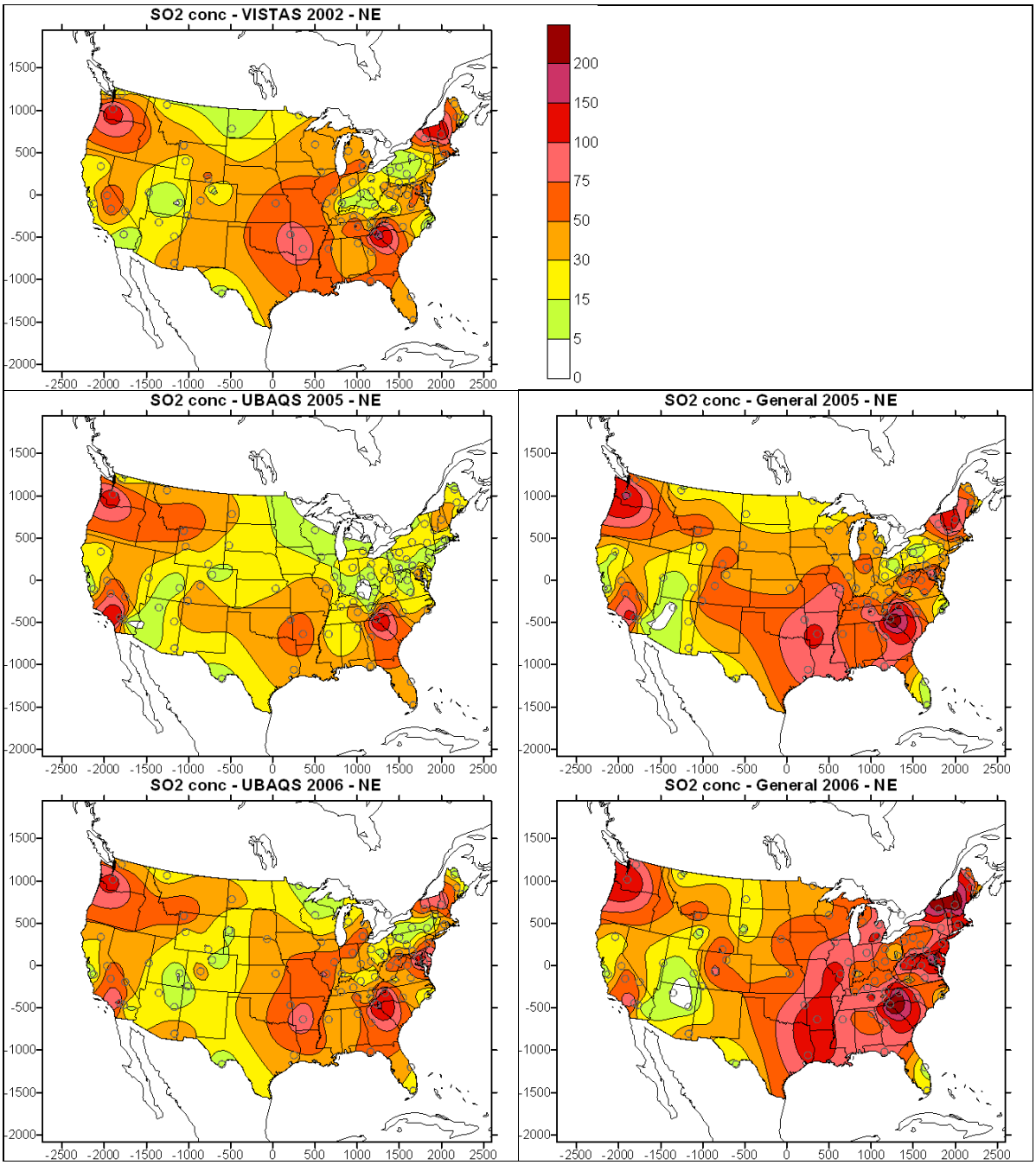

Figure D2-2. Normalized error (%) of modeled annual average SO_2 concentrations using Kriging interpolation of values at the CASTNET monitoring sites (circle markers): CMAQ (left) and CAMx (right) model simulations for 2002 (top), 2005 (middle) and 2006 (bottom).

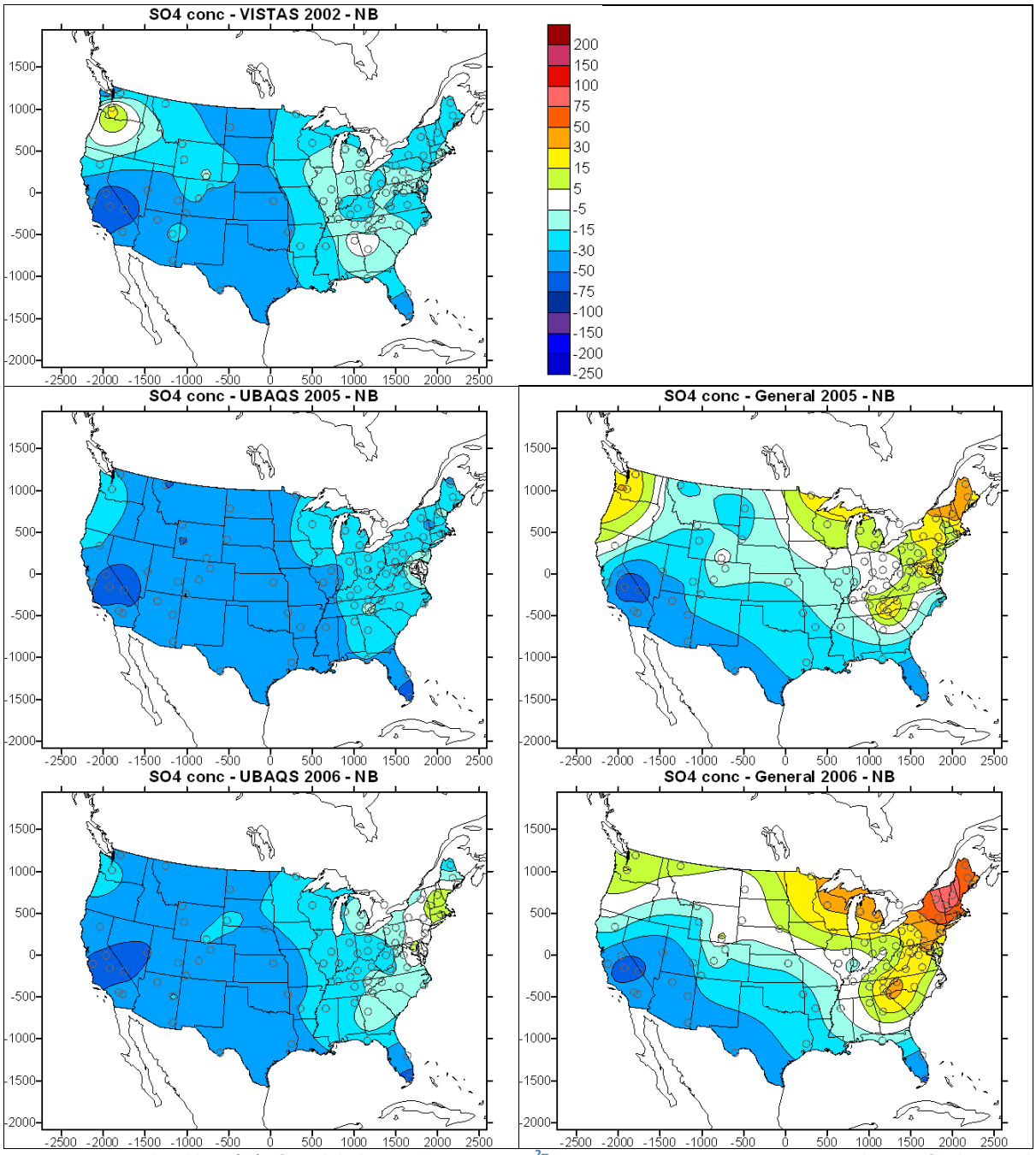

Figure D2-3. Normalized bias (%) of modeled annual average SO_4^{2-} concentrations using Kriging interpolation of values at the CASTNET monitoring sites (circle markers): CMAQ (left) and CAMx (right) model simulations for 2002 (top), 2005 (middle) and 2006 (bottom).

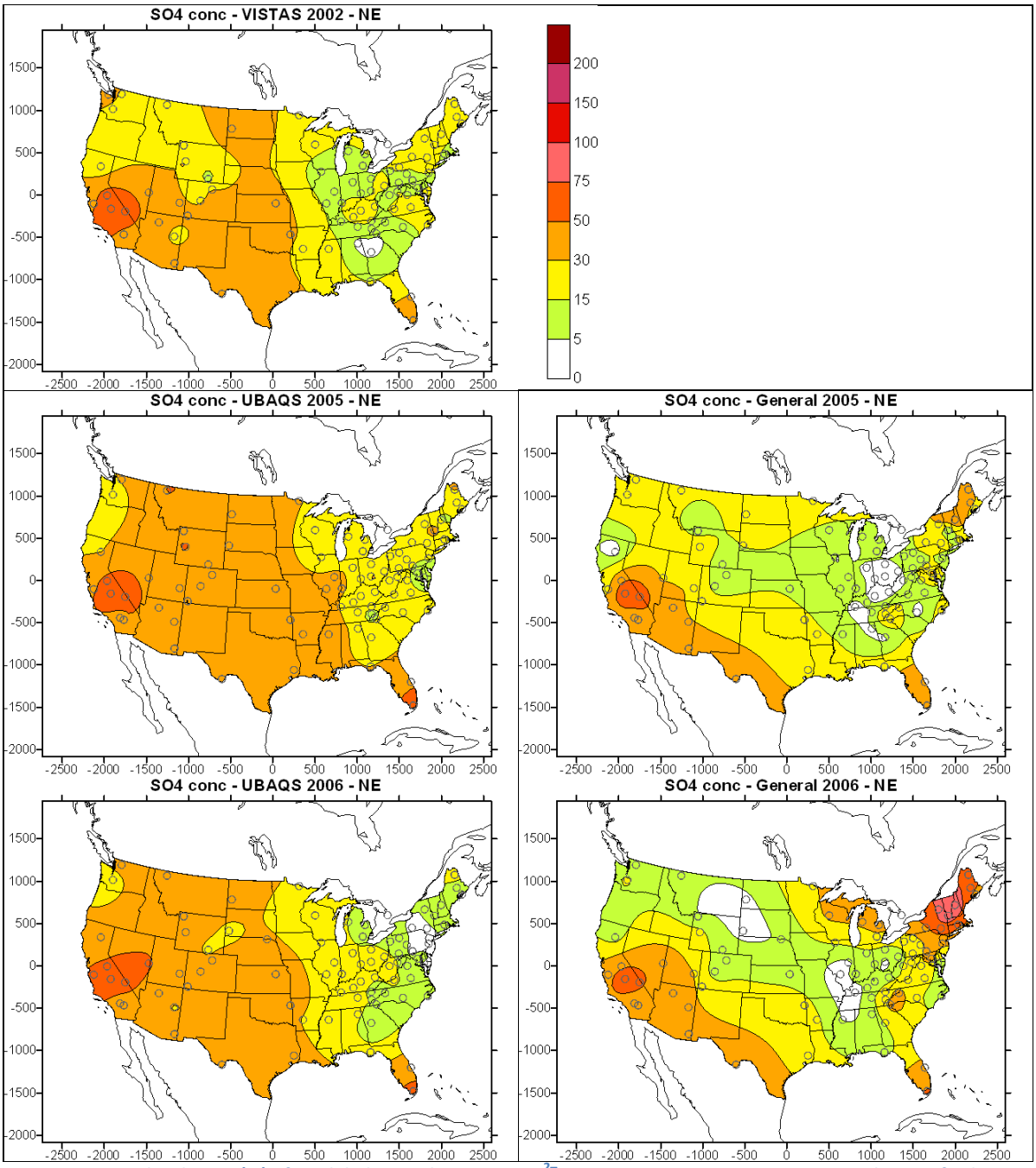

Figure D2-4. Normalized error (%) of modeled annual average SO_4^{2-} concentrations using Kriging interpolation of values at the CASTNET monitoring sites (circle markers): CMAQ (left) and CAMx (right) model simulations for 2002 (top), 2005 (middle) and 2006 (bottom).

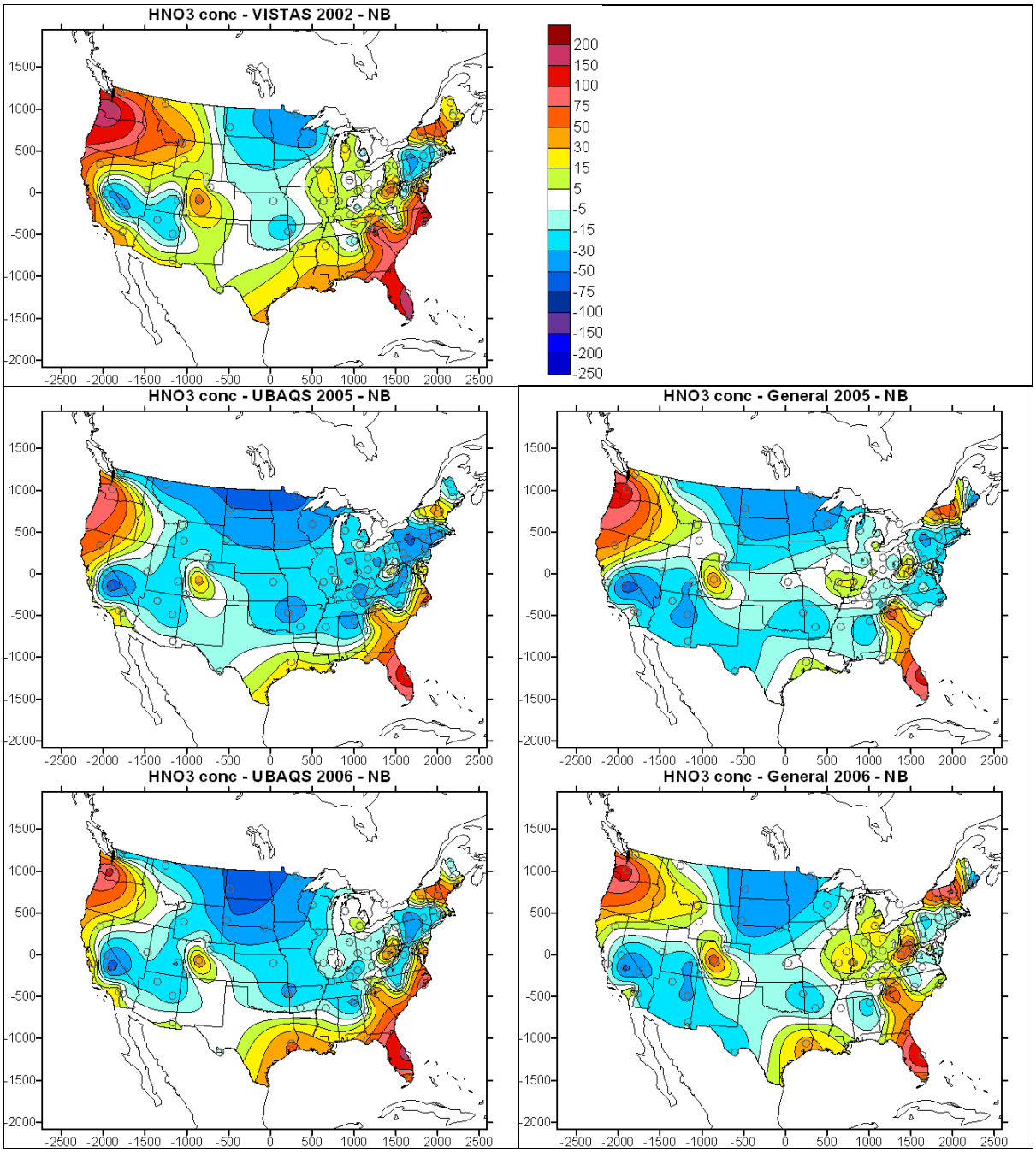

Figure D2-5. Normalized bias (%) of modeled annual average HNO_3 concentrations using Kriging interpolation of values at the CASTNET monitoring sites (circle markers): CMAQ (left) and CAMx (right) model simulations for 2002 (top), 2005 (middle) and 2006 (bottom).

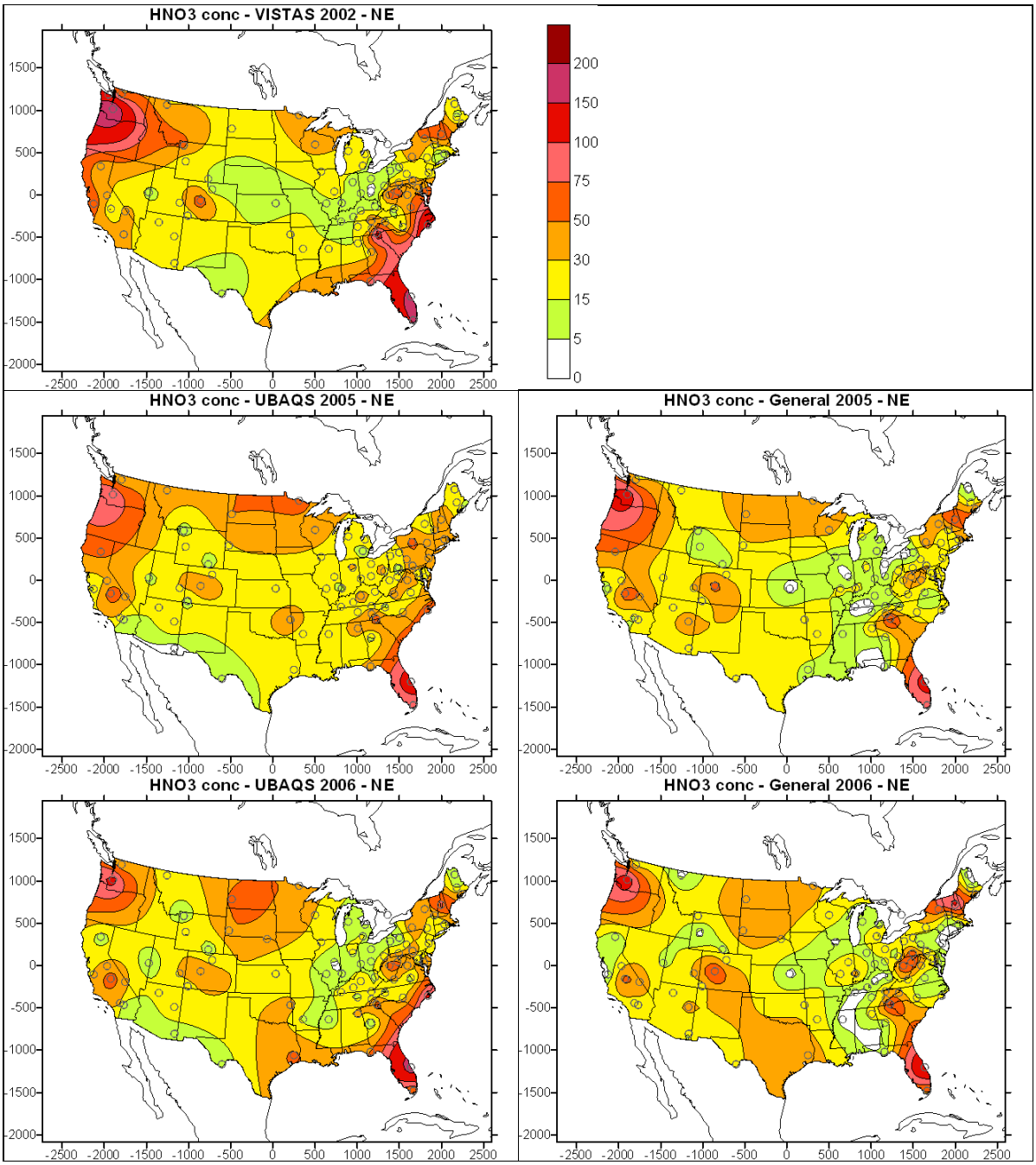

Figure D2-6. Normalized error (%) of modeled annual average HNO_3 concentrations using Kriging interpolation of values at the CASTNET monitoring sites (circle markers): CMAQ (left) and CAMx (right) model simulations for 2002 (top), 2005 (middle) and 2006 (bottom).

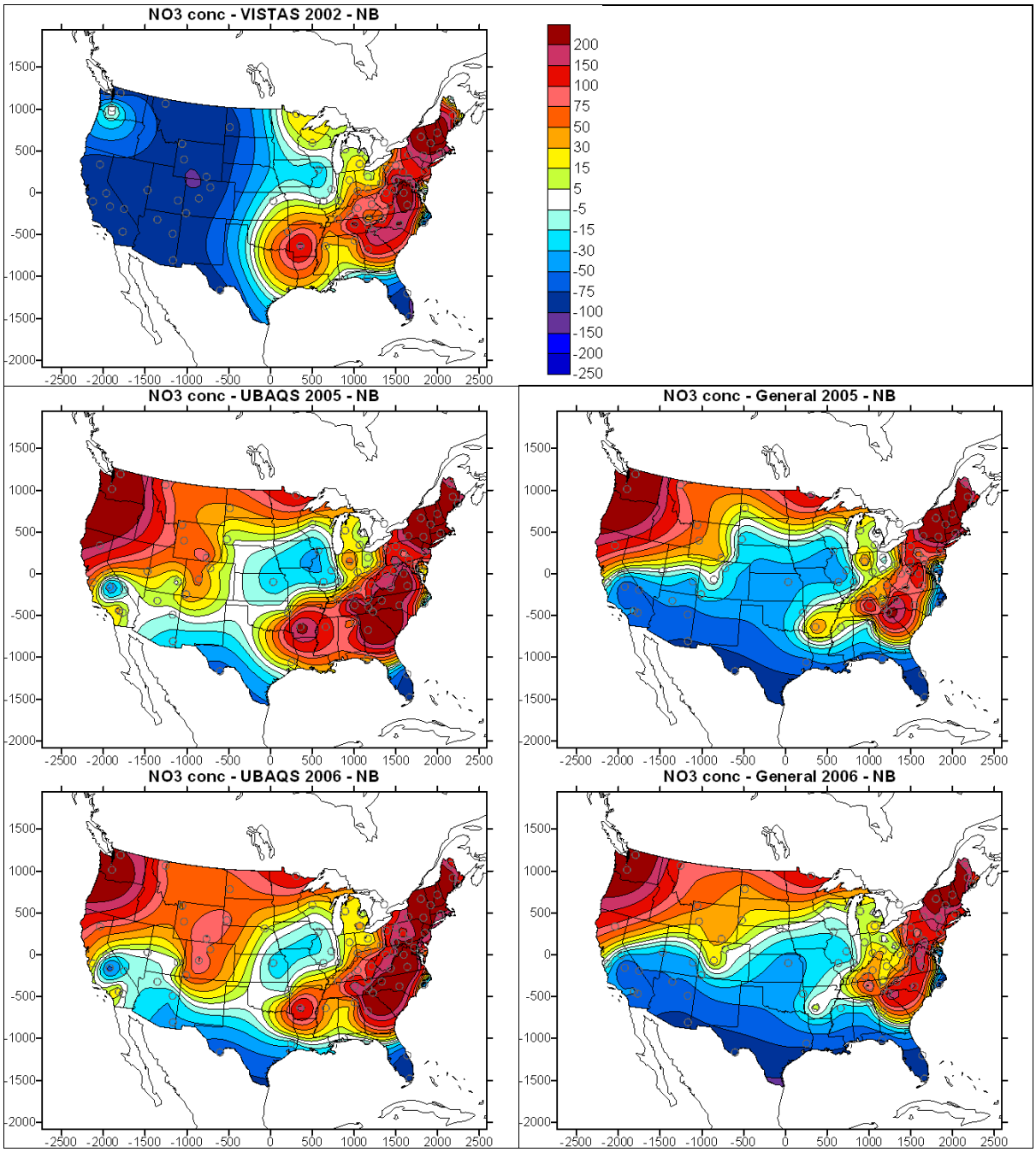

Figure D2-7. Normalized bias (%) of modeled annual average NO_3^- concentrations using Kriging interpolation of values at the CASTNET monitoring sites (circle markers): CMAQ (left) and CAMx (right) model simulations for 2002 (top), 2005 (middle) and 2006 (bottom).

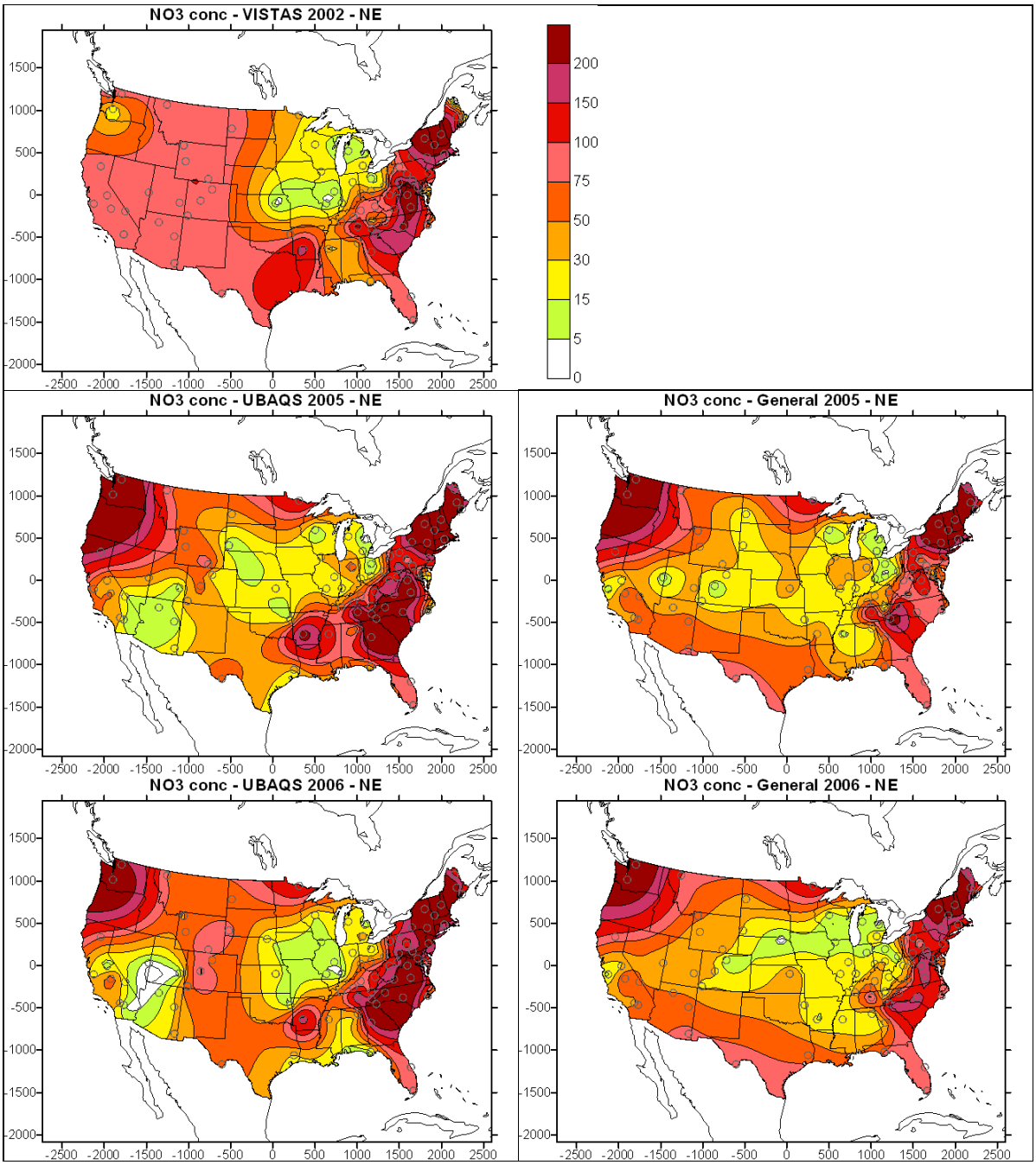

Figure D2-8. Normalized error (%) of modeled annual average NO_3^- concentrations using Kriging interpolation of values at the CASTNET monitoring sites (circle markers): CMAQ (left) and CAMx (right) model simulations for 2002 (top), 2005 (middle) and 2006 (bottom).

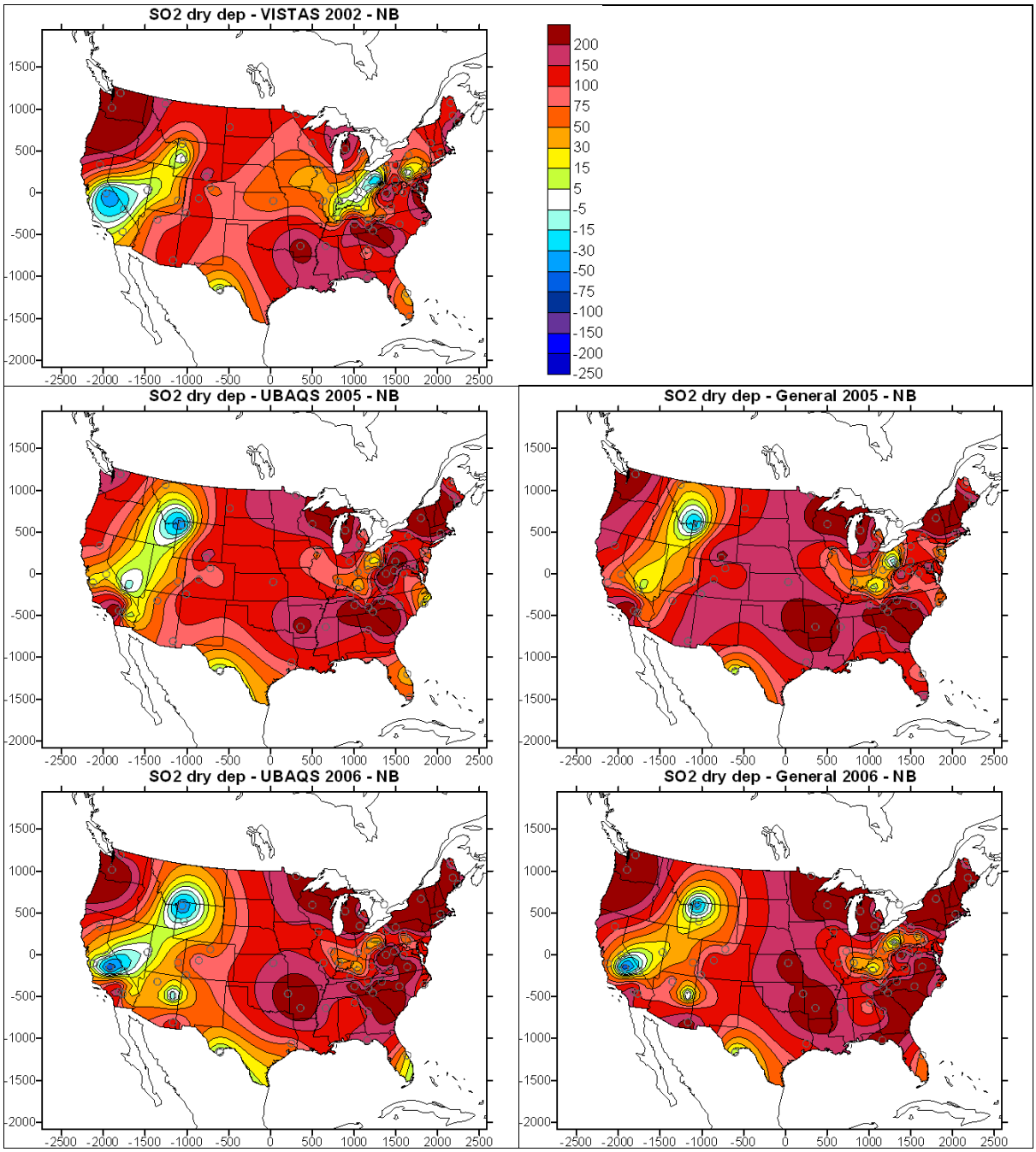

Figure D2-9. Normalized bias (%) of modeled annual total SO_2 dry deposition using Kriging interpolation of values at the CASTNET monitoring sites (circle markers): CMAQ (left) and CAMx (right) model simulations for 2002 (top), 2005 (middle) and 2006 (bottom).

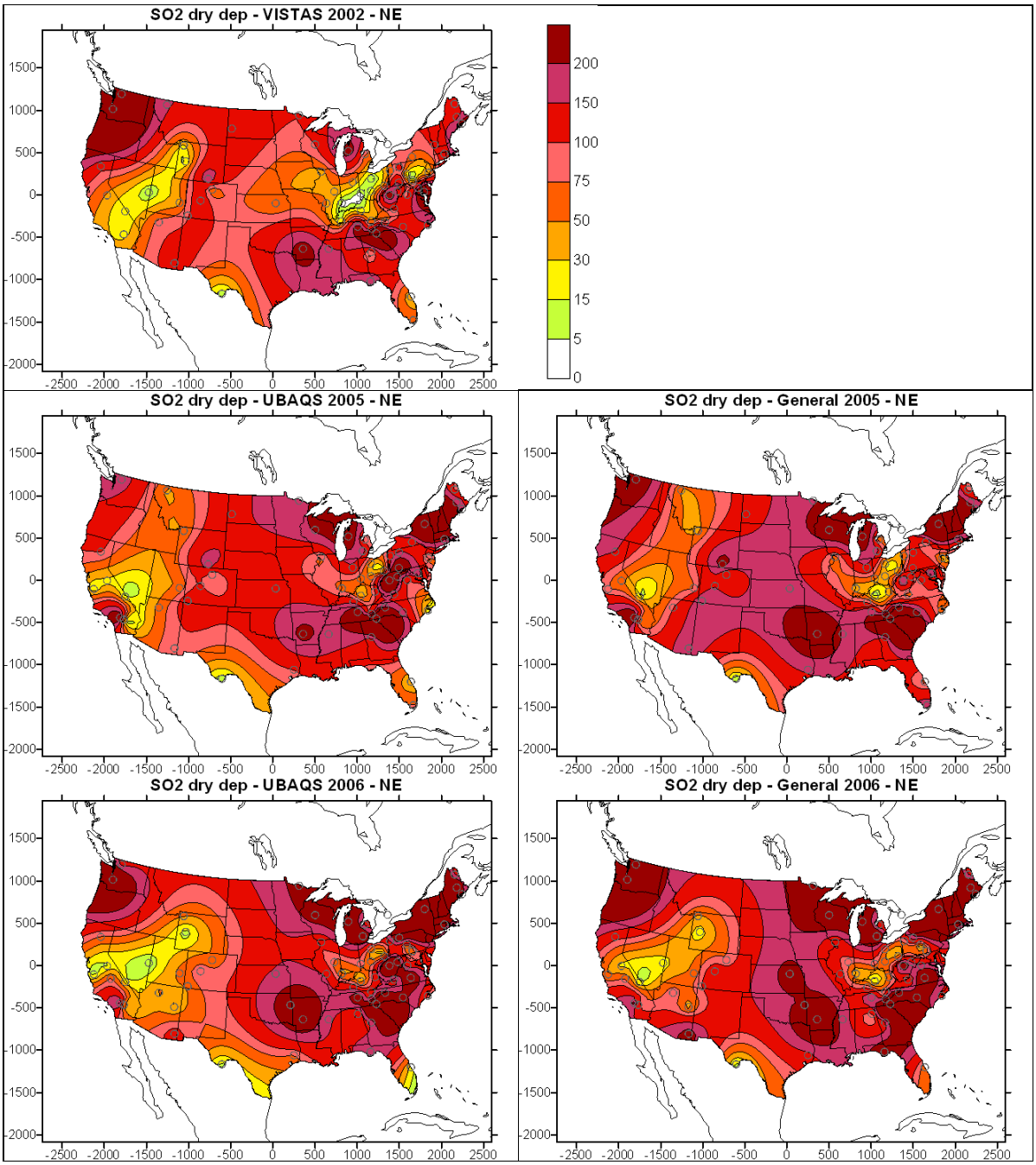

Figure D2-10. Normalized error (%) of modeled annual total SO_2 dry deposition using Kriging interpolation of values at the CASTNET monitoring sites (circle markers): CMAQ (left) and CAMx (right) model simulations for 2002 (top), 2005 (middle) and 2006 (bottom).

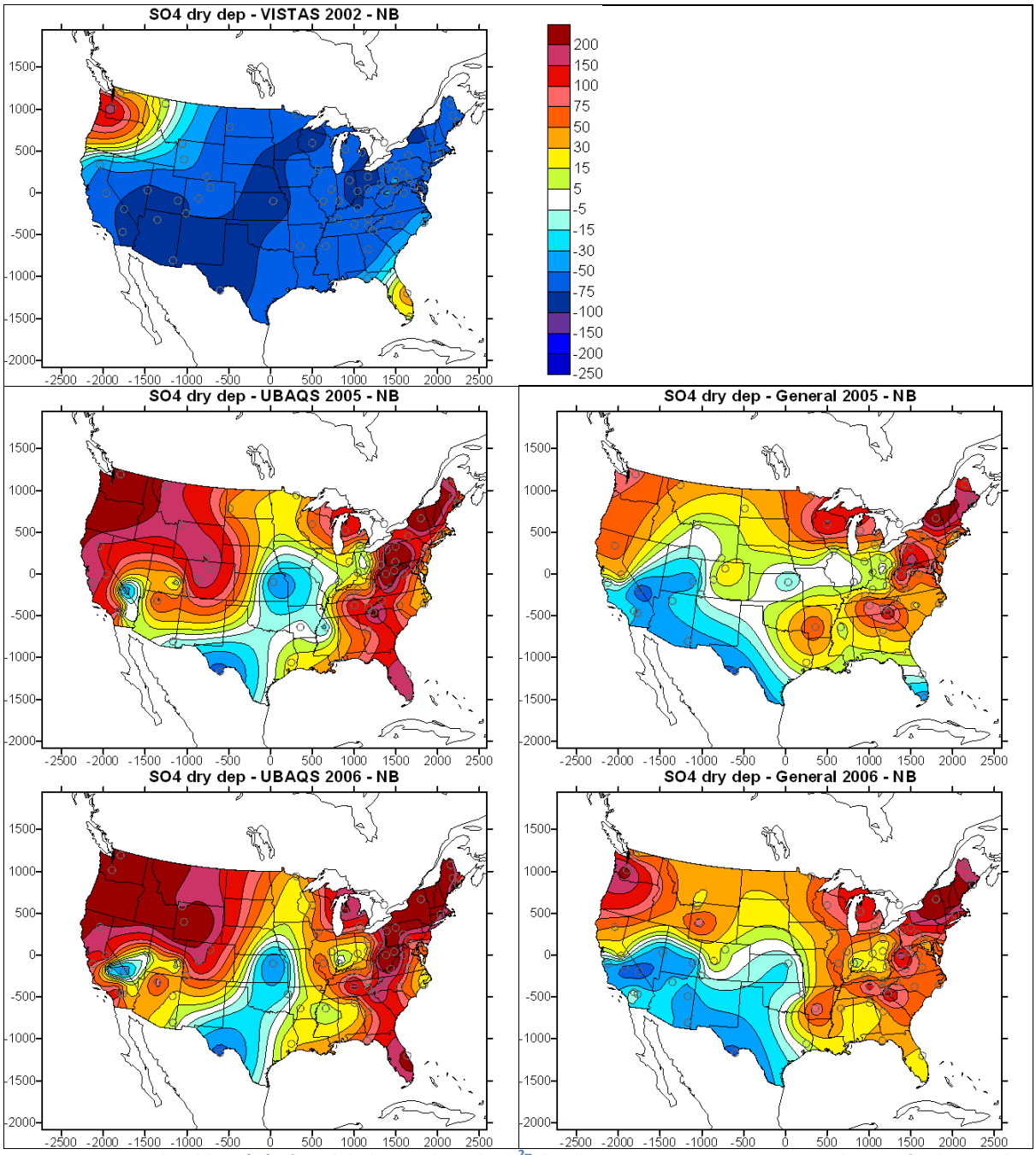

Figure D2-11. Normalized bias (%) of modeled annual total SO_4^{2-} dry deposition using Kriging interpolation of values at the CASTNET monitoring sites (circle markers): CMAQ (left) and CAMx (right) model simulations for 2002 (top), 2005 (middle) and 2006 (bottom).

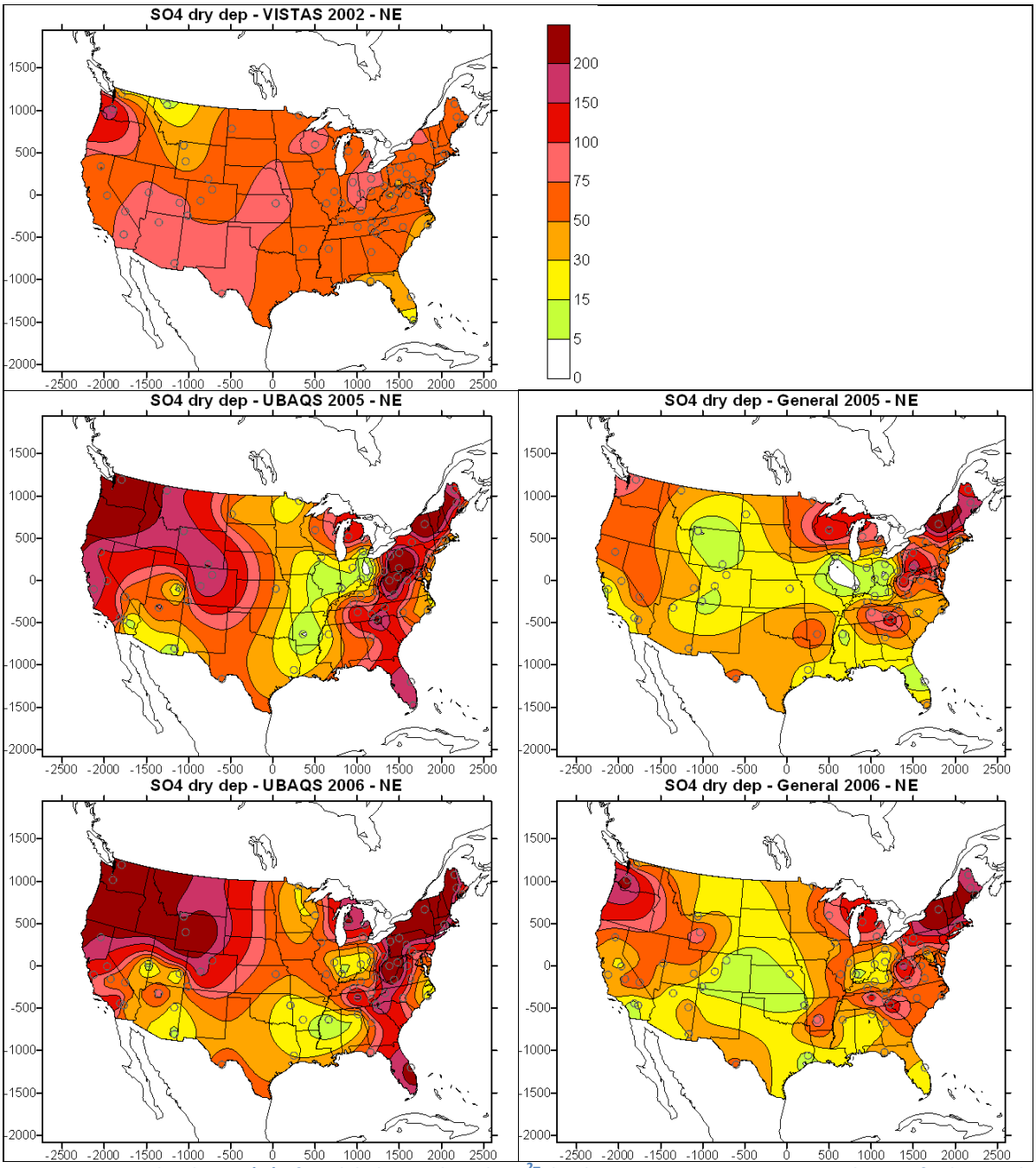

Figure D2-12. Normalized error (%) of modeled annual total SO_4^{2-} dry deposition using Kriging interpolation of values at the CASTNET monitoring sites (circle markers): CMAQ (left) and CAMx (right) model simulations for 2002 (top), 2005 (middle) and 2006 (bottom).

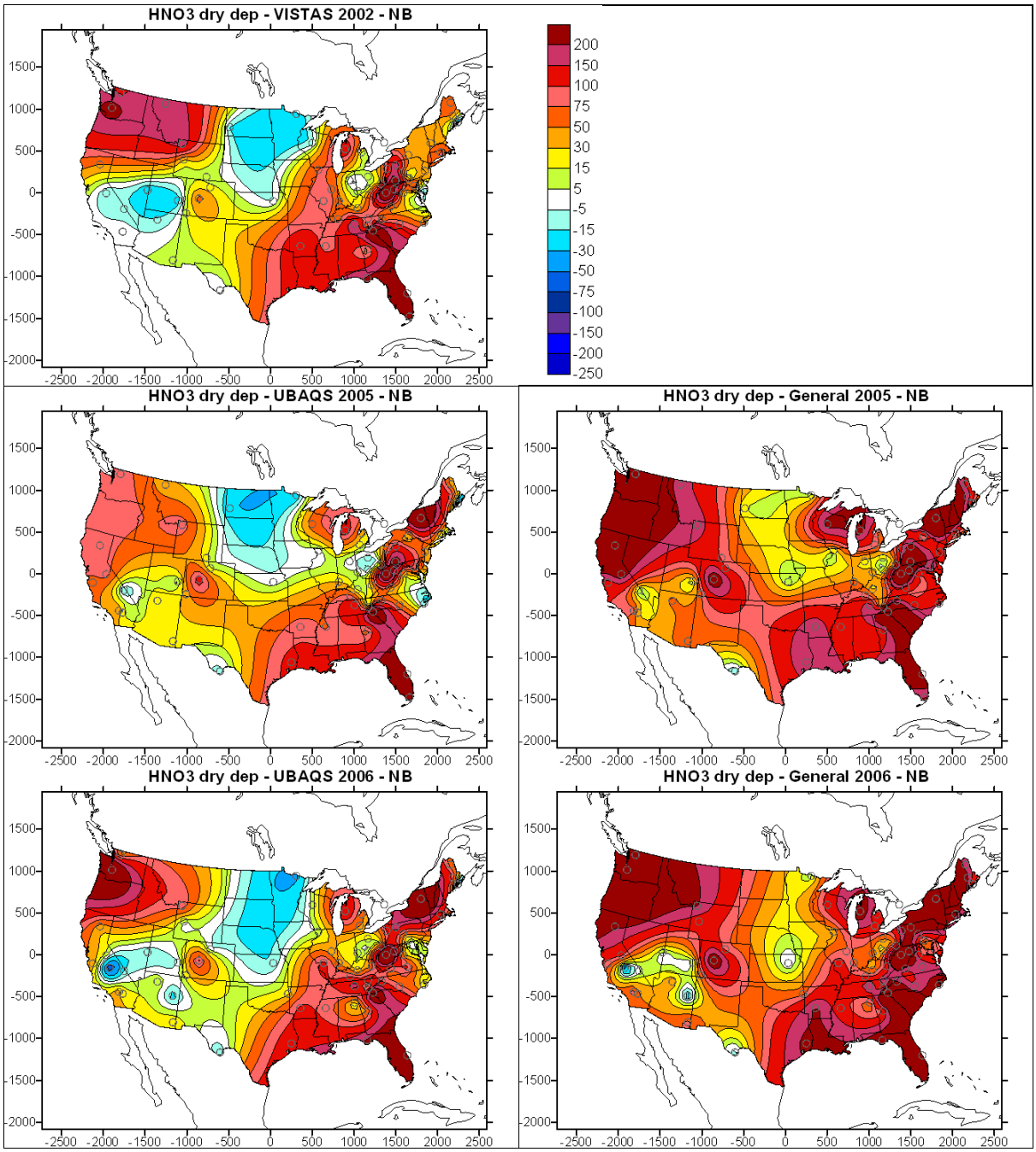

Figure D2-13. Normalized bias (%) of modeled annual total HNO_3 dry deposition using Kriging interpolation of values at the CASTNET monitoring sites (circle markers): CMAQ (left) and CAMx (right) model simulations for 2002 (top), 2005 (middle) and 2006 (bottom).

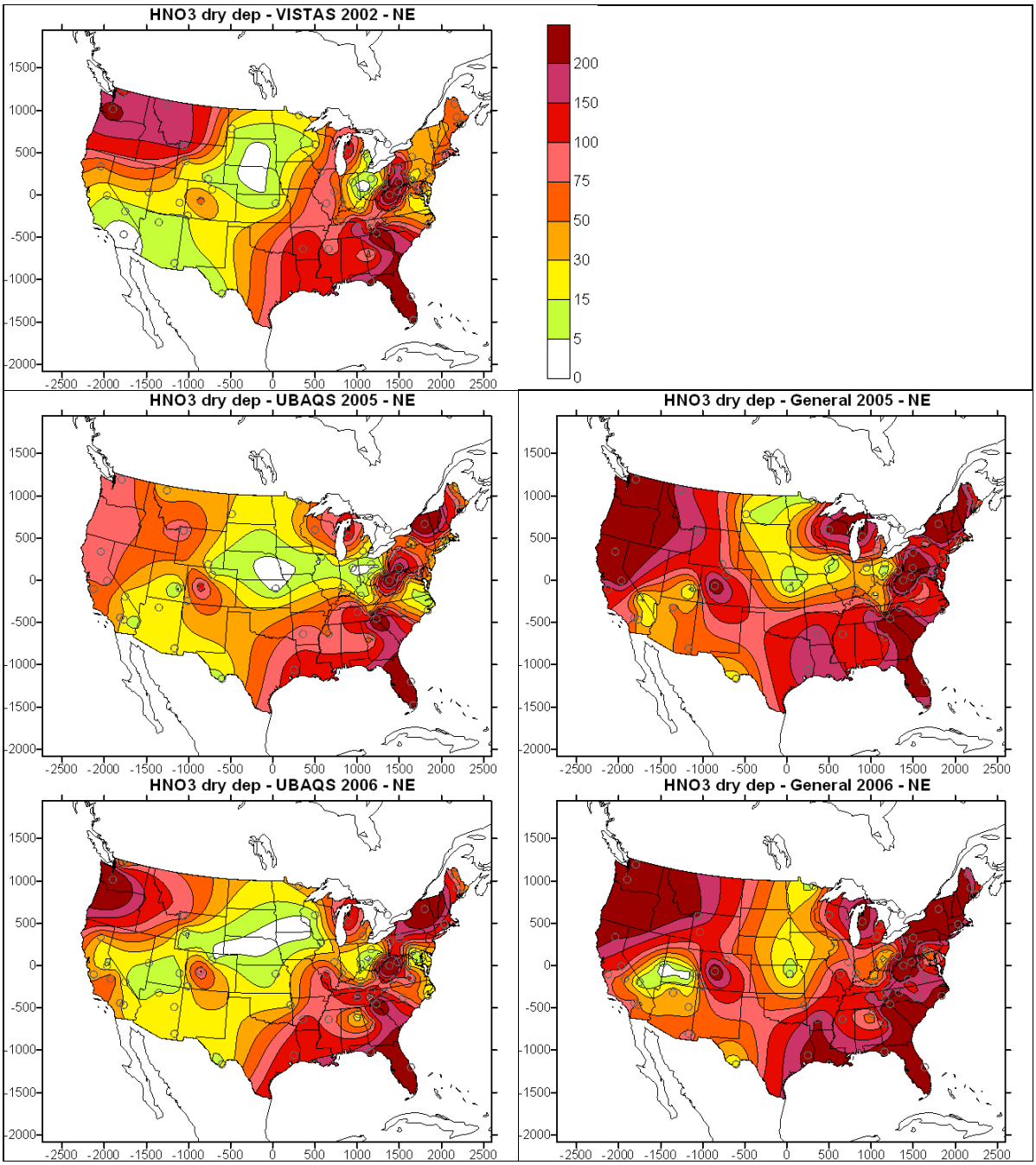

Figure D2-14. Normalized error (%) of modeled annual total HNO_3 dry deposition using Kriging interpolation of values at the CASTNET monitoring sites (circle markers): CMAQ (left) and CAMx (right) model simulations for 2002 (top), 2005 (middle) and 2006 (bottom).

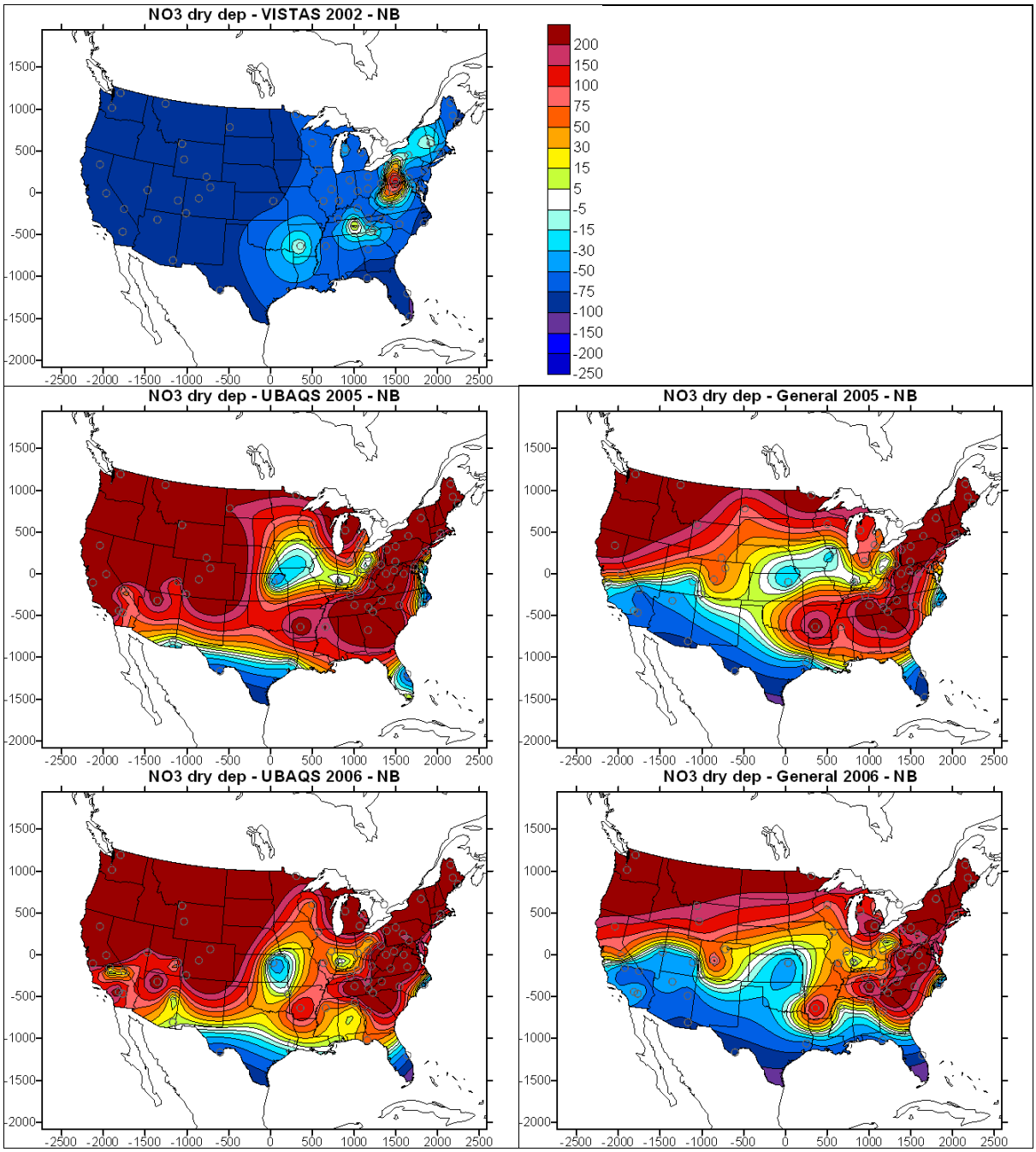

Figure D2-15. Normalized bias (%) of modeled annual total NO_3^- dry deposition using Kriging interpolation of values at the CASTNET monitoring sites (circle markers): CMAQ (left) and CAMx (right) model simulations for 2002 (top), 2005 (middle) and 2006 (bottom).

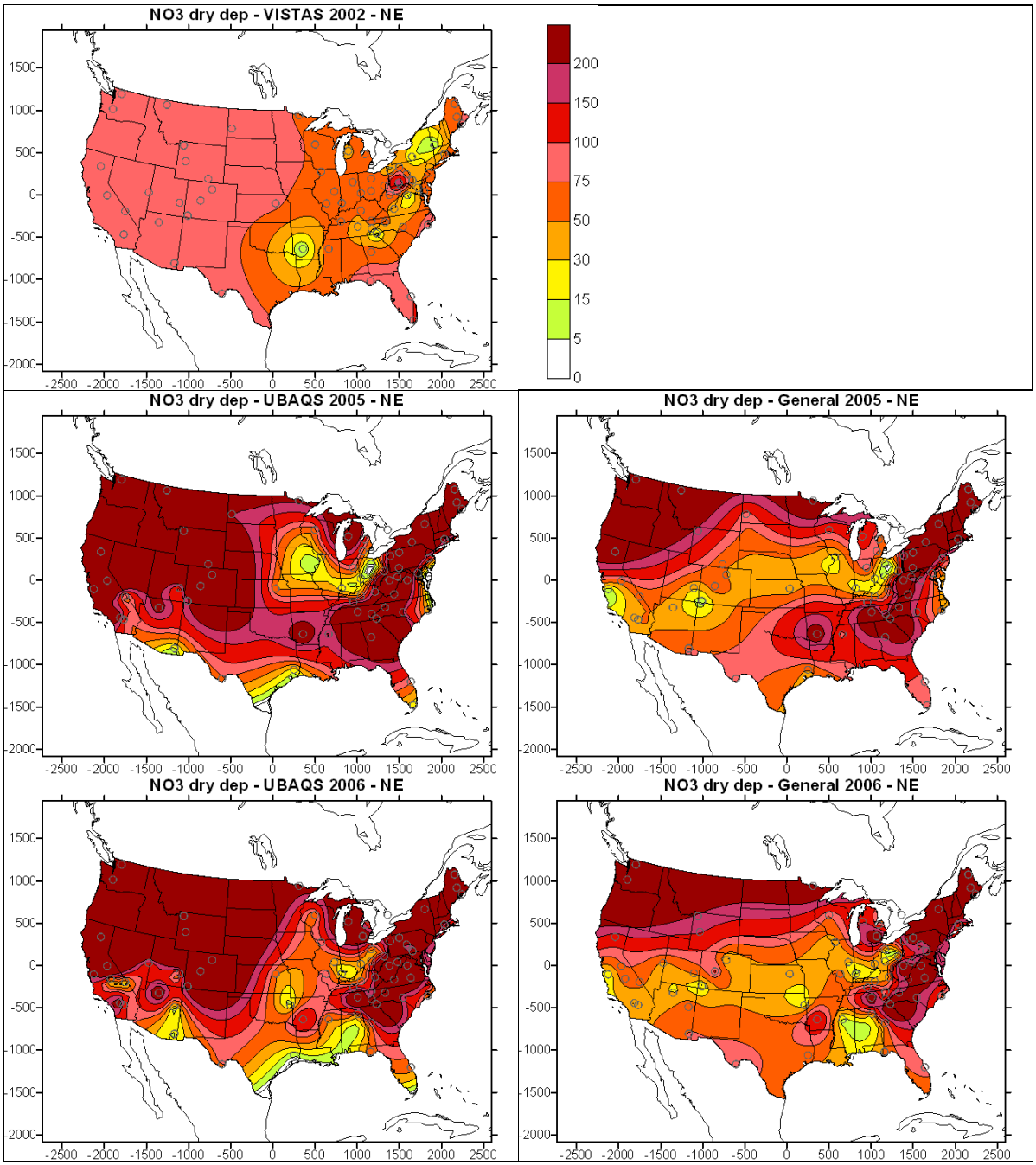

Figure D2-16. Normalized error (%) of modeled annual total NO_3^- dry deposition using Kriging interpolation of values at the CASTNET monitoring sites (circle markers): CMAQ (left) and CAMx (right) model simulations for 2002 (top), 2005 (middle) and 2006 (bottom).

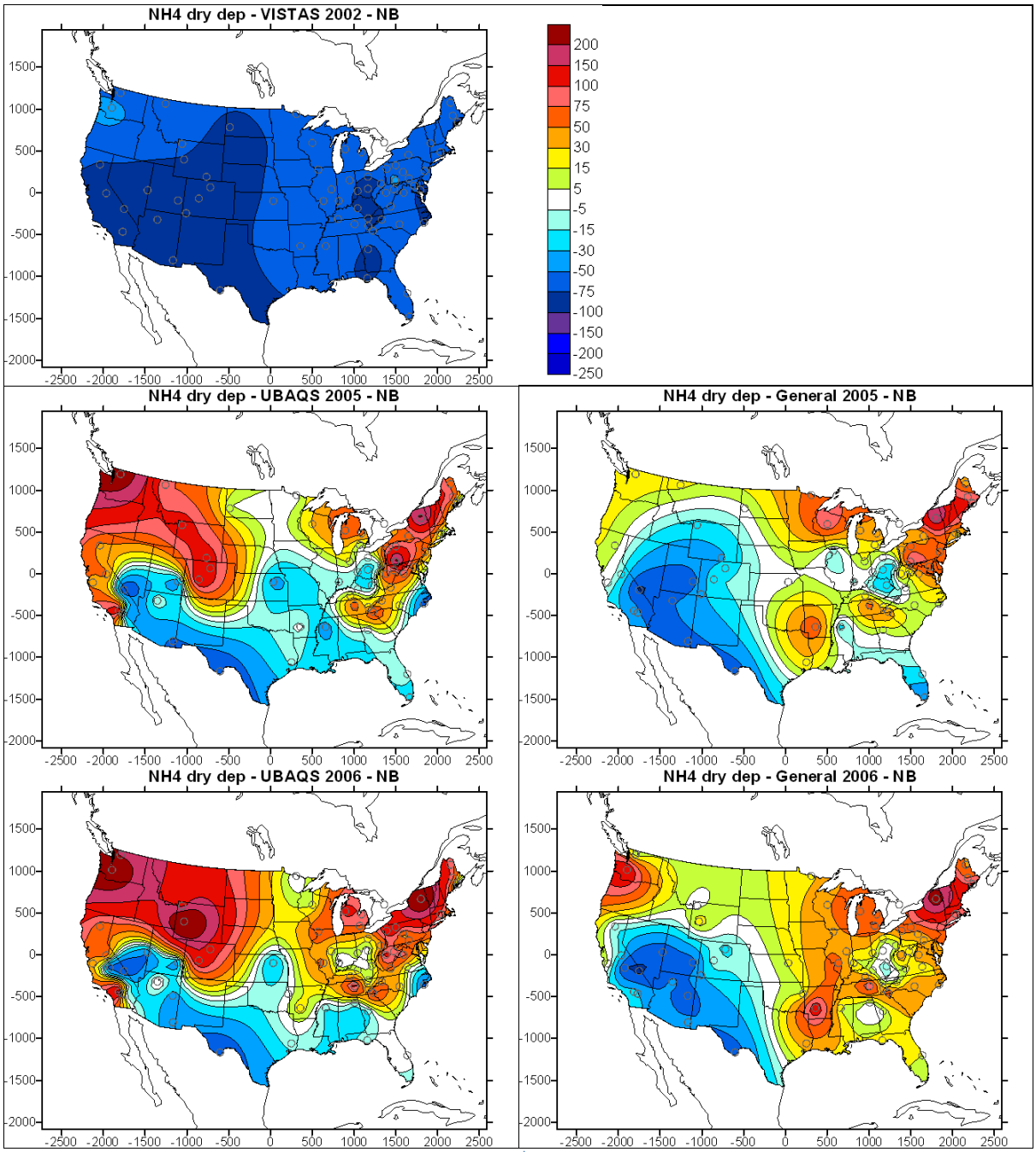

Figure D2-17. Normalized bias (%) of modeled annual total NH_4^+ dry deposition using Kriging interpolation of values at the CASTNET monitoring sites (circle markers): CMAQ (left) and CAMx (right) model simulations for 2002 (top), 2005 (middle) and 2006 (bottom).

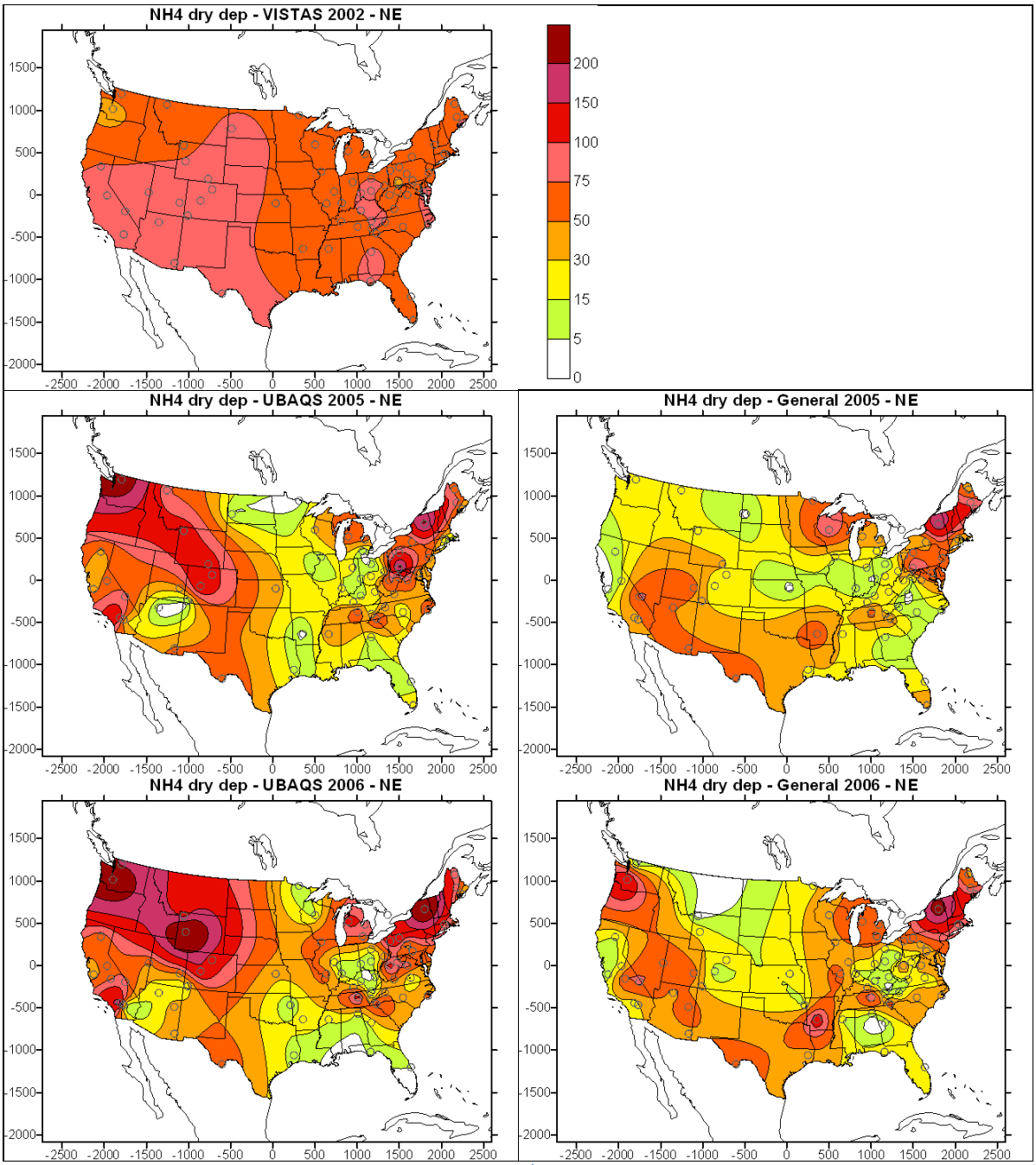

Figure D2-18. Normalized error (%) of modeled annual total NH_4^+ dry deposition using Kriging interpolation of values at the CASTNET monitoring sites (circle markers): CMAQ (left) and CAMx (right) model simulations for 2002 (top), 2005 (middle) and 2006 (bottom).

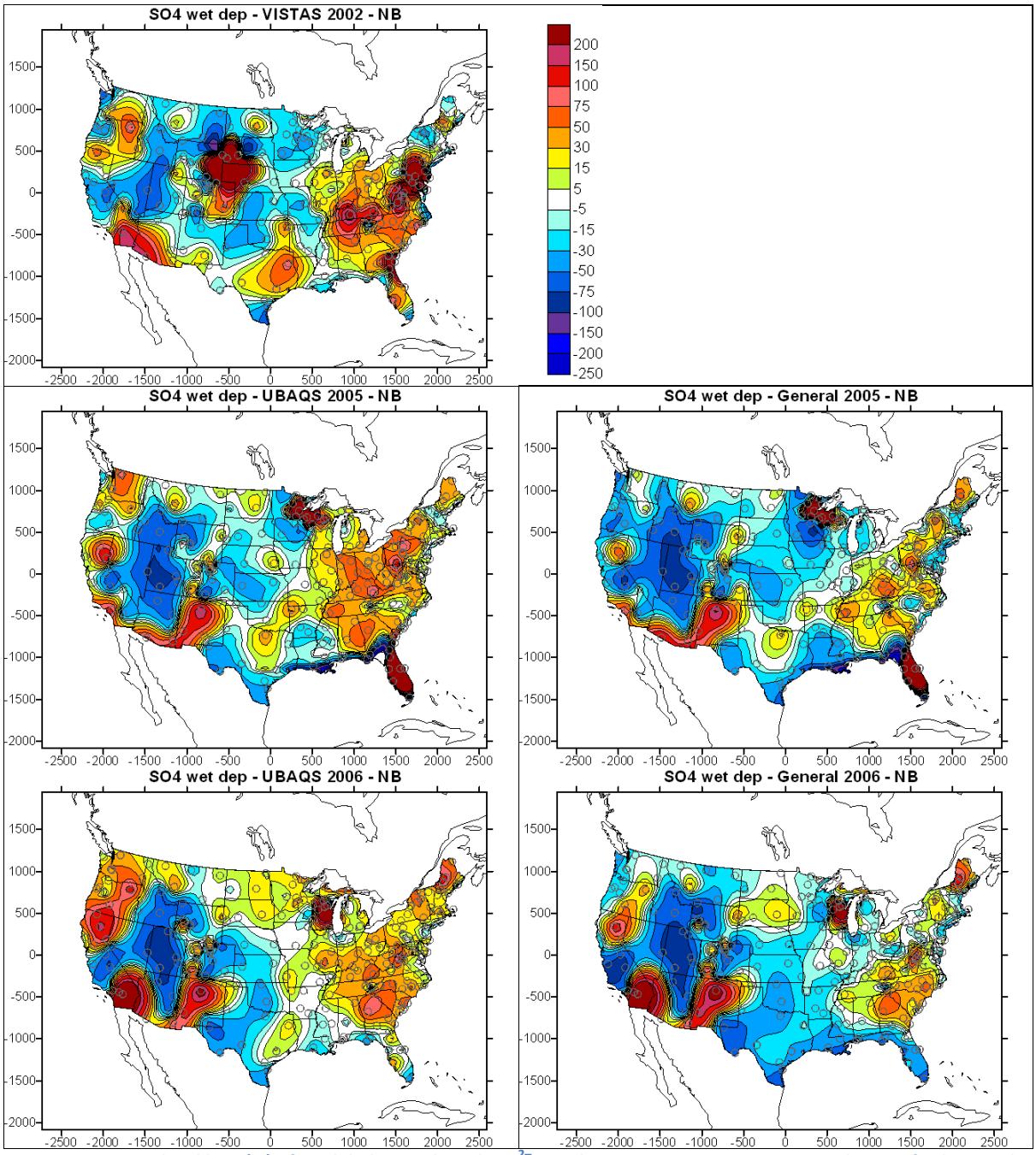

Figure D2-19. Normalized bias (%) of modeled annual total SO_4^{2-} wet deposition using Kriging interpolation of values at the NADP monitoring sites (circle markers): CMAQ (left) and CAMx (right) model simulations for 2002 (top), 2005 (middle) and 2006 (bottom).

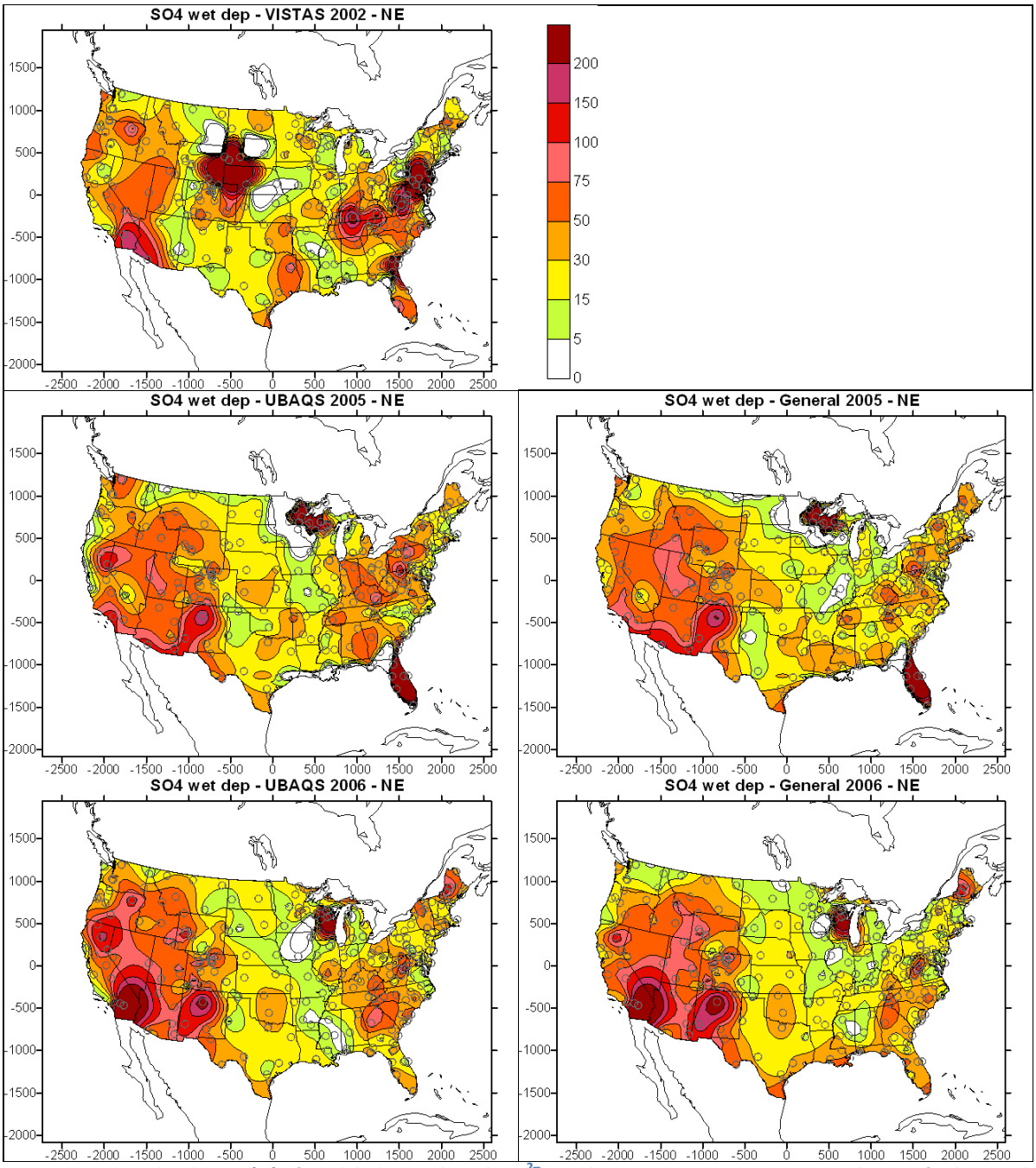

Figure D2-20. Normalized error (%) of modeled annual total SO_4^{2-} wet deposition using Kriging interpolation of values at the NADP monitoring sites (circle markers): CMAQ (left) and CAMx (right) model simulations for 2002 (top), 2005 (middle) and 2006 (bottom).

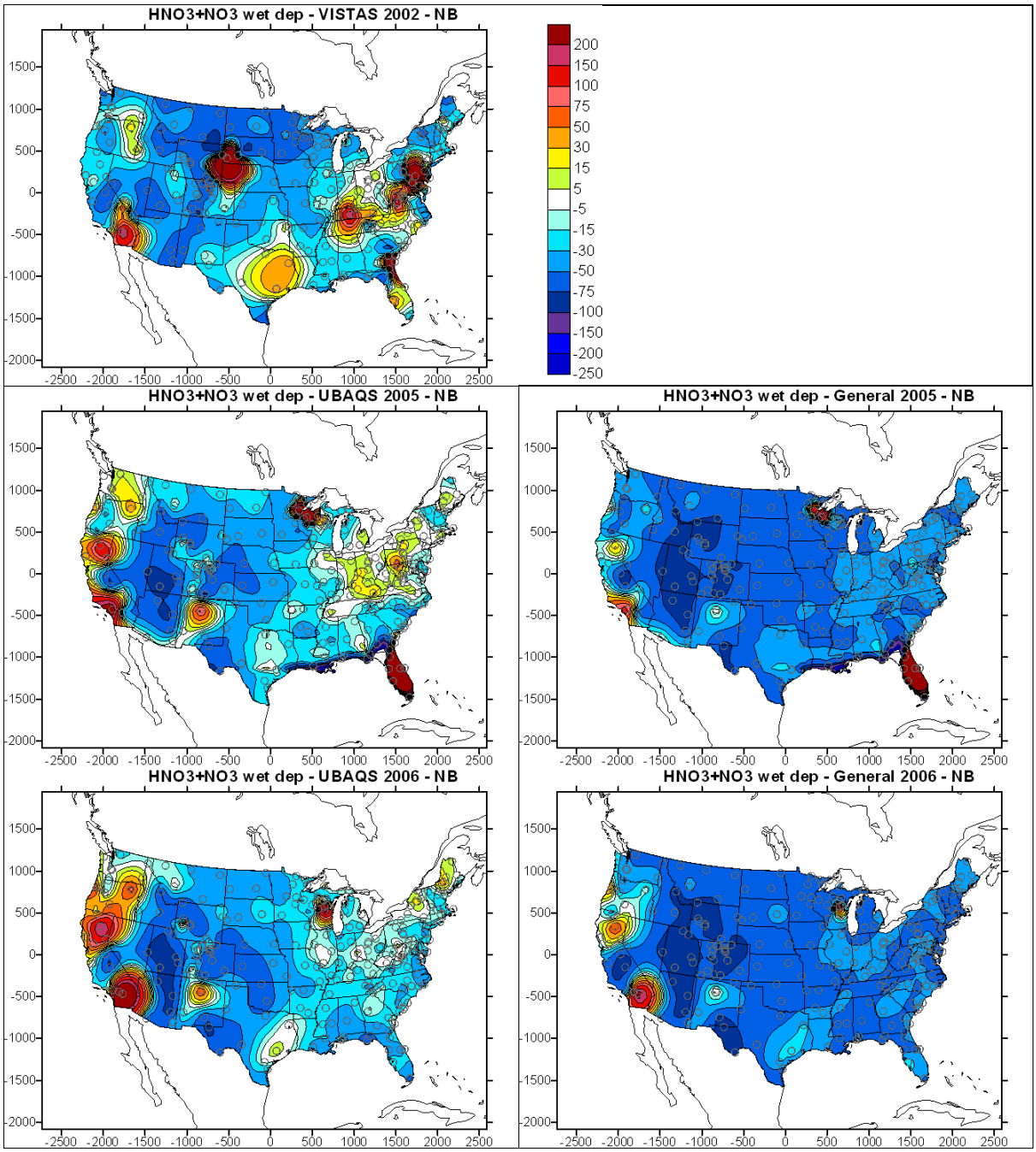

Figure D2-21. Normalized bias (%) of modeled annual total $HNO_3 + NO_3^-$ wet deposition using Kriging interpolation of values at the NADP monitoring sites (circle markers): CMAQ (left) and CAMx (right) model simulations for 2002 (top), 2005 (middle) and 2006 (bottom).

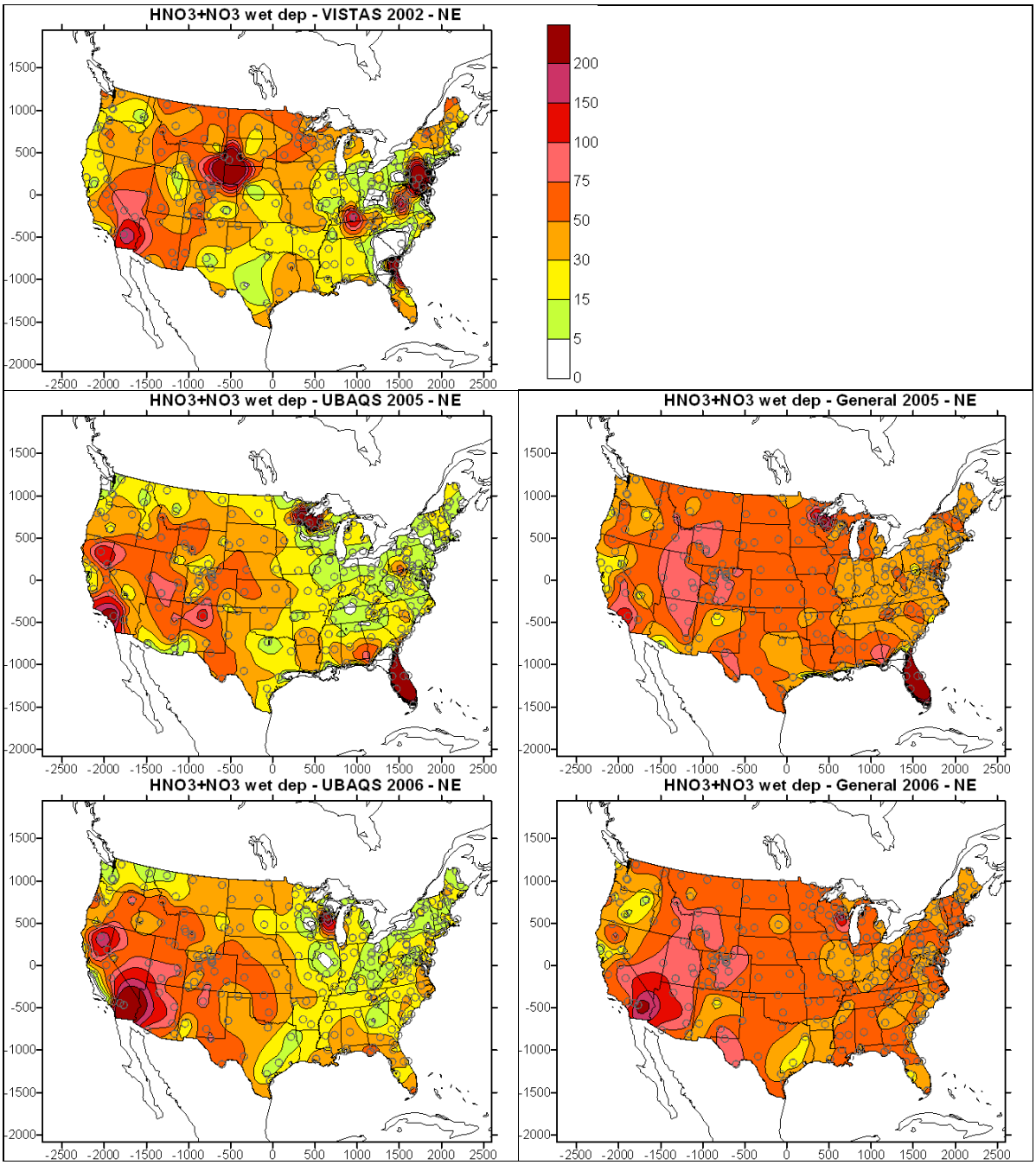

Figure D2-22. Normalized error (%) of modeled annual total $HNO_3 + NO_3^-$ wet deposition using Kriging interpolation of values at the NADP monitoring sites (circle markers): CMAQ (left) and CAMx (right) model simulations for 2002 (top), 2005 (middle) and 2006 (bottom).

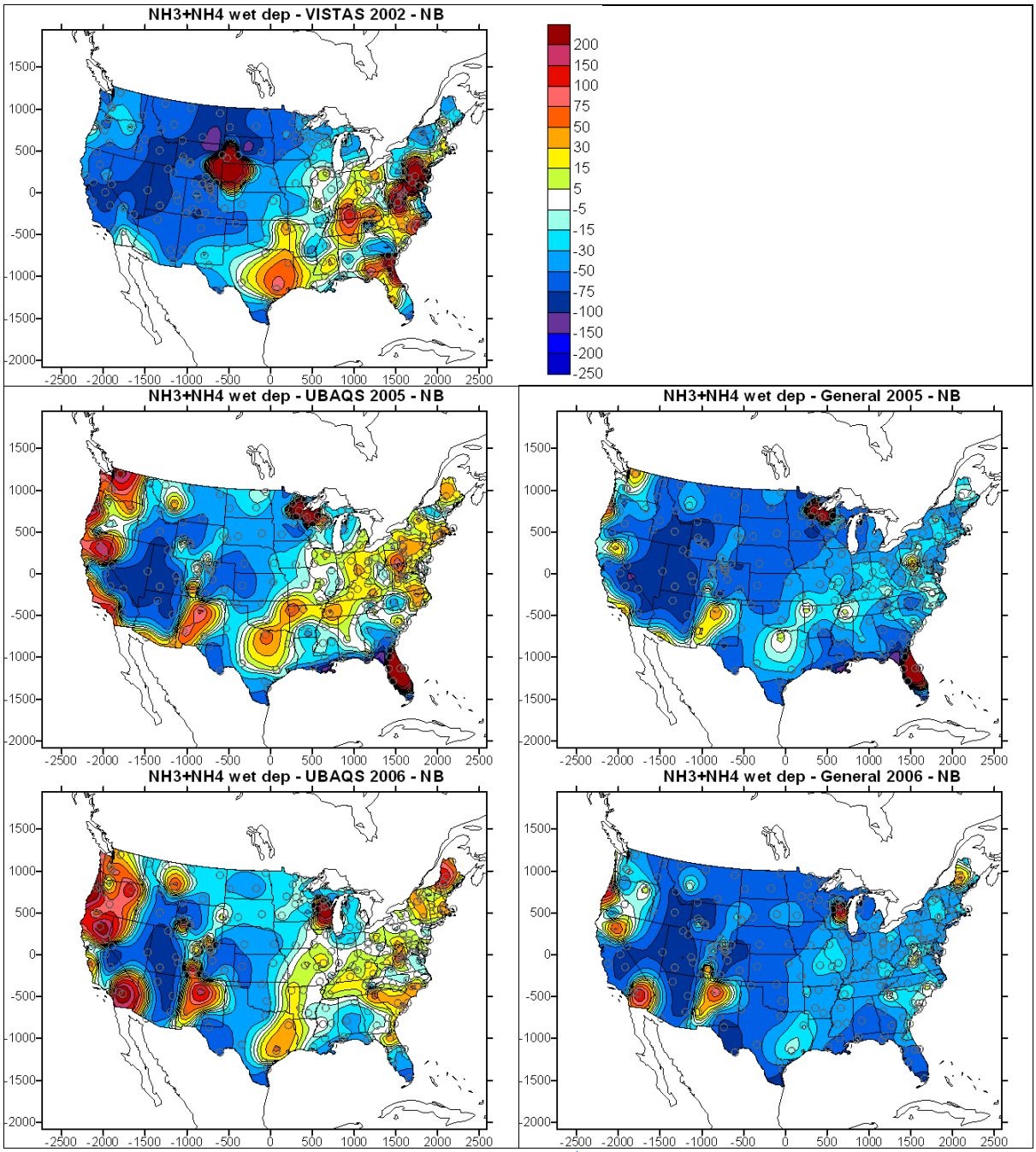

Figure D2-23. Normalized bias (%) of modeled annual total $NH_3 + NH_4^+$ wet deposition using Kriging interpolation of values at the NADP monitoring sites (circle markers): CMAQ (left) and CAMx (right) model simulations for 2002 (top), 2005 (middle) and 2006 (bottom).

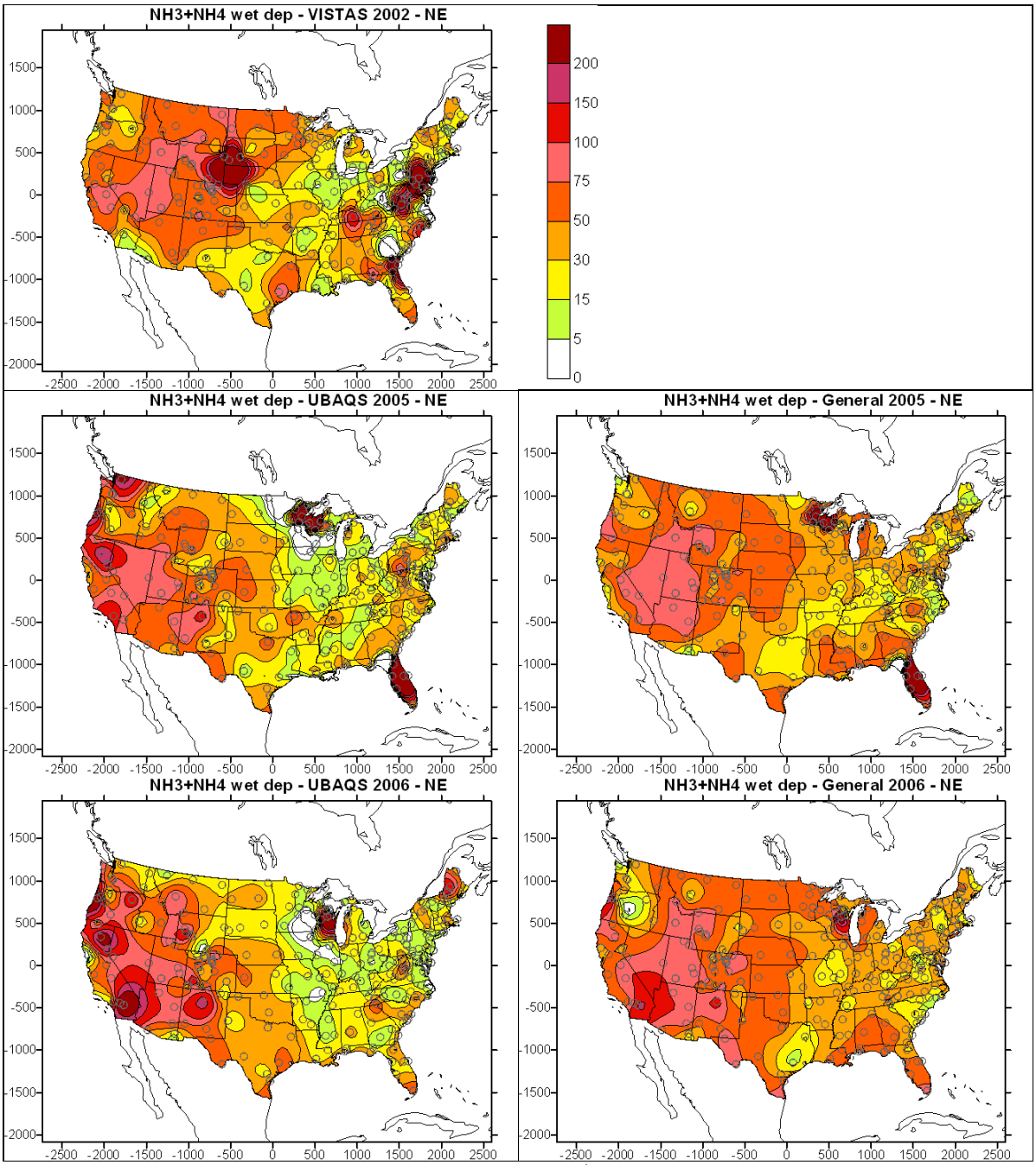

Figure D2-24. Normalized error (%) of modeled annual total NH_3 + NH_4^+ wet deposition using Kriging interpolation of values at the NADP monitoring sites (circle markers): CMAQ (left) and CAMx (right) model simulations for 2002 (top), 2005 (middle) and 2006 (bottom).

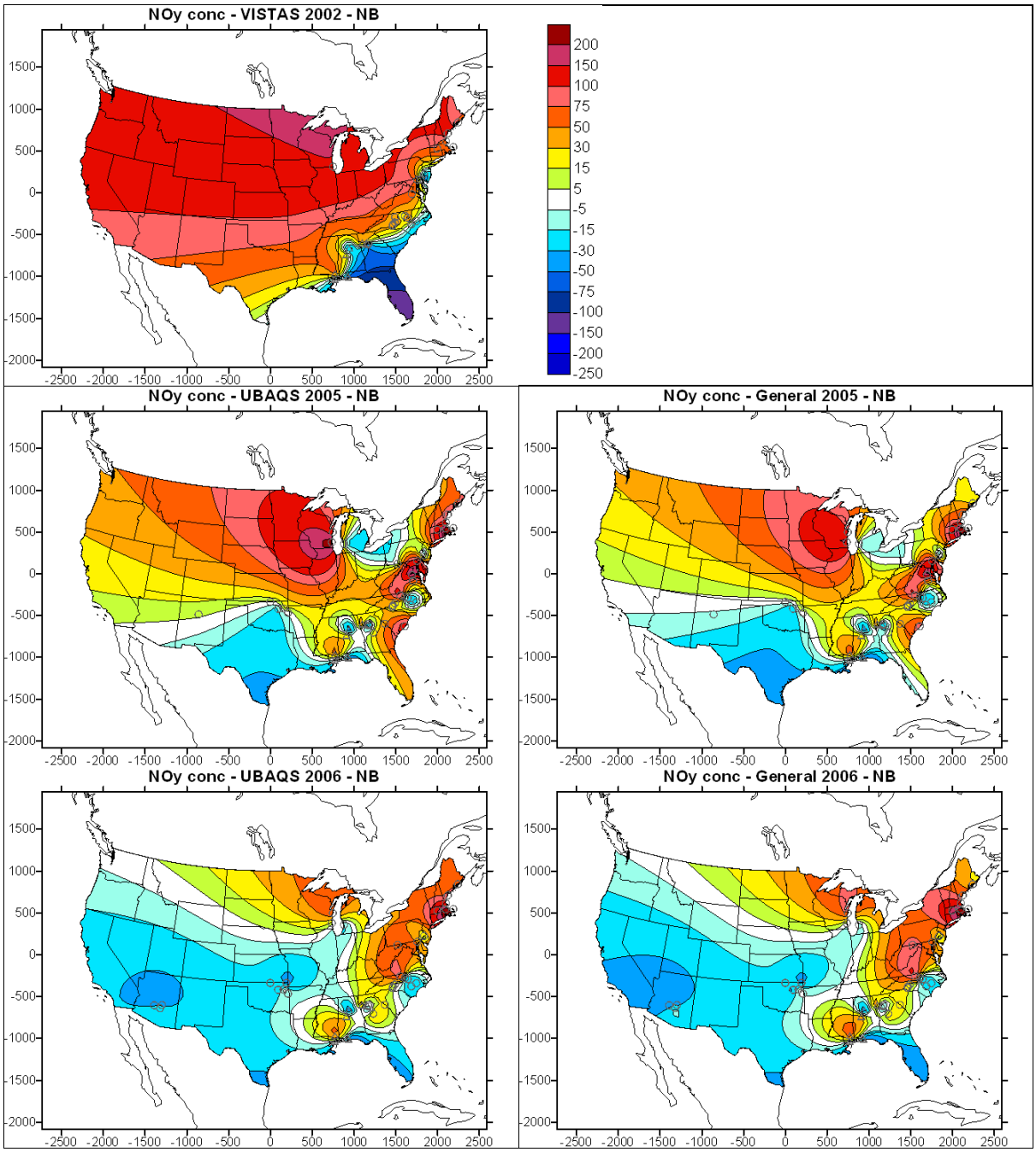

Figure D2-25. Normalized bias (%) of modeled annual average NOy concentrations using Kriging interpolation of values at the AQS (circle markers) and SEARCH (triangle markers) monitoring sites: CMAQ (left) and CAMx (right) model simulations for 2002 (top), 2005 (middle) and 2006 (bottom).

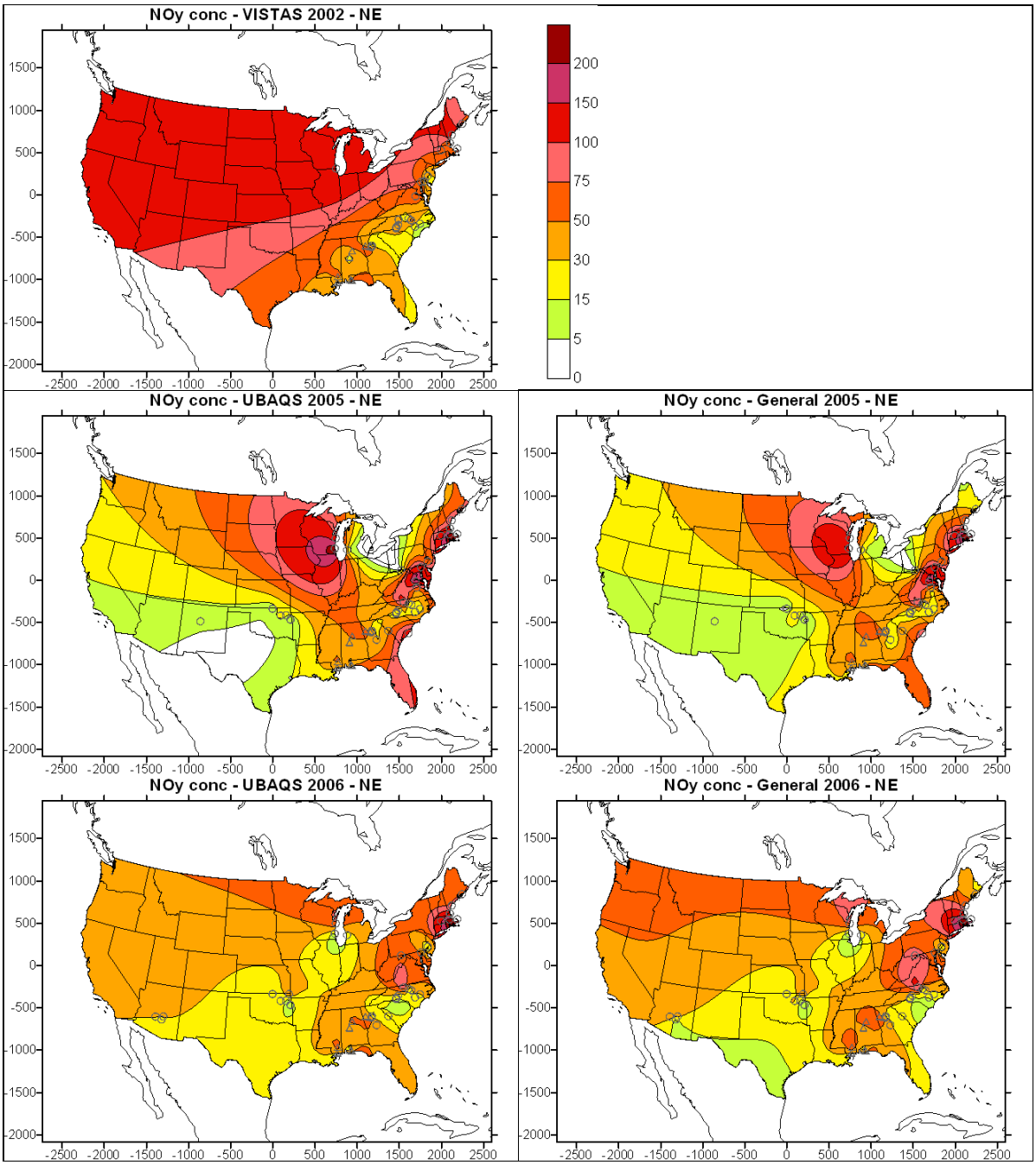

Figure D2-26. Normalized error (%) of modeled annual average NOy concentrations using Kriging interpolation of values at the AQS (circle markers) and SEARCH (triangle markers) monitoring sites: CMAQ (left) and CAMx (right) model simulations for 2002 (top), 2005 (middle) and 2006 (bottom).

Appendix D3: Spatial Maps of Mean Normalized Bias and Error for Concentrations and Deposition of SOx, NOy, and NHx with Native Temporal Resolutions of the Measurements

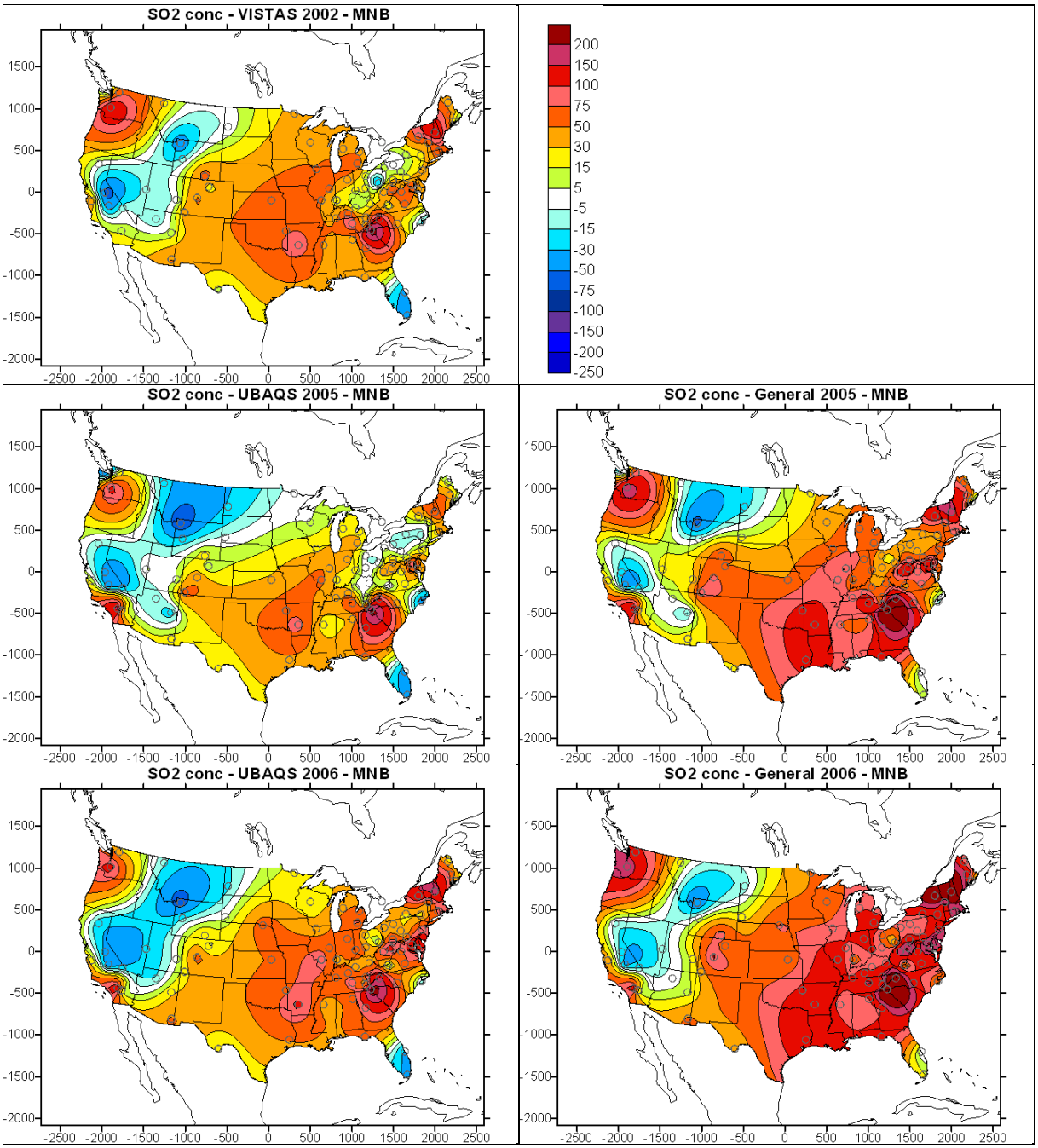

Figure D3-1. Mean normalized bias (%) of modeled weekly average SO_2 concentrations using Kriging interpolation of values at the CASTNET monitoring sites (circle markers): CMAQ (left) and CAMx (right) model simulations for 2002 (top), 2005 (middle) and 2006 (bottom).

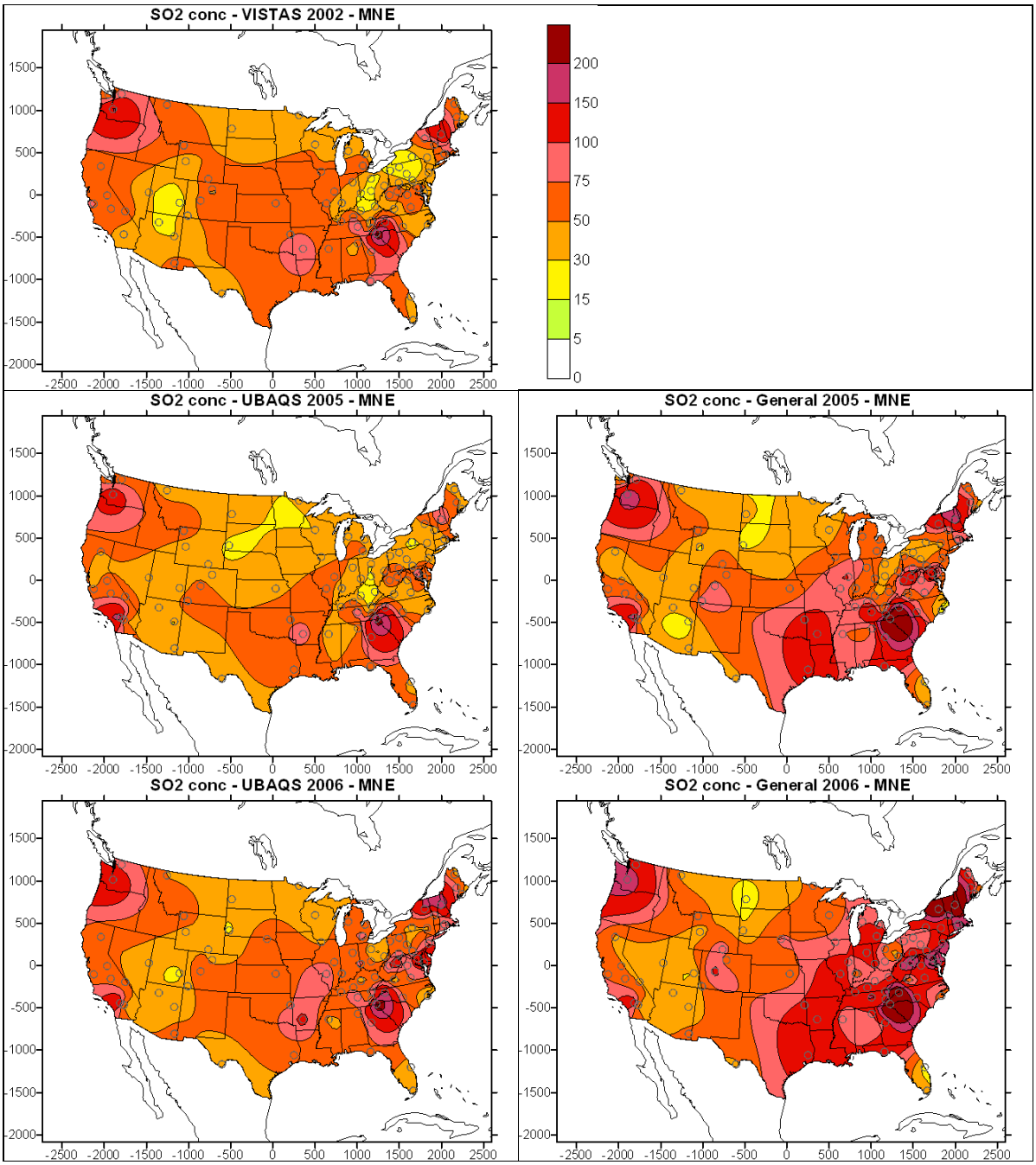

Figure D3-2. Mean normalized error (%) of modeled weekly average SO_2 concentrations using Kriging interpolation of values at the CASTNET monitoring sites (circle markers): CMAQ (left) and CAMx (right) model simulations for 2002 (top), 2005 (middle) and 2006 (bottom).

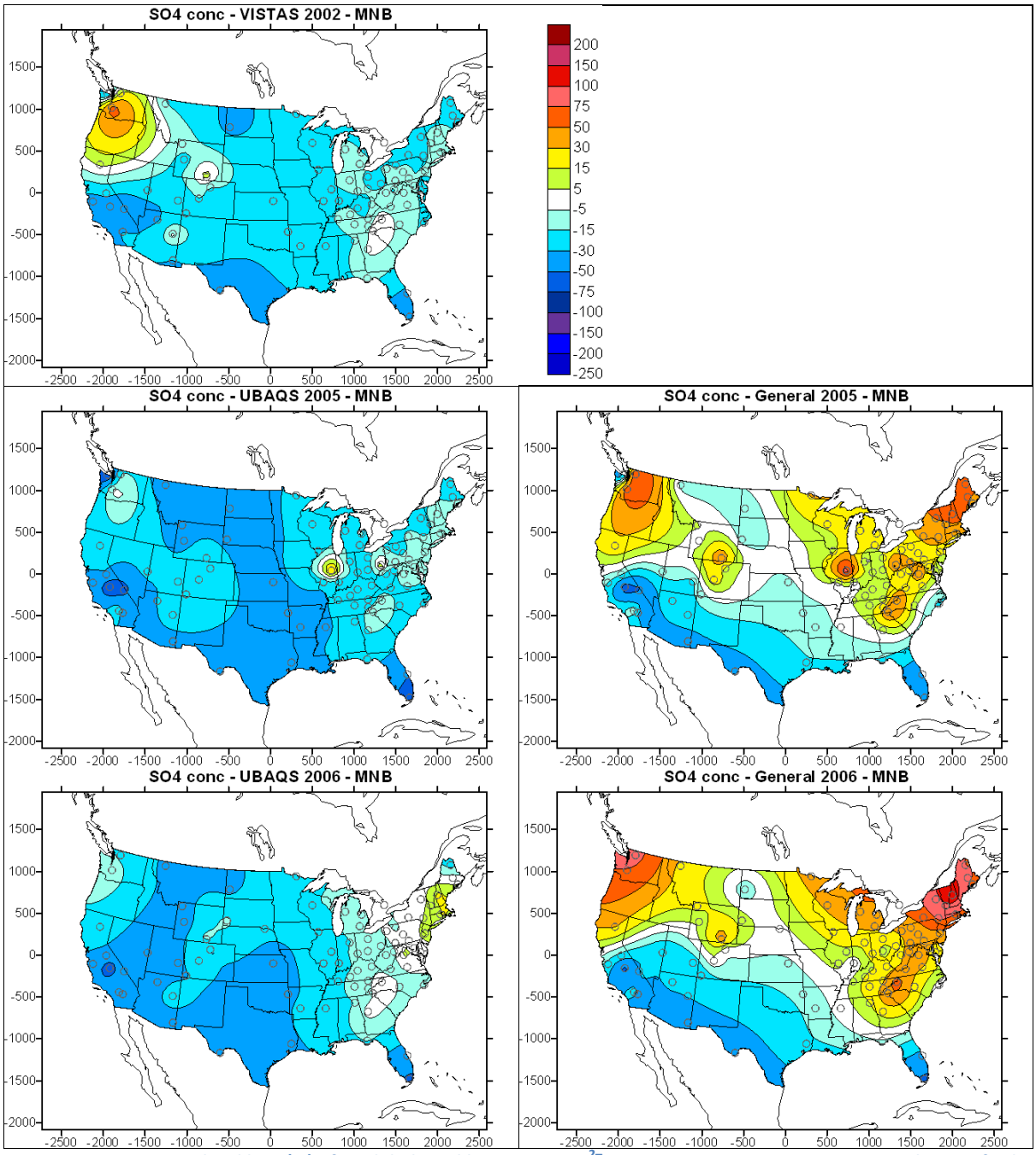

Figure D3-3. Mean normalized bias (%) of modeled weekly average SO_4^{2-} concentrations using Kriging interpolation of values at the CASTNET monitoring sites (circle markers): CMAQ (left) and CAMx (right) model simulations for 2002 (top), 2005 (middle) and 2006 (bottom).

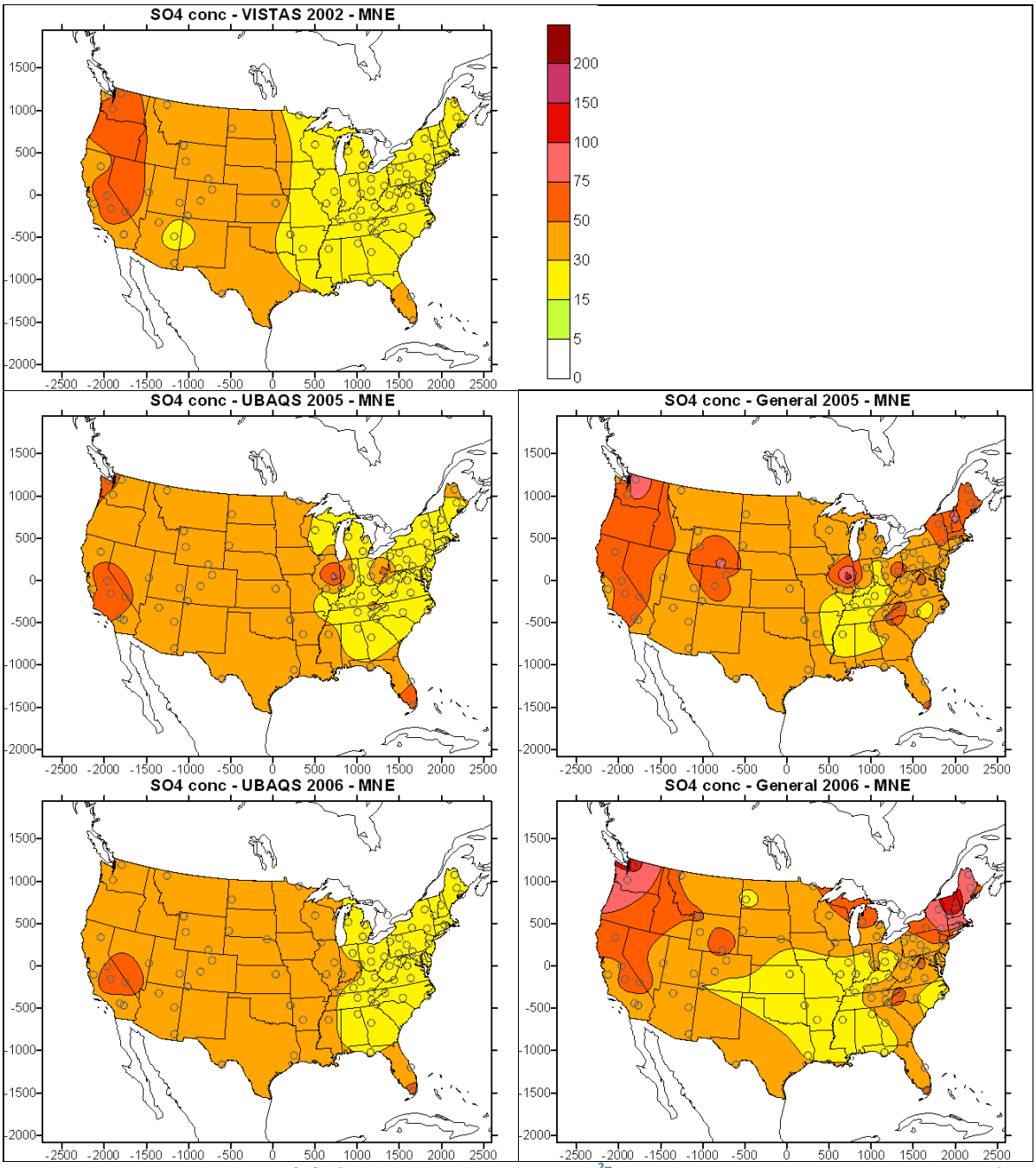

Figure D3-4. Mean normalized error (%) of modeled weekly average SO_4^{2-} concentrations using Kriging interpolation of values at the CASTNET monitoring sites (circle markers): CMAQ (left) and CAMx (right) model simulations for 2002 (top), 2005 (middle) and 2006 (bottom).

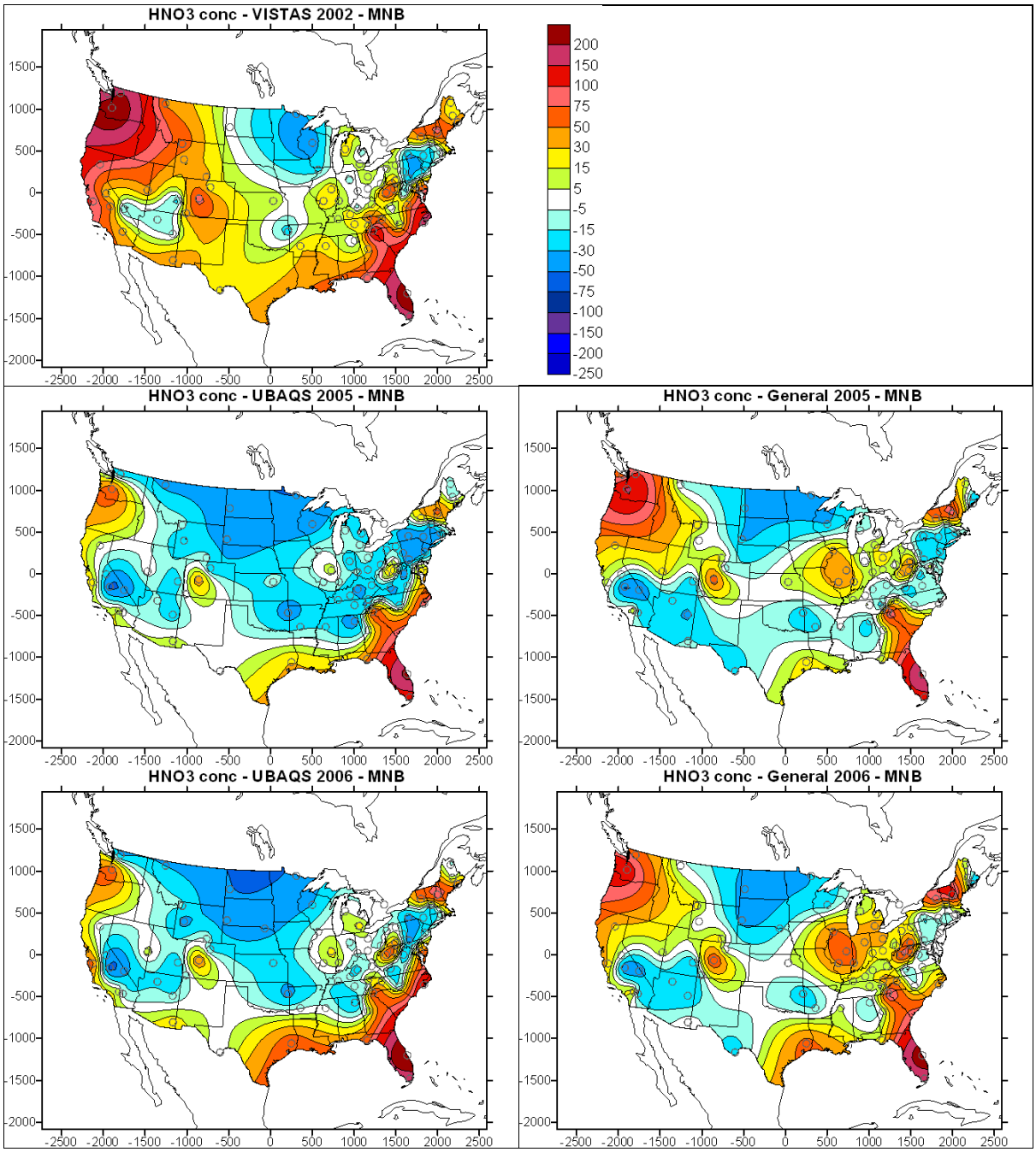

Figure D3-5. Mean normalized bias (%) of modeled weekly average HNO_3 concentrations using Kriging interpolation of values at the CASTNET monitoring sites (circle markers): CMAQ (left) and CAMx (right) model simulations for 2002 (top), 2005 (middle) and 2006 (bottom).

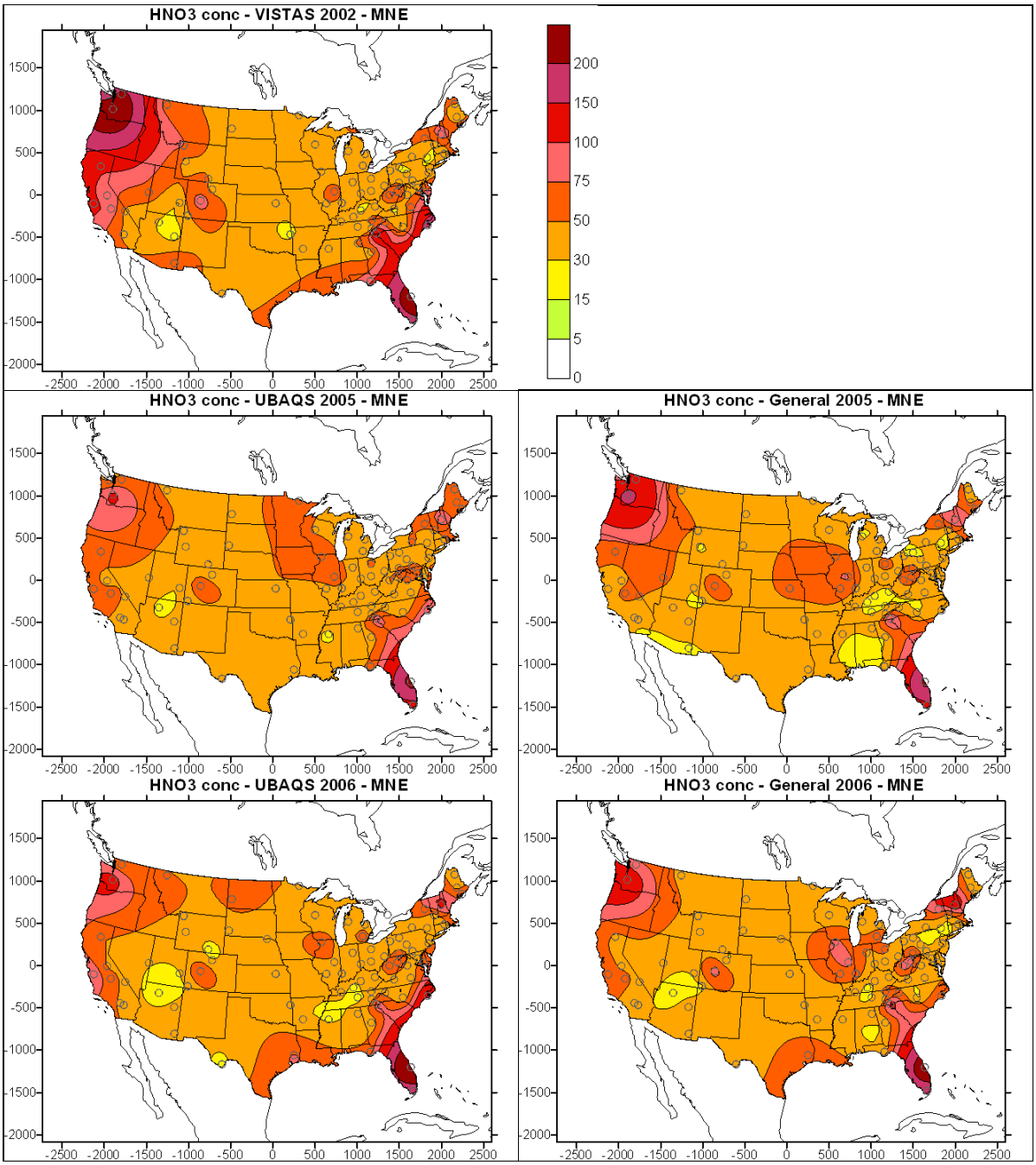

Figure D3-6. Mean normalized error (%) of modeled weekly average HNO_3 concentrations using Kriging interpolation of values at the CASTNET monitoring sites (circle markers): CMAQ (left) and CAMx (right) model simulations for 2002 (top), 2005 (middle) and 2006 (bottom).

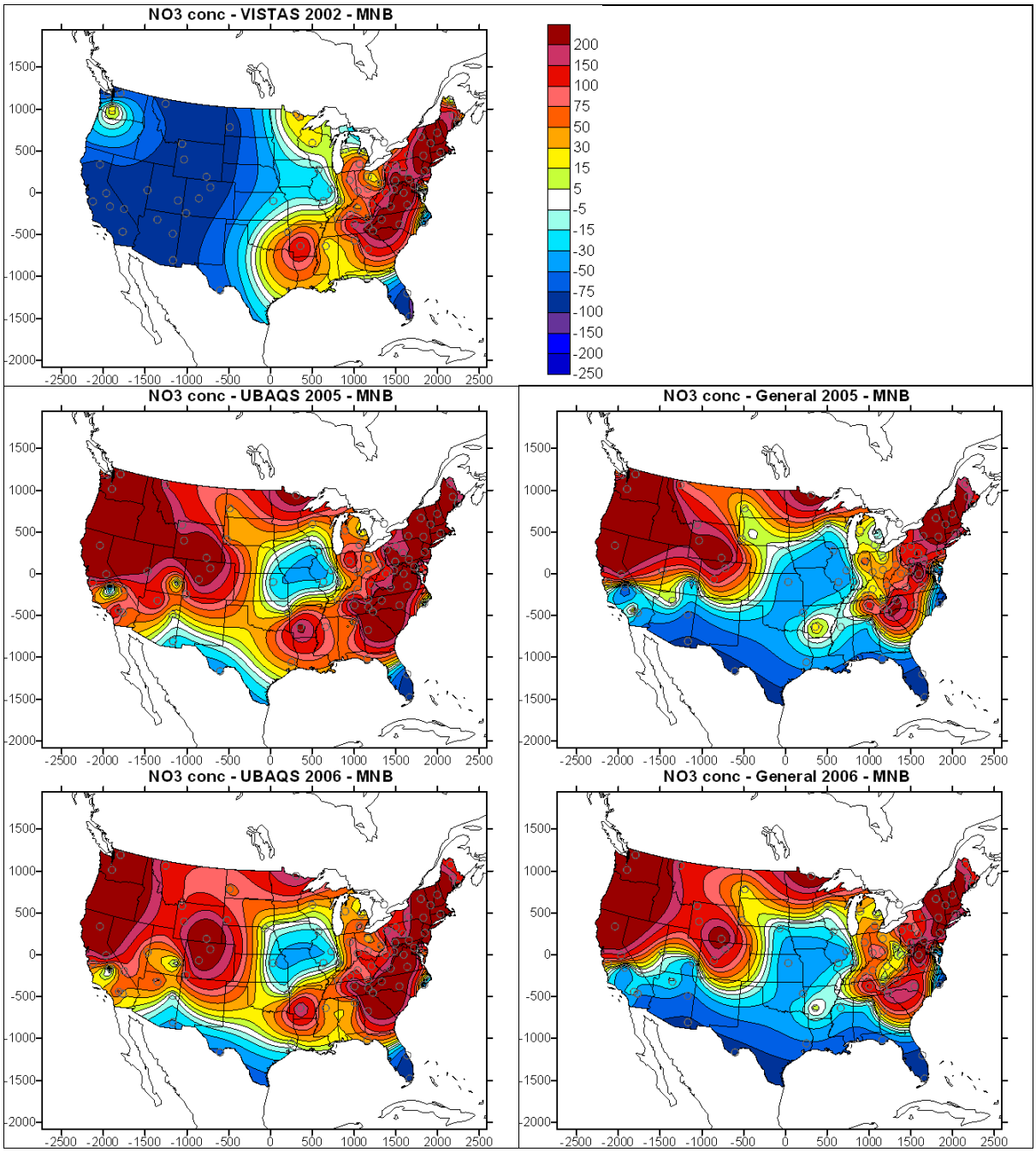

Figure D3-7. Mean normalized bias (%) of modeled weekly average NO_3^- concentrations using Kriging interpolation of values at the CASTNET monitoring sites (circle markers): CMAQ (left) and CAMx (right) model simulations for 2002 (top), 2005 (middle) and 2006 (bottom).

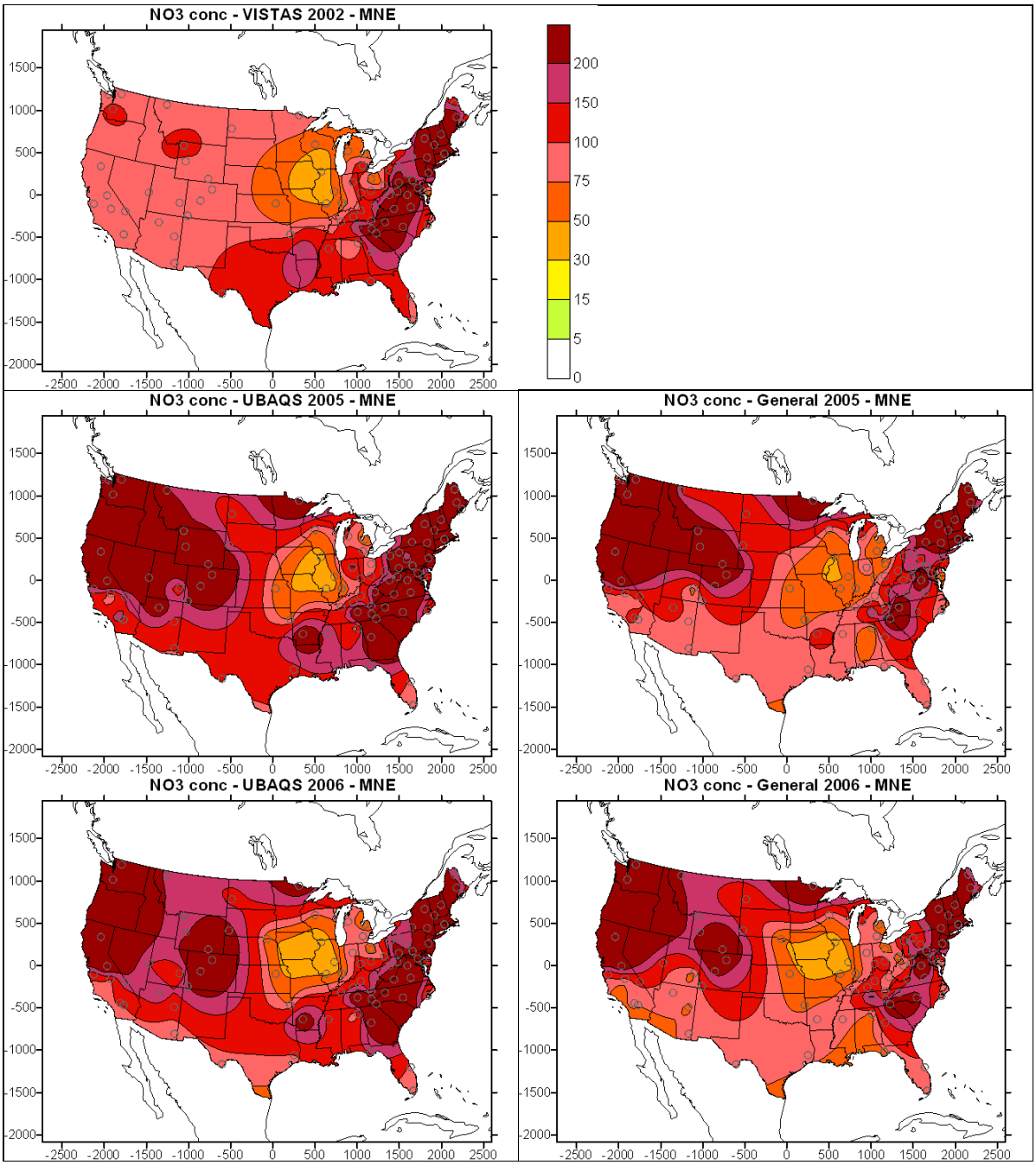

Figure D3-8. Mean normalized error (%) of modeled weekly average NO_3^- concentrations using Kriging interpolation of values at the CASTNET monitoring sites (circle markers): CMAQ (left) and CAMx (right) model simulations for 2002 (top), 2005 (middle) and 2006 (bottom).

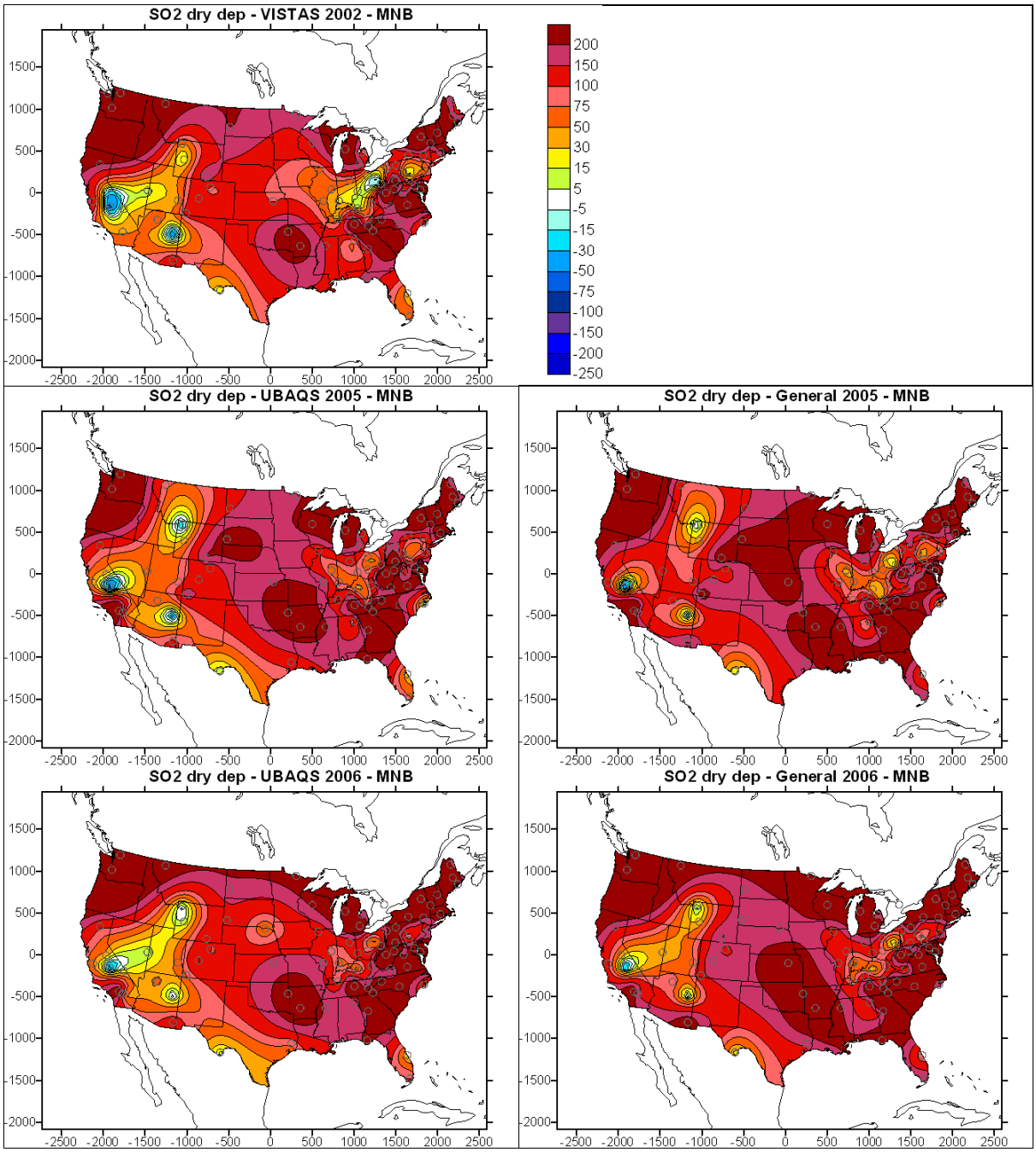

Figure D3-9. Mean normalized bias (%) of modeled weekly total SO_2 dry deposition using Kriging interpolation of values at the CASTNET monitoring sites (circle markers): CMAQ (left) and CAMx (right) model simulations for 2002 (top), 2005 (middle) and 2006 (bottom).

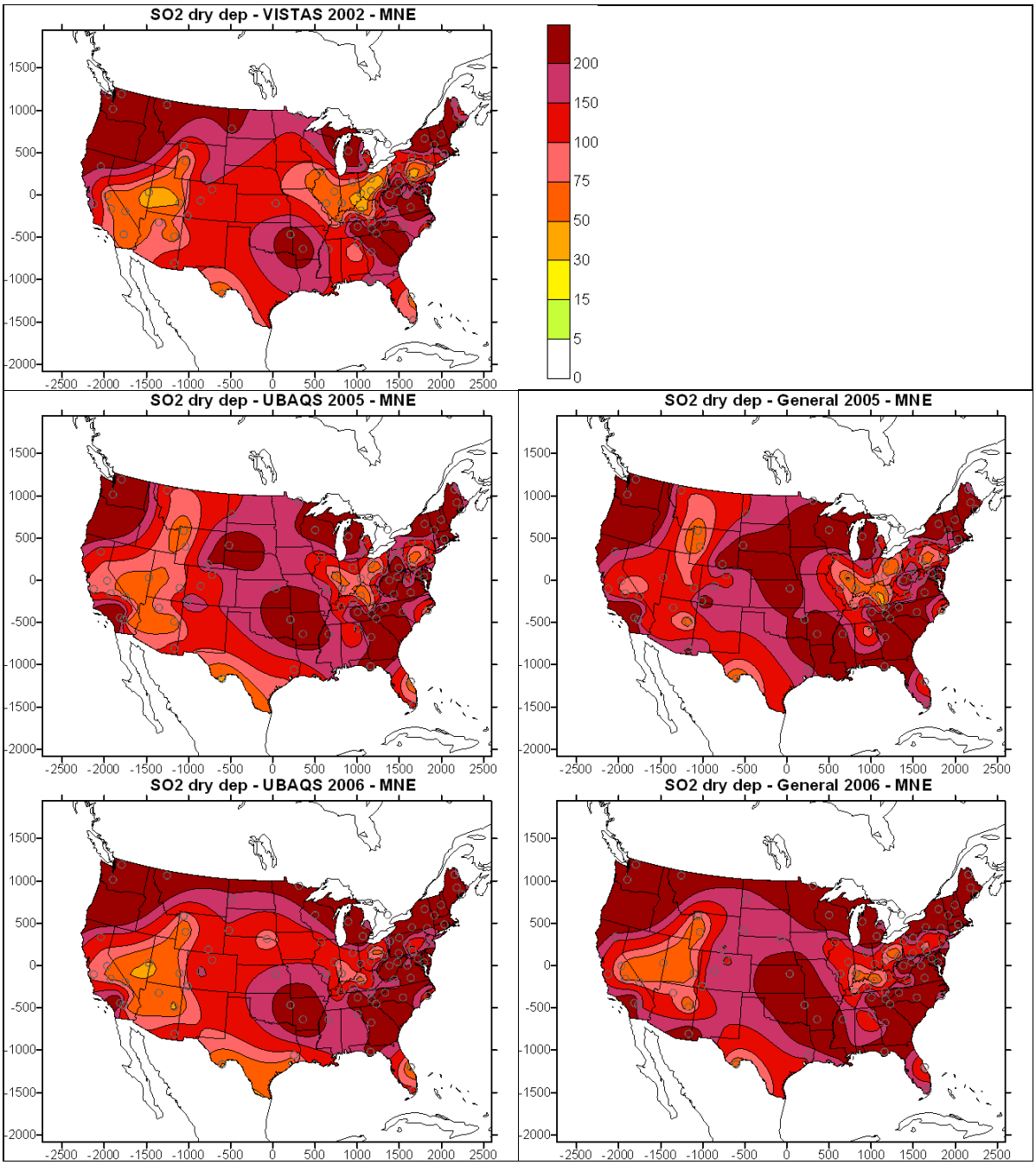

Figure D3-10. Mean normalized error (%) of modeled weekly total SO_2 dry deposition using Kriging interpolation of values at the CASTNET monitoring sites (circle markers): CMAQ (left) and CAMx (right) model simulations for 2002 (top), 2005 (middle) and 2006 (bottom).

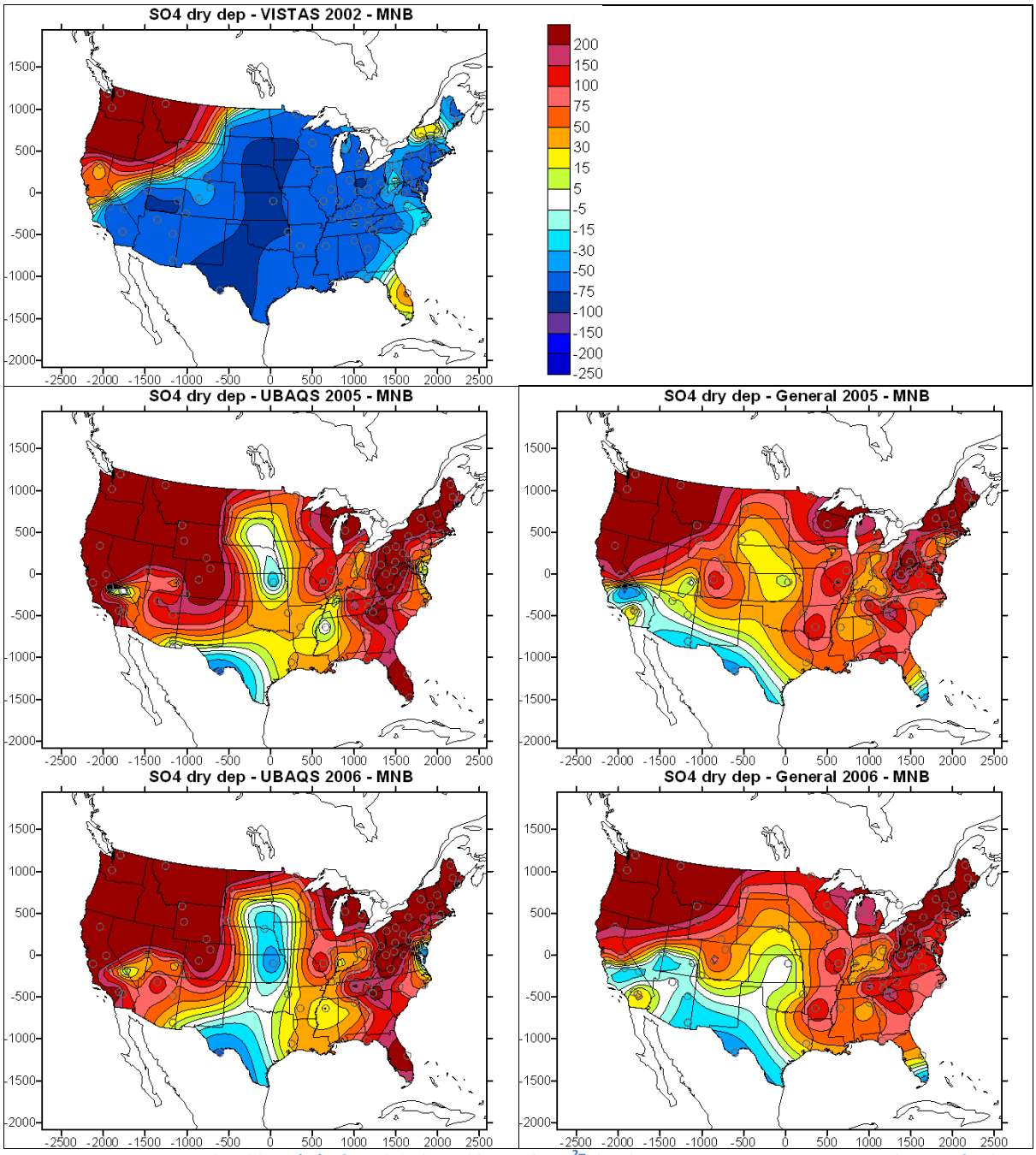

Figure D3-11. Mean normalized bias (%) of modeled weekly total SO_4^{2-} dry deposition using Kriging interpolation of values at the CASTNET monitoring sites (circle markers): CMAQ (left) and CAMx (right) model simulations for 2002 (top), 2005 (middle) and 2006 (bottom).

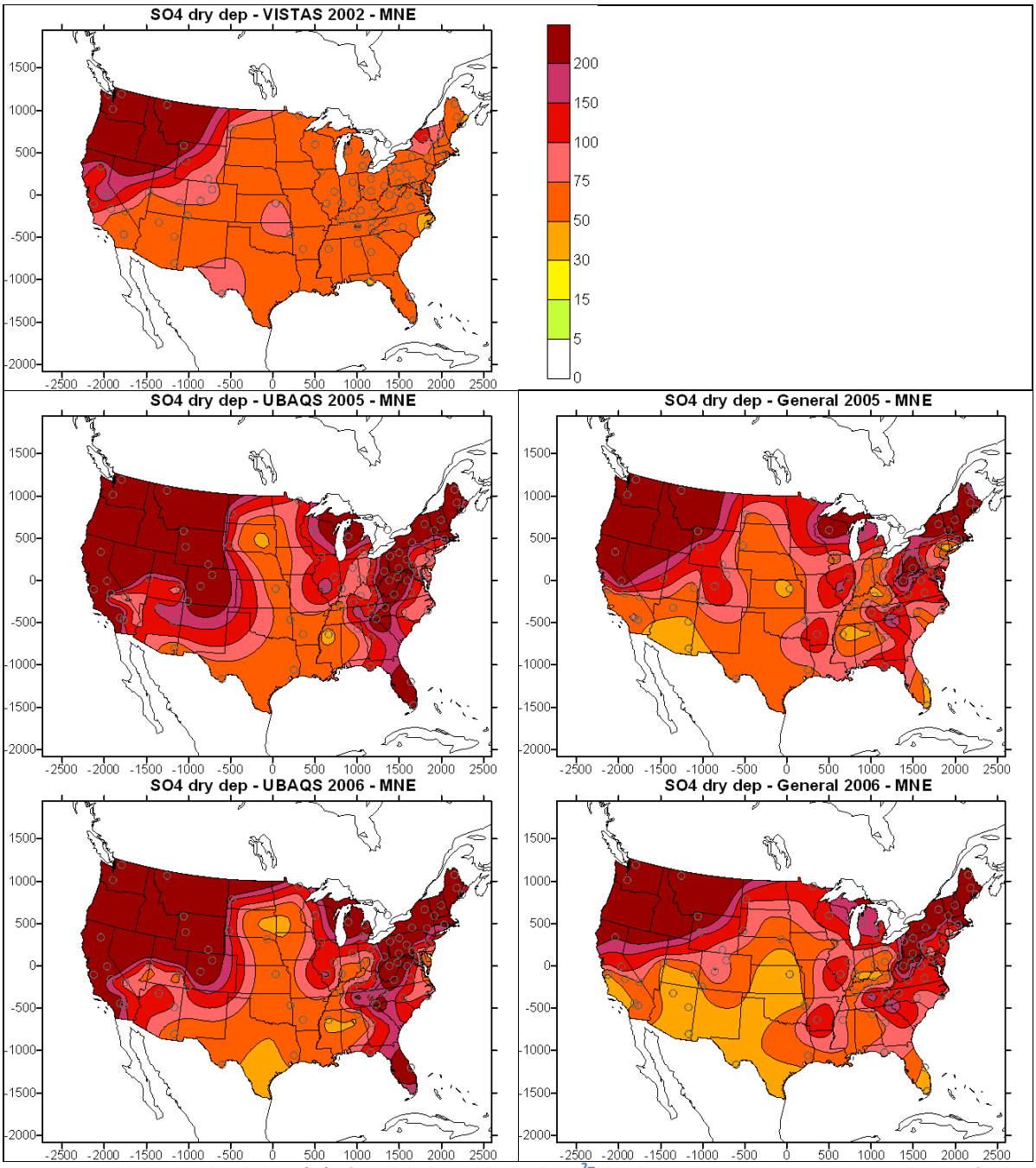

Figure D3-12. Mean normalized error (%) of modeled weekly total SO_4^{2-} dry deposition using Kriging interpolation of values at the CASTNET monitoring sites (circle markers): CMAQ (left) and CAMx (right) model simulations for 2002 (top), 2005 (middle) and 2006 (bottom).

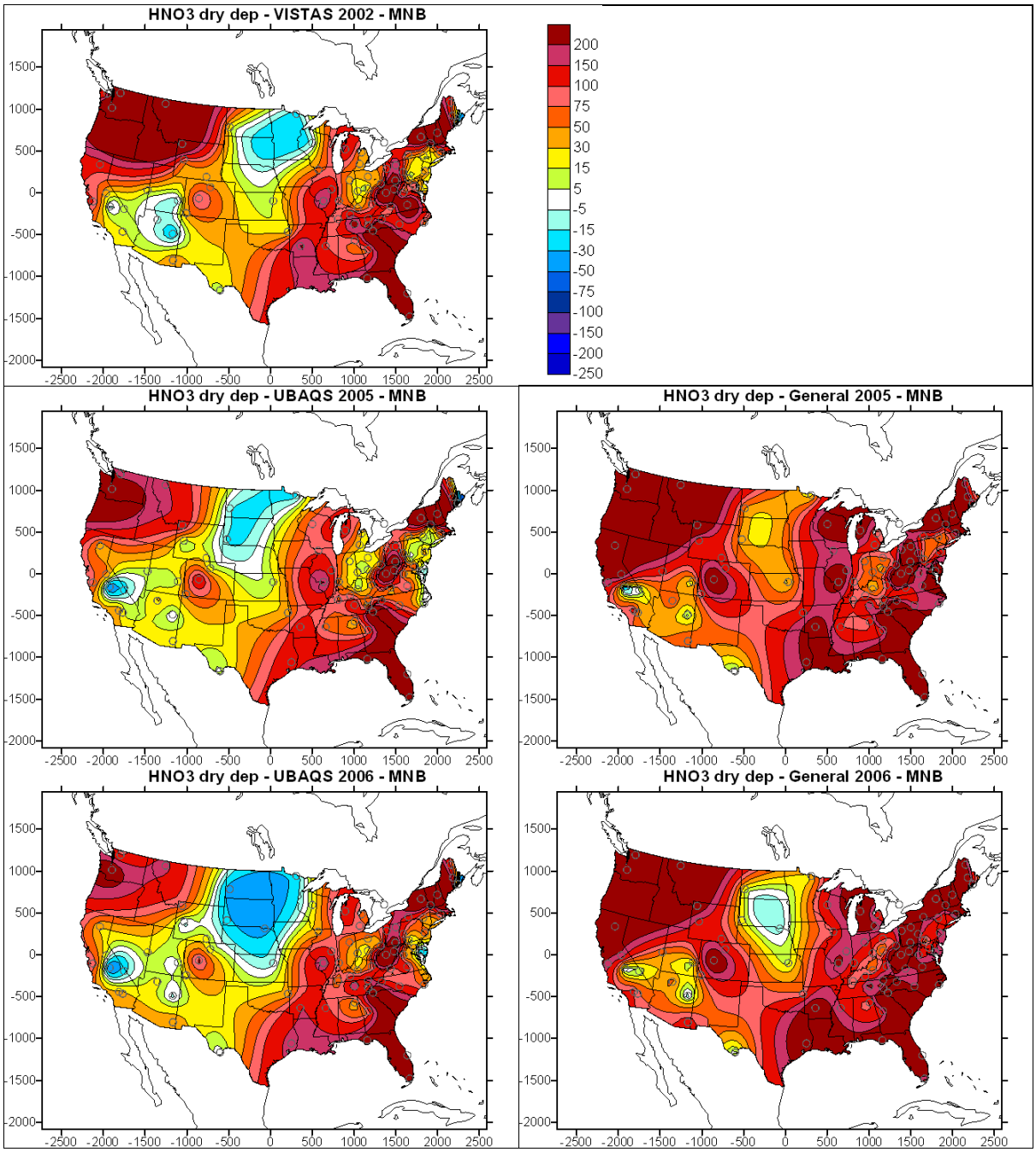

Figure D3-13. Mean normalized bias (%) of modeled weekly total HNO_3 dry deposition using Kriging interpolation of values at the CASTNET monitoring sites (circle markers): CMAQ (left) and CAMx (right) model simulations for 2002 (top), 2005 (middle) and 2006 (bottom).

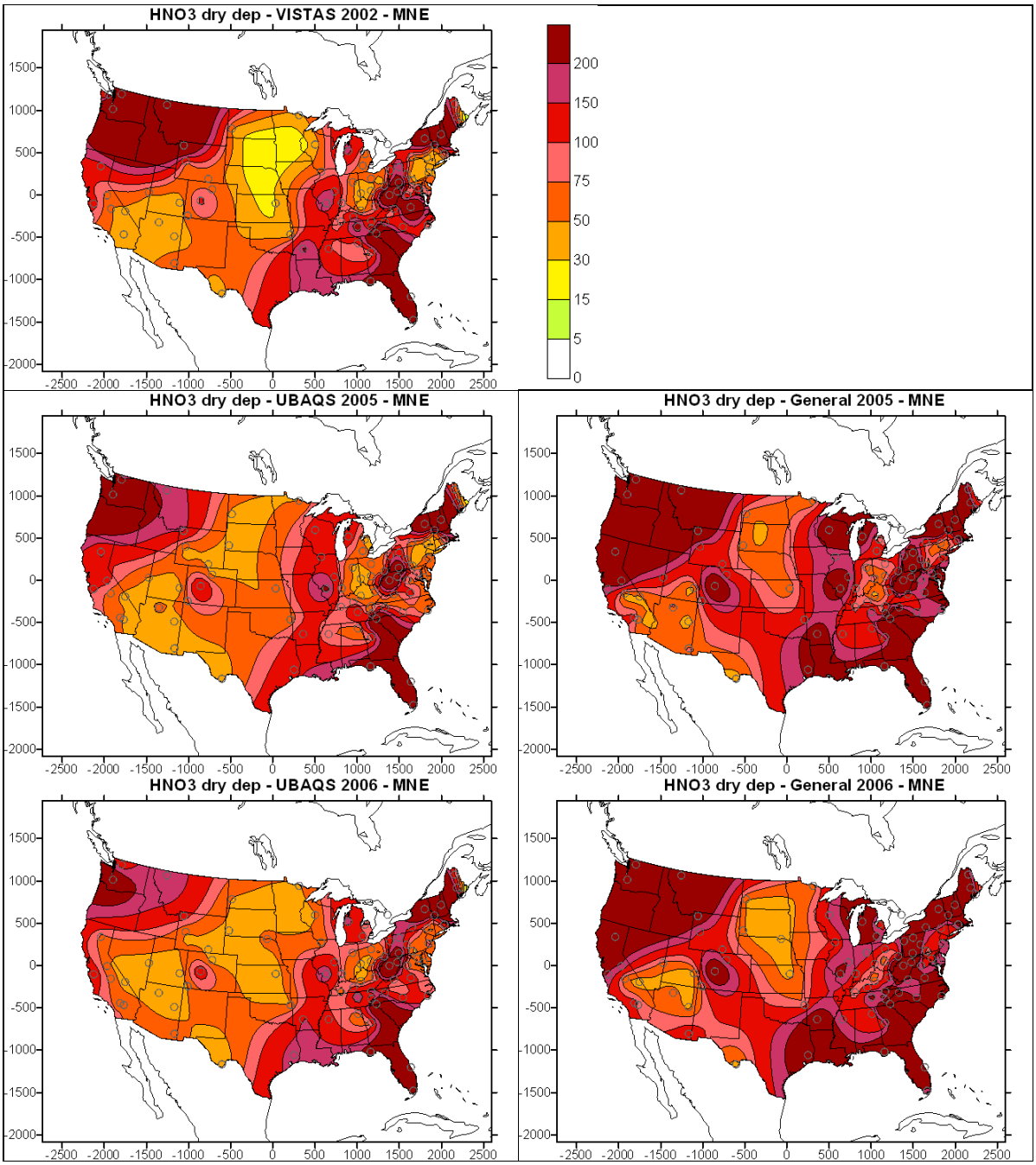

Figure D3-14. Mean normalized error (%) of modeled weekly total HNO_3 dry deposition using Kriging interpolation of values at the CASTNET monitoring sites (circle markers): CMAQ (left) and CAMx (right) model simulations for 2002 (top), 2005 (middle) and 2006 (bottom).

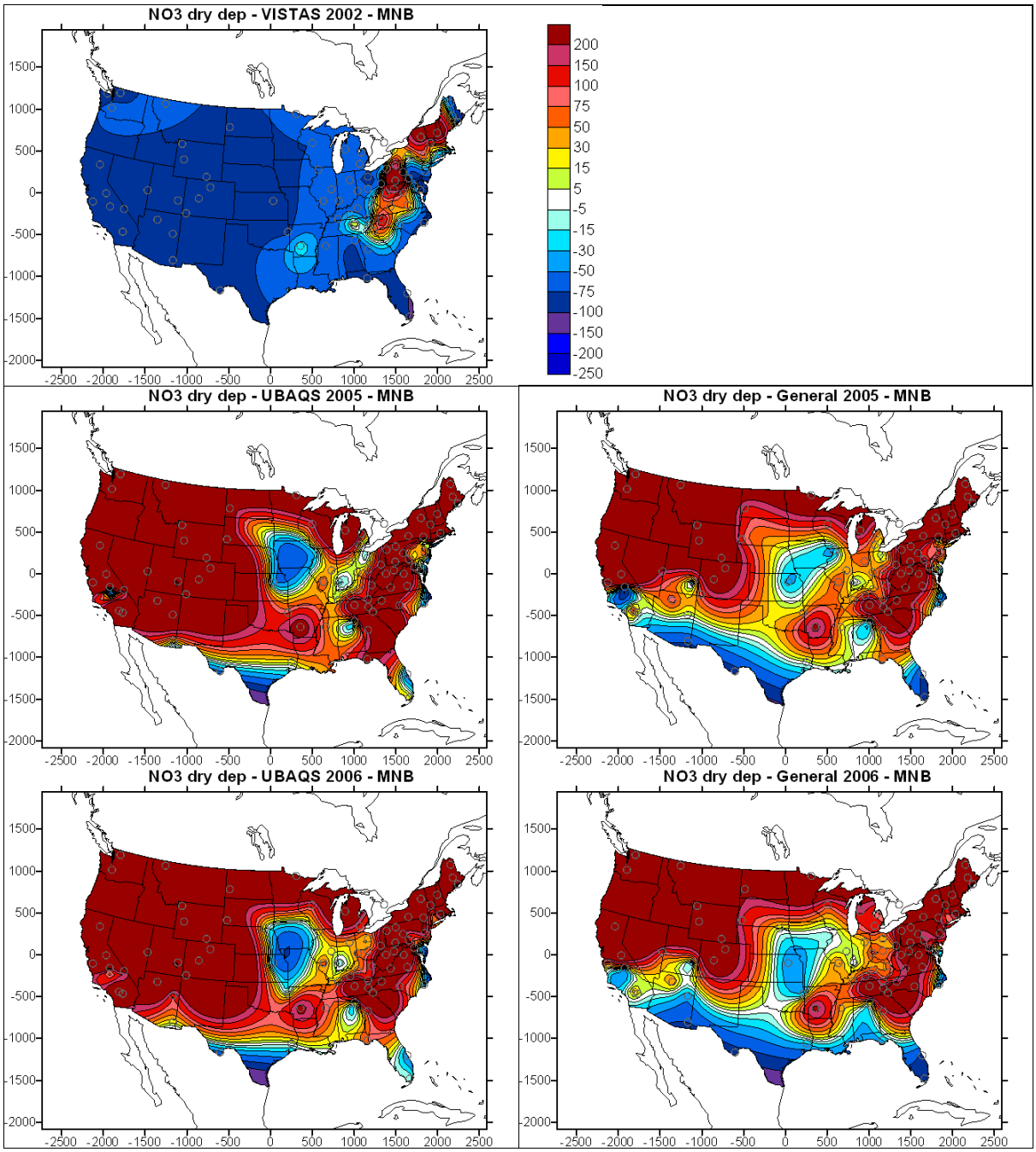

Figure D3-15. Mean normalized bias (%) of modeled weekly total NO_3^- dry deposition using Kriging interpolation of values at the CASTNET monitoring sites (circle markers): CMAQ (left) and CAMx (right) model simulations for 2002 (top), 2005 (middle) and 2006 (bottom).

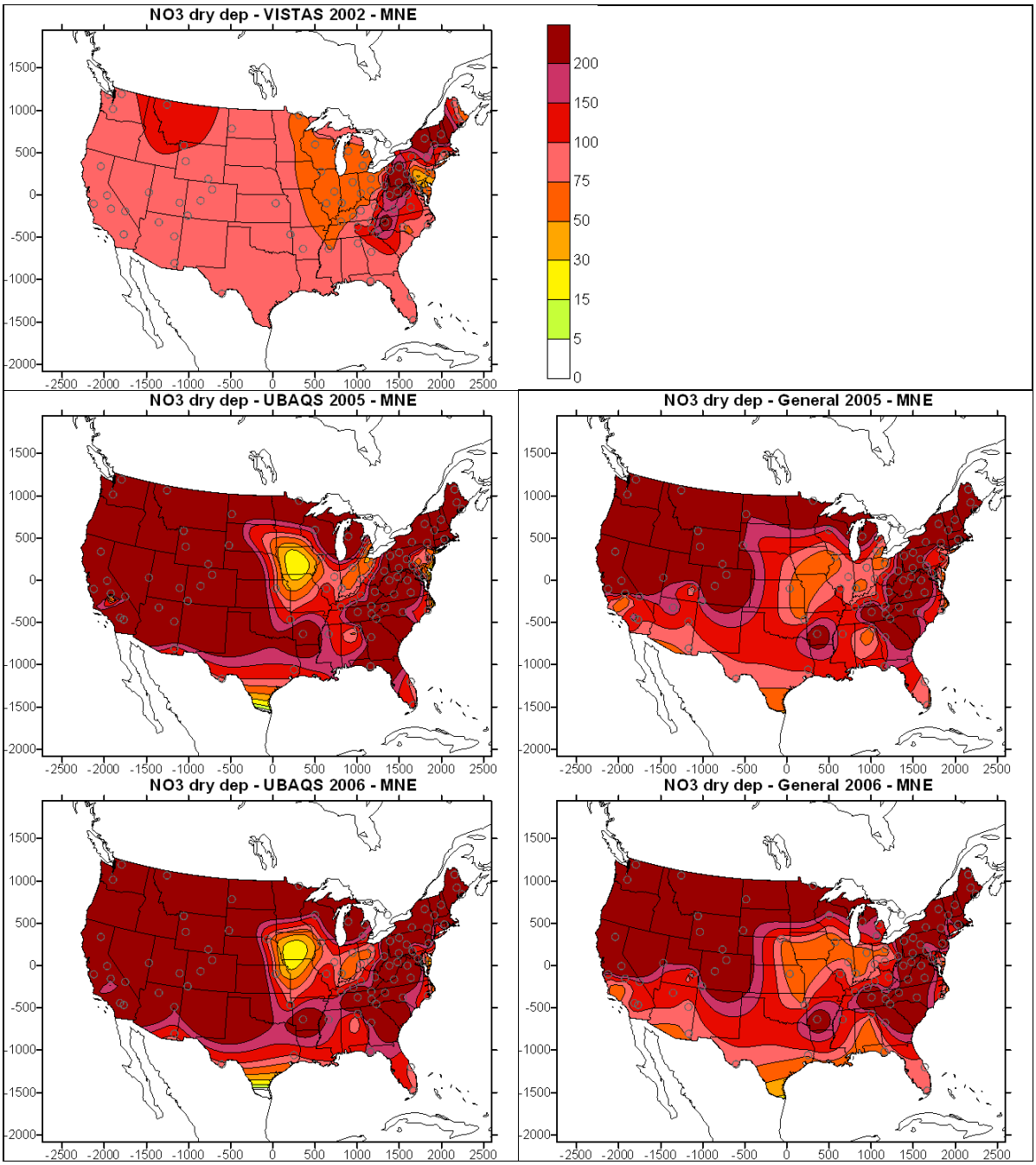

Figure D3-16. Mean normalized error (%) of modeled weekly total NO_3^- dry deposition using Kriging interpolation of values at the CASTNET monitoring sites (circle markers): CMAQ (left) and CAMx (right) model simulations for 2002 (top), 2005 (middle) and 2006 (bottom).

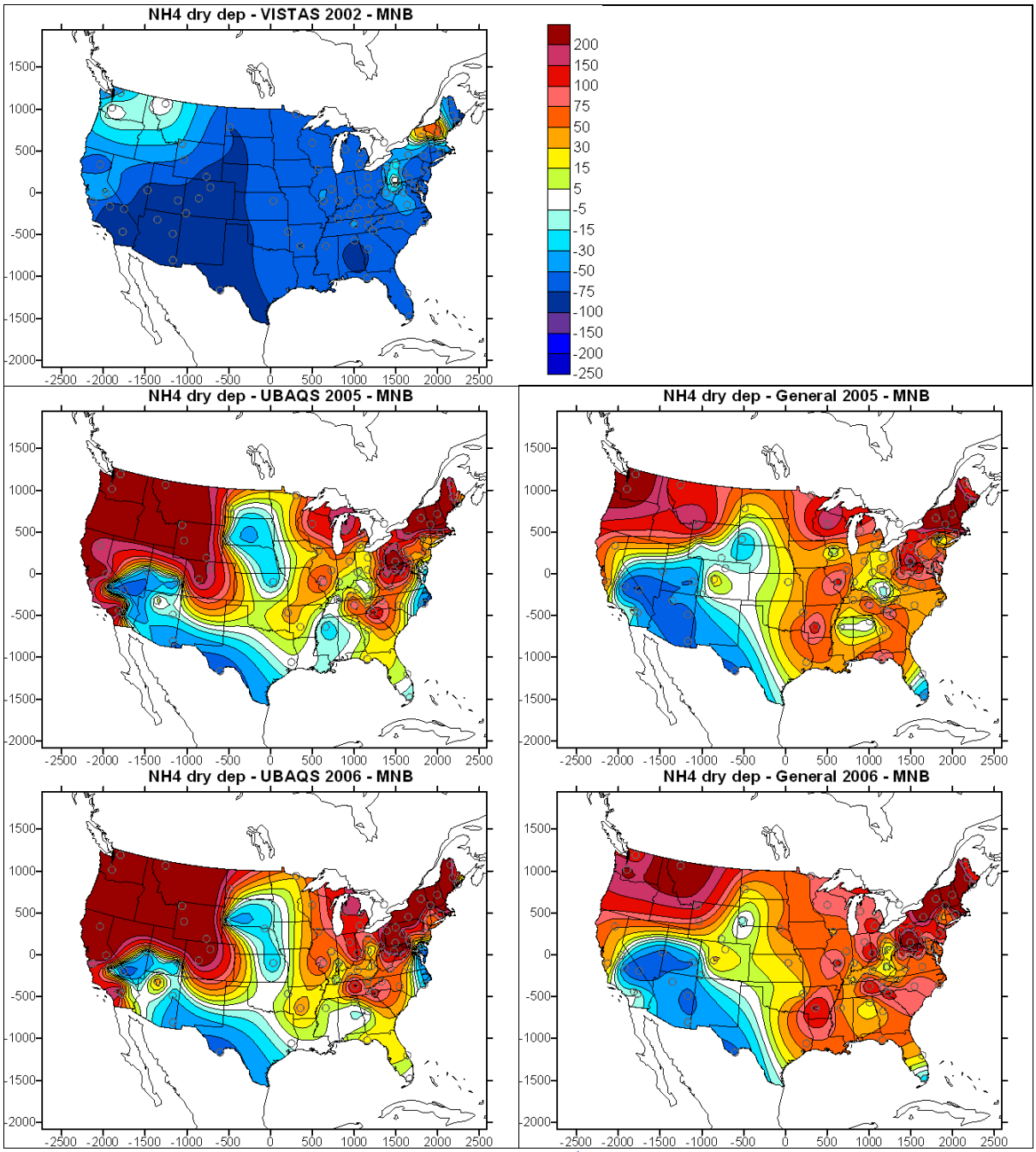

Figure D3-17. Mean normalized bias (%) of modeled weekly total NH_4^+ dry deposition using Kriging interpolation of values at the CASTNET monitoring sites (circle markers): CMAQ (left) and CAMx (right) model simulations for 2002 (top), 2005 (middle) and 2006 (bottom).

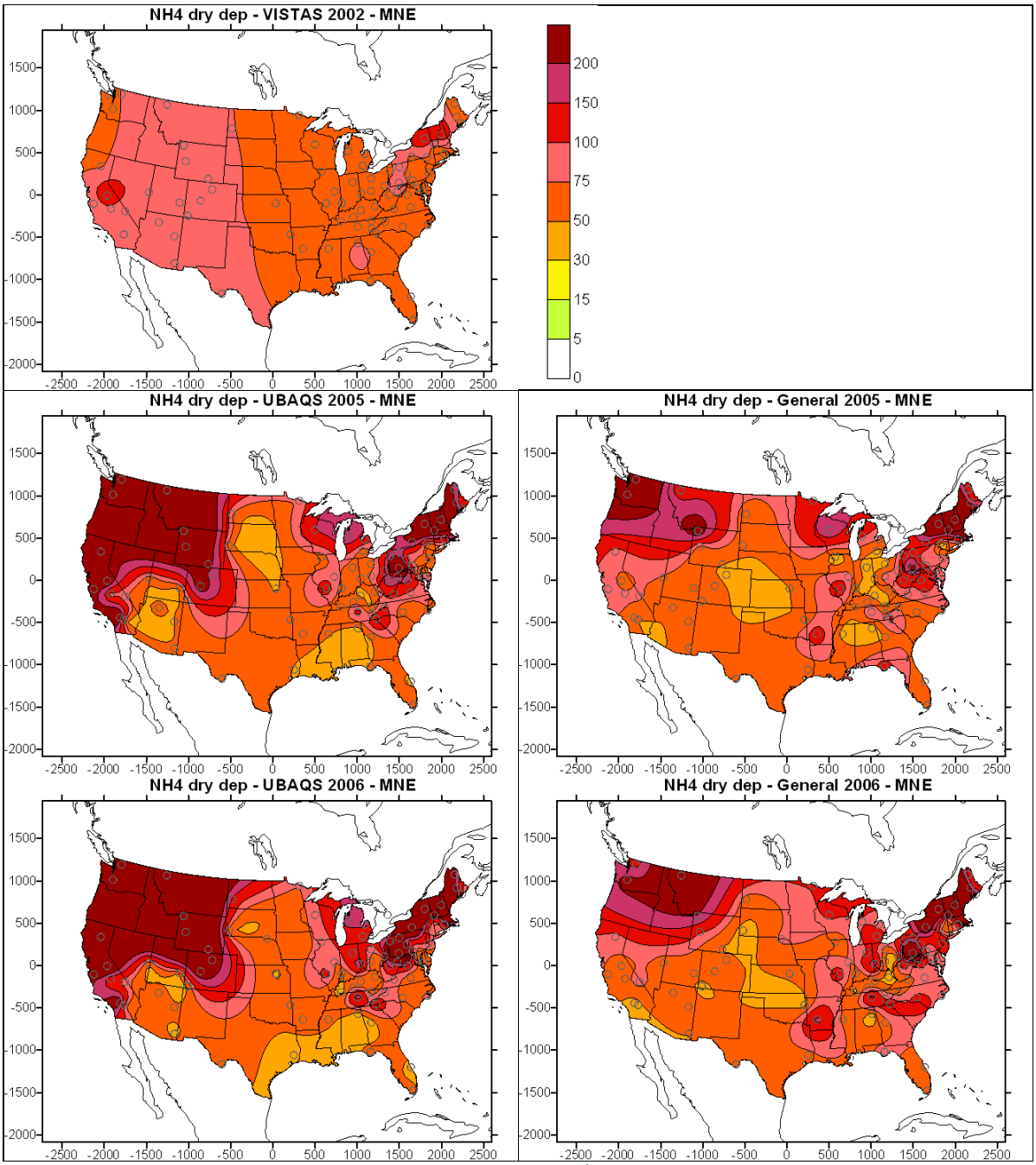

Figure D3-18. Mean normalized error (%) of modeled weekly total NH_4^+ dry deposition using Kriging interpolation of values at the CASTNET monitoring sites (circle markers): CMAQ (left) and CAMx (right) model simulations for 2002 (top), 2005 (middle) and 2006 (bottom).

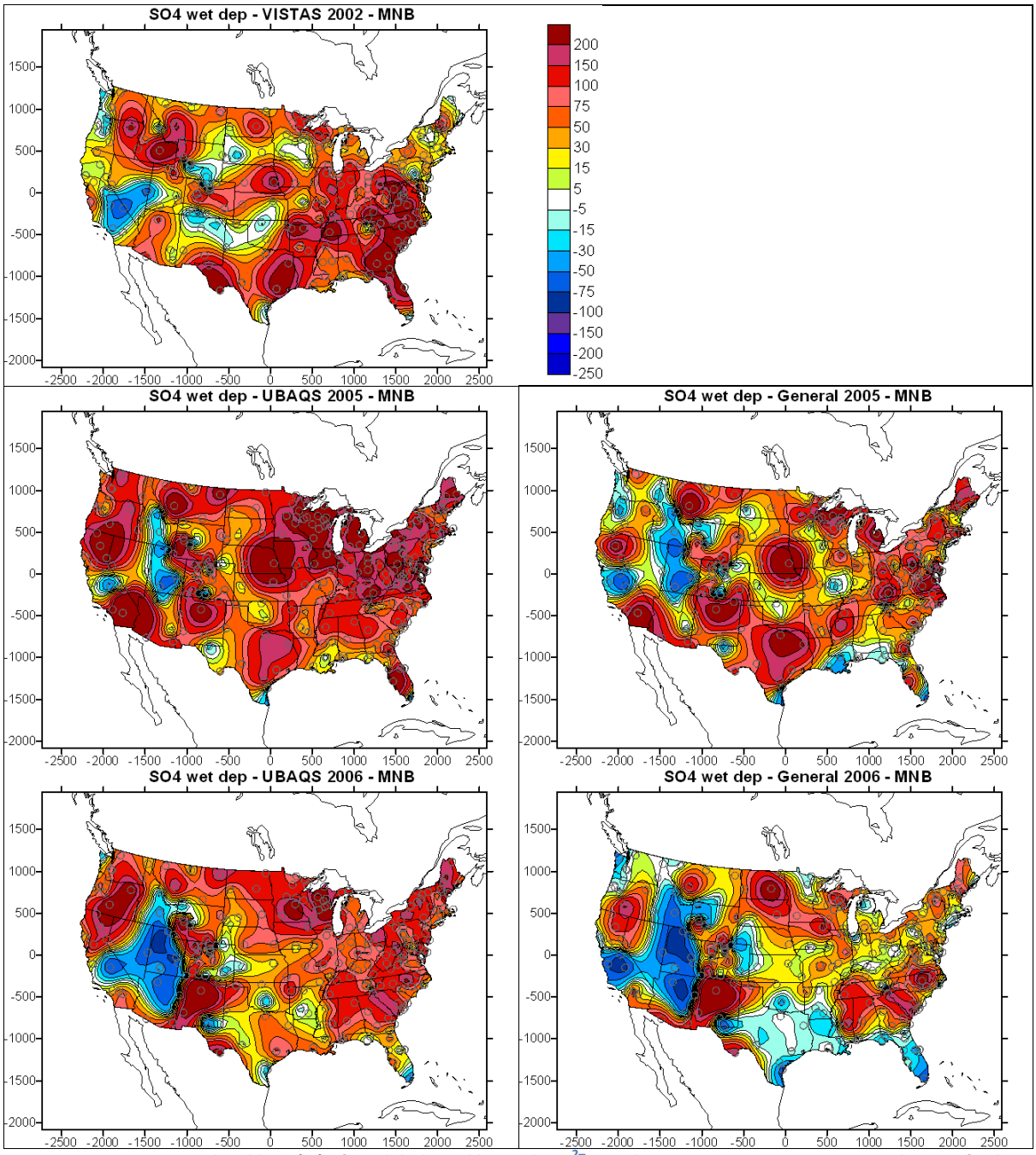

Figure D3-19. Mean normalized bias (%) of modeled weekly total SO_4^{2-} wet deposition using Kriging interpolation of values at the NADP monitoring sites (circle markers): CMAQ (left) and CAMx (right) model simulations for 2002 (top), 2005 (middle) and 2006 (bottom).

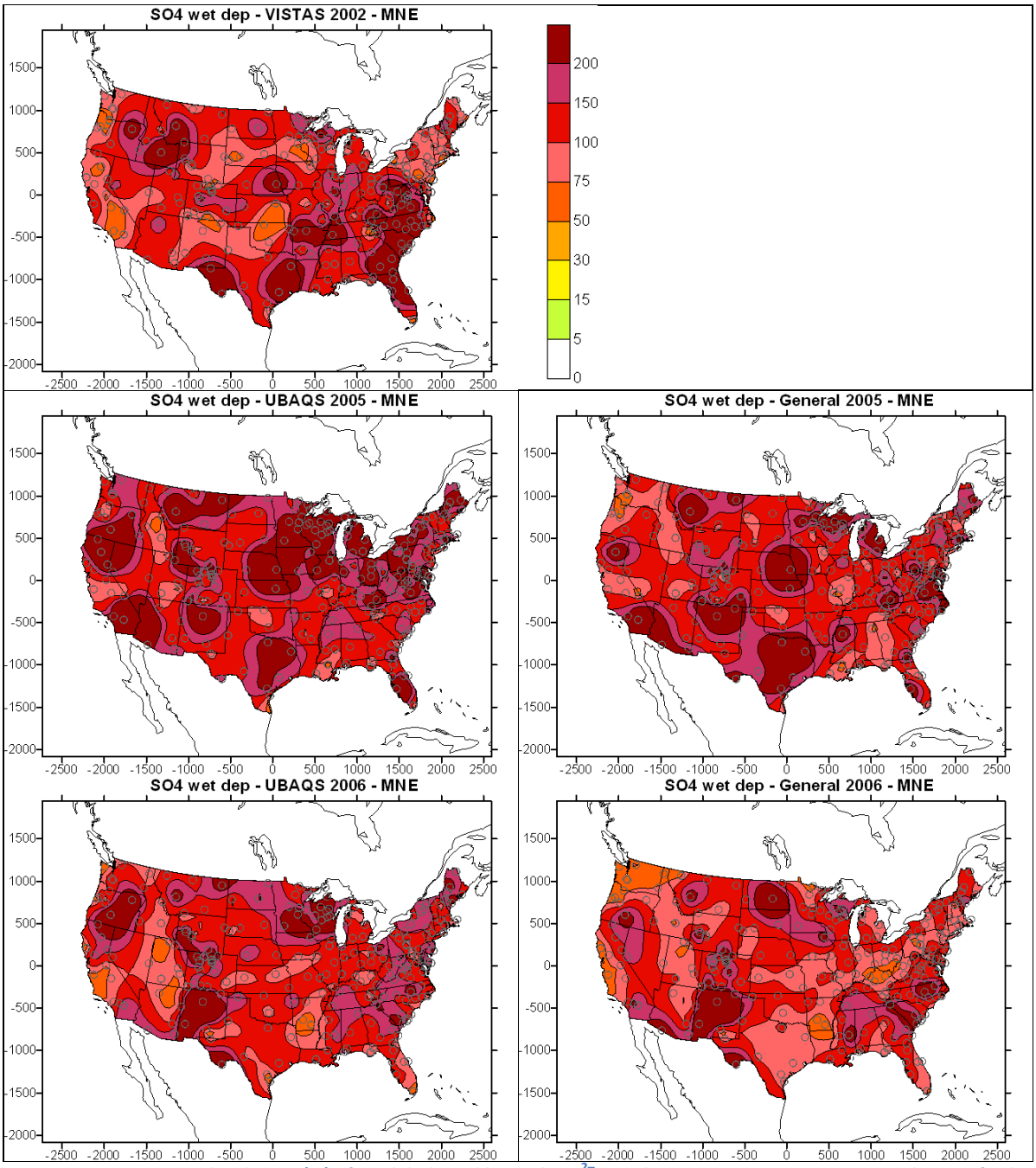

Figure D3-20. Mean normalized error (%) of modeled weekly total SO_4^{2-} wet deposition using Kriging interpolation of values at the NADP monitoring sites (circle markers): CMAQ (left) and CAMx (right) model simulations for 2002 (top), 2005 (middle) and 2006 (bottom).

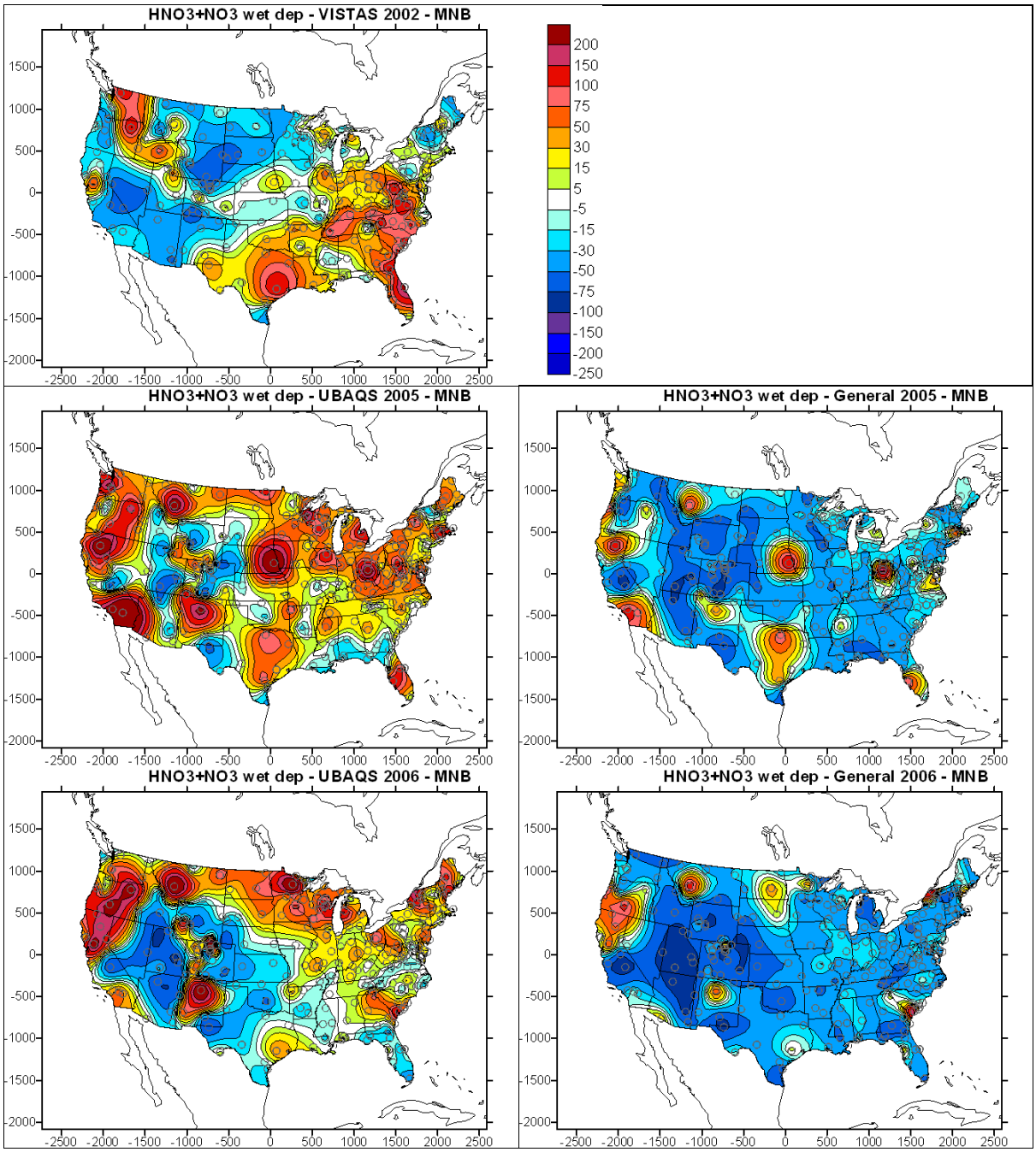

Figure D3-21. Mean normalized bias (%) of modeled weekly total $HNO_3 + NO_3^-$ wet deposition using Kriging interpolation of values at the NADP monitoring sites (circle markers): CMAQ (left) and CAMx (right) model simulations for 2002 (top), 2005 (middle) and 2006 (bottom).

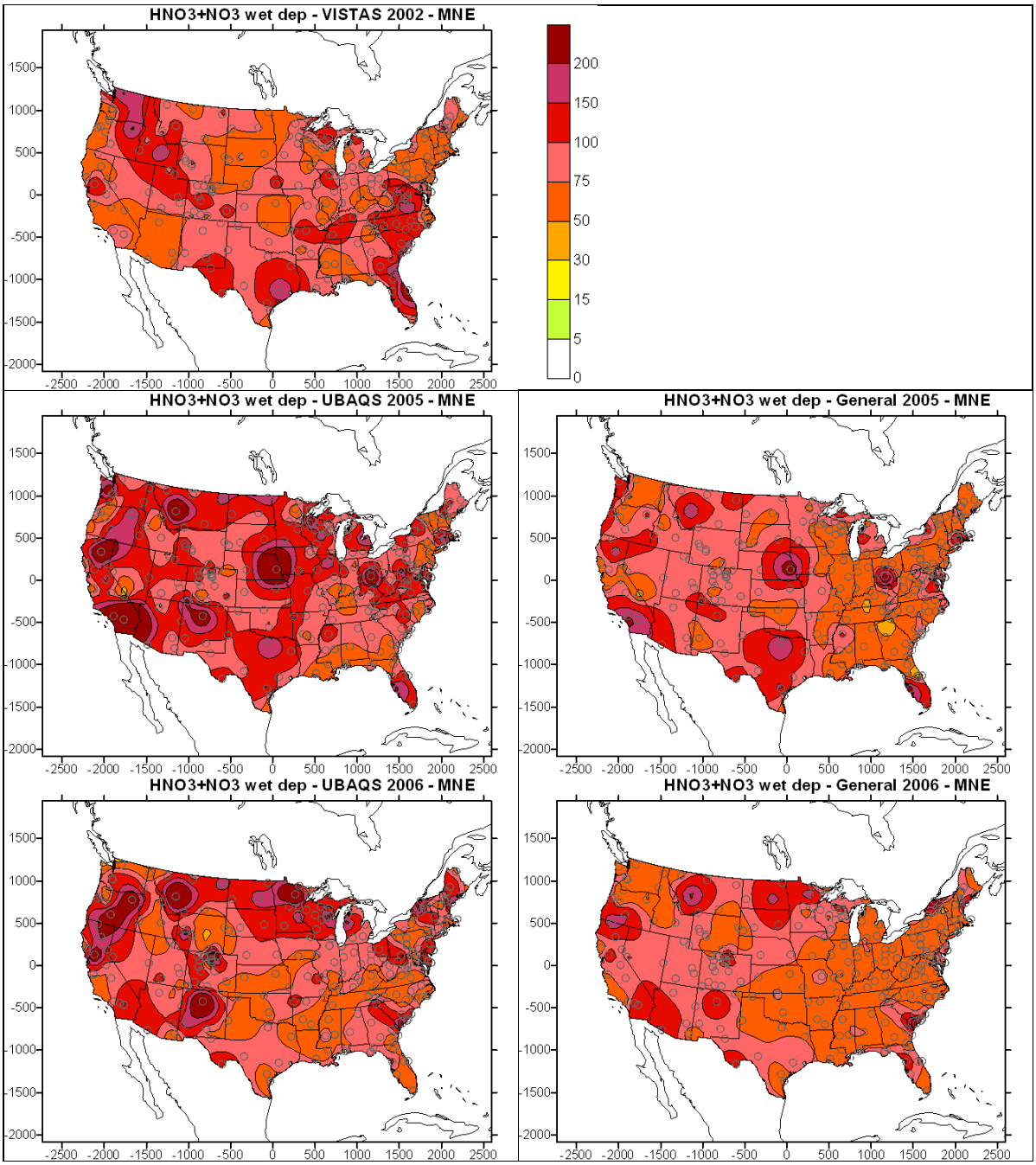

Figure D3-22. Mean normalized error (%) of modeled weekly total $HNO_3 + NO_3^-$ wet deposition using Kriging interpolation of values at the NADP monitoring sites (circle markers): CMAQ (left) and CAMx (right) model simulations for 2002 (top), 2005 (middle) and 2006 (bottom).

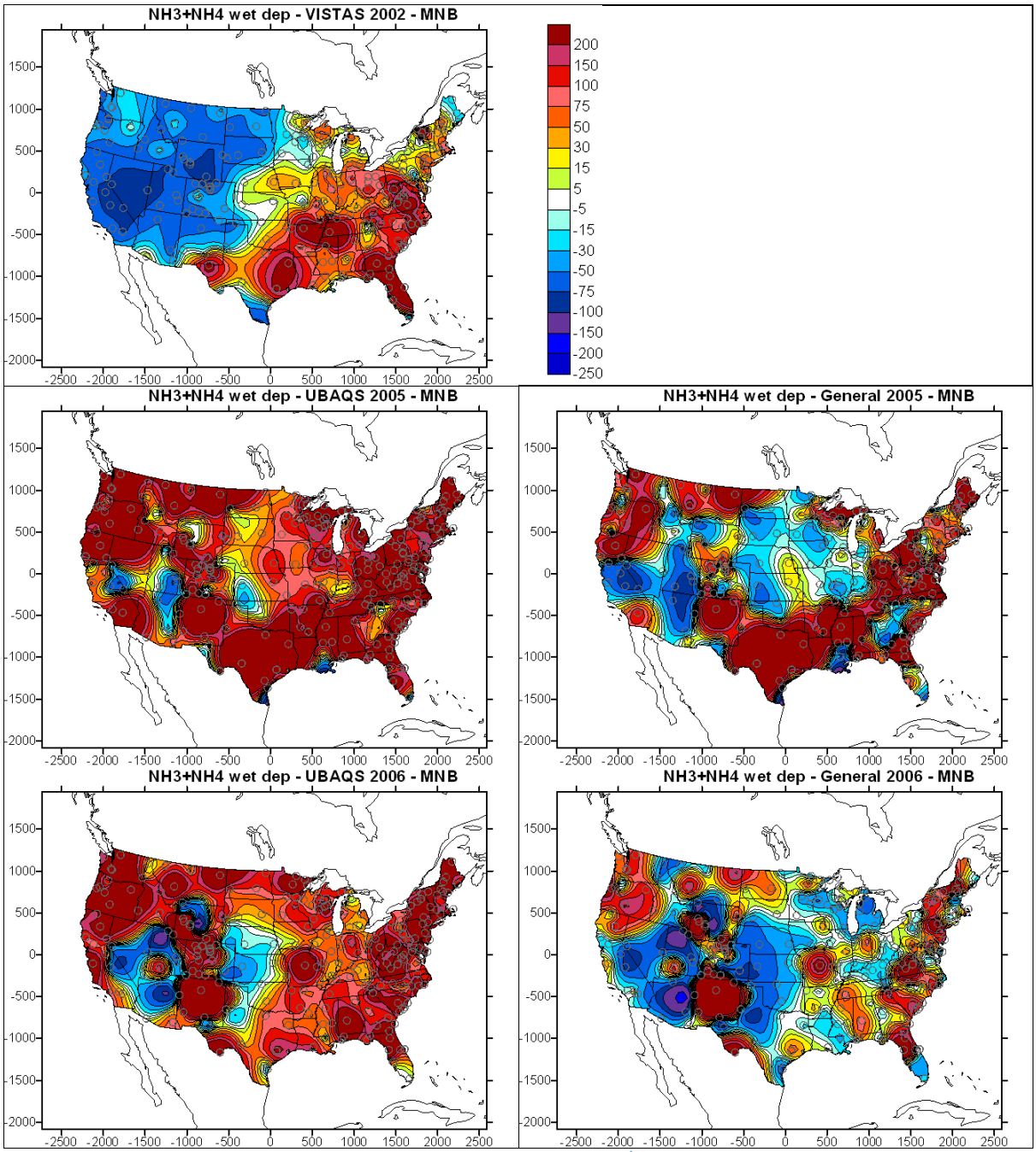

Figure D3-23. Mean normalized bias (%) of modeled weekly total NH_3 + NH_4^+ wet deposition using Kriging interpolation of values at the NADP monitoring sites (circle markers): CMAQ (left) and CAMx (right) model simulations for 2002 (top), 2005 (middle) and 2006 (bottom).

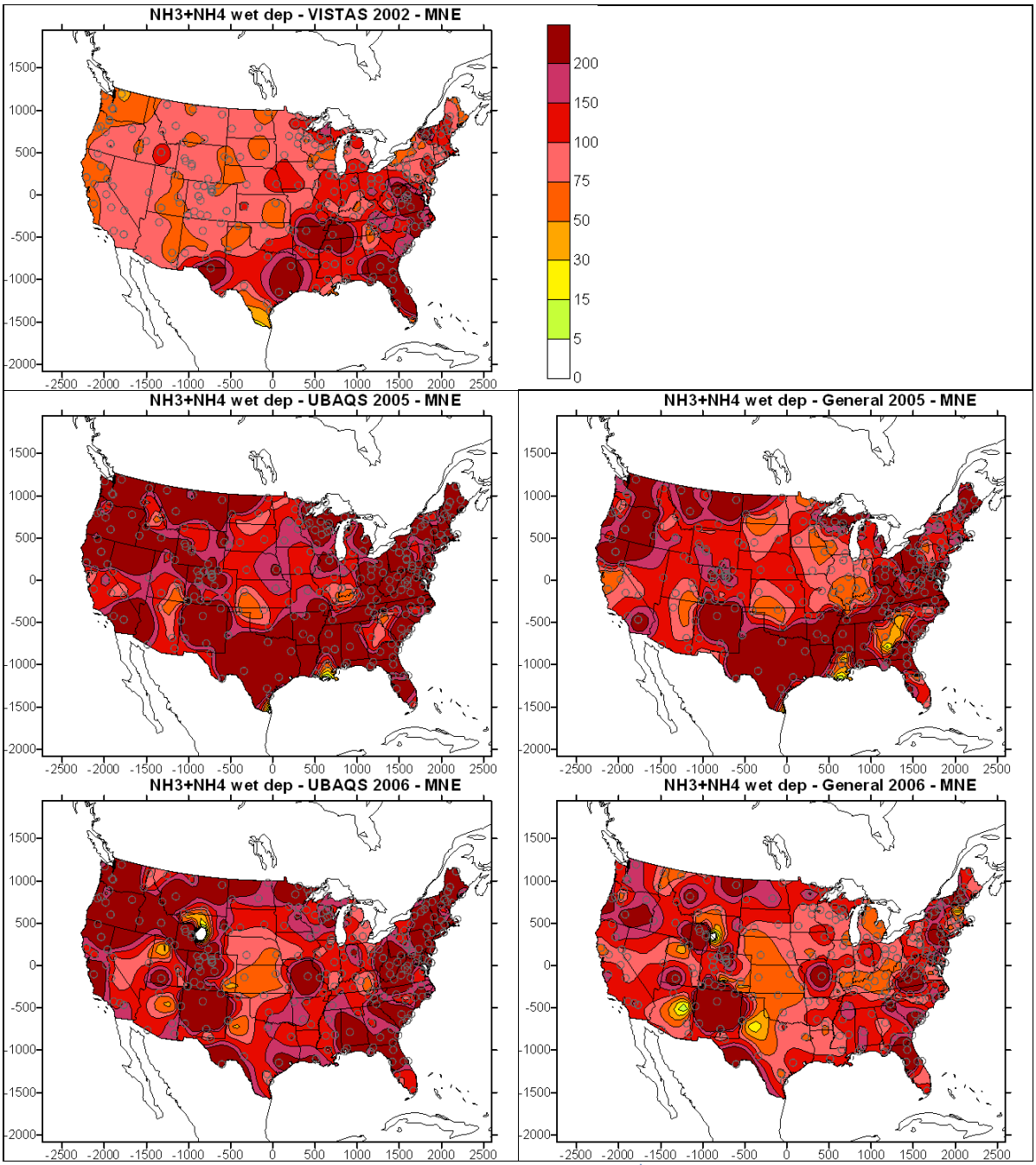

Figure D3-24. Mean normalized error (%) of modeled weekly total NH_3 + NH_4^+ wet deposition using Kriging interpolation of values at the NADP monitoring sites (circle markers): CMAQ (left) and CAMx (right) model simulations for 2002 (top), 2005 (middle) and 2006 (bottom).

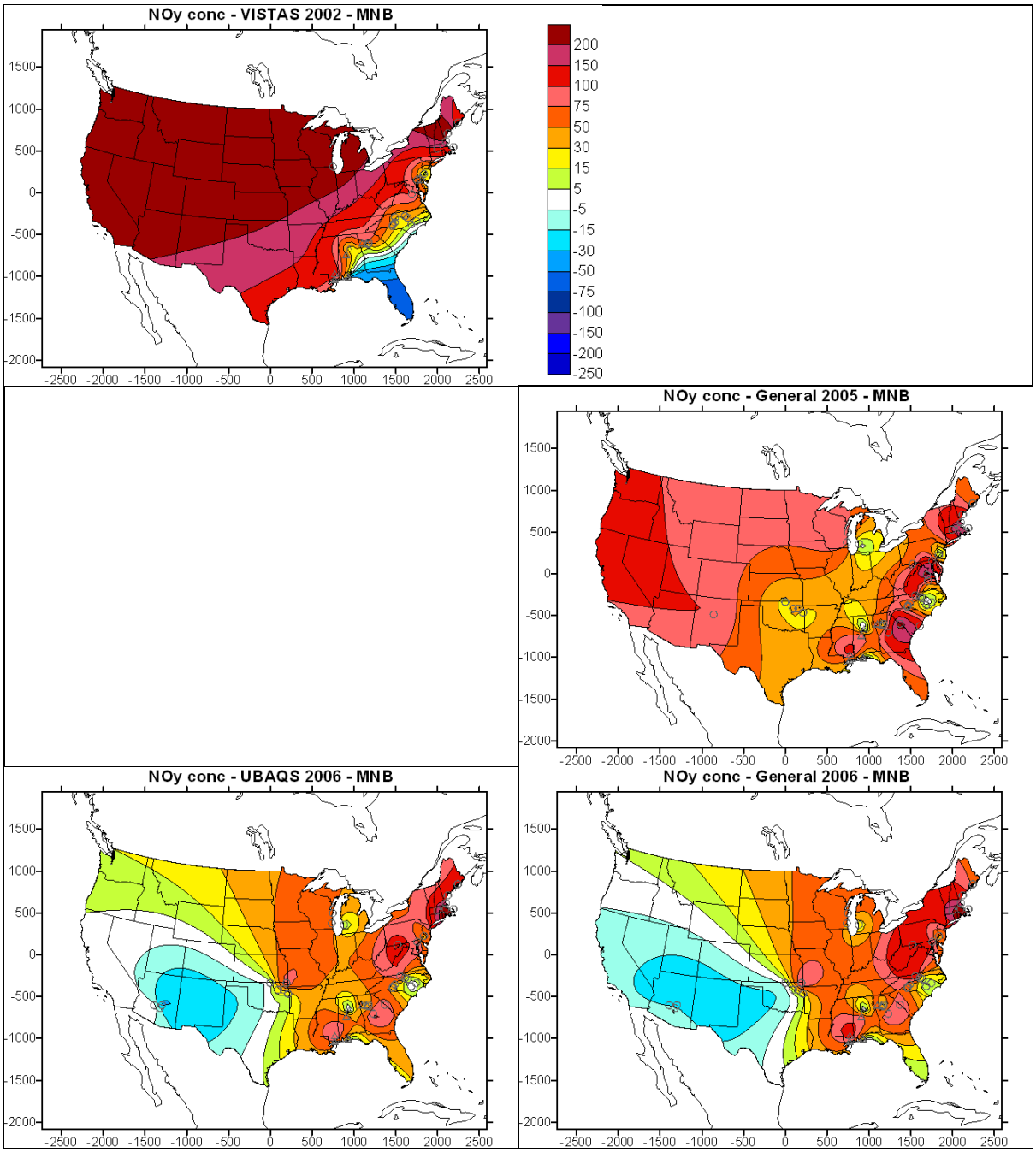

Figure D3-25. Mean normalized bias (%) of modeled hourly average NOy concentrations using Kriging interpolation of values at the AQS (circle markers) and SEARCH (triangle markers) monitoring sites: CMAQ (left) and CAMx (right) model simulations for 2002 (top), 2005 (middle) and 2006 (bottom).

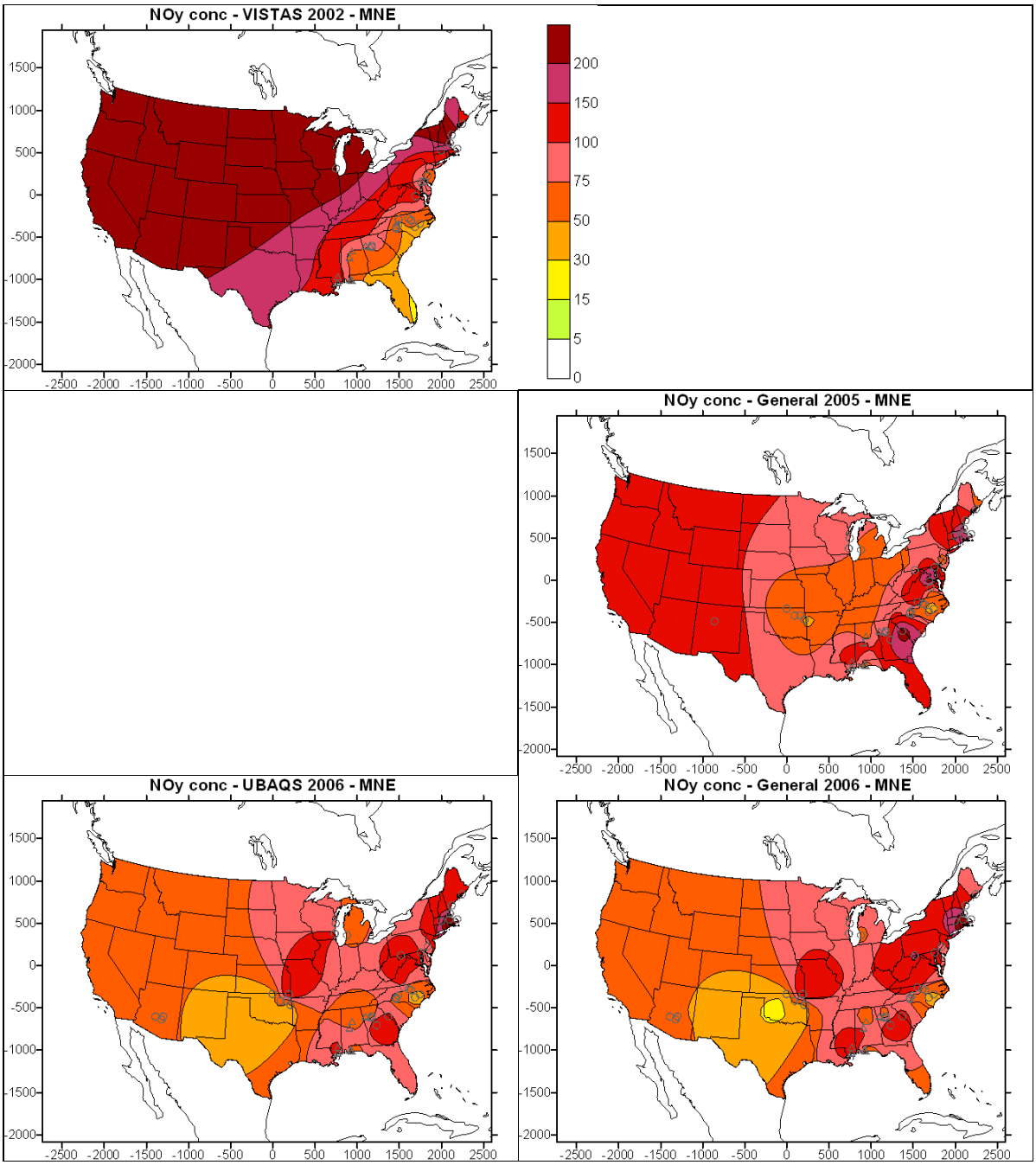

Figure D3-26. Mean normalized error (%) of modeled hourly average NOy concentrations using Kriging interpolation of values at the AQS (circle markers) and SEARCH (triangle markers) monitoring sites: CMAQ (left) and CAMx (right) model simulations for 2002 (top), 2005 (middle) and 2006 (bottom).

Appendix E: Variability in TSOx, TNOy and LNHx over Virginia, Wisconsin, Florida Panhandle, and Ecoregion 9.3.4

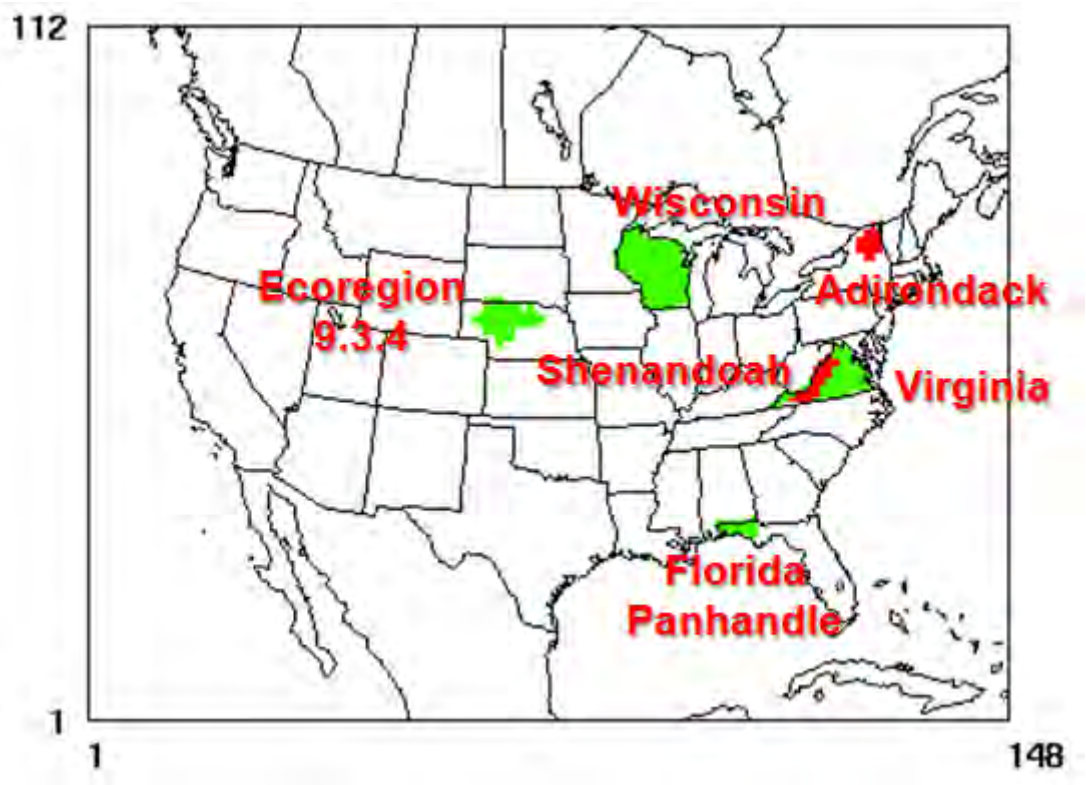

Figure E-1. Additional regions used for variability analysis for TSOx, TNOy and LNHx. Virginia includes 75 grid cells of 36-km resolution or 683 grid cells of 12-km resolution, Wisconsin includes 115 grid cells of 36-km or 1004 grid cells of 12-km, the Florida Panhandle region includes 16 grid cells of 36-km or 150 grid cells of 12-km, and the Ecoregion 9.3.4 includes 51 grid cells of 36-km.

(a) Virginia

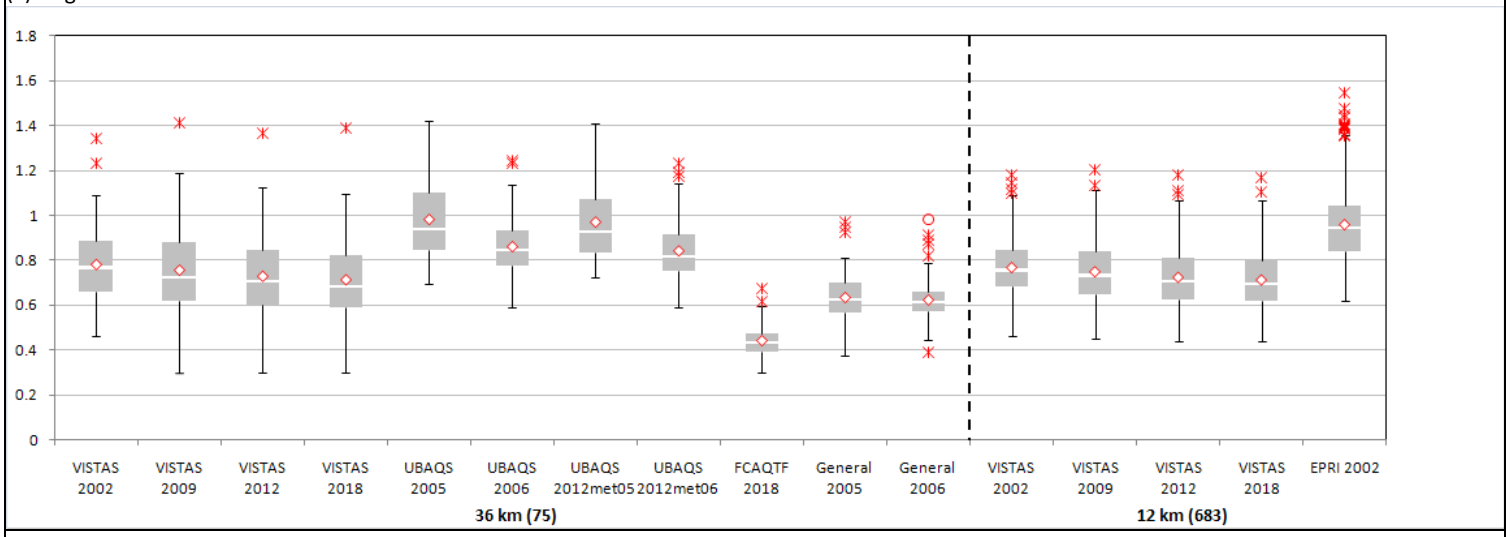

(b) Wisconsin

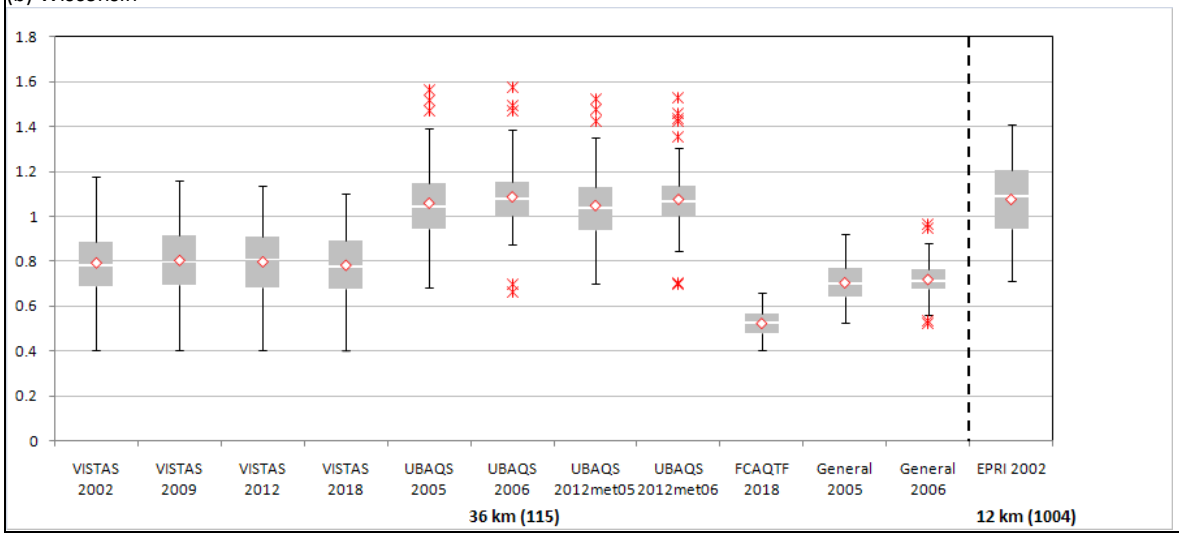

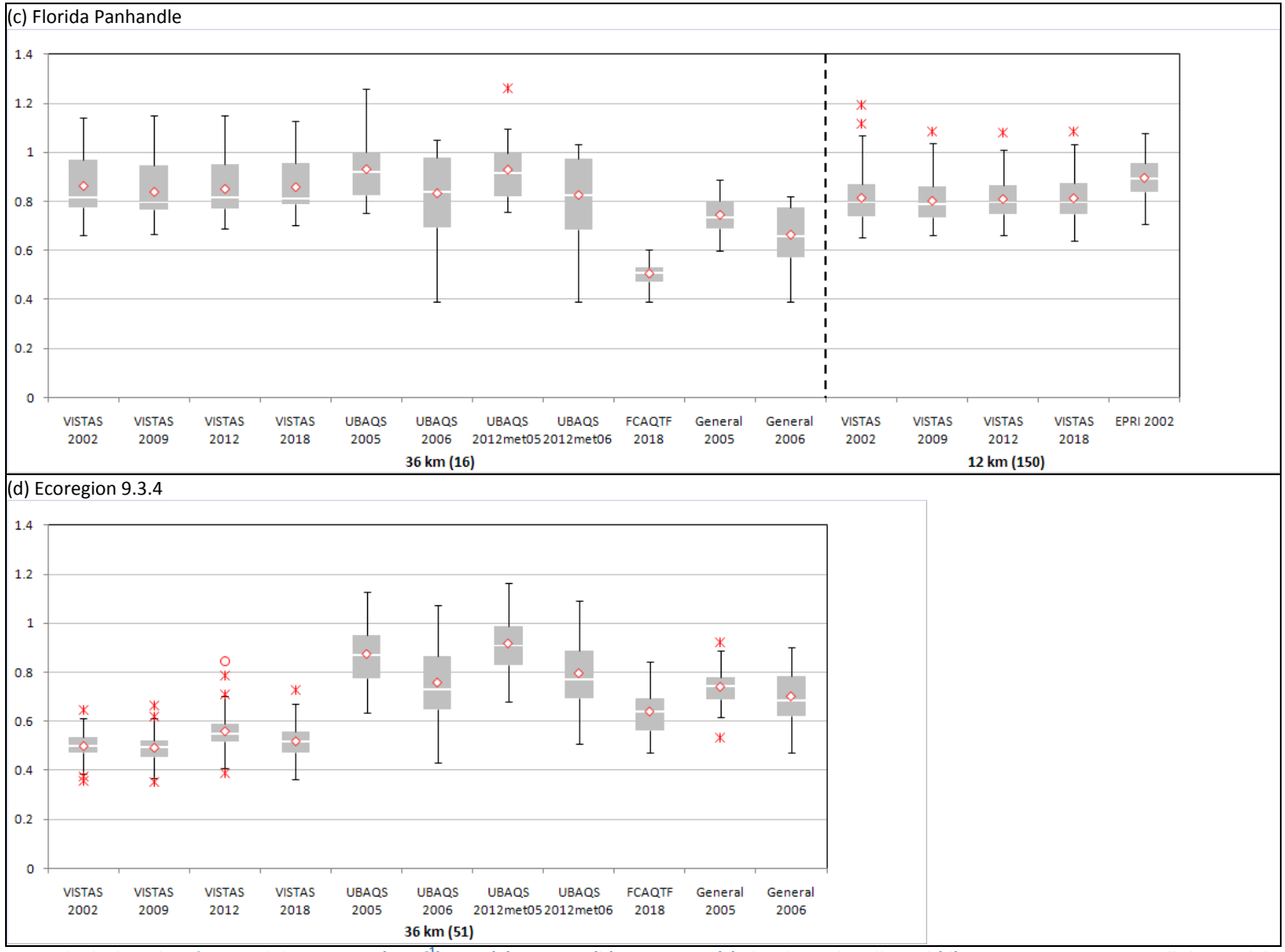

Figure E-2. Box and whisker plots for variability in TSOx (cm s^{-1}) over (a) Virginia, (b) Wisconsin, (c) Florida Panhandle and (d) Ecoregion 9.3.4 across all the model simulations. The number in parentheses represents the number of each sample data.

(a) Virginia

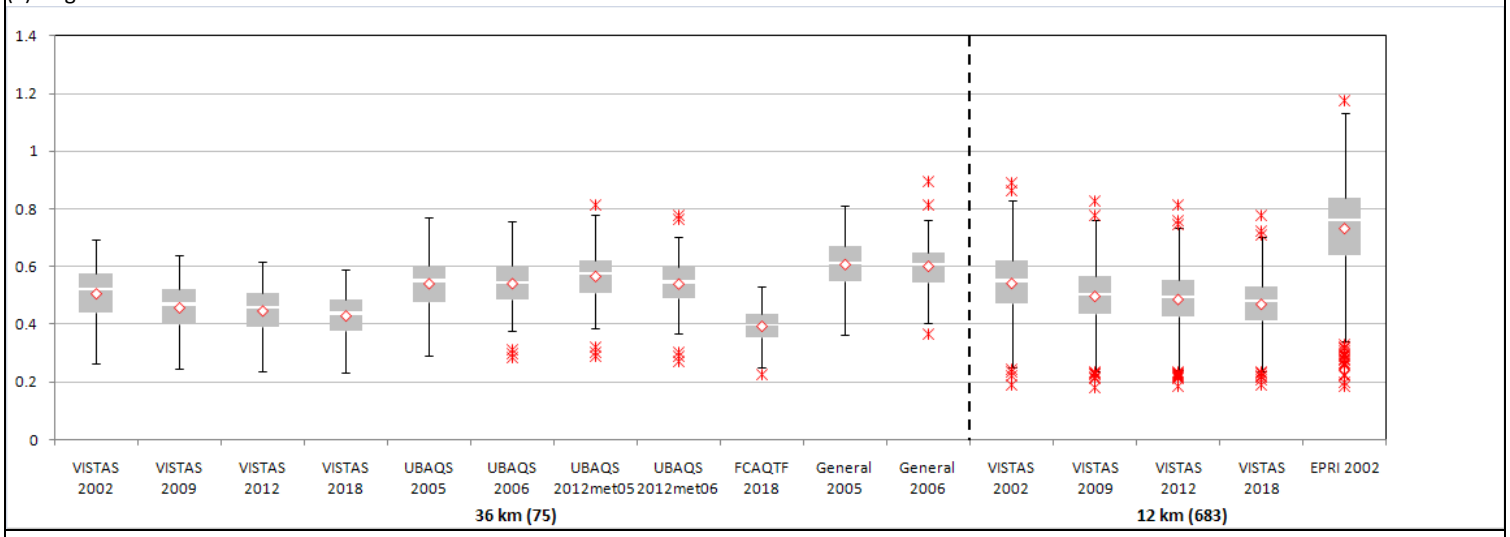

(b) Wisconsin

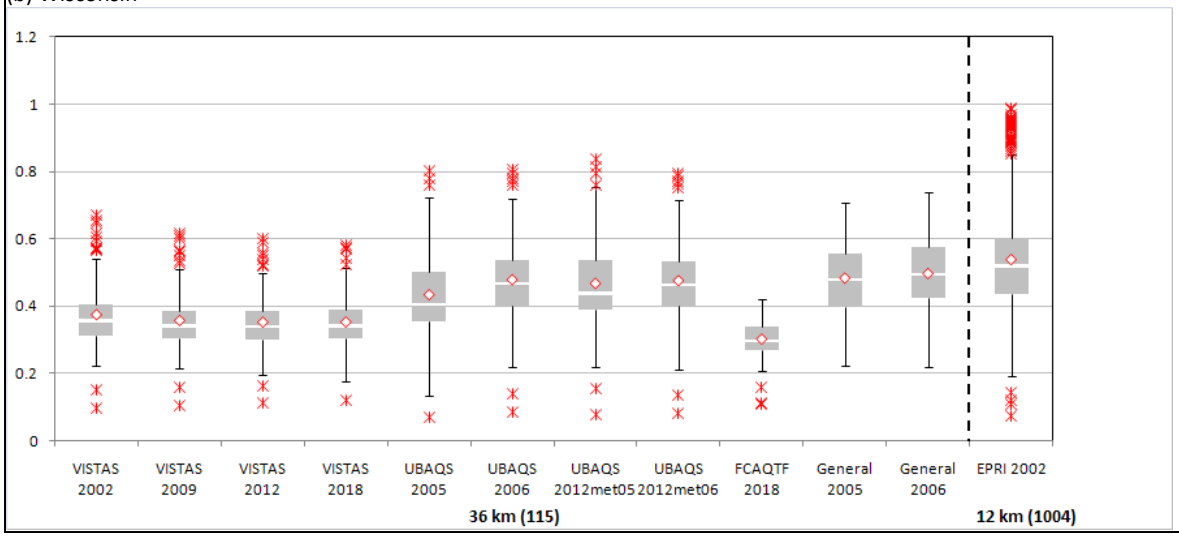

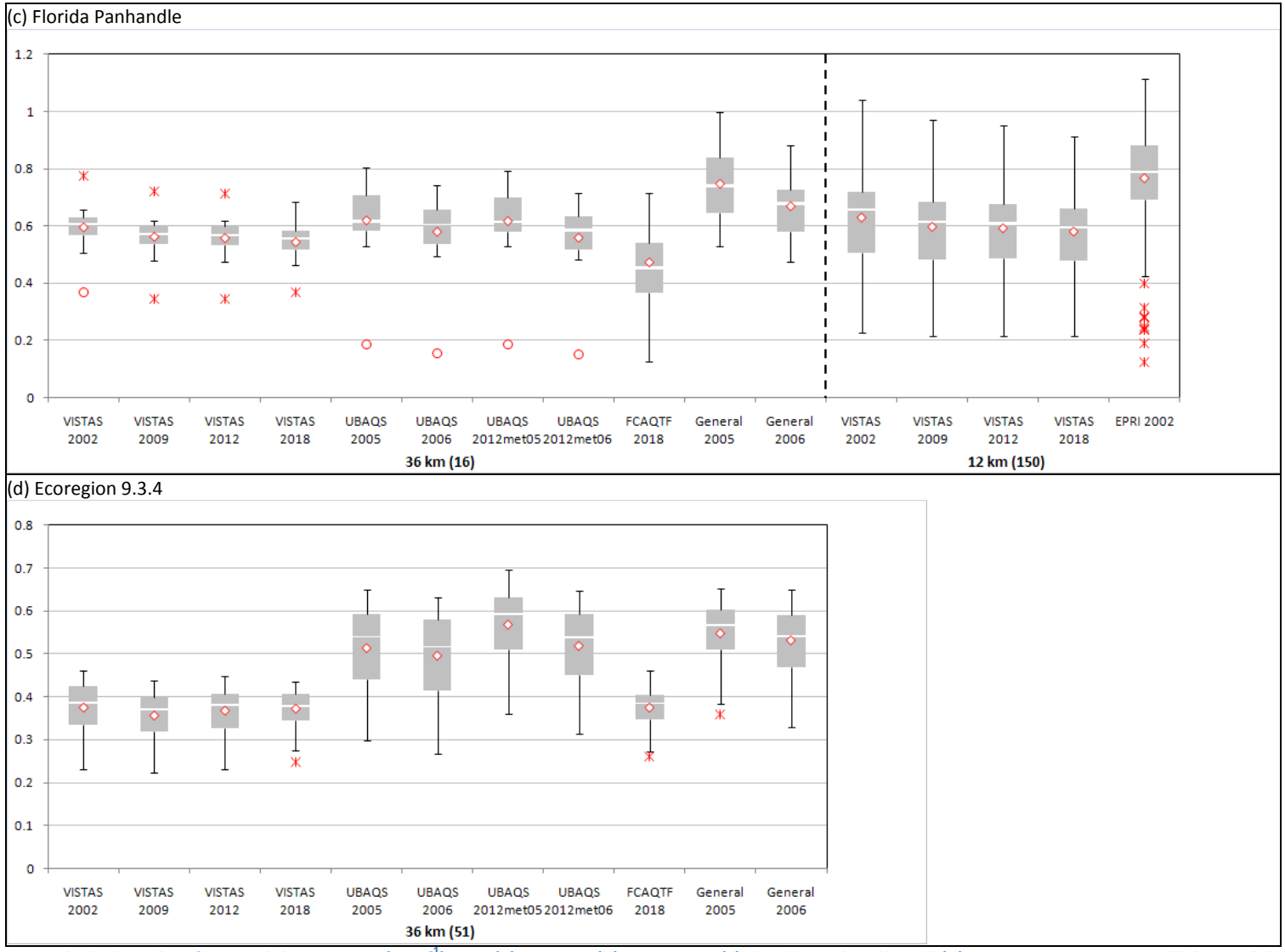

Figure E-3. Box and whisker plots for variability in TNOy (cm s^{-1}) over (a) Virginia, (b) Wisconsin, (c) Florida Panhandle and (d) Ecoregion 9.3.4 across all the model simulations. The number in parentheses represents the number of each sample data.

(a) Virginia

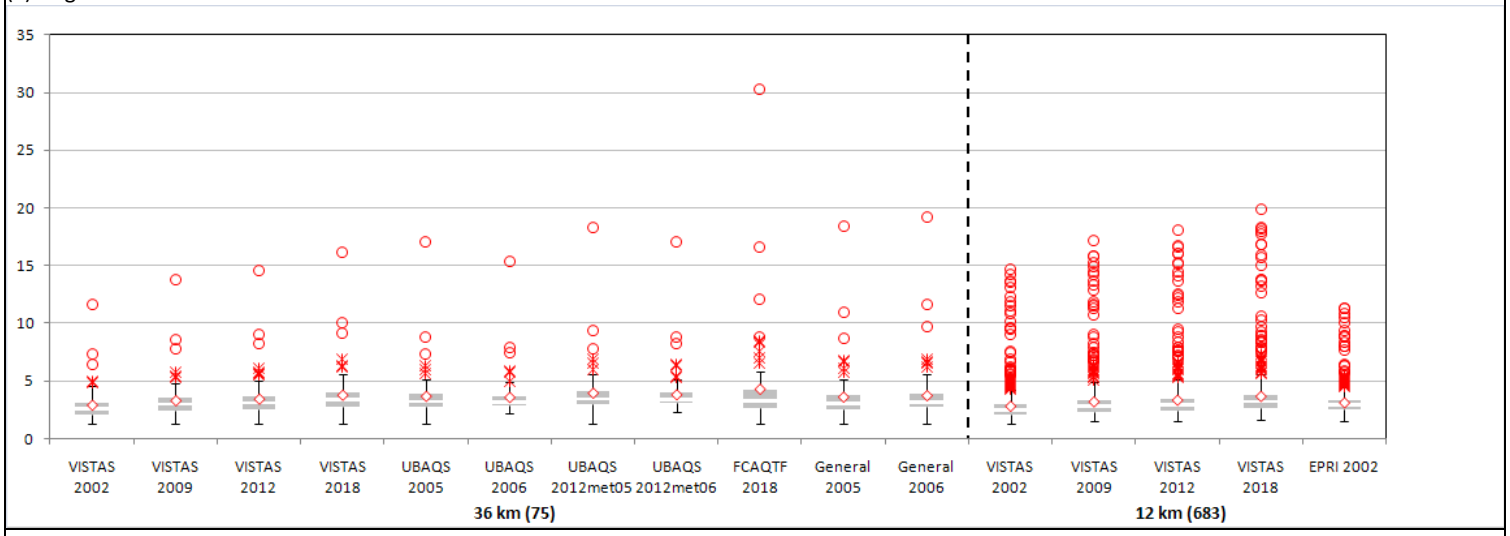

(b) Wisconsin

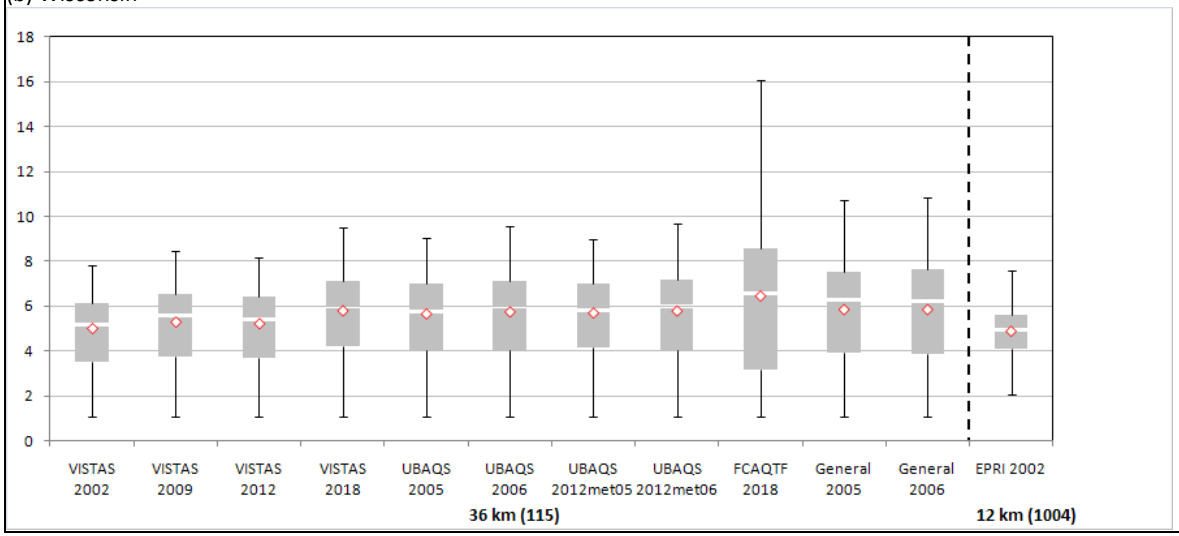

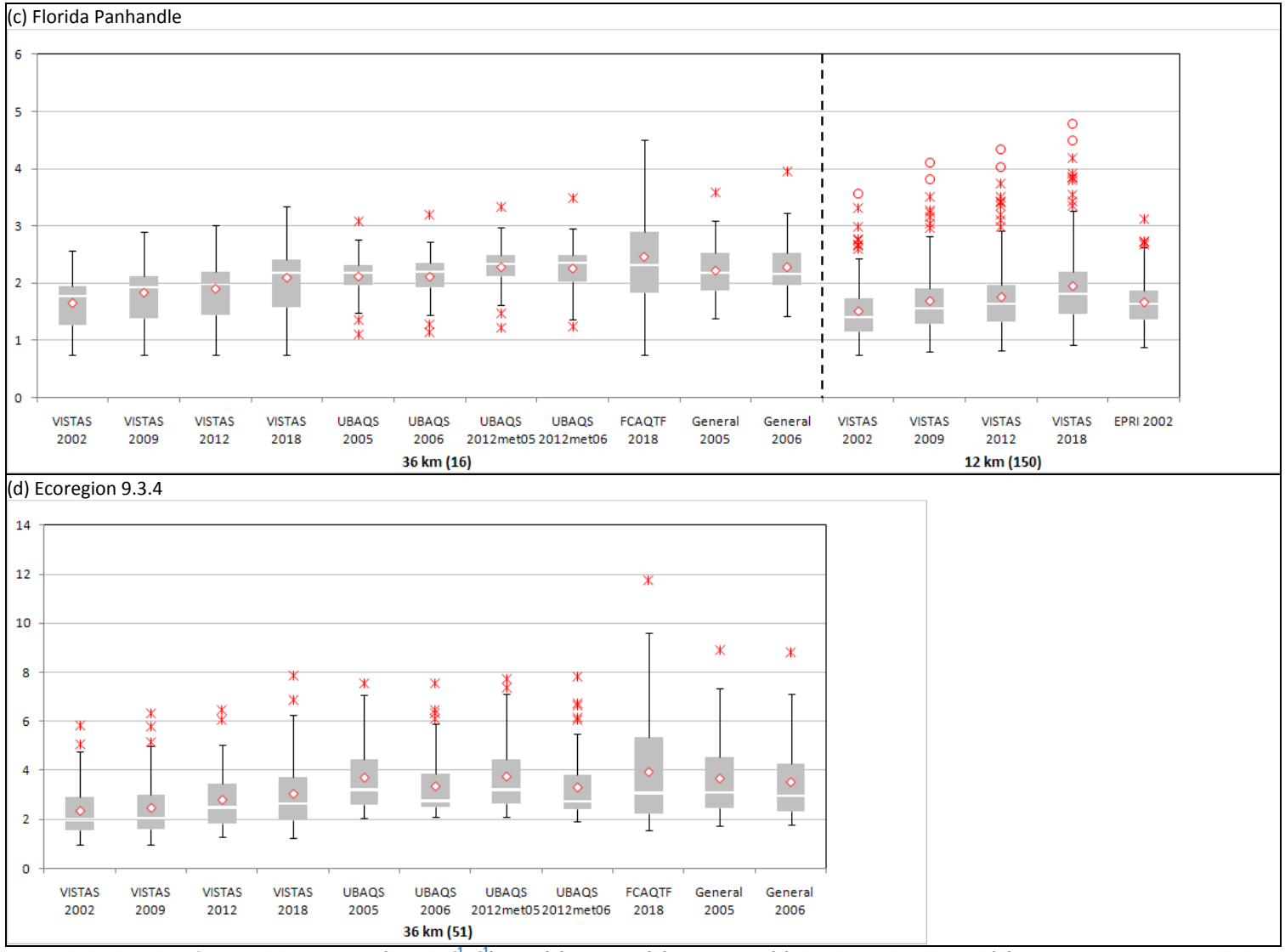

Figure E-4. Box and whisker plots for variability in LNHx (kg-N ha^{-1} y^{-1}) over (a) Virginia, (b) Wisconsin, (c) Florida Panhandle and (d) Ecoregion 9.3.4 across all the model simulations. The number in parentheses represents the number of each sample data.